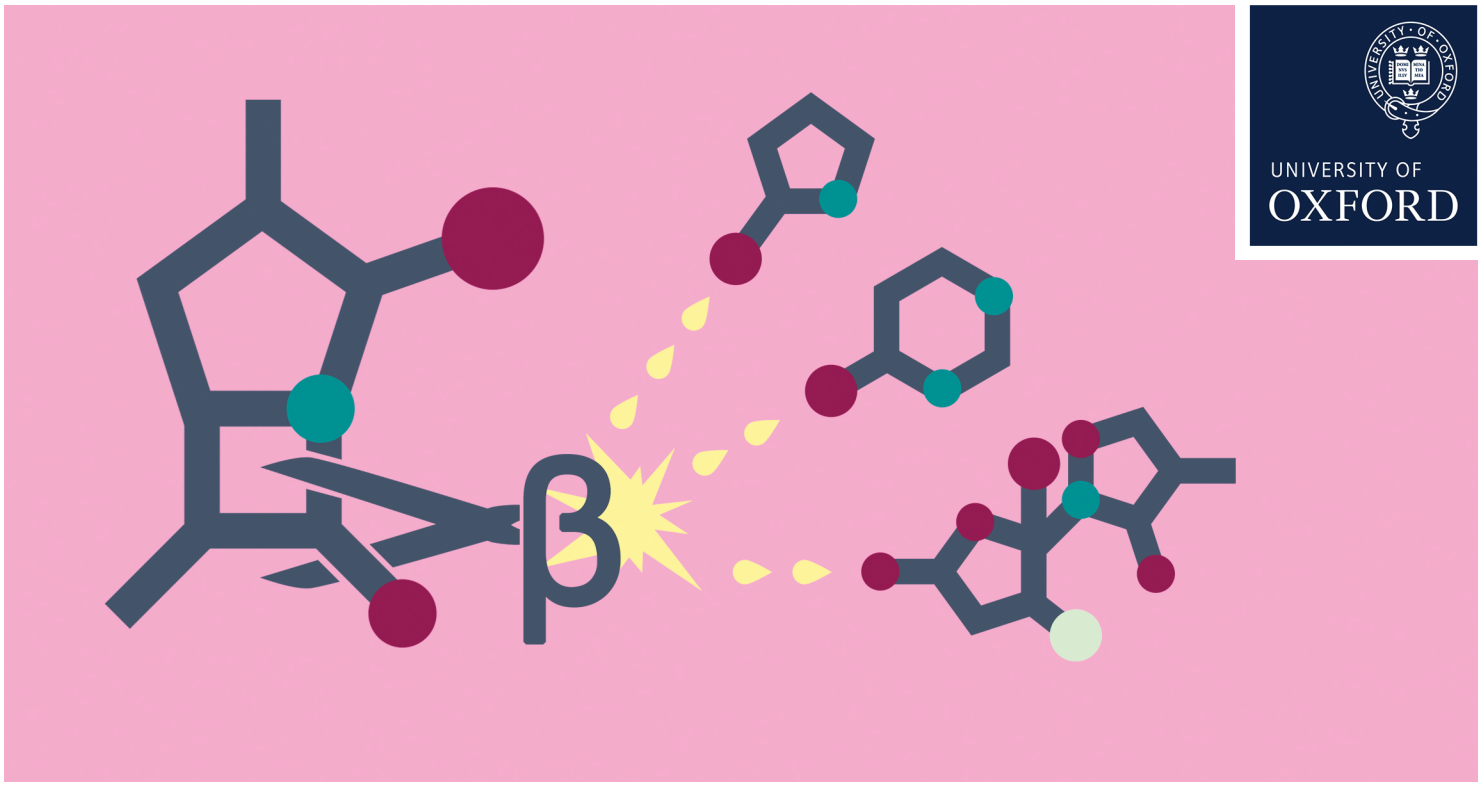
Studies of Novel Antibacterial Agents and Antibiotic Resistance Breakers Towards Combating Multidrug Resistant Bacteria



David Yuxin Wang

Wolfson College

University of Oxford

A thesis submitted for the degree of
Doctor of Philosophy

Michaelmas 2018

Antimicrobial resistance (AMR) within a wide range of infectious agents is a growing public health threat of broad concern to countries and multiple sectors. Increasingly, governments around the world are beginning to pay attention to a problem so serious that it threatens the achievements of modern medicine. A post-antibiotic era – in which common infections and minor injuries can kill – far from being an apocalyptic fantasy, is instead a very real possibility for the 21st century.

Antimicrobial Resistance: Global Report on Surveillance 2014

Word Health Organization

Studies of Novel Antibacterial Agents and Antibiotic Resistance Breakers Towards Combating Multidrug Resistant Bacteria

Abstract

David Yuxin Wang, University of Oxford

A thesis submitted for the degree of Doctor of Philosophy, Michaelmas 2018

β-Lactam containing compounds are the most important antibacterials. Following the discovery of the penicillins, successive generations of *β*-lactams (penicillins, cephalosporins, monobactams, carbapenems) have saved countless lives. Their use is threatened by growing resistance, of which the most important mechanism involves their hydrolysis by *β*-lactamases. There are two types of *β*-lactamases: the serine-*β*-lactamases (SBLs) and the metallo-*β*-lactamases (MBLs). Whereas SBL inhibitors are available, there are no clinically useful MBL inhibitors. This work covered the development of new types of MBL and SBL inhibitors.

One aspect of this work involved the development of new types of MBL inhibitors, in part inspired by structural and high-throughput screening approaches. Extensive chemical synthesis and screening of heteroaryl-carboxylate compounds were performed. Some of these exhibited potent inhibition against a panel of clinically relevant MBLs, including VIM-2.

Lactivicin is the only naturally occurring small molecule that acts similarly to *β*-lactams which does not contain a *β*-lactam ring. However, very little structural-activity relationship studies have been performed on lactivicin. In my work, the synthesis of a novel lactivicin analogue with a modified lactone ring was achieved.

The Class D OXA SBLs are arguably the most worrying of all *β*-lactamases mediated resistance processes. Studies on OXA SBLs were performed with an array of inhibitors; the results inform on the mechanism of OXA inhibition, including the role of protein carbamylation in catalysis and inhibition.

Overall, the results suggest new possibilities for *β*-lactamase inhibition and should contribute to the effort to combat *β*-lactamase mediated resistance.

Contents

Declaration i

Acknowledgements iii

Abbreviations v

1. Introduction 1

1.1. Current strategies to combat antibiotic resistance involving β-lactam antibiotics 3
1.2. The search for a clinically useful metallo-β-lactamase inhibitor 18
1.3. SAR and screening-based drug design of novel β-lactamase inhibitors 28
1.4. Aims and objectives 32
1.5. References 33

2. Fragments Optimisation 45

2.1. Fragments discovery via high-throughput X-ray crystallography platform 47
2.2. Structure-activity relationship and optimisation studies of analogues of **F32** 52
2.3. Development of pyrrole-based analogues of **F32** as MBL inhibitors 58
2.4. Synthesis of a nitropyrrole analogue as a potential MBL detection assay substrate 71
2.5. Synthesis and MBL inhibition studies of thiazole carboxylate derivatives 74
2.6. Structure-activity relationship and optimisation studies of analogues of **F52** 78
2.7. Structure-activity relationship studies of **ELF-128** 85
2.8. Summary of fragment optimisation work and SAR studies 89
2.9. Experimental procedures 91
2.10. References 128

3. γ-Lactam Derivatisation **131**

3.1. Clinical relevance of non *β*-lactam containing antibiotics 133
3.2. Derivatisation of *γ*-lactone for lactivicin synthesis 138
3.3. Towards the synthesis of novel lactivicin analogues 142
3.4. Synthesis of aza-lactivicin derivatives via pyrazolidinones 152
3.5. Summary of synthetic strategies towards novel lactivicin derivatives 155
3.6. Experimental procedures 155
3.7. References 164

4. Studies on OXA β-Lactamases **167**

4.1. Clinical relevance of OXA β-lactamases in antibiotic resistance 169
4.2. Production and purification of OXA-23 and OXA-48 172
4.3. Characterisation of kinetic parameters for OXA-23 and OXA-48 173
4.4. Fluorometric kinetic assays for OXA-23 and OXA-48 with a panel of inhibitors 179
4.5. Fluorometric kinetic assays for OXA-10, OXA-23 and OXA-48 with iodide 185
4.6. Summary of studies on OXA enzymes 198
4.7. Experimental procedures 200
4.8. References 204

5. Conclusions and Future Work **209**

5.1. Conclusions and future work 211
5.2. References 217

Appendix **219**

A1.1. Towards the efficient synthesis of cycloserine 221
A1.2. Experimental procedures 224
A1.3. References 228

Declaration

This thesis describes work carried out in the Chemistry Research Laboratory, Department of Chemistry, University of Oxford between October 2014 and September 2018. The work it describes is entirely my own except where it is specifically indicated in the text.

David Yuxin Wang

Oxford

Trinity Term, 2018

Acknowledgements

The people who made this journey possible…

Recalling the days before starting my DPhil research back in August 2014, I was extremely excited to start my Oxford PhD journey and get my hands dirty in the lab. What eventually greeted me was an amazing project, which far exceeded my initial expectation of a rewarding PhD experience. *Chris*, my supervisor, was not only extremely supportive, but also constantly stretched my academic potential by challenging me with new ideas whilst granting me the space and trust to put my own ideas to the test.

The *Schofield Group* was a magical environment filled many incredible researchers from different parts of the world. I remember a defining moment when I sat down with *Klaus-Daniel* and came up with the idea of pyrrole-based inhibitors in my first year, which ultimately led to a successful part of my project. From this brilliant synthetic chemist, I picked up a vast pool of knowledge that became instrumental in navigating through my research, at the cost of picking up his not-so-good habit of not wearing a lab coat in the lab.

Another incredible individual is *Jürgen*, who has kept my research on the right track and always provided valuable support at times of need. From him, I have picked up a variety of research skills beyond synthetic chemistry, which definitely shaped my appreciation of the interface between chemistry and biology.

Given the highly collaborative nature of my research, I am fortunate to have worked with *Chris L.*, *Sam* and *Gareth* on different projects, some of which have transformed into publications. Some of the projects also would not have happened without external collaborators, including *Patrick* and other colleagues from Diamond Light Source, as well as peers from the University of Bristol and Queen Mary University of London, just to name a few.

Outside of the lab, the Schofield Group has been a vibrant social hub. Over the years, I have bonded with many individuals who were amazing both in and out of the lab, including (in no particular order) *Hide*, *Anete*, *Alex*, *Tharindi*, *Jule* (and her significant other half, *Jens*), *Gonzalo*, *Lucía*, *Aistė*, *Dong*, *Roman*, *Rob*, *Jimmy*, *Jos* and many more.

Special thanks are also extended to *Jenny* and *Zahn*, who made it possible for me to schedule meetings with Chris and decipher his handwritten comments, and *Adam* and *Wendy*, who have kept our lab in a decent state.

Outside of my research group, I was very lucky to be enrolled in *Wolfson College*, which has become my home for the past four years. There are so many wonderful individuals at Wolfson that I would like to thank, including various staff and students. Certainly, I will miss the opportunities to organise bops, balls and other events at Wolfson, which has, interestingly, kickstarted my part-time career as a party DJ.

At Wolfson, I also met a group of amazing friends, including *Wasim*, *Steve*, *Vincent*, *Edd* & *Olivia*, *Sarah* & *Matt*, *Robbie* & *Rachel* and *Karwei*, who became the key social circle in my life outside of research. Dramatic moments at the Wolfson bar will definitely not be forgotten (nor repeated for that matter).

A special shout-out goes to *Marie*, who is by far the most loyal customer to Dave's Kitchen, an initiative I conceptualised in order to bring friends together over a meal. Despite having very tricky dietary preferences, which has proven to make my food preparations unnecessarily challenging, she probably has witnessed both my ups and downs over the years, and I truly appreciate a pair of listening ears.

Lastly, and most importantly, I would like to thank my parents, *Xiwen* (*Steven*) and *Ling*. Coming from an ordinary Chinese family that migrated to Singapore when I was ten years old, I consider myself extremely lucky to be able to pursue higher education overseas with the financial support from my family, because my parents truly believed in the value of education and wanted to provide me a brighter future. As immigrants on foreign soil, the paths chosen by my family have not been the easiest to trek, but I believe I am now equipped with both the intelligence and the adaptability to succeed in the world beyond my PhD.

There are many other individuals who have made my Oxford experience a positive one, but unfortunately, I won't have the opportunity to acknowledge each and every one of them. To all of you (you will know who you are), you have played a special role in my Oxford journey, for which I am more than thankful for!

Abbreviations

2-OG:	2-Oxoglutarate
Ac:	Acetyl
ADME:	Absorption, distribution, metabolism, and excretion
AMA:	Aspergillomarasmine A
AmpC:	Ampicillin class C
AMR:	Antimicrobial resistance
Ar:	Aryl (or argon)
ATMO:	2-Amino-4-thiazolyl methoxyimino
BATSI:	Boronic acid transition state analogue inhibitor
BcII:	*Bacillus cereus* metallo-β-lactamase II
Boc:	*tert*-Butyloxycarbonyl
BrettPhos:	2-(Dicyclohexylphosphino)3,6-dimethoxy-2',4',6'-triisopropyl-1,1′-biphenyl
Bu:	Butyl
CphA:	Carbapenem hydrolysing Aeromonas
CMY:	Cephamycin
COSY:	Correlation Spectroscopy
CTM-X:	Cefotaximase
DBO:	Diazabicyclooctane
DBU:	1,8-Diazabicyclo[5.4.0]undec-7-ene
DCC:	*N*,*N*'-Dicyclohexylcarbodiimide
DEPT:	Distortionless enhancement by polarization transfer
DIAD:	Diisopropyl azodicarboxylate
DIPEA:	*N*,*N*-Diisoproylethylamine
DMAP:	4-(*N*,*N*-Dimethylamino)pyridine
DMF:	*N*,*N*-Dimethylformamide
DMSO:	Dimethyl sulfoxide
EDCI:	1-Ethyl-3-(3-dimethylaminopropyl)carbodiimide
EDTA:	Ethylenediaminetetraacetic acid
Equiv.:	Equivalent
ESBL:	Extended-spectrum *β*-lactamases
Et:	Ethyl
EtOH:	Ethanol
FBDD:	Fragment-Based Drug Discovery
FBLD:	Fragment-Based Lead Discovery
FRET:	Förster Resonance Energy Transfer
FT IR:	Fourier transform infrared spectroscopy

HCMV: Human cytomegalovirus
HMDS: Hexamethyldisilazide
HMQC: Heteronuclear multiple-quantum correlation spectroscopy
HOBt: 1-Hydroxybenzotriazole
HRMS: High resolution mass spectrometry
HTS: High-throughput screening
IC_{50}: Half maximal inhibitory concentration
IMP: Imipenem-resistant *Pseudomonas aeruginosa* producing metallo-β-lactamase
k_{cat}: Catalytic rate (or turnover number)
K_M: Michaelis constant
KPC: *K. pneumoniae* carbapenemase
L1: *β*-Lactamase 1
LBA: Ligand binding assay
LCMS: Liquid chromatography-mass spectrometry
LRMS: Low resolution mass spectrometry
LTV: Lactivicin
MBL: Metallo-*β*-lactamase
Me: Methyl
MeOH: Methanol
min: Minutes
mp: Melting point
MIC: Minimum inhibitory concentration
MRSA: Methicillin-resistant *Staphylococcus aureus*
NAG: *N*-Acetylglucosamine
NAM: *N*-Acetylmuramic acid
NBS: *N*-Bromosuccinimide
NCS: *N*-Chlorosuccinimide
NIS: *N*-Iodosuccinimide
NDM: New Delhi metallo-β-lactamase
NMR: Nuclear magnetic resonance
OMe: Methoxyl/methoxide
OXA: Oxacillinase
PBP: Penicillin-binding protein
Ph: Phenyl
PLE: Porcine liver esterase
PLTV: Phenoxyacetyl-lactivicin
ppm: Parts per million
Pr: Propyl
quant.: Quantitative

R_f: Retardation factor

RuPhos: 2-Dicyclohexylphosphino-2',6'-diisopropoxybiphenyl

SAR: Structure-activity relationship

SBL: Serine-*β*-lactamase

SHV: Sulfhydryl variable

SPR: Surface Plasmon Resonance

TBTO: Tributyltin oxide

^{t}BuXPhos: 2-Di-*tert*-butylphosphino-2',4',6'-triisopropylbiphenyl

TEM: Temoneira

THF: Tetrahydrofuran

TLC: Thin layer chromatography

TOF: Time of flight

Ts: *p*-Toluenesulfonyl

TSTU: *N*,*N*,*N'*,*N'*-Tetramethyl-*O*-(*N*-succinimidyl)uronium tetrafluoroborate

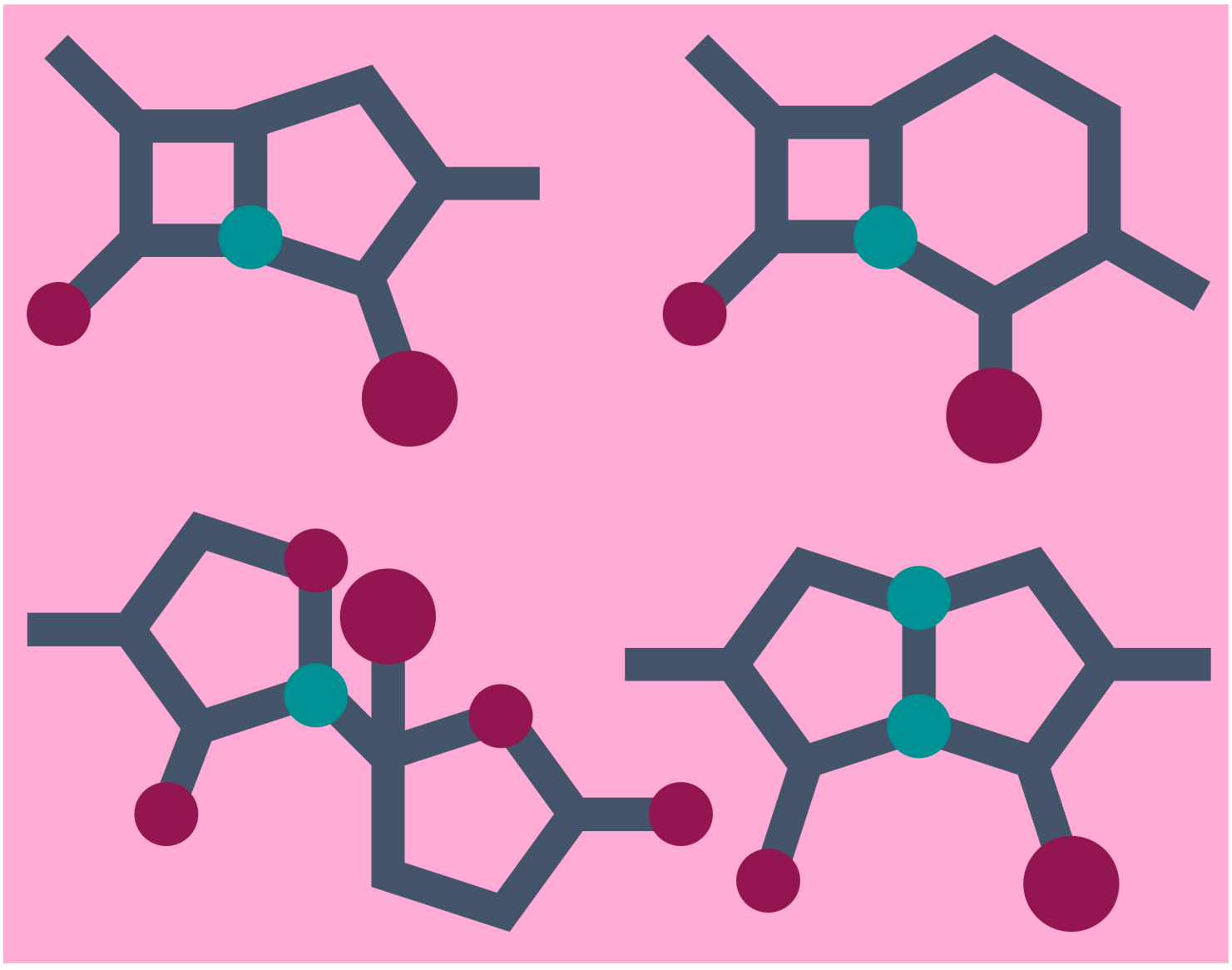
VIM: Verona integron-encoded metallo *β*-lactamase

V_{max}: Maximum rate

WHO: World Health Organization

XPhos: 2-Dicyclohexylphosphino-2',4',6'-triisopropylbiphenyl

Chapter 1.
Introduction



1. Introduction

1.1. Current strategies to combat antibiotic resistance involving β-lactam antibiotics

2018 marks the 90th anniversary of the observation of the activity of the penicillins by Sir Alexander Fleming. Since its pioneering clinical application in 1942, the penicillins, along with other *β*-lactam antibiotics, have become a mainstay of modern medicine. *β*-Lactam antibiotics are widely used in the clinic and in other areas such as agriculture. As compared to other antibiotic classes, the use of the *β*-lactam antibiotics, especially penicillins and cephalosporins, dominates global antibiotic consumption (Figure 1.1)[1]. Since the introduction of the penicillins, the median life expectancy in England and Wales has increased by more than 20%[2]. While other medical technologies have also made significant advances during this time and contributed to improvements in disease treatment, the *β*-lactam antibiotics have played an important part in preventing deaths from commonly observed bacterial infections and in complementing other modern medical procedures which can lead to an increased rate of infection, such as invasive surgical interventions[3].

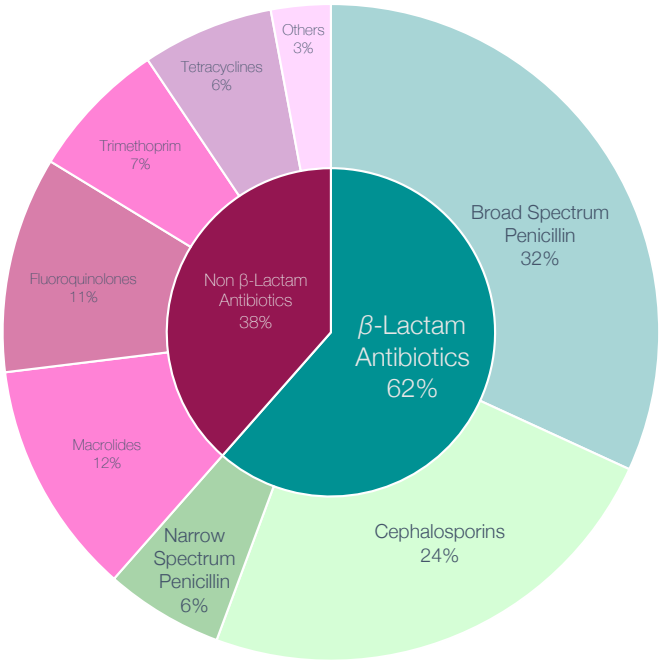


Figure 1.1. Percentage of global market sales of different classes of antibiotics in 2010. *β*-lactam antibiotics contributed to a total of over 62% of global antibiotic consumption. The main contributors are both broad spectrum and narrow spectrum penicillins and cephalosporins. The usage of monobactams and carbapenems, the latter a common last-resort option, although smaller, is also significant[1].

The bactericidal effect of *β*-lactam antibiotics has been described in multiple textbooks and academic syllabi as an example of an extremely successful drug mechanism. Bacteria have a cell wall that protects them from the internal turgor pressure, the result of a concentration gradient across the cell membrane, as well as to provide overall structural integrity[4]. Unlike most other cellular organisms, bacterial cell walls are made up of an inter-linked network of peptidoglycan, a polysaccharide motif typically consisting of alternating *N*-acetylmuramic acid (NAM) and *N*-acetylglucosamine (NAG) residues[5,6]. *β*-Lactam antibiotics act in part by mimicking the terminal D-alanyl-D-alanine residues on peptidoglycan, which are recognised by DD-transpeptidases or penicillin-binding proteins (PBPs)[7,8]. *β*-Lactam antibiotics irreversibly acylate a key serine residue at the active site in PBPs, which inhibits their ability to catalyse the cross-linking of peptidoglycan, thus disrupting cell wall biosynthesis[9,10]. Without an intact cell wall, bacteria cannot survive and lyse due to high cytoplasmic concentration of proteins and other molecules[11]. An outline of biosynthesis of bacterial cell wall and the mechanism of action of *β*-lactam antibiotics on PBPs is given in Figure 1.2. The elegance of *β*-lactam antibiotics not only lies in the fact that they target a fundamentally vital survival mechanism in bacteria, but also in that the peptidoglycan component is highly specific to bacterial species. Therefore, *β*-lactam antibiotics are highly selective and tend not to cause major adverse effects on humans (except when one has an allergic response towards treatment with them).

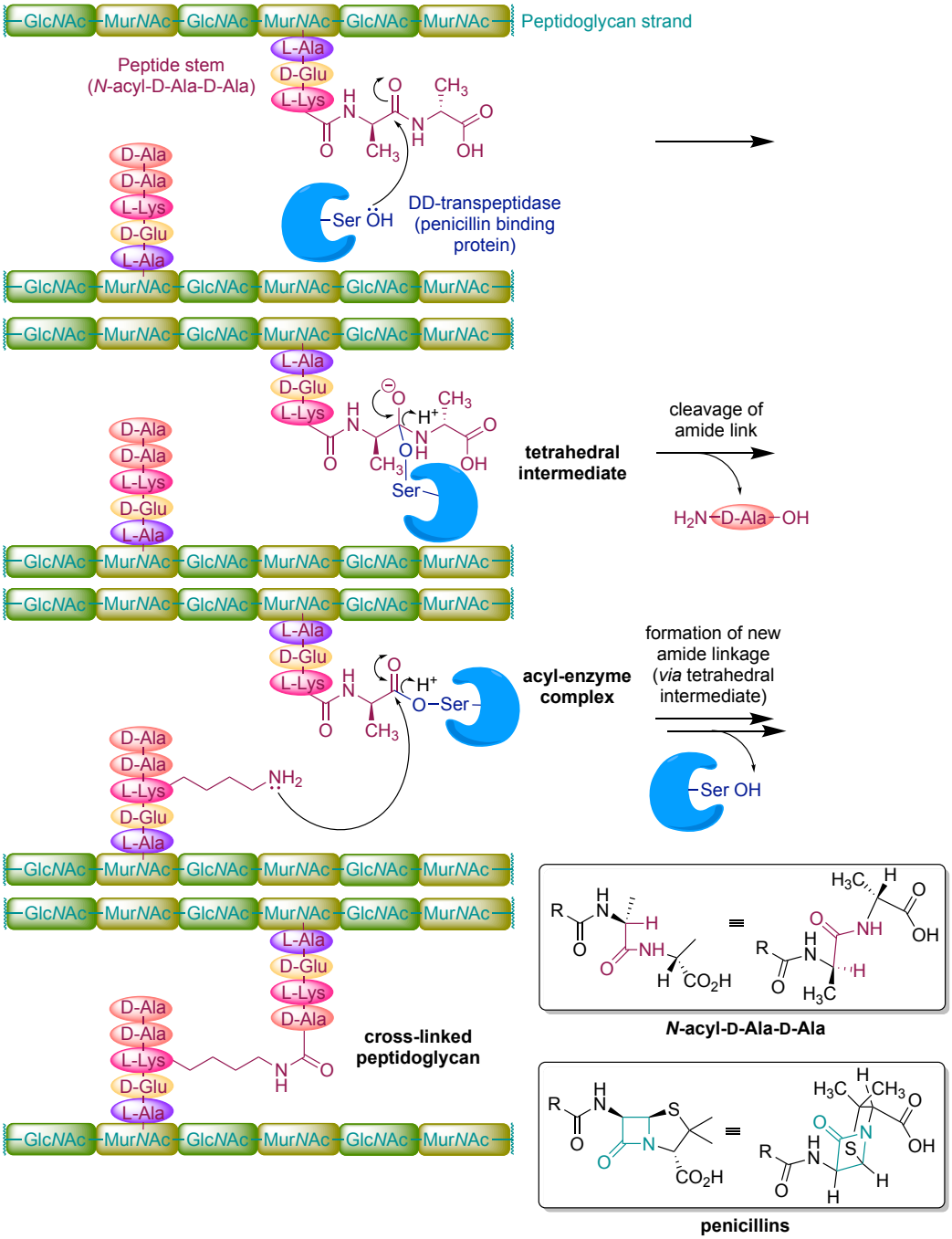


Figure 1.2. Outline of bacterial cell wall biosynthesis, showing the role of DD-transpeptidase[7,8]. The Strominger hypothesis defines the structural similarities between the *N*-acyl-D-alanyl-D-alanine residues and β-lactam antibiotics, exemplified by a general structure of a penicillin in this instance[9,10]. The β-lactam ring, highlighted in green, is compared to the amide backbone of the D-alanyl-D-alanine motif, which is in red.

The use of penicillin and successive generations of β-lactam antibiotics has steadily increased to date and they are used in a broad range of treatments. However, we must acknowledge that what seemed to be the panacea in modern medicine also possesses weaknesses. Ultimately, all organisms are subject to the laws of nature; whilst the human race thought they had discovered "magic bullets" to tackle all bacterial infections[12], bacterial colonies evolved to increase their chances of survival in the face of successive generations of antibiotics. The over-consumption and misuse of antibiotics, both in clinical treatment and in livestock farming[13], has apparently sped the evolution of antibiotic resistant species of bacteria. Newly emerging resistant species act as a threat to our limited existing arsenal of antibiotics, and it would seem to be only a matter of time before humankind loses further ground in this biological arms race, unless breakthroughs in medicinal research offer new solutions. In 2014, the World Health Organization (WHO) recognised antimicrobial resistance (AMR) as a major health threat[14].

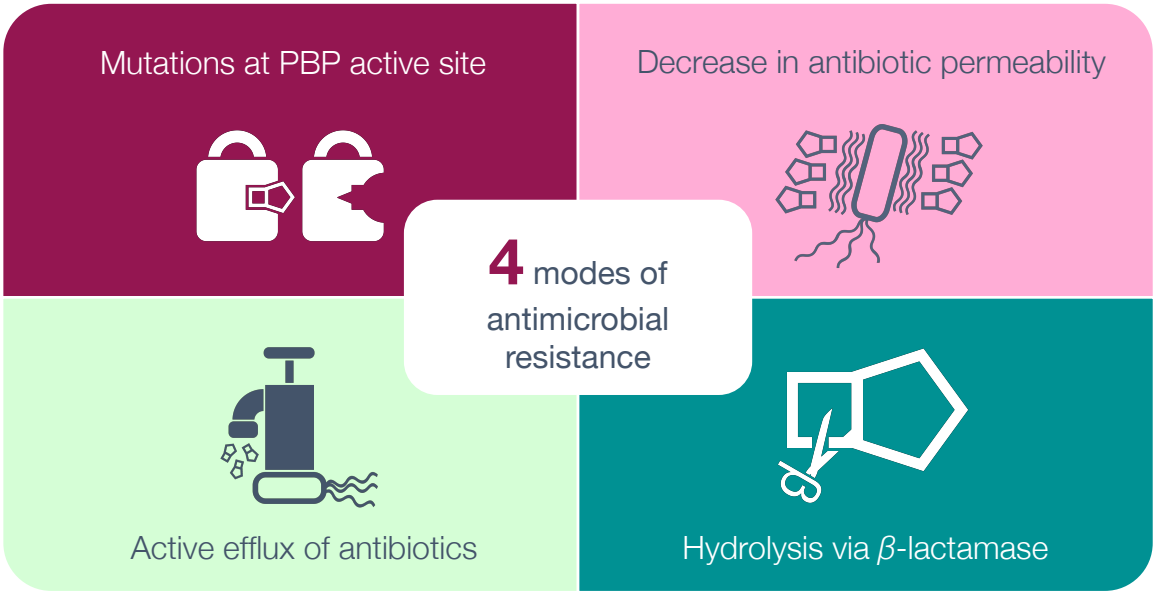


Figure 1.3. Outline of the four major modes of antimicrobial resistance towards β-lactam antibiotics. These comprise PBP active site mutation, decreased drug permeability across bacterial cell membrane, active efflux of the drugs and finally and most importantly, hydrolysis via β-lactamase[15].

There are four main mechanisms to which bacteria have developed resistance towards β-lactam antibiotics (Figure 1.3)[15]. Firstly, the active site of PBPs can mutate to evade the recognition of particular β-lactam antibiotics[16,17]. To expand the scope of activity against various PBPs, medicinal chemists have developed different classes of β-lactam antibiotics, including penicillins, cephalosporins[18], carbapenems[19] and monobactams[20] (Figure 1.4). For each of the classes, in particular cephalosporins, multiple generations featuring different side-chain modifications have been introduced to improve selectivity towards different PBPs[21]. Secondly, the uptake mechanism of β-lactam antibiotics can be altered to reduce membrane permeability

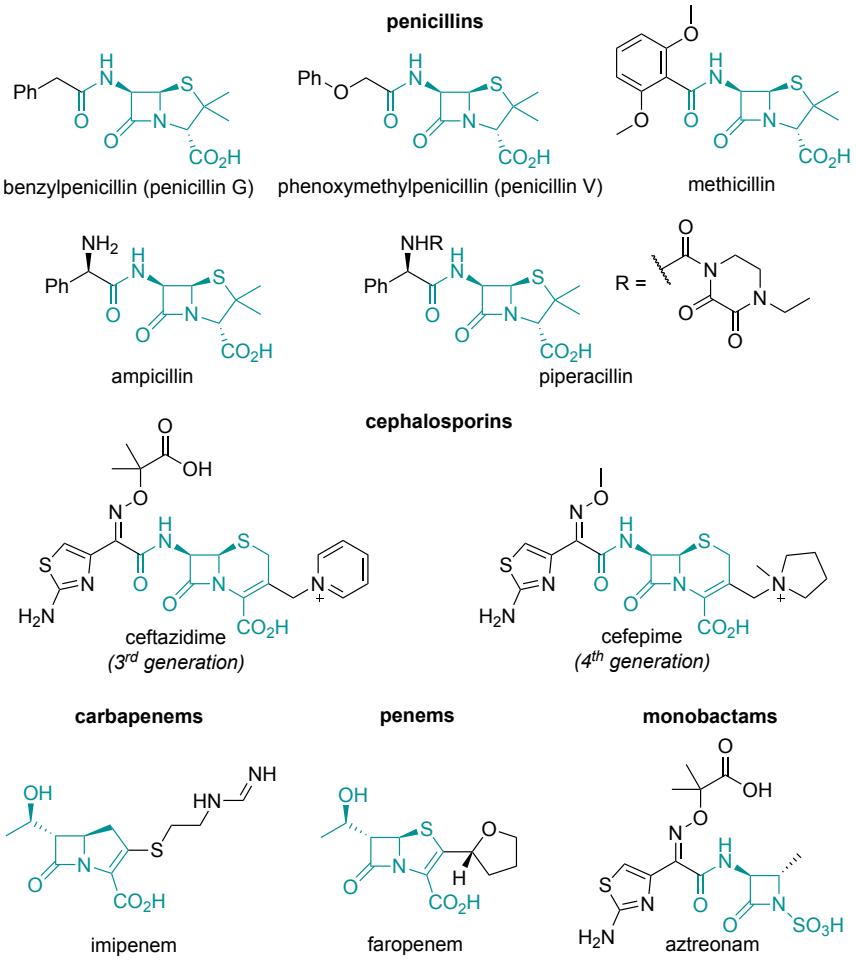


Figure 1.4. Structural examples of clinically relevant β-lactam containing antibiotics. The recurring β-lactam motif is coloured in green. The penicillin and cephalosporin[18] classes are most widely used[1], with a large number of derivatives in each class. The other classes are less commonly prescribed in the clinic, with carbapenems often reserved as a last-resort option in treating bacterial infections[19].

towards β-lactam antibiotics, thus lowering their intracellular concentration and, by extension, the extent of PBP acylation[22]. Bactera also can develop active efflux mechanisms to exclude β-lactam antibiotics from the cytoplasm or the periplasmic space[23,24].

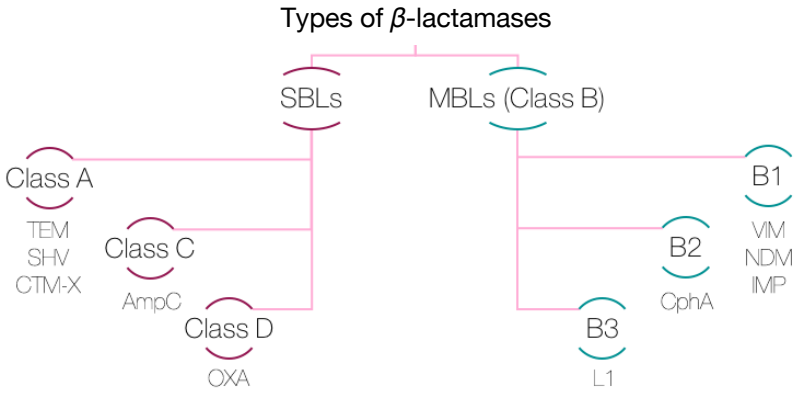


Figure 1.5. β-Lactamases can be divided into serine-β-lactamases (SBLs) and metallo-β-lactamases (MBLs). The Ambler classification of β-lactamases is based on amino acid sequence homology[28]. Classes A, C and D enzymes are SBLs and Class B are MBLs. Clinically relevant examples of each class are given.

Lastly, and perhaps most importantly, bacteria can produce resistance mediating enzymes known as β-lactamases. As their name suggests, β-lactamases catalyse the hydrolysis of the β-lactam ring, which renders β-lactam antibiotics ineffective towards inhibiting PBPs. The first penicillin-destroying enzyme was discovered in *Escherichia coli*[25]. However, even prior to the clinical introduction of penicillin, penicillinase, as it was called by Sir Edward Penley Abraham and Sir Ernst Borie Chain, was thought to harbour little threat to the great clinical potential held by penicillin, which was then used to target Gram-positive strains such as *Staphylococcus* and *Streptococcus*[25]. Unfortunately, in this particular instance, the two scientists who pioneered the large-scale production and clinical usage of penicillin and cephalosporin underestimated the peril of β-lactamases, likely in a large part caused by the selective pressure we have placed upon bacteria through wider use (and maybe overconsumption) of β-

lactam antibiotics[26]. Nearly 80 years after the discovery of the first β-lactamase, more than 850 β-lactamases have been identified, many of which have already caused significant problems to current β-lactam chemotherapies[27]. The production of β-lactamases in bacteria can be either plasmid-mediated[28] or chromosomal-mediated[29]. While the β-lactamases discovered in the early days manifested high selectivity, likely in response to only a narrow spectrum of β-lactam antibiotics, the growing emergence of plasmid-encoded extended-spectrum β-lactamases (ESBLs) are now threatening the entire line of clinically useful β-lactam antibiotics[30,31].

Using the Ambler classification, β-lactamases are divided into four classes based on amino acid sequence similarities (Figure 1.5)[32]. Classes A, C, and D comprise serine-β-lactamases (SBLs), which contain an active site serine residue that is transiently acylated by β-lactam antibiotics, in a fashion that is analogous to PBP inhibition (Figure 1.6A)[33,34]. Class A SBLs, such as TEM (Temoneira), SHV (sulfhydryl variable) and CTM-X (cefotaximase), share a common Ser-70 residue at their active site, which act as the nucleophile in the acylation of β-lactam antibiotics[35,36,37]. Most Class A enzymes are effective penicillinases, although some also recognise cephalosporins[38], and even carbapenems in some cases (such as KPC [*K. pneumoniae* carbapenemase])[39]. Class C SBLs, such as AmpC (ampicillin class C) and CMY (cephamycinase), also possess an essential nucleophilic serine (Ser-64) that is involved in nucleophilic attack. In terms of their scope of activity, the Class C enzymes display high selectivity towards cephalosporins[40]. A distinctive feacture of the Class D β-lactamases, or OXA (oxacillinases), is the presence of a Lys-70 residue which, in the presence of carbon dioxide, is carbamylated without any external enzymatic assistance to yield a carbamic acid[41]. The carbamylation state of this lysine residue

is very important, as the carbamic acid likely plays the role of a general acid and base during catalysis, including by the nucleophilic Ser-67 residue and activating the hydrolytic water molecule involved in deacylation[42]. By contrast, the other SBLs typically use a combination of a lysine and a glutamate to enable general acid/base catalysis[33,34].

The OXA enzymes were one of the earlier *β*-lactamases to be discovered and were once thought to pose little threat to public health, in part because most production of OXA enzymes is plasmid-mediated[41]. However, the discovery of chromosomally-encoded OXA enzymes in *Acinetobacter baumannii*, some of which can hydrolyse carbapenems, has escalated their clinical importance[43]. Carbapenems are usually unaffected by most SBLs except ESBLs[19]. Unlike penicillins and cephalosporins, which are made semi-synthetically from precursors harvested from robust fermentation processes, carbapenem synthesis requires challenging chemical methodologies, as no biosynthetic routes to efficiently produce carbapenems have been developed[44,45,46]. The use of carbapenems is often restricted in the clinic and they are used as last resort therapies for treating highly resistant bacterial infections[16]. Although the carbapenemase activities of most OXA enzymes are comparatively low, their hydrolytic ability can be exacerbated synergistically by the presence of other resistance mechanisms[47], which can breach one of our last lines of defence against resistant species. Commonly observed OXA *β*-lactamases include OXA-10, -23 and -48[41].

The Class B *β*-lactamases are both structurally and mechanistically different from the other three Ambler classes (Figure 1.6B)[48]. Otherwise known as the metallo-*β*-lactamases (MBLs), the active sites of the Class B enzymes contain either one or two

zinc ions that coordinate to a hydroxide ion that acts as the nucleophile to achieve hydrolysis[48]. An aspartate (Asp-120) is proposed to be involved in providing further stabilisation of the intermediate nucleophilic hydroxide/water[49]. The source of the proton, which protonates the lactam-derived nitrogen, is currently under investigation and may come from either Asp-120 or a water molecule[48]. Although SBLs and MBLs bear little overall structural resemblance, they share some general mechanistic similarities. For example, regardless of whether the initial acting nucleophile is a serine residue or a zinc-stabilised hydroxide, it attacks the *β*-lactam ring to form a tetrahedral intermediate[50]. In both cases, the resultant acyl-enzyme complex is rapidly hydrolysed by a water molecule/hydroxide present in the active site, which causes irreversible opening of the *β*-lactam ring to give an inactive *β*-amino acid[48].

From an evolutionary standpoint, MBLs have emerged from a lineage that is distinct from the other *β*-lactamase classes[51]. Given their unique structural features, their scope of activity is extremely broad. Not only are they capable of hydrolysing commonly used penicillins and cephalosporins, but they also exhibit the ability to hydrolyse carbapenems[52]. Commonly observed MBL classes that are of clinical relevance include the Verona integron-encoded metallo-*β*-lactamase (VIM), the Imipenemases (IMP) and the New Delhli metallo-*β*-lactamase (NDM), all of which belong to the B1 class of MBLs[53]. Other well-studied MBLs include CphA (carbapenem hydrolysing *Aeromonas hydrophilia*), a B2 MBL[54] and the mono-zinc L1 (*β*-lactamase 1 from *Strenotrophomonas maltophilia*), a B3 MBL[55] (Figure 1.5). Whilst initial identifications of these MBLs were isolated within specific geographical boundaries, concurrently with the rise of international travel, over a period of three decades, they have now become widespread globally.

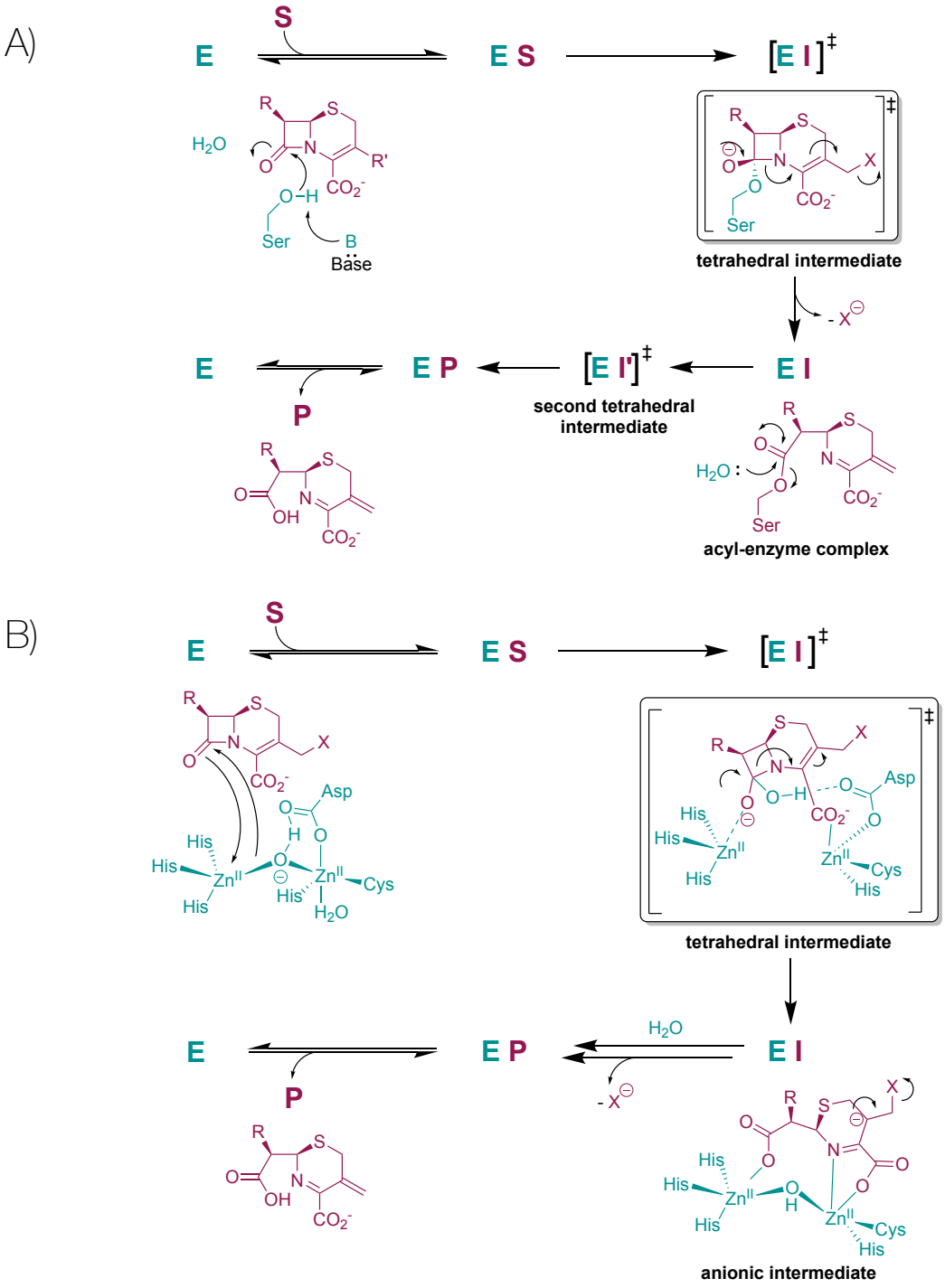


Figure 1.6. Outline of the mechanisms of action for SBLs (A) and MBLs (B), exemplified by the hydrolysis of a cephalosporin. Whilst the source of the initial nucleophilic attack differs (serine residue vs. zinc-bridged hydroxide), there are common features, such as the formation of a tetrahedral intermediate and the eventual hydrolysis of the acyl-enzyme complex by a water molecule[48,49,50].

Scientists have developed some effective strategies to inhibit β-lactamases. The β-lactamase inhibitors that are currently used in the clinic are shown in Figure 1.7. The pioneering example of a clinically valuable β-lactamase inhibitor is clavulanic acid, which was discovered by the Beecham Group in 1974[56]. Clavulanic acid is naturally produced by fermentation of a Gram-positive bacterium, *Streptomyces clavuligerus*[56]. Unlike the classical β-lactam antibiotics, clavulanic acid did not exhibit substantial PBP inhibition[56]. However, it displays a remarkable ability to inhibit Class A SBLs, via the mode of action outlined in Figure 1.8[57]. This property ultimately led to the creation of the first combination therapy (Augmentin®), involving a β-lactam antibiotic (amoxicillin) and a β-lactamase inhibitor, clavulanic acid, to treat bacterial infection. By counteracting the action of SBLs on amoxicillin, the PBPs will be inhibited and consequently, bacterial cell wall biosynthesis will be disrupted[58].

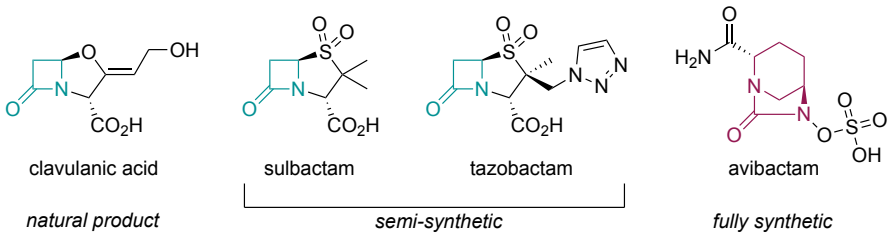


Figure 1.7. β-Lactamase inhibitors used in the clinic. Clavulanic acid, sulbactam and tazobactam are structurally related to the β-lactam antibiotics. They are effective against Class A and some Class C SBLs but lack bactericidal properties as they do not inhibit PBPs[56, 57,58,59,60]. Avibactam has been recently introduced to clinical use and its activity is expanded to cover Class C and some Class D SBLs[63,64]. However, none of these compounds are effective against MBLs[61,62]. The β-lactam ring, highlighted in green, is present in the first three compounds. This is contrasted with the cyclic urea motif in avibactam, which is emphasised in red. Both structural features result in the same mechanism of action against β-lactamase.

Following the clinical success of clavulanic acid, researchers subsequently developed two other β-lactam containing β-lactamase inhibitors, sulbactam and tazobactam, via chemical modification of natural products[59, 60]. Sulbactam is commonly co-administered with ampicillin (Unasyn®)[61], whereas tazobactam is used

in conjunction with piperacillin (Tazocin®)[62]. These combination therapies (and various other combinations) have found significant clinical use against infections caused by a wide range of Gram-negative bacteria, such as *Pseudomonas aeruginosa*[62]. However, while these β-lactam containing β-lactamase inhibitors can effectively inhibit most Class A β-lactamases, they are less effective against Class C β-lactamases. As for Class D and Class B (MBLs) β-lactamases, they are futile[63,64].

The recent clinical introduction of avibactam, which was developed by Actavis Generics and AstraZeneca[65], promises a significant improvement in our ability to manage resistance caused by β-lactamases[66]. In addition to echoing the success of its β-lactam containing predecessors in inhibiting Class A β-lactamases, avibactam manifests the ability to inhibit Class C β-lactamases (such as AmpC) and some Class D β-lactamases (OXA)[67,68,69]. This has led to the launch of a new combination therapy, Avycaz®, consisting of avibactam and ceftazidime, which is useful against bacterial infections showing clinical resistance towards cephalosporins[70].

In terms of its chemical structure, unlike earlier β-lactamase inhibitors avibactam bears no immediate resemblance to any of the β-lactam containing antibiotics. However, its mode of action is related to that of the β-lactam containing β-lactamase inhibitors. The fused diazabicyclooctane (DBO) ring system in avibactam involves a cyclic urea motif. In addition to its broader breadth of activity, avibactam also offers a breakthrough in the design and development of β-lactamase inhibitors, in that the structural scope is no longer restricted to compounds carrying a β-lactam ring.

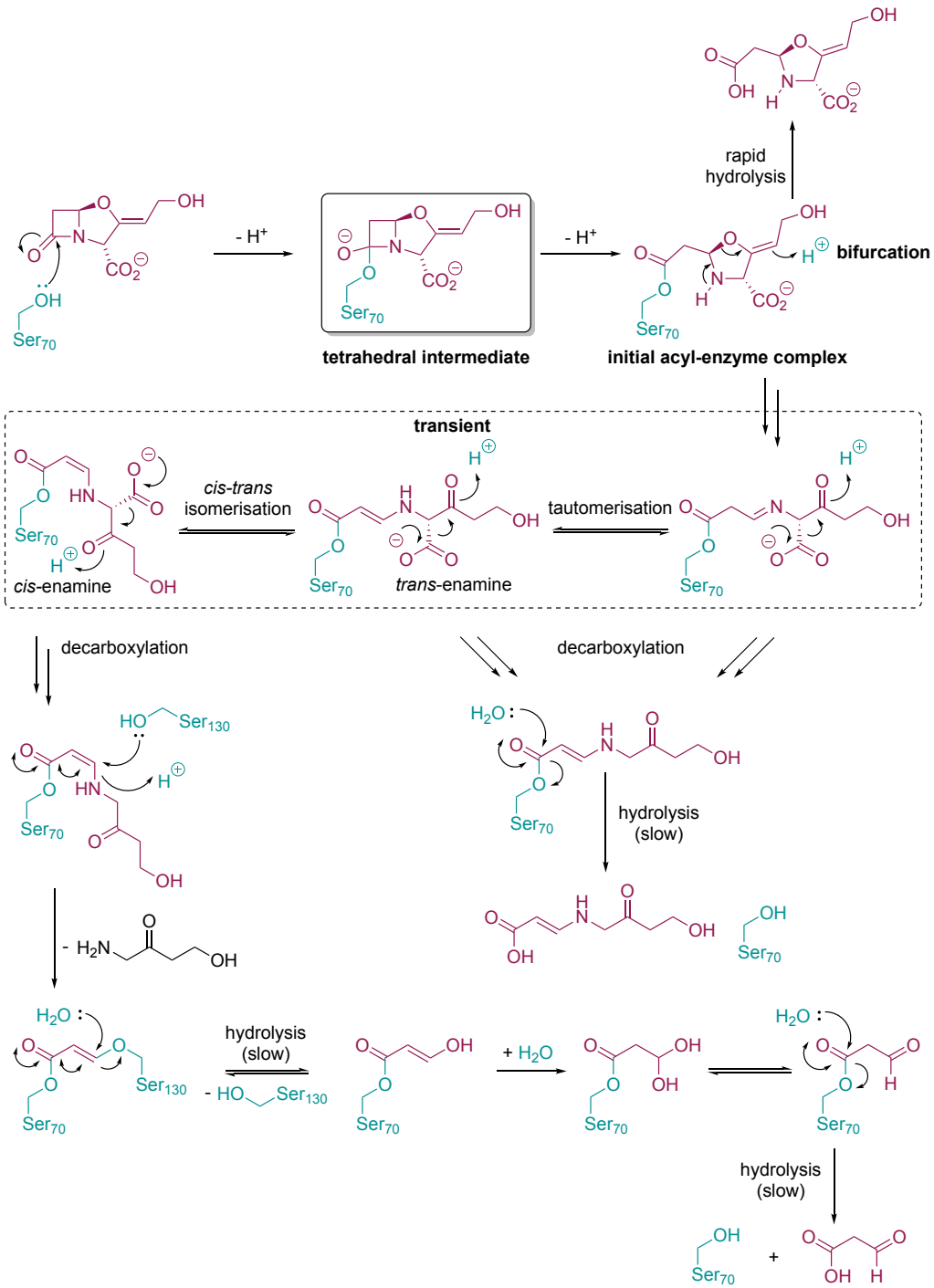


Figure 1.8. Outline of the mode of action of clavulanic acid, the first clinically useful dedicated *β*-lactamase inhibitor[57].

The mechanism of action of avibactam bears some similarity to other β-lactam containing β-lactamase inhibitors (Figure 1.9)[71,72]. However, unlike clavulanic acid, the inhibition of β-lactamase by avibactam is apparently linear from a kinetic perspective[73]. From a medicinal chemistry perspective, the structure of avibactam possesses a primary amide moiety, which offers a convenient starting point for the introduction of more complex side chains to improve potency and selectivity. Besides attempting to optimise activity via modification of the primary amide moiety, carboxylate analogues of avibactam have also been explored[74], since the sulfate group acts by mimicking the carboxylate group that is present in β-lactam containing β-lactamase inhibitors. Overall, avibactam became the first of a new class of SBL inhibitors – the diazabicyclooctanes, (DBOs) (Figure 1.10), with some examples acting as dual inhibitors of SBLs and PBPs[75].

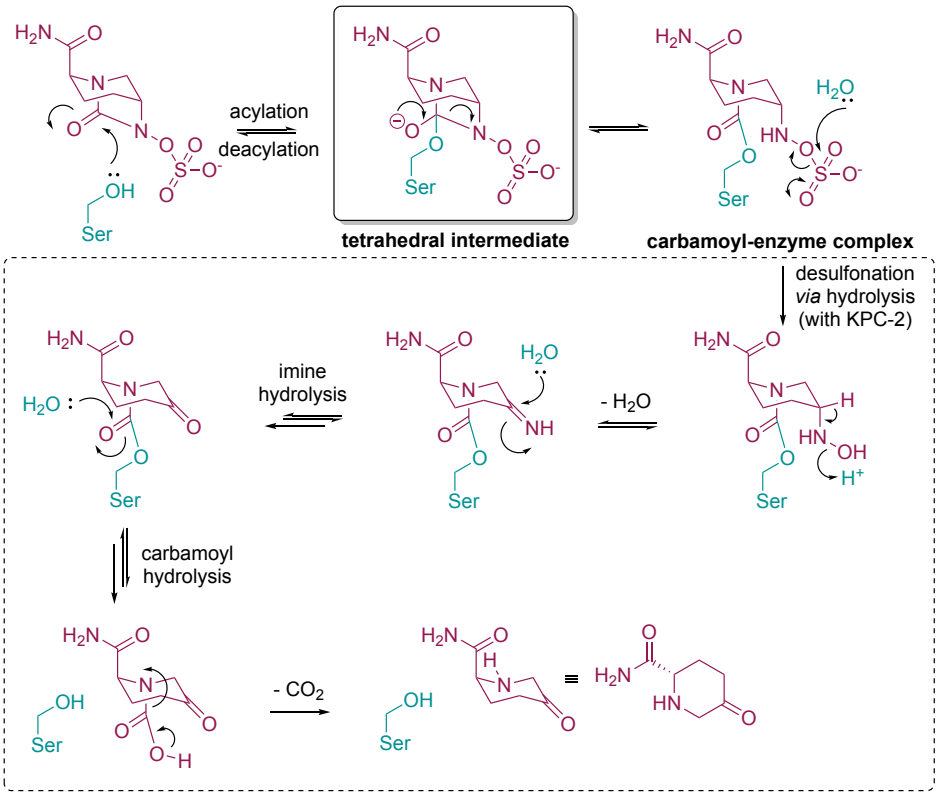


Figure 1.9. Mechanism of action of avibactam inhibiting a β-lactamase. Despite lacking a β-lactam ring, the cyclic urea moiety permits acylation[71,72]. In the presence of a β-lactamase that is not susceptible, avibactam can be hydrolysed, or may undergo decarbamoylation to release a six-membered ring[69].

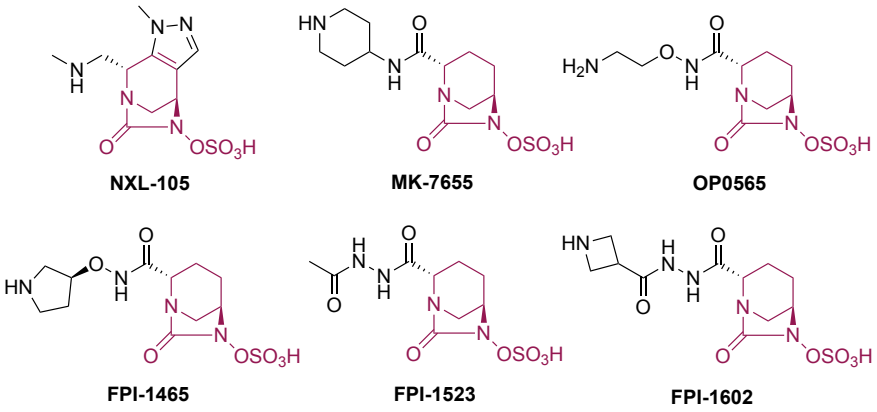


Figure 1.10. Examples of avibactam and related synthetic DBO analogues[66], showing the common bicyclic urea system with a sulfate group (red).

While there have been advances in tackling resistance cause by clinically relevant SBLs, there has not yet been a breakthrough for inhibiting MBLs. MBLs are relatively recent in medical history, with some of the first identifications (of BcII [*Bacillus cereus* metallo-*β*-lactamase]) being made in the 1980s[76]. Although they have not yet caused any major global healthcare crisis, the potential impact of these *β*-lactamases is alarming. This is due to the fact that many MBLs can effectively hydrolyse, in addition to other commonly prescribed *β*-lactam antibiotics (except monobactams), carbapenems[35]. MBLs can thus threaten the efficacy of most of our existing *β*-lactam antibiotic portfolio down to the very last line of defence. Given that the mechanism of action of MBLs is different from that of SBLs (which bear greater similarity towards the PBPs) the development of clinically suitable MBL inhibitors is a challenge for chemists and biologists. To date, no clinically relevant MBL inhibitor has been reported, but the emergence of MBLs in the clinic is rising[77], highlighting the need to develop a clinically useful solution to avoid a “superbug” scenario.

1.2. The search for a clinically useful metallo-β-lactamase inhibitor

In searching for a potential small-molecule inhibitor of MBLs, different approaches have been explored. By examining the mechanism of action of the hydrolysis of a *β*-lactam antibiotic by an MBL, two general approaches to inhibition can be identified (Figure 1.11).

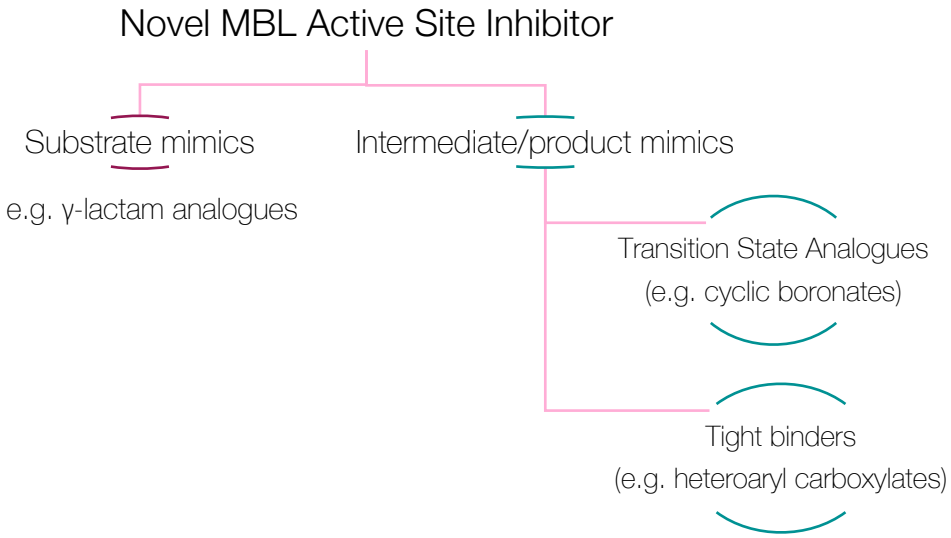


Figure 1.11. Summary of strategies to design inhibitors of MBLs based on their mechanism. It may be possible to achieve inhibition at the active site via substrate mimicry or intermediate/product mimicry.

First, one may explore the scope of compounds that mimic the natural substrates of MBLs, i.e. *β*-lactam antibiotics, which are more stable to hydrolysis. One possibility is to examine compounds with a different lactam ring size. Sir Jack Baldwin and others hypothesised that the *β*-lactam ring was not essential to antibiotic function[78]. Subsequent research involving other serine proteases revealed that *γ*-lactam analogues of *β*-lactam inhibitors can react reversibly with nucleophilic serine enzymes, possibly reflecting the kinetically more favourable formation of five-, compared to four-, membered ring (Figure 1.12)[79,80]. Therefore, an MBL substrate bearing a *γ*-lactam may be more resistant towards hydrolysis as it could recyclise to regenerate the intact molecule (the five-membered ring is also thermodynamically

more stable). In a case when the said MBL substrate is also an inhibitor of PBPs, this could yield exciting results. The concept of recyclisation (at least for the enzyme-inhibitor complex) has been validated by the mode of action of avibactam[81] and may contribute to the clinical success of this compound.

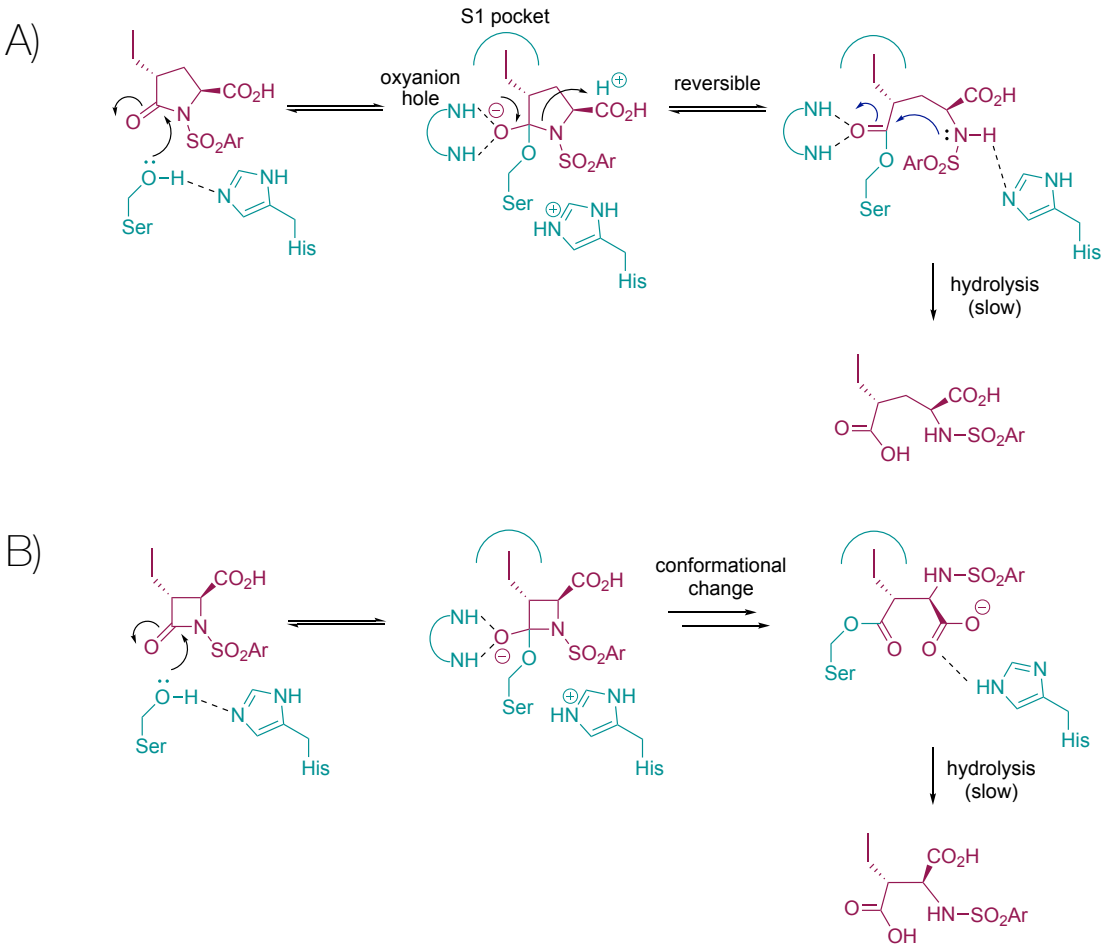


Figure 1.12. The reversible reaction of a *γ*-lactam (**A**), compared with the irreversible reaction of a *β*-lactam analogue (**B**), with a serine protease[79,80]. Formation of a five-membered ring is normally kinetically favoured compared to a analogous four-membered ring. This is consistent with the observations of recyclisation with avibactam made by the Schofield group and others[81].

In the late 80s, researchers from Takeda Laboratories in Japan isolated an antibacterial compound from fermentation broths of *Empedobacter lactamgenus* and *Lysobacter albus*. The compound was named as lactivicin (**LTV**)[82,83]. Lactivicin has two five-membered rings, one of which is a cycloserine derivative, and the other a *γ*-

lactone (Figure 1.13A). **LTV** and another lactivicin derivative, **PLTV**, have shown moderate antimicrobial activities against a wide range of Gram-negative bacteria, such as *E coli*, and exhibit potent activity against Gram-positive bacteria, such as *Bacillus subtilis*[84,85,86]. Researchers from China also synthesised lactivicin derivatives, some of which have shown moderate antibacterial properties[87].

The mechanism of action of PBP inhibition by lactivicin is related to that of the bicyclic *β*-lactam antibiotics such as cephalosporins (Figure 1.13B)[88]. Although lactivicin is susceptible to *β*-lactamase inactivation, the presence of a five-membered lactam-like ring renders its hydrolysis significantly slower in some cases as compared to *β*-lactams[89], even in the case of MBLs, as ongoing research in the Schofield Group has indicated. A recent example of lactivicin derivatisation involves the addition of a siderophore by Pfizer (Figure 1.13A); this derivative manifests improved uptake and good activity in microbiological studies[90,91]. These studies indicate that investigations into the chemistry of new derivatives of lactivicin could result in better performing antibacterial candidates.

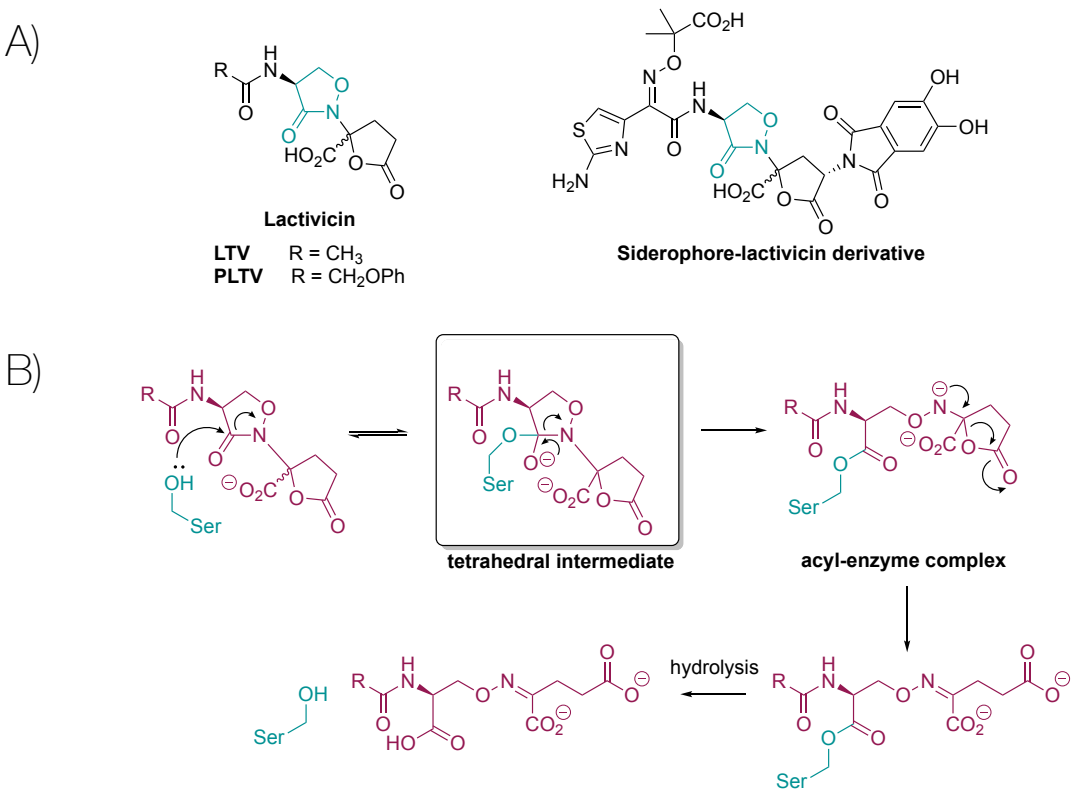


Figure 1.13. Structural features of lactivicin and its analogues (A) and its mechanism of action (B)[88]. The lactivicins inhibit some PBPs and is a substrate for some SBLs[89].

Scientists have also explored *γ*-lactam analogues of penems and carbapenems, especially [5-5] fused bicyclic systems. Some of these compounds were synthesised and investigated by the Baldwin Group[92, 93, 94, 95] and Takeda[96]. Many of these analogues did not display antibacterial activity, but some penem analogues showed promising inhibitory activity. Researchers at Lilly made fused bicyclic systems involving pyrazolidinones with a nitrogen atom replacing C-5[97,98]. With an appropriate electron-withdrawing group in the 3-position of the ring system, these compounds manifested antibacterial activity[99] (Figure 1.14A). However, due to a lack of financial interest in antibiotics, many pharmaceutical companies subsequently abandoned research in the field of new antibacterial chemotherapies. Consequently, the susceptibility of many of these *β*-lactam antibiotic mimics towards 'modern' *β*-lactamases has never been thoroughly investigated.

However, with the success of avibactam and a renewed interest in lactivicins, interest in experimenting with non *β*-lactam PBP/*β*-lactamase inhibitors is increasing. New strategies, such as introducing siderophores to increase drug uptake[100], may also shed light on avenues to optimise existing chemotherapies.

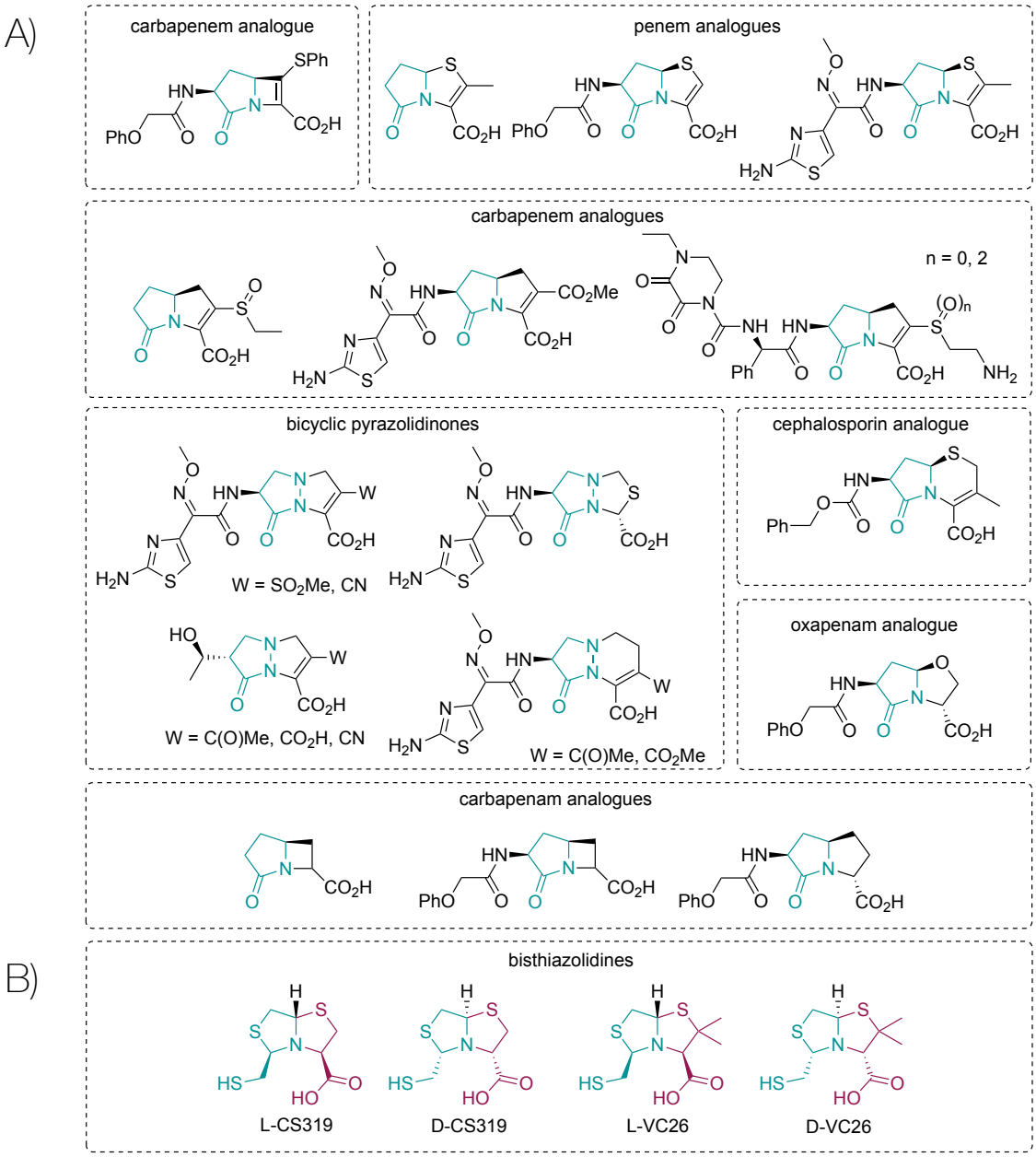


Figure 1.14. Examples of fused bicyclic ring systems containing *γ*-lactam rings and similar five-membered rings (in green), such as pyrazolidinones (**A**)[92-98], and bisthiazolidines (**B**)[101,102]. These compounds were designed to mimic existing classes of *β*-lactam antibiotics. The susceptibility of compounds in **A** towards *β*-lactamases remains unknown. The bisthiazolidines in **B** may mimic penams (similarities shown in red) and show inhibition of some MBLs, e.g. NDM-1[101,102].

One class of compounds with potential as MBL inhibitors is the bisthiazolidines, which are mimics of the penams (Figure 1.14B)[101,102]. While structurally resembling a classic penicillin in its thiazolidine ring, these compounds also contain another five-membered ring core, which may imitate the *β*-lactam ring. The bicyclic system in the bisthiazolidines resonates with the 5-5 bicyclic systems of earlier works by the Baldwin Group, Takeda and Lilly 30 years ago.

Another approach to achieve MBL inhibition involves examining the intermediates and products formed during MBL-mediated hydrolysis of *β*-lactam antibiotics. The reaction of *β*-lactams with MBLs involves formation of a tetrahedral intermediate prior to collapse to form a thiazolidine or thiazine carboxylate intermediate (Figure 1.6B)[48,49,50], which may be mimicked by a five- or six-membered heteroaryl (or aryl) carboxylate.

One can envisage compounds which, upon binding to an MBL, form a complex that mimics a high energy intermediate (transition state analogue approach). Examples of this approach that are being explored include boronic acid transition state analogue inhibitors (BATSIs)[27]. In these BATSIs, the unique Lewis acidic nature of boron is exploited as it can accept an additional lone pair of electrons, including from the nucleophilic water molecule or hydroxide ion (or serine in the case of SBLs). Two such examples are vaborbactam, which was developed by Rempex Pharmaceuticals and which is now approved for use in the US for use in combination with meropenem (marketed as Vabomere)[103,104], and CR161, which was developed jointly by Therabor Pharmaceuticals and University of California[105,106,107] (Figure 1.15). Within the scope of MBLs, an ongoing collaboration amongst the Schofield group, the University of Bristol, Queen Mary University of London and the University of Leeds has shown

promising results for some bicyclic boronates (Figure 1.15), which are active against all classes of β-lactamases, including MBLs[108,109].

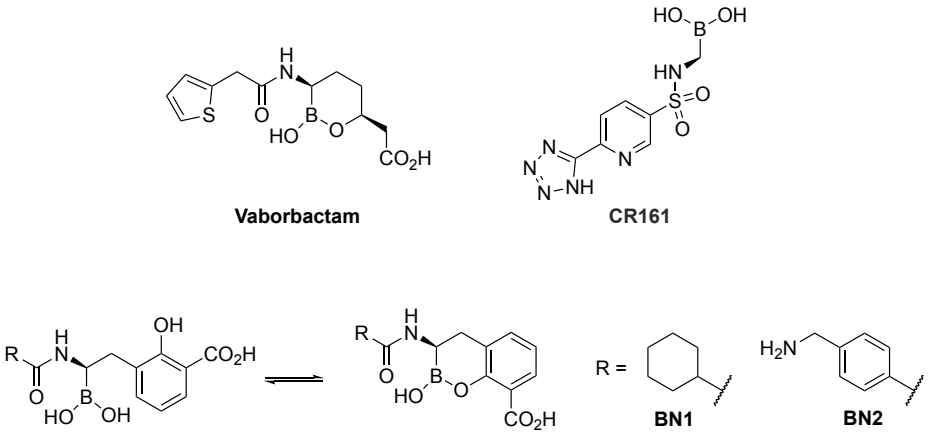


Figure 1.15. Examples of boronate compounds that have been explored in academic and pharmaceutical research, targeting β-lactamase inhibition. Notable examples include and vaborbactam[103,104] and CR161[105,106,107], which are designed to target serine β-lactamase. Cyclic boronates such as BN1 and BN2 have also been found to inhibit all classes of β-lactamase[108,109].

One can also design compounds that optimise other non-covalent interactions with the MBL active site. By examining the hydrolysed product structure, one can draw structural similarities between the resultant nitrogen-containing heterocycle and five- or six-membered heteroaryl carboxylates (Figure 1.16). Picolinates and pyridine dicarboxylates have attracted the attention in the field of MBL inhibitors[110,111]. Other heteroaryl carboxylates that have surfaced include thiazole 4-carboxylate compounds synthesised by Antabio[112,113], as well as a pyrimidine 4-carboxylate lead compound that was identified in a collaboration between the Schofield Group and the European Lead Factory.

Heterocyclic chemistry is a very well-developed area in synthetic chemistry, partially owing to the emphasis placed upon heterocyclic compounds by the pharmaceutical industry. Bemis and Murcko clustering, in which the main molecular scaffold is derived from removing side chain atoms, reveals that the top-scoring frameworks in

drug molecules include five-membered and six-membered ring systems, as well as bicyclic 5-6 systems[114]. Recent advances in C-H functionalisation and photoredox catalysis are expanding the value of heterocycles in medicinal chemistry, in addition to the many established methodologies to functionalise these ring systems, such as various metal-catalysed coupling reactions. Thus, simple heteroaryl leads for MBL inhibition are of interest.

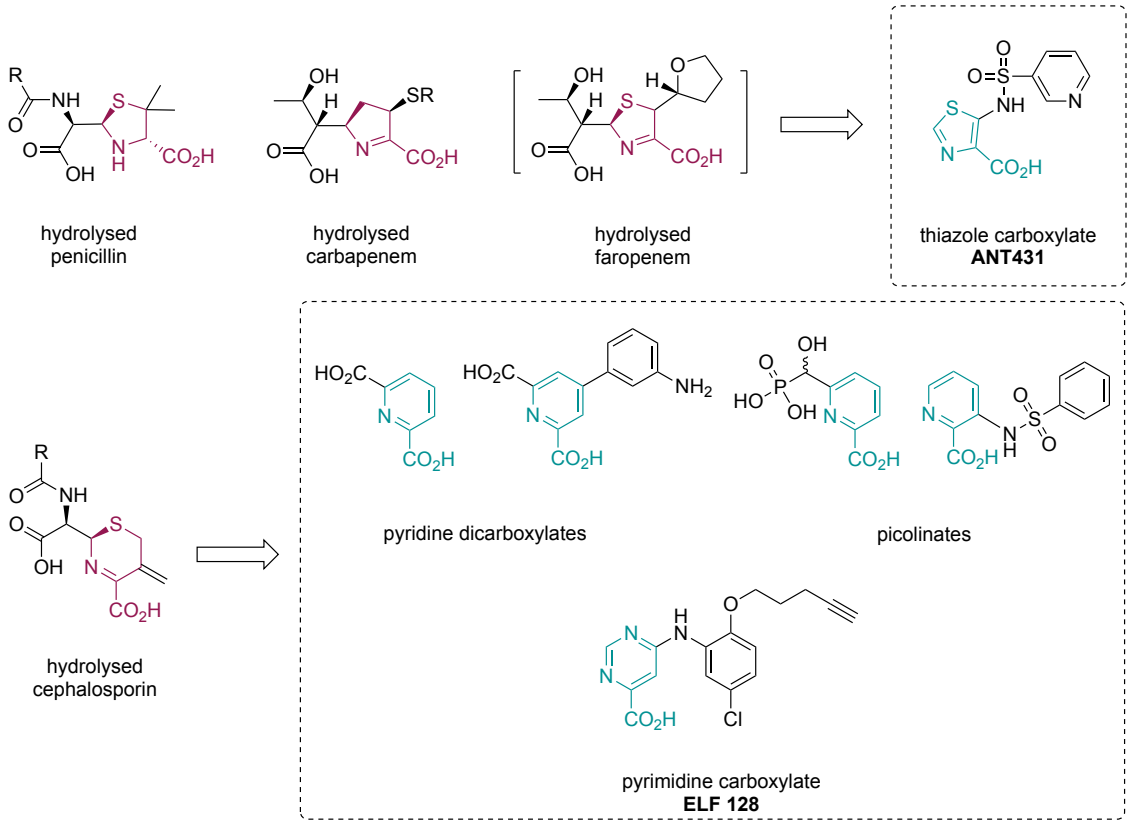


Figure 1.16. Structural similarities between the heterocycle that results from the hydrolysis of a penicillin or a cephalosporin (red) and the aromatic heterocyclic systems in some MBL inhibitors [110-113] (green). ELF 128 was investigated as part of this work.

Given MBLs possess one or two zinc ions, one approach to achieve inhibition is to use a chelator that binds to the zinc ions. This strategy, however, poses a drawback: metalloproteins are vital in human biology[115]. Consequently, the specificity of metal chelation for a prospective zinc chelator is crucial in order to avoid undesired side effects. One example of a nonspecific zinc ion chelating MBL inhibitor is

ethylenediaminetetraacetic acid (EDTA). [116, 117] A more refined example is aspergillomarasmine A (AMA), an MBL inhibitor that displayed *in vivo* activities towards MBLs, but not SBLs[118,119] (Figure 1.17A).

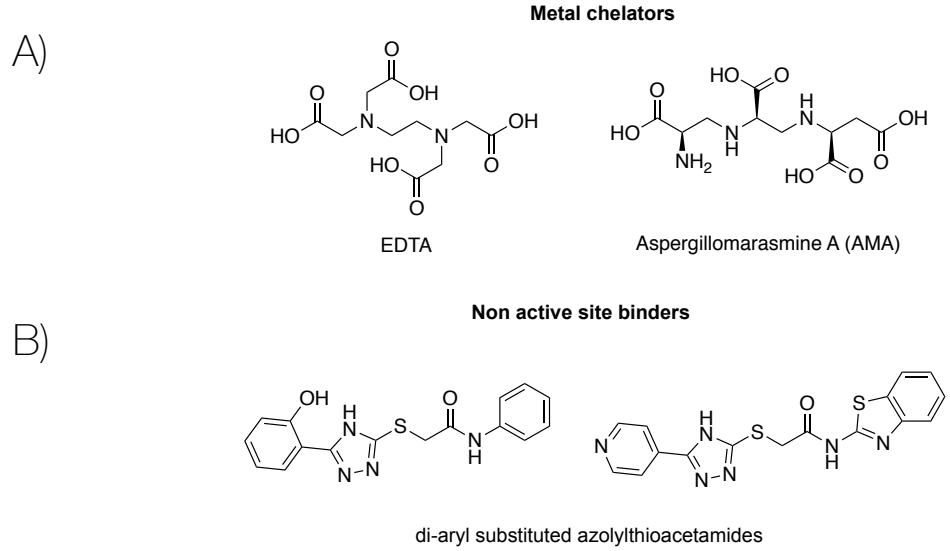


Figure 1.17. Examples of MBL inhibitors chelating to zinc[116-119] (**A**). Certain compounds can also form non-active site interactions with MBLs, which results in conformational change and loss of activity (**B**) [120,121].

Another approach involves non-active site targeting. Given that the emergence of MBLs is relatively recent and that many of them bear significant structural differences outside of the active site, more research needs to be conducted in order to design a successful non-active site inhibitor. Thus, the clinical relevance of such inhibitors for MBLs is speculative, and it could be that resistance will be a problem. A potential candidate series from this category of inhibitors are the di-aryl substituted azolylthioacetamides (Figure 1.17B)[120,121].

Several other interesting compounds have been identified as potential inhibitors of *β*-lactamases. The development of *β*-lactam containing *β*-lactamase inhibitors has led to the synthesis of oxapenems by Amura (e.g. AM-112)[122] and tricyclic carbapenems by GSK and Lek Pharmaceuticals (e.g. LK-157)[123]; the latter shows promising inhibitory activities against serine *β*-lactamases[124,125].

Other inhibitors of nucleophilic serine enzymes/proteases could also be adapted for *β*-lactamase inhibition. For example, trans-lactams, which were developed as an inhibitor for the human cytomegalovirus (HCMV) protease, contain a *γ*-lactam core that acts as an electrophilic centre for acylation[126]. This may relate to *β*-lactamase inhibition via *β*-lactam substrate mimicry. The strigolactones, which are plant hormones derived from plant roots[127], bear a *γ*-lactone moiety, which may potentially act like a *β*-lactam. Similarly, a steroidal natural product isolated from *Lantana camara*, or more commonly known as wild-sage, has been found to display inhibition towards human *α*-thrombin properties[128], but the use of this core against bacteria remain untested. Thiol-containing compounds are well established zinc enzyme inhibitors and have been found to possess promising *β*-lactamase inhibition, especially as MBL inhibitors[129]. Some examples include thiomandelic acid[130], captopril[131] and fragments derived from rhodamine hydrolysis[132]. Examples from each of these potential strategies to achieve MBL inhibition are summarised (Figure 1.18).

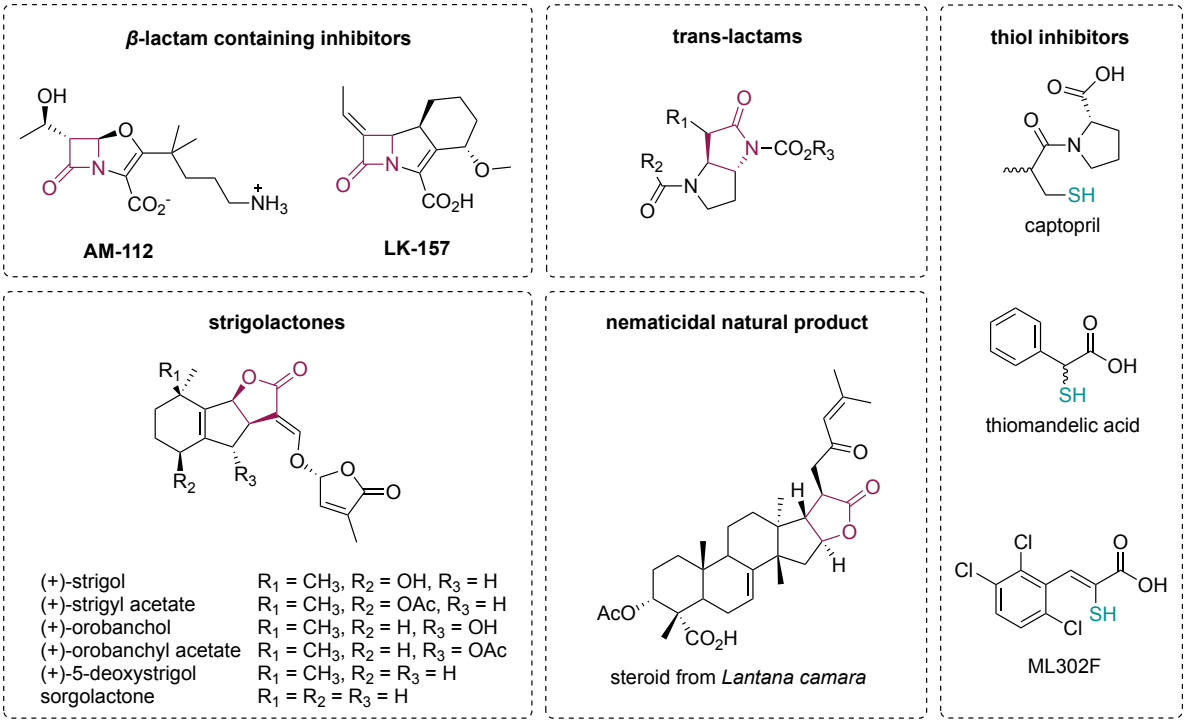


Figure 1.18. Examples of potential inhibitors for SBLs and MBLs[122-132].

1.3. SAR and screening-based drug design of novel β-lactamase inhibitors

As highlighted in the previous section of this chapter, one approach to developing novel MBL inhibitors is to consider either the substrate structure or the intermediate/product structure. In order to design a therapeutic molecule that is either a substrate mimic or an intermediate/product mimic, one can employ either a structure-activity relationships (SAR) approach, involving chemical modifications on a molecule that exhibits known effects on a target enzyme and correlating changes in activity to structural alterations. An example of such an approach to medicinal chemistry is the development of nonselective beta blockers, such as propranolol based on dichloroisoproterenol, which was discovered to be a *β*-antagonist (Figure 1.19)[133]. The synthesis of compounds resembling MBL substrates, such as lactivicin and bicyclic pyrazolidinone derivatives, employing this SAR approach is described in Chapter 3.

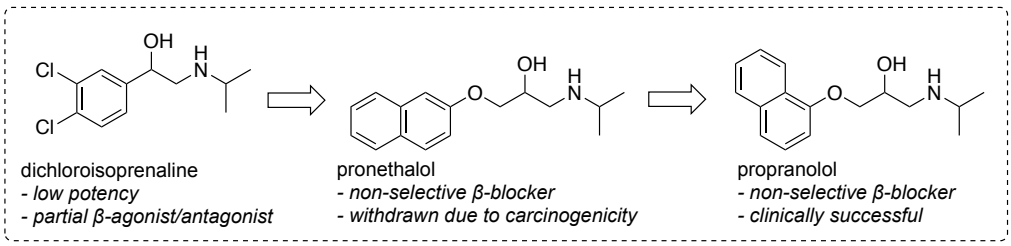


Figure 1.19. An early success in rational drug design, which led to the first clinically relevant non-selective *β*-blocker, propranolol[133].

An alternative is to employ a screening-based approach, starting from a large collection of molecules with the aim of identifying “hits”. Advances in enzymology, biological assays and experimental apparatus have led to the development of various robust high-throughput screening (HTS) platforms, complemented by large libraries of molecules[134]. However, the number of compounds required to be screened in a classical HTS approach is often hundreds of thousands. The compounds identified

as hits tend to bind less efficiently to the enzyme target since the binding energies per unit molecular mass is relatively low. When a compound is identified as a hit from HTS, the subsequent lead optimisation process can prove challenging as the molecular masses of compounds from an HTS library often tend to be relatively large[135]. Therefore, the fragment-based drug discovery (FBDD) approach, sometimes known as the fragment-based lead discovery (FBLD) approach, is being increasingly used[136]. FBDD surfaced 20 years ago and involves screening a library of low molecular weight "fragments" using techniques such as NMR, X-ray and mass spectrometry (MS) in order to identify (weak) binders of a target[137]. These fragments are significantly smaller than compounds utilised in classical HTS, and a common set of rules that apply to designing a compound library is often known as the "rule of three" (Figure 1.20), which is analogous to Lipinski's rule of five to evaluate druglikeness[138]. Other rules can be imposed upon the compounds within a given library, such as ease of chemical synthesis and functionalisation. The identified fragment binders can form the backbones for further synthesis to evolve potent lead compounds. The FBDD approach is arguably more efficient as it requires screening a relatively smaller library of compounds (typically a few thousand fragments) and fewer synthetic steps to arrive at the lead compound[138]. Recent successes of the FBDD approach include the development and eventual clinical approval of vemurafenib (a BRAF inhibitor for the treatment of late-stage melanoma) by Plexxikon, and venetoclax (a Bcl-2 inhibitor for the treatment of chronic lymphocytic leukaemia) by AbbVie and Genentech, respectively (Figure 1.20)[135,139].

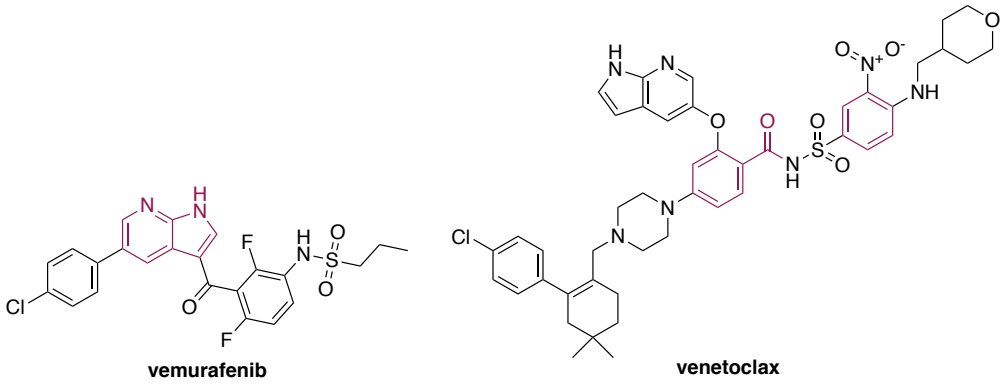


Figure 1.20. Structures of vemurafenib (left; BRAF inhibitor for late stage melanoma) and venetoclax (right; Bcl-2 inhibitor for chronic lymphocytic leukaemia), both of which exemplify the recent success of the fragment-based drug design (FBDD) approach. Components from the original fragment(s) are coloured in red.[135,139]

The success of the FBDD approach is heavily reliant on the screening approach employed, which normally must possess a high sensitivity to accurately detect weak fragment-enzyme binding in the first instance[135]. The most common screening techniques are NMR (nuclear magnetic resonance) and SPR (surface plasmon resonance) [140]. NMR assays often measure the change in chemical shift when fragments bind to isotope-labelled (^{15}N and/or ^{13}C) proteins[135]. Therefore, they generally require a large amount of isotope-labelled proteins and tend to be more useful for proteins with molecular weights below 50 kDa[135]. On the other hand, SPR assays detect changes in refractive index elicited by an increase in mass when fragments bind to proteins immobilised to sensor chips. However, allosteric ligands may be flagged as false positives in SPR[135]. Thus, the utilisation of other screening techniques is of interest in complementing FBDD. They include the use of mass spectrometry (MS), Förster Resonance Energy Transfer (FRET) [141,142], and X-ray crystallography. Traditional X-ray crystallography protocols are time-consuming. However, technological advances, including the use of synchrotrons, has led to the development of high-throughput X-ray crystallography (HTX) screening platforms.

Although an FBDD approach has yet to be reported for lead discovery of a PBP/*β*-lactamase inhibitor, the use of X-ray crystallography in antibiotic discovery is not new. In 1945, Dorothy Hodgkin solved the structure of the newly-discovered penicillin using this method[143], which ultimately led to our understanding of the importance of the *β*-lactam ring. The Schofield Group, in conjunction with Diamond Light Source (Didcot, UK), has successfully developed a platform specifically for the discovery of novel MBL inhibitors. The hits from this experiment have led to several interesting lead compounds. The synthesis and activity profile of these compounds is discussed in Chapter 2. The identification as well as subsequent optimisation of lead compound have relied on correlation between activity assays and binding assays, including a well-established and reliable platform to probe MBL inhibition developed in the Schofield Group uses FC-5 as a fluorogenic substrate, which released umbelliferone upon hydrolysis by *β*-lactamases (Figure 1.21)[144], as applied in the research described in both Chapters 2 and 4 of this thesis.

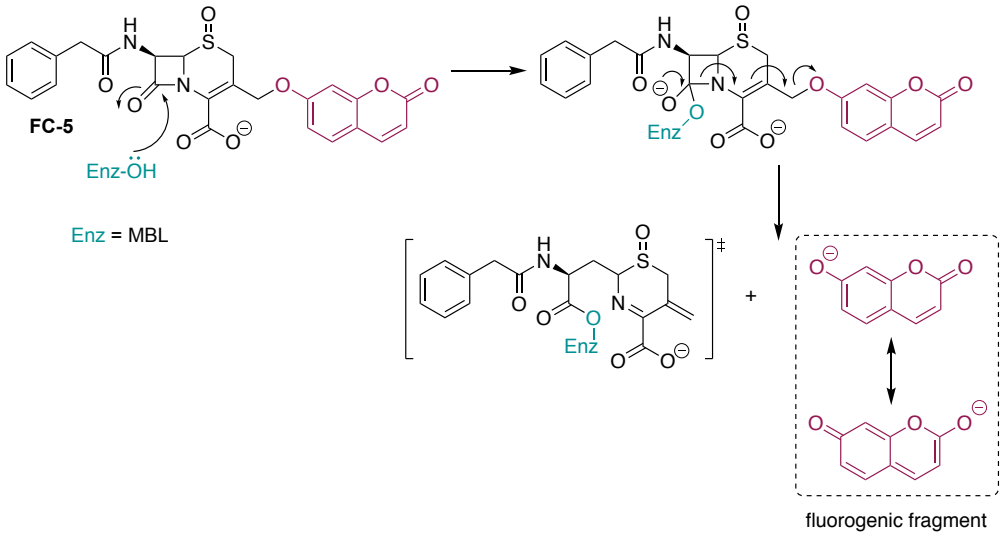


Figure 1.21. FC-5 as a fluorogenic substrate for detecting MBL inhibition[144]. FC-5 contains a cephalosporin core that bears a penicillin G amide side chain and a sulfoxide. FC-5 possesses an umbelliferone as a leaving group which, upon hydrolysis mediated by an MBL, detaches itself and emits fluorescent energy[144].

1.4. Aims and objectives

The experimental work described in this thesis aimed to enable insights towards developing a solution to β-lactamase mediated antimicrobial resistance. In particular, the work involved exploration of various small-molecule structures as potential inhibitors of MBLs, as well as investigations into OXA β-lactamases, which are of increasing clinical relevance.

One aspect of this work involved the development of new types of MBL inhibitors, in part inspired by an FBDD approach, as described in Chapter 2. Extensive chemical synthesis based on initial fragment hits and screening of further optimised heteroaryl-carboxylate compounds were performed by colleagues from the Schofield Group using an FC-5 assay platform. Some of these exhibited potent inhibition against a panel of clinically relevant MBLs, including VIM-2.

Lactivicin is the only naturally occurring small molecule that acts similarly to β-lactams which does not contain a β-lactam ring. However, very little structural-activity relationship studies have been performed on lactivicin, partly due to synthetic challenges in accessing new lactivicin analogues. In Chapter 3 of this thesis, the synthesis of a novel lactivicin analogue with a modified lactone ring was achieved.

The Class D OXA SBLs are arguably the most worrying of all β-lactamases mediated resistance processes[145,146]. Studies on OXA SBLs were performed with a set of inhibitors; the results, which are reported in Chapter 4, inform on the mechanism of OXA inhibition, including the role of protein carbamylation in catalysis and inhibition.

The thesis concludes with a view into the future and a discussion of ideas inspired by this project, suggesting new possibilities for *β*-lactamase inhibition that may contribute to efforts to combat *β*-lactamase mediated resistance.

1.5. References

[1] Boeckel, T. P. V.; Gandra, S.; Ashok, A.; Caudron, Q.; Grenfell, B. T.; Levin, S. A.; Laxminarayan, R. *Lancet Infect. Dis.* **2014**, *14*, 742–750.

[2] Mortality in England and Wales: Average life span, 2010 https://www.ons.gov.uk/peoplepopulationandcommunity/birthsdeathsandmarriages/deaths/articles/mortalityinenglandandwales/2012-12-17 (accessed Jun 6, 2018).

[3] Bohnen, J. M. A. Surgical treatment evidence-based and problem-oriented; Zuckschwerdt: München, 2001.

[4] Ghuysen, J.-M.; Hakenbeck, R. *Bacterial cell wall*; Elsevier: Amsterdam, 1994.

[5] Anderson, J. S.; Meadow, P. M.; Haskin, M. A.; Strominger, J. L. *Arch. Biochem. Biophys.* **1996**, *116*, 487–515.

[6] Buynak, J.D. *ACS Chem. Biol.* **2007**, *2*, 602–605.

[7] Tipper, D. J.; Strominger, J. L. *Proc. Natl. Acad. Sci. U.S.A.* **1965**, *54*, 1133–1141.

[8] Waxman, D. J.; Strominger, J. L. *Annu. Rev. Biochem.* **1983**, *52*, 825–869.

[9] Yocum, R. R.; Rasmussen, J. R.; Strominger, J. L. *J. Biol. Chem.* **1980**, *255*, 3977–3986.

[10] Frère, J. M. *J. Pharm. Belg.* **1988**, *43*, 107–115.

[11] Tomasz, A. *Ann. Rev. Microbiol.* **1979**, *33*, 113–137.

[12] Strebhardt, K.; Ullrich, A. *Nat. Rev. Cancer* **2008**, *8*, 473–480.

[13] Silbergeld, E. K.; Graham, J.; Price, L. B. *Annu. Rev. Public Health* **2008**, *29*, 151–169.

[14] World Health Organization. *Antimicrobial Resistance: Global Report on Surveillance*; rep.

[15] Frère, J. M.; Joris, B.; Granier, B.; Matagne, A.; Jacob, F.; Bourguignon-Bellefroid, C. *Res. Microbiol.* **1991**, *142*, 705–710.

[16] Neu, H. C. *Curr. Clin. Top. Infect. Dis.* **1987**, *8*, 37–61.

[17] Georgopapadakou, N. H. *Antimicrob. Agents Chemother.* **1993**, *37*, 2045–2053.

[18] Hamilton-Miller, J. *Int. J. Antimicrob. Agents* **2008**, *31*, 189–192.

[19] Papp-Wallace, K. M.; Endimiani, A.; Taracila, M. A.; Bonomo, R. A. *Antimicrob. Agents Chemother.* **2011**, *55*, 4943–4960.

[20] Sykes, R. B.; Bonner, D. P. *Clin. Infect. Dis.* **1985**, *7*, S579–93.

[21] Page, M. G. *Expert Opin. Investig. Drugs* **2004**, *13*, 973–985.

[22] Maass, E. A.; Johnson, M. J. *J. Bacteriol.* **1949**, 57, 415–422.

[23] Okusu, H.; Ma, D.; Nikaido, H. *J. Bacteriol.* **1996**, *178*, 306–308.

[24] Webber, M. A.; Piddock, L. J. *J. Antimicrob. Chemother.* **2003**, *51*, 9–11.

[25] Abraham, E. P.; Chain, E. *Nature* **1940**, *146*, 837–837.

[26] Ventola, C. L. *P. T.* **2015**, *40*, 277–283.

[27] Drawz, S. M.; Bonomo, R. A. *Clin. Microbiol. Rev.* **2010**, *23*, 160–201.

[28] Medeiros, A.; Mayer, K. H.; Opal, S. M. *Antimicrob. Newslett.* **1988**, *5*, 61–65.

[29] Asheshov, E. H. *Nature* **1966**, *210*, 804–806.

[30] Paterson, D. L.; Bonomo, R. A. *Clin. Microbiol. Rev.* **2005**, *18*, 657–686.

[31] Bush, K. *Curr. Opin. Microbiol.* **2010**, *13*, 558–564.

[32] Bush, K.; Jacoby, G. A. *Antimicrob. Agents Chemother.* **2009**, *54*, 969–976.

[33] Lamotte-Brasseur, J.; Knox, J.; Kelly, J. A.; Charlier, P.; Fonzé, E.; Dideberg, O.; Frère, J.-M. *Biotechnol. Genet. Eng. Rev.* **1994**, *12*, 189–230.

[34] Galleni, M.; Lamotte-Brasseur, J.; Raquet, X.; Dubus, A.; Monnaie, D.; Knox, J. R.; Frère, J.-M. *Biochem. Pharmacol.* **1995**, *49*, 1171–1178.

[35] Herzberg, O.; Moult, J. *Science* **1987**, *236*, 694–701.

[36] Herzberg, O.; Moult, J. *J. Mol. Biol.* **1991**, *217*, 701–719.

[37] Lamotte-Brasseur, J.; Dive, G.; Dideberg, O.; Charlier, P.; Frère, J. M.; Ghuysen, J. M. *Biochem. J.* **1991**, *279*, 213–221.

[38] Paterson, D. L.; Bonomo, R. A. *Clin. Microb. Rev.* **2005**, *18*, 657–686.

[39] Queenan, A. M.; Busk, K. *Clin. Microb. Rev.* **2007**, *20*, 440–458.

[40] Lobkovsky, E.; Moews, P. C.; Liu, H.; Zhao, H.; Frère, J. M.; Knox, J. R. *Proc. Natl. Acad. Sci. U.S.A.* **1993**, *90*, 11257–11261.

[41] Evans, B. A.; Amyes, S. G. B. *Clin. Microbiol. Rev.* **2014**, *27*, 241–263.

[42] Golemi, D.; Maveyraud, L.; Vakulenko, S.; Samama, J.-P.; Mobashery, S. *Proc. Natl. Acad. Sci. U.S.A.* **2001**, *98*, 14280–14285.

[43] Brown, S.; Amyes, S. *J. Antimicrob. Chemother.* **2006**, *57*, 1–3.

[44] Ito, Y.; Kawabata, T.; Terashima, S. *Tetrahedron Lett.* **1986**, *27*, 5751–5754.

[45] Sasaki, A.; Goda, K.; Enomoto, M.; Sunagawa, M. *Chem. Pharm. Bull.* **1992**, *40*, 1094–1097.

[46] Grzeszczyk, B.; Stecko, S.; Mucha, Ł.; Staszewska-Krajewska, O.; Chmielewski, M.; Furman, B. *J. Antibiot.* **2013**, *66*, 161–163.

[47] Heritier, C.; Poirel, L.; Lambert, T.; Nordmann, P. *Antimicrob. Agents Chemother.* **2005**, *49*, 3198–3202.

[48] Crowder, M. W.; Spencer, J.; Vila, A. J. *Acc. Chem. Res.* **2006**, *39*, 721–728.

[49] Crisp, J.; Conners, R.; Garrity, J. D.; Carenbauer, A. L.; Crowder, M. W.; Spencer, J. *Biochemistry* **2007**, *46*, 10664–10674.

[50] Meini, M.-R.; Llarrull, L. I.; Vila, A. J. *FEBS Lett.* **2015**, *589*, 3419–3432.

[51] Meini, M.-R.; Llarrull, L.; Vila, A. *Antibiotics* **2014**, *3*, 285–316.

[52] Walsh, T. R. *Int. J. Antimicrob. Agents* **2010**, *36*, S8–14.

[53] Mojica, M. F.; Bonomo, R. A.; Fast, W. *Curr. Drug Targets* **2016**, *17*, 1029–1050.

[54] Xu, D.; Xie, D.; Guo, H. *J. Biol. Chem.* **2006**, *281*, 8740–8747.

[55] Simm, A. M.; Higgins, C. S.; Carenbauer, A. L.; Crowder, M. W.; Bateson, J. H.; Bennett, P. M.; Clarke, A. R.; Halford, S. E.; Walsh, T. R. *J. Biol. Chem.* **2002**, *277*, 24744–24752.

[56] Brown, A. G. *Drug Des. Deliv.* **1986**, *1*, 1–21.

[57] Therrien, C.; Levesque, R. C. *FEMS Microbiol. Rev.* **2000**, *24*, 251–262.

[58] Ball, A.; Davey, P. G.; Geddes, A. M.; Farrell, I. D.; Brookes, G. R. *Lancet* **1980**, *315*, 620–623.

[59] Pfizer. Penicillanic acid 1,1-dioxides as beta-lactamase inhibitors. United States Patent US 4234579 A, Nov 18, 1980.

[60] Taiho Pharmaceutical Co Ltd. Penicillin derivatives and process for preparation of the same. European Patent EP 0097466 A1, Jan 4, 1984.

[61] Campoli-Richards, D. M.; Brogden, R. N. *Drugs* **1987**, *33*, 577–609.

[62] Wise, R. *J. Antimicrob. Chemother.* **1993**, *31*, 97–104.

[63] Poirel, L.; Potron, A.; Nordmann, P. *J. Antimicrob. Chemother.* **2012**, *67*, 1597–1606.

[64] Walsh, T. R.; Toleman, M. A.; Poirel, L.; Nordmann, P. *Clin. Microbiol. Rev.* **2005**, *18*, 306–325.

[65] AstraZeneca. Process For Preparing Heterocyclic Compounds Including Trans-7-Oxo-6-(Sulphooxy)-1,6-Diazabicyclo[3,2,1]Octane-2-Carboxamide And Salts Thereof. International Patent WO 2012/172368 A1, December 20, 2012.

[66] Wang, D. Y.; Abboud, M. I.; Markoulides, M. S.; Brem, J.; Schofield, C. J. *Future Med. Chem.* **2016**, *8*, 1063–1084.

[67] Stachyra, T.; Pechereau, M. C.; Bruneau, J. M.; Claudon, M.; Frère, J. M.; Miossec, C.; Coleman, K.; Black, M. T. *Antimicrob. Agents Chemotherap.* **2010**, *54*, 5132–5138.

[68] Coleman, K. *Curr. Opin. Microbiol.* **2011**, *14*, 550–555.

[69] Ehmann, D. E.; Jahić, H.; Ross, P. L.; Gu, R.-F.; Hu, J.; Durand-Réville, T. F.; Lahiri, S. D.; Thresher, J.; Livchak, S.; Gao, N.; Palmer, T.; Walkup, G. K.; Fisher, S. L. *J. Biol. Chem.* **2013**, *288*, 27960–27971.

[70] Mosley, J. F.; Smith, L. L.; Parke, C. K.; Brown, J. A.; Wilson, A. L.; Gibbs, L. V. *P. T.* **2016**, *41*, 479–483.

[71] Lahiri S. D; Mangani, S.; Durand-Reville, T. F.; Benvenuti, M.; De Luca, F.; Sanyl, G.; Docquier, J. D. *Antimicrob. Agents Chemotherap.* **2013**, *57*, 2496–2505.

[72]Krishnan, N. P.; Nguyen, N. Q.; Papp-Wallace, K. M.; Bonomo, R. A.; van den Akker, F. *PLoS ONE* **2015**, *10*, e0136813.

[73] Ehmann, D. E.; Jahic, H.; Ross, P. L.; Gu, R. F.; Kern, G.; Walkup, G. K.; Fisher, S. L. *Proc. Natl Acad. Sc. U.S.A.* **2012**, *109*, 11663–11668.

[74] Meiji Seika Pharma Col, Ltd. Optically-active diazocyclooctane derivative and method for manufacturing same. World Patent Office WO 2012/086241 A1, Jun 28, 2012.

[75] King, A. M.; King, D. T.; French, S.; Brouillette, E.; Asli, A.; Alexander, J. A. N.; Vuckovic, M.; Maiti, S. N.; Parr, T. R.; Brown, E. D.; Malouin, F.; Strynadka, N. C. J.; Wright, G. D. *ACS Chem. Biol.* **2016**, *11*, 864–868.

[76] Lim, H. M.; Pene, J. J.; Shaw, R. W. *J. Bacteriol.* **1988**, *170*, 2873–2878.

[77] Walsh, T. R. *Clin. Microbiol. Infect.* **2007**, *13*, 113.

[78] Baldwin, J. E.; Lynch, G. P.; Pitlik, J. *J. Antibiot.* **1991**, *44*, 1–24.

[79] Wilmouth, R. C.; Westwood, N. J.; Anderson, K.; Brownlee, W.; Claridge, T. D.; Clifton, I. J.; Pritchard, G. J.; Aplin, R. T.; Schofield, C. J. *Biochemistry* **1998**, *37*, 17506–17513.

[80] Wilmouth, R. C.; Kassamally, S.; Westwood, N. J.; Sheppard, R. J.; Claridge, T. D.; Aplin, R. T.; Wright, P. A.; Pritchard, G. J.; Schofield, C. J. *Biochemistry* **1999**, *38*, 7989–7998.

[81] Choi, H.; Paton, R. S.; Park, H.; Schofield, C. J. *Org. Biomol. Chem.* **2016**, *14*, 4116–4128.

[82] Harada, S.; Tsubotani, S.; Hida, T.; Ono, H.; Okazaki, H. *Tetrahedron Lett.* **1986**, *27*, 6229–6232.

[83] Nozaki, Y.; Katayama, N.; Ono, H.; Tsubotani, S.; Harada, S.; Okazaki H.; Nakao, Y. *Nature* **1987**, *325*, 179–180.

[84] Tamura, N.; Matsushita, Y.; Yoshioka, K.; Ochiai, M. *Tetrahedron* **1988**, *44*, 3231–3240.

[85] Harada, S.; Tsubotani, S.; Hida, T.; Koyana, K.; Kondo, M.; Ono, H. *Tetrahedron* **1988**, *44*, 6589–6606.

[86] Nozaki, Y.; Katayama, N.; Harada, S.; Ono, H.; Okazaki, H. *J. Antibiot.* **1989**, *42*, 84–93.

[87] Zhou, A.; Li, Z.; Li, M.; Wang, J. *Chin. J. Antibiot.* **1994**, *19*, 194–199.

[88] Macheboeuf, P.; Fisher, D.; Brown, T.; Zervosen, A.; Joris, B.; Luxen, A.; Dessen, A.; Schofield, C. J. *Nature Chem. Bio.* **2007**, *3*, 565–569.

[89] Brown, T. Jr.; Charlier, P.; Herman, R.; Schofield, C. J.; Sauvage, E. *J. Med. Chem.* **2010**, *53*, 5890–5894.

[90] Starr, J.; Brown, M. F.; Aschenbrenner, L.; Caspers, N.; Che, Y.; Gerstenberger, B. S.; Huband, M.; Knafels, J. D.; Lemmon, M. M.; Li, C.; Mccurdy, S. P.; Mcelroy, E.; Rauckhorst, M. R.; Tomaras, A. P.; Young, J. A.; Zaniewski, R. P.; Shanmugasundaram, V.; Han, S. *J. Med. Chem.* **2014**, *57*, 3845–3855.

[91] Calvopiña, K.; Umland, K.-D.; Rydzik, A. M.; Hinchliffe, P.; Brem, J.; Spencer, J.; Schofield, C. J.; Avison, M. B. *Antimicrob. Agents Chemother.* **2016**, *60*, 4170–4175.

[92] Baldwin, J. E.; Adlington, R. M.; Jones, R. H.; Schofield, C. J.; Zaracostas, C.; Greengrass, C. W. *J. Chem. Soc. Chem. Commun.* **1985**, *1985*, 194–196.

[93] Baldwin, J. E.; Lowe, C.; Schofield, C. J.; Lee, E. *Tetrahedron Lett.* **1986**, *27*, 3461–3464.

[94] Baldwin, J. E.; Freeman, R. T.; Schofield, C. J. *Tetrahedron Lett.* **1989**, *30*, 4019–4020.

[95] Baldwin, J. E.; Lynch, G. P.; Pitlik, J. *J. Antibiot.* **1991**, *44*, 1–24.

[96] Hashiguchi, S.; Natsugari, H.; Ochiai, M. *J. Chem. Soc. Perkin. Trans. 1* **1988**, *1988*, 2345–2352.

[97] Jungheim, L. N.; Barnett, C. J.; Gray, J. E.; Horcher, L. H.; Shepherd, T. A.; Sigmund, S. K. *Tetrahedron* **1988**, *44*, 3119–3126.

[98] Shepherd, T. A.; Jungheim, L. N. *Tetrahedron Lett.* **1988**, *29*, 5061–5064.

[99] Ternansky, R. J.; Draheim, S. E.; Pike, A. J.; Counter, F. T.; Eudaly, J. A.; Kasher, J. S. *J. Med. Chem.* **1993**, *36*, 3224–3229.

[100] Kurth, C.; Kage, H.; Nett, M. *Org. Biomol. Chem.* **2016**, *14*, 8212–8227.

[101] González, M. M.; Kosmopoulou, M.; Mojica, M. F.; Castillo, V.; Hinchliffe, P.; Pettinati, I.; Brem, J.; Schofield, C. J.; Mahler, G.; Bonomo, R. A.; Llarrull, L. I.; Spencer, J.; Vila, A. J. *ACS Infect. Dis.* **2015**, *1*, 544–554.

[102] Hinchliffe, P.; González, M. M.; Mojica, M. F.; González, J. M.; Castillo, V.; Saiz, C.; Kosmopoulou, M.; Tooke, C. L.; Llarrull, L. I.; Mahler, G.; Bonomo, R. A.; Vila, A. J.; Spencer, J. *Proc. Natl. Acad. Sci. U.S.A.* **2016**, *113*, E3745–3754.

[103] Hecker, S. J.; Reddy, K. R.; Totrov, M.; Hirst, G. C.; Lomovskaya, O.; Griffith, D. C.; King, P.; Tsivkovski, R.; Sun, D.; Sabet, M.; Tarazi, Z.; Clifton, M. C.; Atkins, K.; Raymond, A.; Potts, K. T.; Abendroth, J.; Boyer, S. H.; Loutit, J. S.; Morgan, E. E.; Durso, S.; Dudley, M. N. *J. Med. Chem.* **2015**, *58*, 3682–3692.

[104] Goldstein, E. J. C.; Citron, D. M.; Tyrrell, K. L.; Merriam, C. V. *Antimicrob. Agents Chemother.* **2013**, *57*, 2620–2630.

[105] Eidam, O.; Romagnoli, C.; Caselli, E.; Babaoglu, K.; Pohlhaus, D. T.; Karpiak, J.; Bonnet, R.; Shoichet, B. K.; Prati, F. *J. Med. Chem.* **2010**, *53*, 7852–7863.

[106] Eidam, O.; Romagnoli, C.; Dalmasso, G.; Barelier, S.; Caselli, E.; Bonnet, R.; Shoichet, B. K.; Prati, F. *Proc. Natl. Acad. Sci. U.S.A.* **2012**, *109*, 17448–17453.

[107] Bouza, A. A.; Swanson, H. C.; Smolen, K. A.; Vandine, A. L.; Taracila, M. A.; Romagnoli, C.; Caselli, E.; Prati, F.; Bonomo, R. A.; Powers, R. A.; Wallar, B. J. *ACS Infect. Dis.* **2017**, *4*, 325–336.

[108] Brem, J.; Cain, R.; Cahill, S.; Mcdonough, M. A.; Clifton, I. J.; Jiménez-Castellanos, J.-C.; Avison, M. B.; Spencer, J.; Fishwick, C. W. G.; Schofield, C. J. *Nat. Commun.* **2016**, *7*, 12406.

[109] Cahill, S. T.; Cain, R.; Wang, D. Y.; Lohans, C. T.; Wareham, D. W.; Oswin, H. P.; Mohammed, J.; Spencer, J.; Fishwick, C. W. G.; Mcdonough, M. A.; Schofield, C. J.; Brem, J. *Antimicrob. Agents Chemother.* **2017**, *61*, e02260–16.

[110] Horsfall, L. E.; Garau, G.; Lienard, B. M. R.; Dideberg, O.; Schofield, C. J.; Frere, J. M.; Galleni, M. *Antimicrob. Agents Chemother.* **2007**, *51*, 2136–2142.

[111] Chen, A. Y.; Thomas, P. W.; Stewart, A. C.; Bergstrom, A.; Cheng, Z.; Miller, C.; Bethel, C. R.; Marshall, S. H.; Credille, C. V.; Riley, C. L.; Page, R. C.; Bonomo, R. A.; Crowder, M. W.; Tierney, D. L.; Fast, W.; Cohen, S. M. *J. Med. Chem.* **2017,** *60*, 7267–7283.

[112] Antabio SAS. Antibacterial Thiazolecarboxylic Acids. International Patent WO 2014/198849 A1, Dec 18, 2014.

[113] Everett, M.; Sprynski, N.; Coelho, A.; Castandet, J.; Bayet, M.; Bougnon, J.; Lozano, C.; Davies, D. T.; Leiris, S.; Zalacain, M.; Morrissey, I.; Magnet, S.; Holden, K.; Warn, P.; Luca, F. D.; Docquier, J.-D.; Lemonnier, M. *Antimicrob. Agents Chemother.* **2018**, *62*, e00074–18.

[114] Bemis, G. W.; Murcko, M. A. *J. Med. Chem.* **1996**, *39* (15), 2887–2893.

[115] Pettinati, I.; Brem, J.; Lee, S. Y.; Mchugh, P. J.; Schofield, C. J. *Trends Biochem. Sci.* **2016**, *41*, 338–355.

[116] Aoki, N.; Ishii, Y.; Tateda, K.; Saga, T.; Kimura, S.; Kikuchi, Y.; Kobayashi, T.; Tanabe, Y.; Tsukada, H.; Gejyo, F.; Yamaguchi, K. *Antimicrob. Agents Chemother.* **2010**, *54*, 4582–4588.

[117] Yoshizumi, A.; Ishii, Y.; Livermore, D. M.; Woodford, N.; Kimura, S.; Saga, T.; Harada, S.; Yamaguchi, K.; Tateda, K. *J. Infect. Chemother*. **2013**, 19, 992–995.

[118] Chouchani, C.; Marrakchi, R.; Ferchichi, L.; Salabi, A. E.; Walsh, T. R. *ACS Infectious Diseases* **2018**, *4*, 135–145.

[119] King, A. M.; Reid-Yu, S. A.; Wang, W.; King, D. T.; Pascale, G. D.; Strynadka, N. C.; Walsh, T. R.; Coombes, B. K.; Wright, G. D. *Nature* **2014**, *510*, 503–506.

[120] Zhang, Y.-L.; Yang, K.-W.; Zhou, Y.-J.; Lacuran, A. E.; Oelschlaeger, P.; Crowder, M. W. *ChemMedChem* **2014**, *9*, 2445–2448.

[121] Xiang, Y.; Chang, Y.-N.; Ge, Y.; Kang, J. S.; Zhang, Y.-L.; Liu, X.-L.; Oelschlaeger, P.; Yang, K.-W. *Bioorg. Med. Chem. Lett.* **2017**, *27*, 5225–5229.

[122] Simpson, I. N.; Urch, C. J.; Hagen, G.; Albrecht, R.; Sprinkart, B.; Pfaendler, H. R. *ChemInform* **2004**, *35*.

[123] LEK Pharmaceuticals dd. New Trinem Antibiotics and Inhibitors of Beta-Lactamases. US Patent US 20110166118A1, July 7, 2011.

[124] Jamieson, C. E.; Lambert, P. A.; Simpson, I. N. *Antimicrob. Agents Chemother.* **2003**, *47*, 1652–1657.

[125] Paukner, S.; Hesse, L.; Prezelj, A.; Solmajer, T.; Urleb, U. *Antimicrob. Agents Chemother.* **2008**, *53*, 505–511.

[126] Borthwick, A. D.; Angier, S. J.; Crame, A. J.; Exall, A. M.; Haley, T. M.; Hart, G. J.; Mason, A. M.; Pennell, A. M. K.; Weingarten, G. G. *J. Med. Chem.* **2000**, *43*, 4452–4464.

[127] Xiong, G.; Wang, Y.; Li, J. *Enzymes* **2014**, *35*, 57–84.

[128] Weir, M. P.; Bethell, S. S.; Cleasby, A.; Campbell, C. J.; Dennis, R. J.; Dix, C. J.; Finch, H.; Jhoti, H.; Mooney, C. J.; Patel, S.; Tang, C.-M.; Ward, M.; Wonacott, A. J.; Wharton, C. W. *Biochemistry* **1998**, *37*, 6645–6657.

[129] Klingler, F. M.; Wichelhaus, T. A.; Frank, D.; Cuesta-Bernal, J.; El-Delik, J.; Muller, H. F.; Sjuts, H.; Gottig, S.; Koenigs, A.; Pos, K. M.; Pogoryelov, D.; Proschak, E. *J. Med. Chem.* **2015**, 58, 3626−3630.

[130] Damblon, C.; Jensen, M.; Ababou, A.; Barsukov, I.; Papamicael, C.; Schofield, C. J.; Olsen, L.; Bauer, R.; Roberts, G. C. K. *J. Biol. Chem.* **2003**, *278*, 29240–29251.

[131] Garcia-Saez, I.; Hopkins, J.; Papamicael, C.; Franceschini, N.; Amicosante, G.; Rossolini, G. M.; Galleni, M.; Frere, J. M.; Dideberg, O. *J. Biol. Chem.* **2003**, 278, 23868−23873.

[132] Brem, J.; Berkel, S. S. V.; Aik, W.; Rydzik, A. M.; Avison, M. B.; Pettinati, I.; Umland, K.-D.; Kawamura, A.; Spencer, J.; Claridge, T. D. W.; Mcdonough, M. A.; Schofield, C. J. *Nat. Chem.* **2014**, *6*, 1084–1090.

[133] Black, J. W.; Crowther, A. F.; Shanks, R. G.; Smith, L. H.; Dornhorst, A. C. *Lancet* **1964**, *1*, 1080–1081.

[134] Macarron, R.; Banks, M. N.; Bojanic, D.; Burns, D. J.; Cirovic, D. A.; Garyantes, T.; Green, D. V. S.; Hertzberg, R. P.; Janzen, W. P.; Paslay, J. W.; Schopfer, U.; Sittampalam, G. S. *Nature Rev. Drug Dis.* **2011**, *10*, 188-195.

[135] Erlanson, D. A.; Fesik, S. W.; Hubbard, R. E.; Jahnke, W.; Jhoti, H. *Nature Rev. Drug Dis.* **2016**, *15*, 605-619.

[136] Murray, C. W.; Rees, D. C. *Nat. Chem.* **2009**, *1*, 187–192.

[137] Rees, D. C.; Congreve, M.; Murray, C. W.; Carr, R. *Nature Rev. Drug Dis.* **2004**, *3*, 660-672.

[138] Congreve, M.; Carr, R.; Murray, C.; Jhoti, H. *Drug Discov. Today* **2003**, *8*, 876–877.

[139] Lamoree, B.; Hubbard, R. E. *Essays Biochem.* **2017**, *61*, 453-464.

[140] Christopeit, T.; Carlsen, T. J. O.; Helland, R.; Leiros, H.-K. S. *J. Med. Chem.* **2015**, *58*, 8671–8682.

[141] Kim, Y. S.; Cha, H. J. *Antimicrob. Agents Chemother.* **2006**, *50*, 3330–3335.

[142] Stone, M. R. L.; Butler, M. S.; Phetsang, W.; Cooper, M. A.; Blaskovich, M. A. *Trends Biotech.* **2018**, *36*, 523–536.

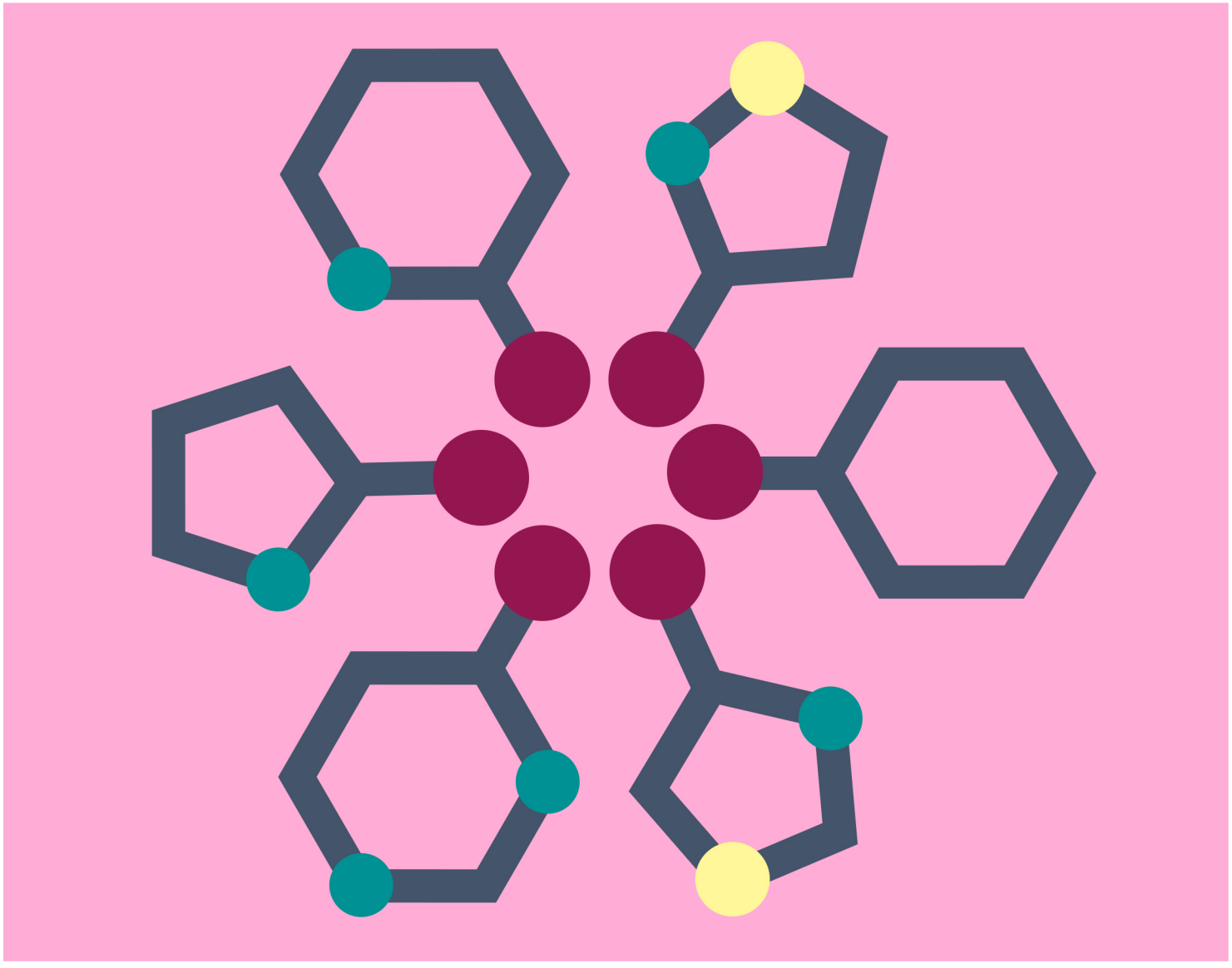
[143] Crowfoot, D.; Bunn, C. W.; Rogers-Low, B. W.; Turner-Jones, A. In *The Chemistry of Penicillin*; Princeton University Press: Princeton, New Jersey, 1949; p 310.

[144] Berkel, S. S. V.; Brem, J.; Rydzik, A. M.; Salimraj, R.; Cain, R.; Verma, A.; Owens, R. J.; Fishwick, C. W. G.; Spencer, J.; Schofield, C. J. *J. Med. Chem.* **2013**, *56*, 6945–6953.

[145] Antunes, N. T.; Lamoureaux, T. L.; Toth, M.; Stewart, N. K.; Frase, H.; Vakulenko, S. B. *Antimicrob. Agents Chemother.* **2014**, *58*, 2119–2125.

[146] Nordmann, P.; Poirel, L. *Clin. Microb. Infect.* **2014**, *20*, 821–830.

Chapter 2.
Fragments Optimisation



2. Fragment Optimisation

2.1. Fragment discovery via a high-throughput X-ray crystallography platform

As described in Chapter 1, the deployment of fragment-based drug discovery (FBDD) in the search for novel antibiotics and resistance breakers is potentially of considerable value. When this technique is coupled to a high-throughput X-ray crystallography platform, the resultant drug discovery process is efficient and can directly provide information on the three-dimensional binding modes of fragments. As a starting point for FBDD for MBLs, the *XChem* platform for VIM-2, a clinically relevant MBL which hydrolyses carbapenems (antibiotics used as a last resort)[1], was developed by Dr. Patrick Collins (Diamond Light Source) and Dr. Jürgen Brem (University of Oxford, Schofield Group) et al. [unpublished results]). The *XChem* platform employs fast crystal soaking using acoustic droplet ejection techniques[2], machine-assisted crystal mounting, and automated X-ray diffraction data collection and processing[3]. The Maybridge Ro3 Diversity Fragment Library, which consists of 2500 fragments, was chosen due to its commercial accessibility. Overall, 1012 crystals were soaked yielded a total of 580 refined datasets with an average resolution of 1.6 Å. Analysis of these 580 datasets using PanDDA revealed electron density for 53 clearly bound fragments (Figure 2.1).

Out of the 53 bound fragments, seven active site zinc coordinating fragments were identified (Figure 2.2). From these seven fragments, some noticeable structural similarities can be observed when compared to the natural substrates as well as to the proposed intermediates and products involved in the MBL-catalysed hydrolysis of β-lactam antibiotics (Figure 2.3).



Figure 2.1. Structures of 53 fragment binders identified from 580 datasets from *XChem*. Initial fragment optimisation focused on the active site zinc coordinating fragments, all of which were carboxylates.

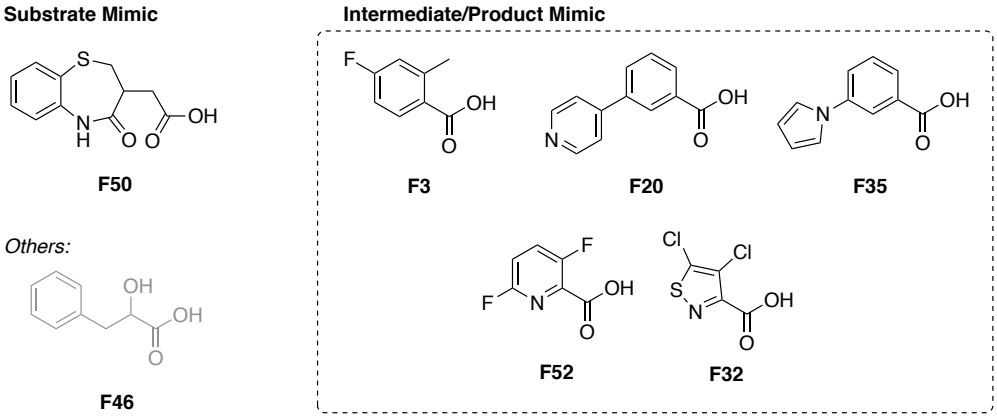


Figure 2.2. The seven fragments that were identified as active site zinc coordinating from a total of 53 'fragment crystal structures', obtained using high-throughput crystallography via the Maybridge Ro3 Diversity Fragment Library and VIM-2. These seven fragments can be further divided into two main categories based on their structural similarities to the intact natural β-lactam substrates as well as to the intermediates and products of the MBL-catalysed hydrolysis of β-lactam antibiotics (Figure 2.3).

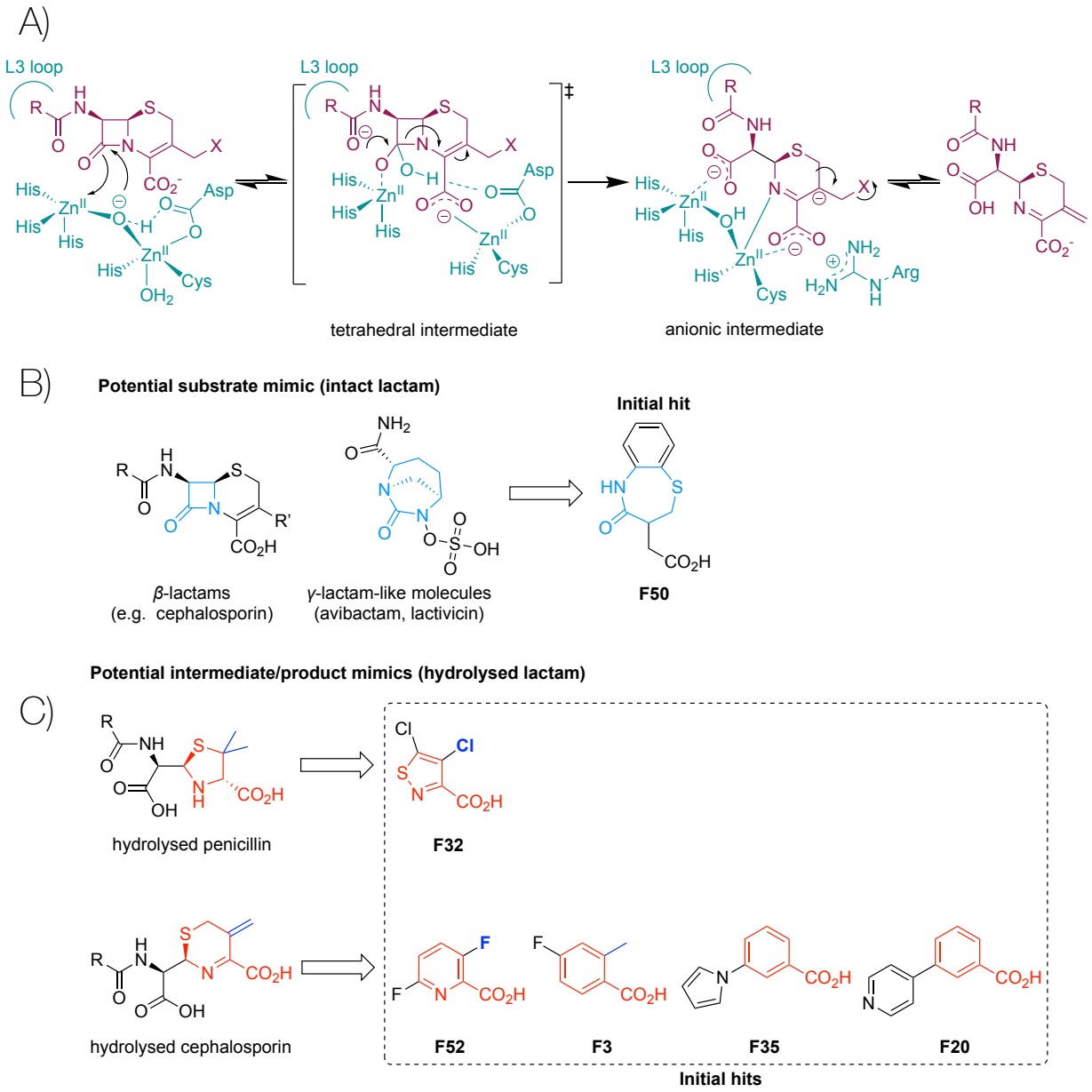


Figure 2.3. MBL-catalysed hydrolysis of a *β*-lactam antibiotic shown for a cephalosporin, depicting key interactions of the antibiotic with the zinc ions and other key active site residues (A). Similarities between F50 and the intact lactam substrate (B) as well as between F3, F20, F32, F35 and F52, and hydrolysed lactam substrates (C) can be proposed.

F50 bears a seven-membered *ε*-lactam, which is an expanded form of a *β*-lactam. Coincidentally, avibactam also contains a seven-membered ring. Therefore, it was thought, at least in some aspects, that **F50** could mimic avibactam, an MBL substrate, in terms of its binding mode.

In some regards, the aryl and heteroaryl carboxylates, such as **F3**, **F20**, **F32**, **F35** and **F52**, resemble the structures of the hydrolysed products of *β*-lactam antibiotics. It was envisioned that five-membered aromatic rings, such as **F32**, which features an isothiazole core, could mimic the hydrolysed product of penicillins or carbapenems; six-membered ring fragments such as **F3**, **F20**, **F35** and **F52**, similarly, could mimic the hydrolysed products of cephalosporins. The use of heteroaryl carboxylates in MBL inhibition is not novel, which can be traced back to investigations of picolinates and pyridine dicarboxylates as potential MBL inhibitors with zinc-chelating properties[4,5]. More recent developments have featured other heteroaryl cores, such as the thiazoles in a series of MBL inhibitors explored by Antabio (France)[6,7]. These molecules are compared with various hydrolysed *β*-lactam products (Figure 2.4).

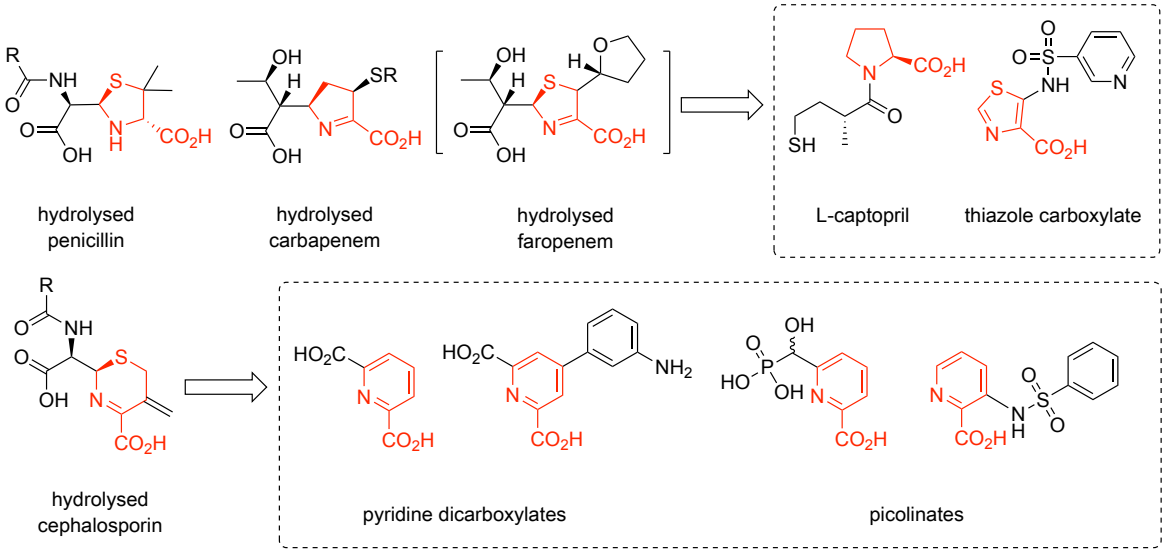


Figure 2.4. Examples of heteroaryl carboxylate structures that have been explored as plausible MBL inhibitors in the literature. Heteroaryl carboxylates have an inherent ability to chelate to zinc (or other metals), which provides them a natural potential to achieve MBL inhibition.

In order to validate the results obtained from the *XChem* platform, solution-based assays were performed by Dr. Jürgen Brem and Dr. Gareth Langley from the Schofield Group in order to determine the remaining activity of VIM-2 in the presence

of various fragments at different concentrations using a fluorogenic assay platform[8]. The focus was shifted towards five fragments, four of which came from the initial active site zinc coordinating pool, and an additional fragment, **F47**, which was an initial active site non-zinc coordinating hit. All five fragments caused some decrease in remaining activity of VIM-2 at a concentration of 100 μM, between 5% and 34% (Figure 2.5).

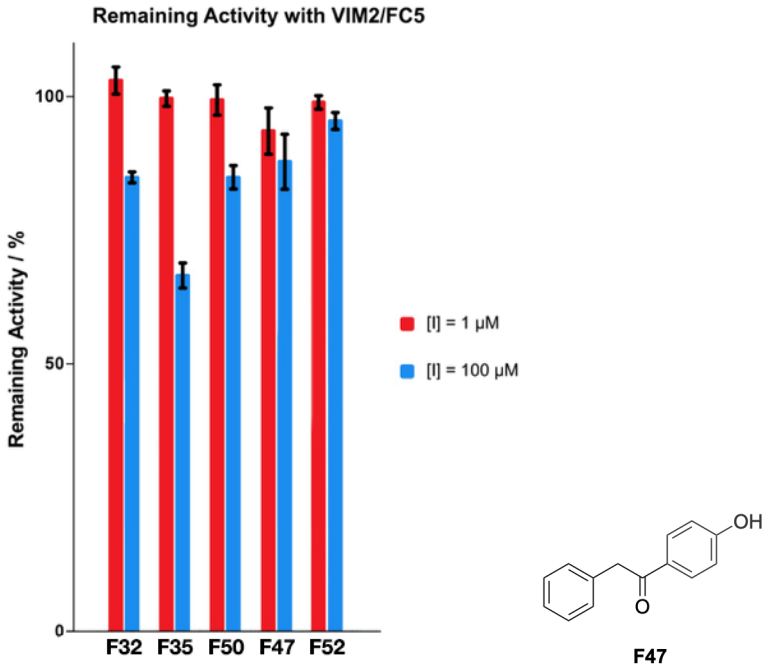


Figure 2.5. Remaining activity of VIM-2 against a panel of active site binding fragments (as suggested by the results from X-ray crystallography screening). Using FC-5 as a fluorogenic assay substrate[8], all five fragments caused an appreciable level of remaining activity reduction at a concentration of 100 μM, with F35, a benzoic acid derivative, displaying the highest reduction.

Subsequently, these five fragments were chosen to be optimised via, firstly, constructing a structure-activity relationship (SAR) profile for each fragment. Work from Dr. Anna Rydzik (former Schofield Group member) suggested that **F50** did not offer much scope for optimisation. The focus was then shifted to exploring the potential of various heteroaryl cores as potent MBL inhibitors. In the interest of clarity, the research highlighted in Chapter 2 is presented according to the hydrolysed β-

lactam products each compound may mimic, i.e. hydrolysed penams mimicked by five-membered aromatic systems (**F32** and related compounds), followed by hydrolysed cephems mimicked by six-membered aromatic systems (**F35**, **F52** and related compounds).

2.2. Structure-activity relationship and optimisation studies of analogues of F32

F32, an isothiazole 2-carboxylate, was considered as a starting point for validation and optimisation. From a crystal structure first with of **F32** complexed with VIM-2 (Figure 2.6), an interaction between the 5-chloro group with Phe-61 from the L3 loop is clearly apparent. Zn2 of VIM-2 is chelated by both the nitrogen atom of the **F32** heteroaryl core and the C-3 carboxylate group of **F32**. It was also noted that a water molecule (or hydroxide), W1, which bridges the zinc ions, is located relatively far from **F32**, thus suggesting that in this instance it may not directly participate in fragment binding.

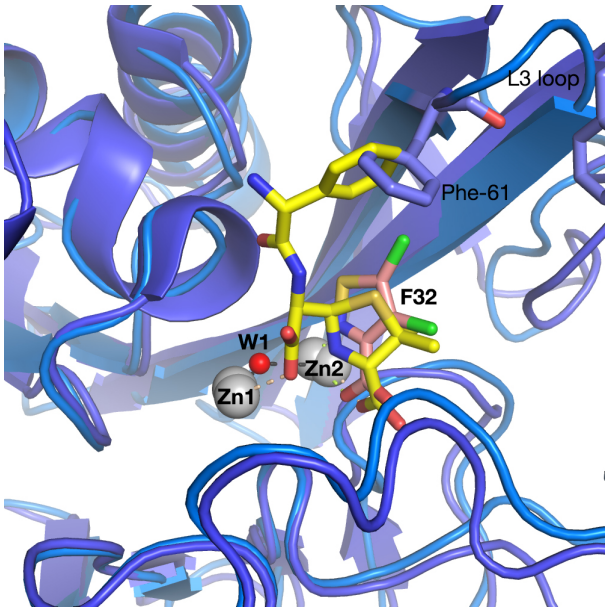
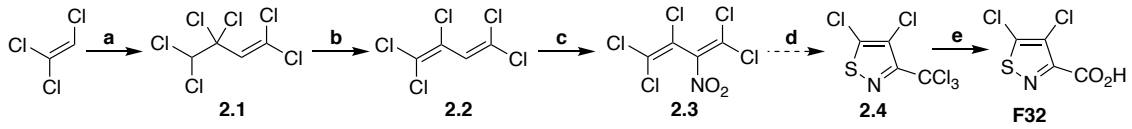


Figure 2.6. View from a crystal structure of F32 (pink) with VIM-2, illustrating key active site interactions including those between the 5-chloro group and Phe-61 of the L3 loop, the nitrogen atom of the heteroaryl ring and Zn2, and the C-3 carboxylate group of F32 and Zn2. Note that interactions with the bridging water molecule, W1, are not observed and that the mechanism of binding appears to be primarily via zinc chelation. This crystal structure is overlaid via a crystal structure of hydrolysed ampicillin (yellow) with NDM-1 with PyMOL. The overlay shows a close resemblance in the binding of F32 and the isothiazole five-membered ring from hydrolysed ampicillin. *(RCSB PDB ID: 5ZGE)*

In order to enhance the potency of MBL inhibitors based upon the structure of **F32**, methods were explored to achieve the in-house synthesis of both **F32** and its derivatives, especially for C-5 functionalisation of isothiazole. In the attempts to resynthesise **F32**, the only synthetic precedent in the literature comprised a series of reactions, some of which were ill-documented and archived in former USSR journals (Scheme 2.1)[9]. This route was modified and attempted.

From trichloroethylene, 1,1,3,3,4,4-hexachlorobut-1-ene was synthesised via a free radical reaction using a catalytic amount of dibenzoyl peroxide as an initiator (Scheme 2.1). After refluxing for 96 hours, the reaction gave **2.1** in 44% yield. An elimination reaction was then carried out on **2.1** in alkaline conditions comprising a slight excess of 28% sodium methoxide in methanol, which was added at 0 °C. The reaction was allowed to warm to room temperature, then stirred overnight to form **2.2** (1,1,2,4,4-pentachlorobuta-1,3-diene) in 64% yield. Next, nitration was performed on **2.2** by the addition of concentrated nitric acid and a small amount of concentrated sulfuric acid (10:1 v/v) at 0 °C followed by stirring at room temperature for two days, to afford **2.3** in 66% yield. To obtain the isothiazole **2.4**, an aromatic cyclisation reaction was then executed under a high temperature of 200 °C in the presence of sulfur powder; however, after two days no product formation was observed[9] (Scheme 2.1). Further literature search did not reveal any mechanistic description of this series of reactions, especially the cyclisation step that yields **2.4**, as the experimental procedures of these reactions have not been detailed in literature. Further, it should also be noted that the spectroscopic data obtained for **2.1**, **2.2** and **2.3** were inconclusive in supporting their structures, and comparison with literature data was not possible as the latter were not available.

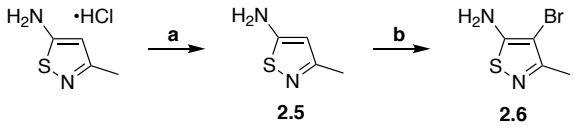


Scheme 2.1. *Synthetic route to F32*[9]*:*

a) Benzoyl peroxide (1.2 mol. %), reflux, 96 h, 44%; b) 28% NaOMe in MeOH (1.5 equiv.), MeOH, 0 ºC to r.t., overnight, 64%; c) conc. nitric acid (1.5 equiv.) and conc. sulfuric acid (10:1 v/v), 0 ºC to r.t., 2 days, 66%; d) sulfur (1.6 equiv.), 200 ºC, 2 days, reaction unsuccessful; e) *theoretical conditions:* fuming HNO_3 (8 equiv.), 0 – 5 ºC for 3 h then 10 – 15 ºC for 1 day, 90% (theoretical yield)[9].

In parallel, synthetic plans to produce analogues of **F32** were considered. 3-Methyl-5-aminoisothiazole was identified as a potentially viable and commercially available precursor with the flexibility of potentially offering both functionalisation on the amino position, e.g. amide (and sulfonamide) coupling, as well as oxidation on the C-3 methyl group to yield the indispensable carboxylate group. It was also envisioned that the C-4 position of a 3-methyl-5-aminoisothiazole could be halogenated to enable functionalisation at this position.

Initially, following a literature method[10], 5-amino-3-methylisothiazole (**2.5**) was produced from 5-amino-3-methylisothiazole hydrochloride by adjusting to pH 10 with the addition of 1 M sodium hydroxide solution. Following extraction of the organic phase using diethyl ether, the combined organic extracts was washed with brine, dried over anhydrous sodium sulfate and concentrated *in vacuo*. This afforded **2.5** in 92% yield, which was used in the next step without further purification. Using tetrachloromethane as a solvent, *N*-bromosuccinimide (NBS) was added to **2.5** at room temperature, then stirred at 65 ºC for two hours to produce **2.6** in 67% yield (Scheme 2.2).

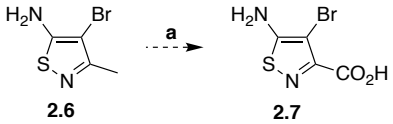


Scheme 2.2. *C-4 bromination of an isothiazole precursor[10]:*

a) 1 M NaOH (aq.), adjusted to pH 10, H_2O, 5 min, 92%; b) NBS* (1 equiv.), CCl_4, r.t. to 65 °C, N_2, 2 h, 67%.

**N*-Bromosuccinimide.

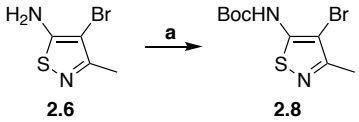
From **2.6**, a single-step oxidation reaction of the C-3 methyl group into a carboxylate group was attempted (Scheme 2.3). Using chromium(VI) trioxide in concentrated sulfuric acid, which was added to **2.6** portion-wise while maintaining a temperature under 30 °C, the mixture was then allowed to warm to room temperature overnight. However, none of the desired product was observed, although the starting material had reacted, as observed by TLC.



Scheme 2.3. *Attempted single-step oxidation of 2.6:*

a) CrO_3 (3 equiv.), conc. H_2SO_4, r.t., overnight, reaction unsuccessful.

In a different strategy, **2.6** was first Boc-protected using di-*tert*-butyl dicarbonate (Boc anhydride) and triethylamine in dichloromethane. After four hours, the desired product, **2.8**, was afforded in 25% yield (Scheme 2.4). It was envisaged that a Boc protection could enable later-stage C-5 amine functionalisations.

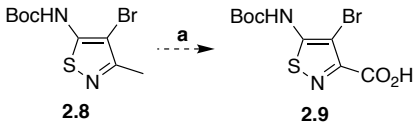


Scheme 2.4. *Boc protection of 2.6:*

a) Boc_2O (1.5 equiv.), Et_3N (3 equiv.), N_2, r.t., 4 h, 25%.

A single-step oxidation of **2.8** using chromium(VI) trioxide in concentrated sulfuric acid was then attempted (Scheme 2.5), but none of the desired product was isolated. The starting material did not survive the harsh reaction conditions as shown by TLC.

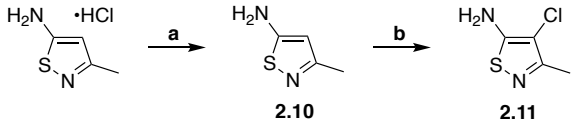
The Boc group was particularly vulnerable to deprotection by acidic reaction conditions.



Scheme 2.5. *Attempted single-step oxidation of 2.8:*

a) CrO_3 (3 equiv.), conc. H_2SO_4, r.t., overnight, reaction unsuccessful.

Since C-4 bromination of 5-amino-3-methylisothiazole had been possible, C-4 chlorination was also investigated. From 5-amino-3-methylisothiazole hydrochloride, 5-amino-3-methylisothiazole (**2.10**) was obtained using a reported method[10] (Scheme 2.2). Next, following a literature method[11], *N*-chlorosuccinimide (NCS) was added portion-wise, using chloroform as a solvent. After refluxing for four hours, **2.11** was produced in quantitative yield (Scheme 2.6).

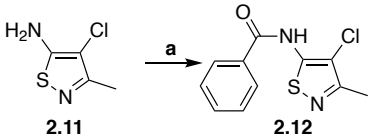


Scheme 2.6. *C-4 chlorination of an isothiazole precursor[11]:*

a) 1 M NaOH (aq.), adjusted to pH 10, H_2O, 5 min, 67%; b) NCS* (1 equiv.), chloroform, reflux, 4 h, quant.

**N*-Chlorosuccinimide.

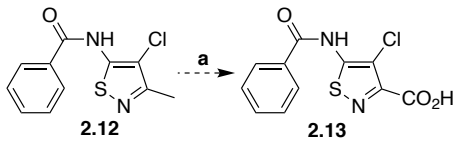
Given the potential lability of the Boc protecting group, especially towards the conditions used for oxidation, functionalisation of the C-5 amine group on **2.11** was performed via an amide formation. Reacting **2.11** with benzoyl chloride in pyridine, 18 hours (room temperature) gave **2.12** in 73% yield (Scheme 2.7).



Scheme 2.7. *Amide formation from 2.11:*

a) PhCOCl (1.3 equiv.), pyridine, r.t., 18 h, 73%.

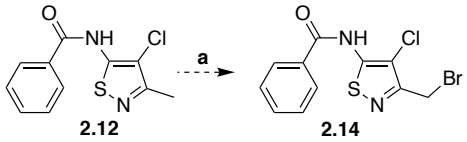
From **2.12**, three milder sets of oxidation reaction conditions were attempted, aiming to achieve the single-step oxidation of the C-3 methyl group (Scheme 2.8). **2.12** was first reacted with potassium permanganate in the presence of sodium carbonate in water, which was refluxed for 20 hours. The reaction failed to proceed and starting material was recovered. Then, **2.12** was reacted with potassium permanganate in the presence of pyridine and water (1:3 v/v) at 50 ºC for 24 hours. Again, the reaction did not proceed and the starting material was recovered. Finally, reacting **2.12** with selenium(IV) dioxide in pyridine at 55 ºC (two hours) then 80 ºC (3.5 hours), and subsequently room temperature overnight, the starting material was again recovered without any sign of the desired oxidation.



Scheme 2.8. *Attempted single-step oxidation of 2.12:*

a) Method A: $KMnO_4$ (2.5 equiv.), Na_2CO_3 (0.5 equiv.), H_2O, reflux, 20 h, reaction unsuccessful; method B: $KMnO_4$ (3 equiv.), pyridine/water (1:3 v/v), 50 ºC, 24 h, reaction unsuccessful; method C: SeO_2 (1.5 equiv.), pyridine, 55 ºC for 2 h, then 80 ºC for 3.5 h, then overnight at r.t., reaction unsuccessful.

Since a single-step oxidation of the C-3 methyl group of **2.12** into a carboxylate group had so far proven to be not possible, a stepwise approach was proposed, involving halogenation of the methyl group. Adapting a literature method[12], **2.12** with NBS in carbon tetrachloride, using benzoyl peroxide (BPO) as an initiator, was refluxed for 24 hours, but the desired product was not obtained (Scheme 2.9).



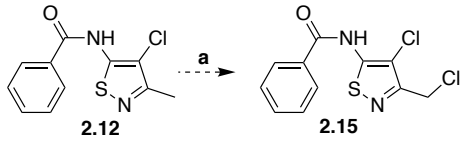
Scheme 2.9. *Attempted bromination of C-3 methyl group of **2.12**[12]:*

a) NBS* (1 equiv.), BPO** (15 mol. %), reflux, 24 h, reaction unsuccessful.

**N*-Bromosuccinimide.

***Benzoyl peroxide.

In addition to bromination, chlorination on the same C-3 methyl group of **2.12** was also attempted. **2.12** was reacted with sulfuryl chloride in acetic acid at room temperature for 48 hours. When no reaction was found to take place, another portion of sulfuryl chloride was added. However, after stirring the reaction mixture at room temperature for a further 48 hours, no sign of the required reaction was observed by TLC (Scheme 2.10).



Scheme 2.10. *Attempted chlorination of C-3 methyl group of **2.12**:*

a) SO_2Cl_2 (excess), AcOH, r.t., 96 h, reaction unsuccessful.

Given that both single-step oxidation and stepwise oxidation were unsuccessful, work on producing the isothiazole-related compounds was halted and the focus was shifted towards more productive investigation lines (see below).

2.3. Development of pyrrole-based analogues of F32 as MBL inhibitors

During the early stages of the isothiazole synthesis, it was recognised that an MBL inhibitor bearing an isothiazole core may possess limitations. In addition to synthetic challenges as well as *in vivo* toxicity issues[13], an isothiazole carboxylate core only

bears two sites of functionalisation, i.e. at C-4 and C-5. Therefore, attention was turned to other heteroaromatic rings which may offer greater flexibility.

Pyrroles have footprints in various successful pharmaceutical products, including the top-selling statin drug atorvastatin[14], as well as nonsteroidal anti-inflammatory drugs such as tolmetin[15] and ketorolac[16]. Naphthoylpyrroles such as **JWH-030**, a potent class of synthetic cannabinoids[17], are also occurring in the increasingly problematic street drug commonly known as "spice" (Figure 2.7).

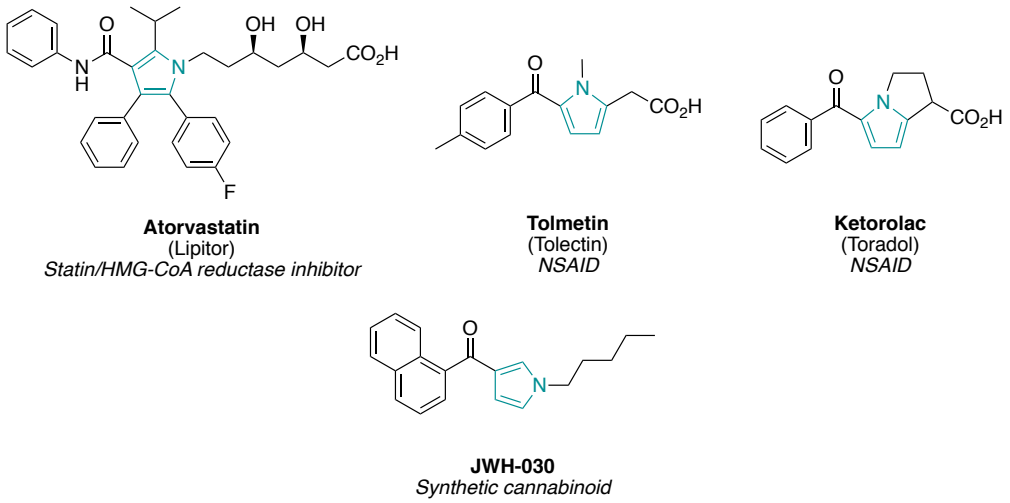


Figure 2.7. Examples of pyrrole-based pharmaceutical products include atorvastatin, a statin (or HMG-CoA reductase inhibitor) that is one of the best-selling medicines in history[14], as well as nonsteroidal anti-inflammatory drugs (NSAID) such as tolmentin[15] and ketorolac[16]. There has been an increase in the recreational use of synthetic cannabinoid, where examples of pyrrole-containing compounds, such as JWH-030[17], occur.

It was considered that it may be possible to replace isothiazole 3-carboxylate of **F32** with a pyrrole 2-carboxylate, so enabling binding/inhibition and functionalisation at the C-5 pyrrole position. It was, however, noted that the presence of an acidic proton on the pyrrole may compromise zinc chelation. In order to alleviate this potential concern, the mode of action of MBLs was re-examined (Figure 2.3A). MBL-mediated hydrolysis of β-lactams involves a nucleophilic hydroxide bridging between the two

zinc ions for the B1 and B3 MBLs (or complexed to one zinc ion as in the case of the mono-zinc B2 MBLs). It was predicted that instead of chelating to the zincs, pyrroles have the potential to hydrogen-bond to the hydroxide nucleophile, enabling inhibition to occur via a mechanism that differs from the isothiazole progenitors. Simple *in silico* analyses using PyMOL using energy minimisation suggested that pyrroles could interact with MBLs via a different mechanism compared to that obtained for **F32**, involving forming interactions with the Phe-61 on the L3 loop as well as the zinc ions. In the potential pyrrole-based inhibitors, it was predicted that towards Zn1, which enables stronger interactions between the 2-carboxylate group and Zn1, alongside weakening of interactions between the pyrrole heteroatom and Zn2, may occur (Figure 2.8). In addition, enhancement of interactions to improve potency of inhibition at other sites may be possible, such as via C-4 and C-5 pyrrole functionalisations (Figure 2.8).

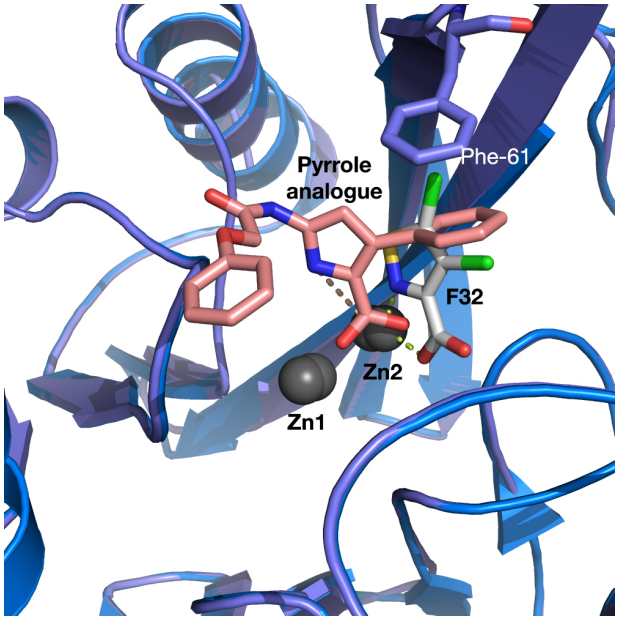
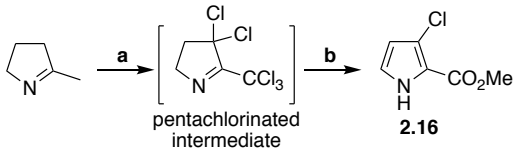


Figure 2.8. Example of a potential pyrrole-based MBL inhibitor (pink) docked and overlaid with the binding mode that was observed for the crystal structure of F32 (grey) with VIM-2 (figure prepared using PyMOL). It was speculated that the carboxylate group of the pyrrole core could shift closer to Zn1 while the heteroatom of the pyrrole core could edge further away from Zn2, relative to the binding of F32. Functionalisation at C-3 could enable interactions with Phe61 at the L3 loop, whereas functionalisation in C-5 could enhance other interactions at the active site.

As a proof of concept, six simple pyrrole 2-carboxylate derivatives with different C-3 functionalisation were synthesised. A convenient and affordable synthetic literature route[18] permitted access of **2.16**, i.e. 3-chloro-pyrrole 2-carboxylate methyl ester,

from 2-methyl-1-pyrroline, in two steps, as shown below in Scheme 2.11. In the presence of a large excess of NCS at 55 ºC, chlorination of 2-methyl-1-pyrroline was performed via electrophilic addition at both the C-2 methyl and the C-3 positions of 2-methyl-1-pyrroline, giving a pentachlorinated intermediate, which was used in the subsequent step without further purification. The conversion from the pentachlorinated intermediate to **2.16** involves a series of elimination and nucleophilic substitution reactions in the presence of alkali (28% sodium methoxide in methanol) in methanol at room temperature; these reactions afforded **2.16** in yield of 87% over two steps (Scheme 2.11).



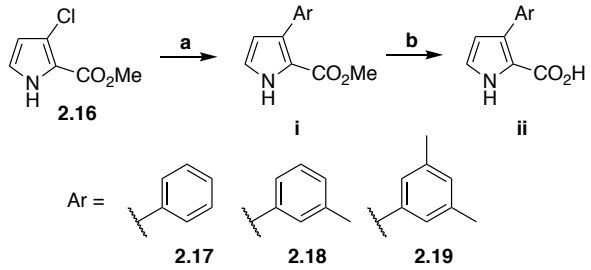
Scheme 2.11. *Synthesis of **2.16**[18]:*

a) NCS (8 equiv.), THF, 55 ºC, 1 h; b) 28% NaOMe-MeOH (6 equiv.), MeOH, r.t., 2 h, 87% over 2 steps.

It was envisioned that **2.16** would be subjected to Suzuki and/or Sonogashira coupling reactions to access aromatic analogues at C-3. While attempts to carry out Sonogashira reactions were unsuccessful, Suzuki reactions with **2.16** led to compounds **2.17i**, **2.18i** and **2.19i**, using phenylboronic acid, *m*-tolylboronic acid, and 3,5-dimethylboronic acid, respectively. The Suzuki reactions employed palladium(II) acetate as a catalyst, 2-dicyclohexylphosphino-2',4',6'-triisopropylbiphenyl (XPhos) as a ligand, and potassium carbonate as a base (in 1,4-dioxane and water [5:1 v/v]). The yields of the Suzuki reactions ranged from 81 to 86% (Scheme 2.12 and Table 2.1). **2.17i**, **2.18i** and **2.19i** were then hydrolysed under alkaline conditions using lithium hydroxide monohydrate in methanol and water (2:1 v/v). After overnight reactions, **2.17ii**, **2.18ii** and **2.19ii** were successfully synthesised in yields between 33

and 84% (Scheme 2.12 and Table 2.1). Despite their successful synthesis, **2.17ii**, **2.18ii** and **2.19ii**, did not exhibit any signs of inhibition at 100 μM against VIM-2 using a standard FC-5-based assay[8], possibly due to the lack of interaction of the inhibitors with the L3 loop of VIM-2, given the structural simplicity of these compounds (Figure 2.3A).

Interestingly, the 1,2-disubstituted pyrrole analogues (**2.16** to **2.19**) revealed an unexpected multiplicity for the two pyrrole protons. Instead of appearing as doublets (or doublets of doublets should they couple to pyrrole N-H), they appear as distinct triplets instead. These observations are in agreement with the reported NMR literature spectra[19,20]. A possible explanation can be found in NMR studies of substituted pyrroles, which speculates that the extent of coupling between in the two pyrrole protons is identical to the extent of coupling with the pyrrole N-H[21].



Scheme 2.12. *Synthesis of various pyrrole analogues via Suzuki coupling and ester hydrolysis:*
a) Ar-$B(OH)_2$ (1.2 equiv.), $Pd(OAc)_2$ (10 mol. %), XPhos* (20 mol. %), K_2CO_3 (3 equiv.), 1,4-dioxane/H_2O (5:1 v/v), N_2, 100 ºC, 2 h, see Table 2.1; b) $LiOH \bullet H_2O$ (5 equiv.), MeOH/H_2O (2:1 v/v), r.t., overnight, See Table 2.1.
*2-Dicyclohexylphosphino-2',4',6'-triisopropylbiphenyl.

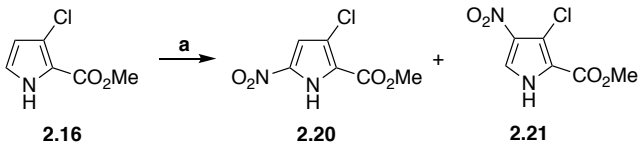
Table 2.1. Boronic acid reagents and yields for the synthesis of 2.17 to 2.19i via Suzuki coupling, followed by the synthesis of 2.17 to 2.19ii via methyl ester hydrolysis, showing the reaction yields.

Compound	Boronic acid	Yield of **i**	Yield of **ii**
2.17	Phenylboronic acid	83%	84%
2.18	*m*-Tolylboronic acid	86%	33%
2.19	3,5-Dimethylboronic acid	81%	61%

In order to increase the potency of inhibition, it was envisaged that more complex pyrrole analogues may be required, especially with functionalisation at the C-5 (or C-4) position(s) of the pyrrole 2-carboxylate core, e.g. nitration of the methyl ester intermediate **2.16** could lead to useful functionalisations. Given that pyrroles are sensitive towards strongly acidic conditions, nitration typically has to be carried out under relatively mild conditions with acetic anhydride and the slow addition of concentrated nitric acid at low temperatures[22], thus generating *in situ* the active nitrating agent, acetyl nitrate (Scheme 2.13). The lower the temperature, the greater the selectivity of nitration towards C-5 as opposed to the C-4 position[22]. However, by lowering the temperature, the overall yield of the reaction also decreases[22]. Noting the effect of temperature on pyrrole nitration, concentrated nitric acid was slowly added to **2.16** in acetic anhydride at -40 ºC. After 2.5 hours, a mixture of the nitrated isomers, **2.20** and **2.21** (nitrated at C-5 and C-4 respectively) was obtained, with yields varying from 13 to 40%, and the C-5:C-4 isomeric ratio between 2:1 and 1:1. **2.20** and **2.21** could be distinguished from their proton NMR spectra. With pyrroles, a proton in the C-5 position (**2.21**) will result in a proton shift that is significantly more downfield (8.19 ppm) than a proton in the C-4 position (7.05 ppm; **2.20**), due to the electronegativity of the pyrrole nitrogen atom (N-1).

The reaction intermediate, acetyl nitrate, is known to be shock sensitive and explosive, and must be handled with care[23]. Therefore, other nitration methods with significantly better thermal stability were explored, including a method involving sodium nitrate, sulfur trioxide-pyridine (SO_3-pyridine), sodium bisulfate and sodium sulfate in acetonitrile (Scheme 2.13)[24]. In the literature, this reaction is reported to proceed with

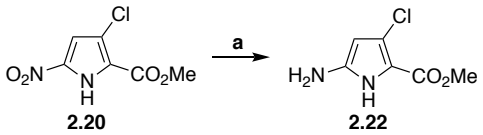
a different pyrrole at room temperature. However, by applying the modified method on **2.16**, no reaction was observed after 24 hours.



Scheme 2.13. *Nitration of 2.16*[22,24]*:*

a) method 1[22]: conc. nitric acid (1.5 equiv.), acetic anhydride, -40 °C, 2.5 h, 13 to 40%, 2:1 to 1:1 selectivity (2.20:2.21); method 2[24]: $NaNO_3$ (3 equiv.), $NaHSO_4$ (1.125 equiv.), Na_2SO_4 (0.375 equiv.), SO_3-pyridine (1.55 equiv.), MeCN, N_2, r.t., 24 h, reaction unsuccessful.

From the nitrated intermediates, **2.20** and **2.21**, reduction of the nitro group was envisaged. An iron-mediated reduction procedure was used by reacting **2.20** with iron power and ammonium chloride in ethanol and water (10:1 v/v) under reflux, which gave **2.22** in quantitative yield (Scheme 2.14)[25].

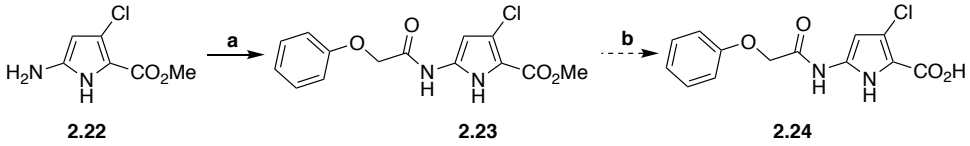


Scheme 2.14. *Reduction of the 5-nitro group of 2.20*[25]*:*

a) Fe (5.5 equiv.), NH_4Cl (0.7 equiv.), EtOH/H_2O (10:1 v/v), reflux, 1 h, quant.

Initially, an amide coupling reaction was attempted on **2.22** in order to mimic the amide side chain in penicillin V, in part hoping to achieve some similarities with the natural *β*-lactam substrate in its binding mode with MBLs (Figure 2.9). Reacting **2.22** with phenoxylacetyl chloride and 1-hydroxylbenzotriazole hydrate (HOBt) in anhydrous acetonitrile and pyridine (4:1 v/v), gave **2.23** after 21 hours in 52% yield. The subsequent hydrolysis of **2.23** in basic aqueous conditions proved to be challenging, likely due to the presence of acidic protons in **2.23** as well as the effects of solvent. With sodium hydroxide in tetrahydrofuran (THF) and water (1:1 v/v), no product was observed after an overnight reaction with **2.23** at room temperature. It

was speculated that the presence of additional acidic proton on the amide side chain may hinder alkaline hydrolysis. **2.23** was also found to be relatively insoluble in methanol and ethanol (Scheme 2.15).



2.22 **2.23** **2.24**

Scheme 2.15. *Amine functionalisation of 2.22 via an amide coupling reaction and ester hydrolysis:* **a)** $PhOCH_2COCl$ (5 equiv.), HOBt* (5 equiv.), anhydrous MeCN/pyridine (4:1 v/v), N_2, 0 °C to r.t., overnight, 52%; **b)** NaOH (5 equiv.), THF/H_2O (1:1 v/v), r.t., overnight, reaction unsuccessful. *1-Hydroxylbenzotriazole hydrate.

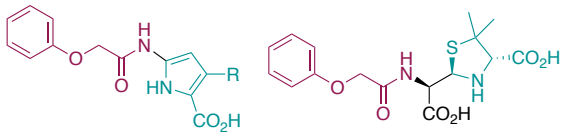
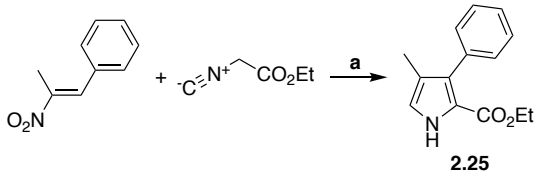


Figure 2.9. The phenoxyacetyl side chain was chosen to be expanded upon the C-5 position of the pyrrole core (red). A pyrrole core may mimic the five-membered ring of hydrolysed penicillin substrate (green).

An alternative synthetic route, which may grant access to a new precursor, **2.25**, with a methyl substitution at the C-4 position of the pyrrole ring was envisaged. This employed a Barton-Zard reaction featuring a (3-2) cycloaddition between a vinyl nitrate and an isonitrile [26] . Reacting *trans*-β-methyl-β-nitrostyrene, ethyl isocyanoacetate and 1,8-diazabicyclo[5.4.0]undec-7-ene (DBU) in THF and isopropanol (3:1 v/v) for four hours afforded **2.25** in 93% yield (Scheme 2.16)[26].



2.25

Scheme 2.16. *Barton-Zard synthesis of a pyrrole precursor* ***2.25***[26]*:*
a) DBU (2 equiv.), THF/^{i}PrOH (3:1 v/v), 10 °C to r.t., 4 h, 93%.

Using a similar scheme with additional steps, another pyrrole analogue, **EBL-1291** was synthesised by Dr. Tharindi Panduwawala in the Schofield Group (Figure 2.10). **EBL-1291** displays potent inhibition against a panel of clinically relevant MBLs, including a pIC_{50} of 8.9 against VIM-2. This positive result further reaffirmed the potential of pyrrole 2-carboxylate derivatives as promising leads for MBL inhibition. From a crystal structure of **EBL-1291** with VIM-2 (Figure 2.10), which was obtained by Dr. Jürgen Brem in the Schofield group, the pyrrole binding mode involving interactions between the nitrogen atom of the pyrrole ring with the bridging hydrolytic water was revealed. While the same nitrogen atom as well as the 2-carboxylate group are likely to bind to Zn2, interactions with surrounding active site residues may not be optimal, as interactions between aryl substitutions of **EBL-1291** at both C-5 and C-3 and hydrophobic residues at the L3 loop, such as Phe-61 and Tyr-66, are relatively 'loose'; the distance observed between the 5-phenyl group of **EBL-1291** and Phe-61 was 4.1Å, while that between the 3-(3,5-dichlorophenyl) group of **EBL-1291** and Tyr-66 was 3.6 Å. This suggests the importance of functionalising the C-3, C-4 and/or C-5 positions in order to improve interactions and potency.

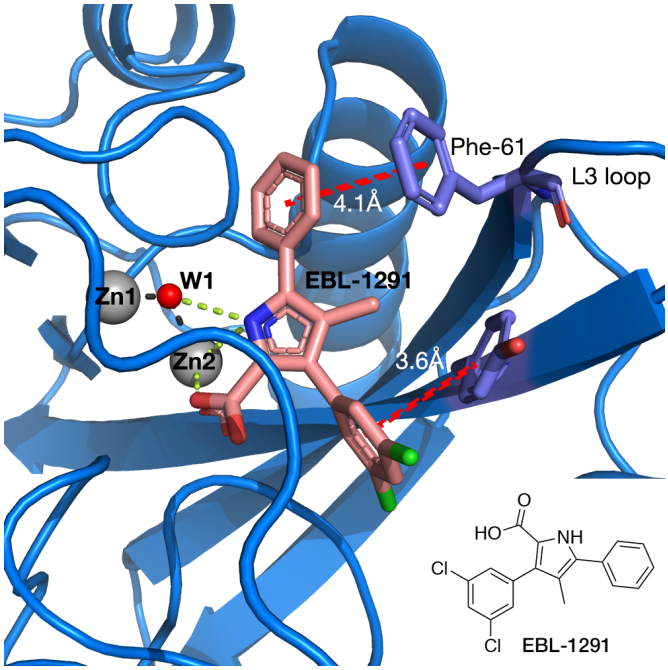
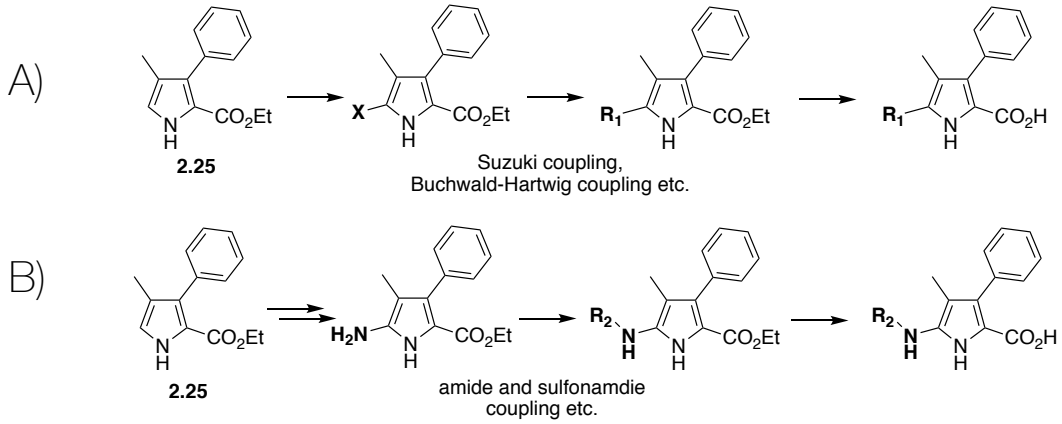


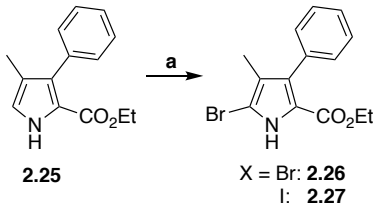
Figure 2.10. View from a crystal structure of **EBL-1291** with VIM-2 using PyMOL. Note that the nitrogen atom of the pyrrole seemingly interacts with both Zn2 and the bridging water molecule W1. The 2-carboxylate group chelates to Zn2. Notably, interactions of the C-3 and C-5 aryl groups with the L3 loop residues, such as Phe-61 and Tyr-66, are relatively 'loose' (red; 4.1 Å and 3.6 Å respectively), suggesting an opportunity to optimise their interactions.

While colleagues in the Schofield Group have focused primarily on the SAR at the C-3 position of the pyrrole core, there was a lack of understanding of how different groups in the C-5 position can affect potency. Therefore, synthetic methods were explored using **2.25** to investigate flexibility at the C-5 position of the pyrrole ring. It was envisioned that this could be achieved via either halogenation of the C-5 position of the pyrrole ring, which would enable further substitution reactions e.g. via Suzuki coupling, or amination, which would enable subsequent coupling reactions to form various amides and sulfonamides (Scheme 2.17).



Scheme 2.17. From compound **2.25**, it was envisioned that C-5 functionalisation could be achieved via two broad strategies: 1) halogenation using reagents such as NBS and NIS could be achieved, followed by metal-catalysed coupling reactions such as Suzuki reactions, Buchwald-Hartwig reactions as well as Ullmann-type reactions (A); 2) reductive amination could be achieved via nitration and from the free amine, it would be possible to carry out a wide array of functionalisation using reactions such as those involving amide and sulfonamide coupling (B).

From **2.25**, a reaction with NBS in *N,N*-dimethylformamide (DMF) after two hours afforded the C-5 brominated product, **2.26**, in 72% yield[27]. Iodination was also performed on **2.25** at the C-5 position using *N*-iodosuccinamide (NIS) in DMF, which produced **2.27** in 75% yield (Scheme 2.18).



Scheme 2.18. *Halogenation of the C-5 position of 2.25*[27]*:*

a) X = Br: NBS* (1.1 equiv.), DMF, r.t., 2 h, 72% or X = I: NIS** (1.1 equiv.), DMF, r.t., 2 h, 75%.

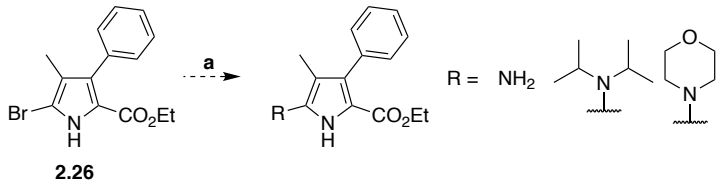
**N*-Bromosuccinimide.

***N*-Iodosuccinimide.

Subsequent attempts to optimise Buchward-Hartwig cross coupling reactions using **2.26** were unsuccessful. Direct formation of an amine in the C-5 position of **2.26** with benzophenone imine, tris(dibenzylideneacetone)dipalladium(0), 2-di-*tert*-butylphosphino-2',4',6'-triisopropylbiphenyl (^{t}BuXPhos) and tripotassium phosphate in dimethoxyethane (DME) was unfruitful[28]; reaction at both 30 and 50 °C afforded no

desired product after 24 hours. To afford a diisopropylamine at the C-5 position, **2.26** was reacted with diisopropylamine, palladium(II) acetate, 2-dicyclohexylphosphino-2',6'-diisopropoxybiphenyl (RuPhos) and LiHMDS in THF, but no reaction was observed after 24 hours. In an attempt to introduce a morpholine ring at the C-5 position, **2.26** was reacted with morpholine, tris(dibenzylideneacetone)dipalladium(0), ^{t}BuXPhos and sodium *tert*-butoxide in toluene at 110 ºC, but again no reaction was observed after 24 hours (Table 2.2).

Table 2.2. Reactions and conditions attempted to achieve Buchwald-Hartwig cross coupling in order to enable C-5 functionalisation of pyrroles from **2.26**. All reactions were unsuccessful.



2.26

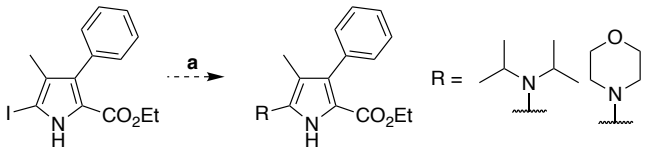
Amine	Catalyst	Phosphine ligand	Base	Solvent	Temperature
Benzophenone imine (1.2 equiv.)[15]	$Pd_2(dba)_3$ (3 mol. %)	^{t}BuXPhos (9 mol. %)	K_3PO_4 (2.5 equiv.)	DME*	30 ºC
Benzophenone imine (1.2 equiv.)[15]	$Pd_2(dba)_3$ (3 mol. %)	^{t}BuXPhos (9 mol. %)	K_3PO_4 (2.5 equiv.)	DME*	50 ºC
Diisopropylamine (1.2 equiv.)	$Pd(OAc)_2$ (1 mol. %)	RuPhos (3 mol. %)	LiHMDS (1.2 equiv.)	THF	r.t.
Morpholine (1.5 equiv.)	$Pd_2(dba)_3$ (2.5 mol. %)	^{t}BuXPhos (10 mol. %)	NaO^{t}Bu (2 equiv.)	Toluene	110 ºC

*Dimethoxyethane.

Attempts to optimise Ullmann-type coupling reactions using **2.27** were also unsuccessful. To afford a diisopropylamine at the C-5 position, **2.27** was reacted with diisopropylamine, copper(I) iodide, 2-isobutyrylcyclohexanone and caesium carbonate in DMF at room temperature, but no reaction was observed after 24 hours. To afford a morpholine at the C-5 position, **2.27** was reacted with morpholine,

copper(I) iodide, 2-isobutyrylcyclohexanone and caesium carbonate in DMF at room temperature, but again no reaction was observed after 24 hours (Table 2.3).

Table 2.3. Reactions and conditions attempted to achieve Ullmann-type coupling reactions in order to enable C-5 functionalisation of pyrroles from **2.27**. All reactions were unsuccessful.

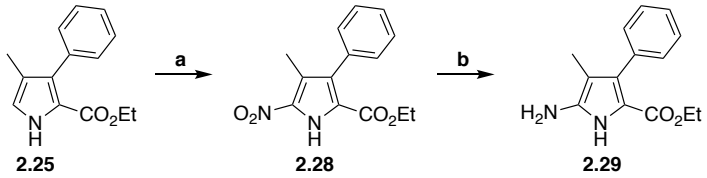


2.27

Amine	Catalyst	Ligand	Base	Solvent	Temperature
Diisopropylamine (1.5 equiv.)	CuI (5 mol. %)	2-Isobutyrylcyclohexanone (20 mol. %)	Cs_2CO_3 (2 equiv.)	DMF	r.t.
Morpholine (1.5 equiv.)	CuI (5 mol. %)	2-Isobutyrylcyclohexanone (20 mol. %))	Cs_2CO_3 (2 equiv.)	DMF	r.t.

Failure to carry out successful Buchwald-Hartwig and Ullmann-type coupling could possibly be due to the fact that 2-pyrrole carboxylates can function as metal chelators, thus rendering the metal catalysts ineffective *in situ*.

As reported earlier, it was proposed that amination at the C-5 position could be achieved via a nitro-containing intermediate (**2.20**). Thus, from **2.25**, a similar nitration was conducted using concentrated nitric acid in acetic anhydride at -40 ºC, to afford **2.28** in 28% yield after two hours[22]. An iron-mediated reduction was then performed on **2.28**, using iron powder, ammonium chloride in ethanol and water (10:1 v/v). After refluxing for an hour, **2.29** was produced in quantitative yield (Scheme 2.19)[25].



Scheme 2.19. *C-5 amination of a pyrrole precursor* ***2.25*** *via nitration followed by reduction*[22,25]*:* **a)** conc. nitric acid (1.5 equiv.), acetic anhydride, -40 °C, 2 h, 28%[22]; **b)** Fe (5.5 equiv.), NH_4Cl (0.7 equiv.), $EtOH/H_2O$ (10:1 v/v), reflux, 1 h, quant[25].

Unfortunately, despite the successful synthesis of various pyrrole analogues, their half-life and coverage of clinically relevant MBL spectrum have, to date, proven to be unsatisfactory as revealed in unpublished results from a collaborative project between the Schofield Group and several other institutions (ENABLE). In comparison, indole analogues, which presented a similar mode of inhibition to the pyrroles, have provided better potential for optimisation. In agreement with the initial hypothesis, pyrrole and indole analogues, unlike **F32**, were found to interact with the di-zinc ion bridging water molecule from crystal structures obtained by Dr. Jürgen Brem. Since the development of indole analogues conferred lower risks of attrition, the pursuit of pyrrole analogues was halted, and no further analogues were synthesised following the successful synthesis of **2.29**.

2.4. Synthesis of a nitropyrrole analogue as a potential MBL detection assay substrate

While the clinical relevance of pyrrole-based MBL inhibitors is not currently evident, their potential use in academic research remains sanguine. As previously discussed, nitropyrrole analogues such as **2.20** and **2.28** could be accessed via mild and calculated nitration conditions. Historically, nitro compounds have been known for their chromophoric properties, caused by unsaturation within the nitro group. For example, nitrocefin, a cephalosporin analogue which contains an extensive conjugated system with two nitro groups (Figure 2.11), is used as a valuable

chromogenic substrate in β-lactamase assays[29]. Therefore, it was envisioned that a nitropyrrole analogue could be exploited in MBL detection assays.

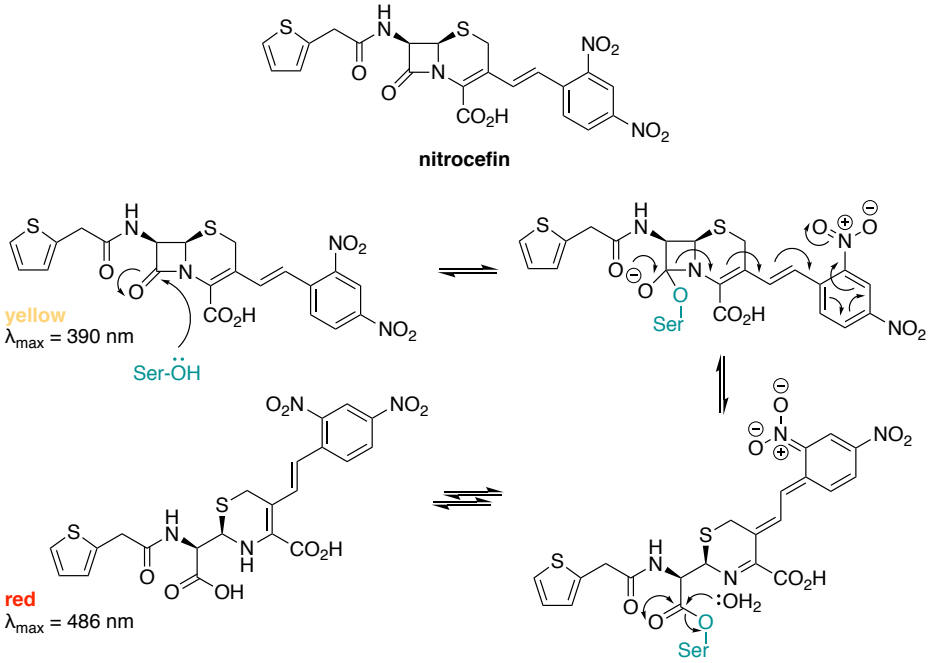
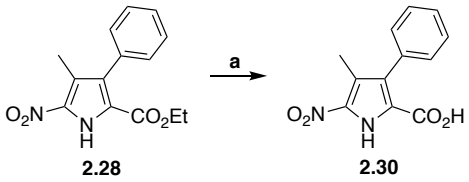


Figure 2.11. The importance of the nitro group in chromogenic assays in the β-lactamase field, as exemplified by nitrocefin. Nitrocefin contains (two) nitro groups, giving an extended conjugation system in a cephalosporin scaffold. In its unhydrolysed form, the maximum absorbance is at 390 nm, which results in a yellow colour. However, upon hydrolysis by an SBL, the ring-opened product has a maximum absorbance at 486 nm, which results in a red colour. This colour change has been successfully exploited in various β-lactamase assays[29].

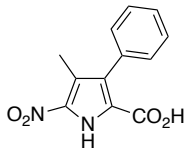
Therefore, a nitropyrrole analogue, **2.30**, was successfully synthesised. Hydrolysis of the ethyl ester (**2.28**) was achieved under aqueous alkaline conditions using 1 M sodium hydroxide aqueous solution (THF/methanol, 3:1 v/v) after a 12-hour reaction at ambient temperature in 66% yield (Scheme 2.20). In an inhibition screening conducted by Corentin Bon (former Schofield Group member) using an existing platform[8], it was revealed that **2.30** displays significant inhibition of VIM-2 (Table 2.4 and Figure 2.12).



Scheme 2.20. *Synthesis of a nitropyrrole inhibitor of MBLs, 2.30:*

a) 1 M NaOH (aq) (5 equiv.), THF/MeOH (3:1 v/v), r.t., 12 h, 66%.

Table 2.4. Inhibition studies of nitropyrrole analogue **2.30** with VIM-2, compared against a known inhibitor, L-captopril.



2.30

Molecular Weight: 246.22
H-bond donors: 2
H-bond acceptors: 4
CLogP: 1.681

	pIC_{50}*
Compound	VIM-2
2.30	7.3 ± 0.02
L-Captopril**	6.1 ± 0.02

*Inhibition studies were performed on a standard fluorogenic assay platform involving FC-5[8] and a panel of clinically relevant MBLs. Courtesy of Corentin Bon (former Schofield Group member).

**L-Captopril was used as a control for positive MBL inhibition.

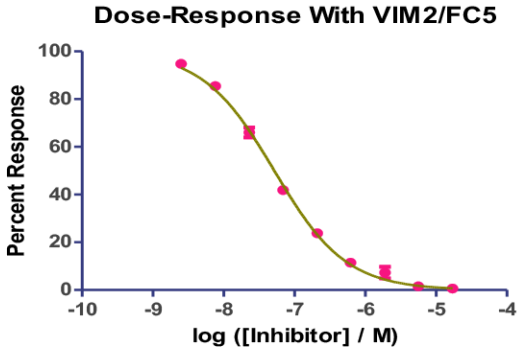


Figure 2.12. Graph showing the inhibition of VIM-2 by **2.30**, measured by the percent response illustrated by the hydrolysis of FC-5, against log (inhibitor concentration, measured in M)[8]. Courtesy of Corentin Bon (former Schofield Group member).

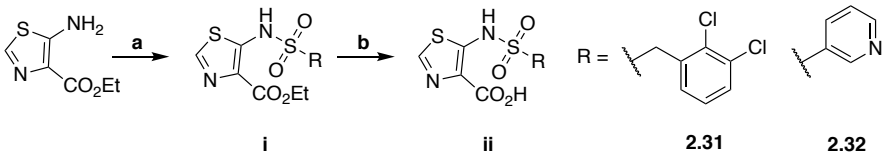
While **2.30** has displayed potent inhibition with VIM-2, its chromogenic properties need to be further investigated before validation as a useful MBL probe. In particular, it remains unknown whether a detectable change in absorbance could be observed when **2.30** is bound to an MBL.

2.5. Synthesis and MBL inhibition studies of thiazole carboxylate derivatives

Given **F32** contains an isothiazole core, it was considered that compounds bearing a thiazole core may be of interest. A series of 4-thiazolecarboxylates have been developed and tested as part of the antibacterial pipeline of Antabio[7]. The structural similarities between the thiazole series and the compounds explored thus far, as well as the apparently positive inhibitory profiles, were of interest. Therefore, two thiazole analogues, **2.31ii** and **2.32ii** were chosen due to their reported MBL inhibition potential and synthesised according to literature procedures[7].

To synthesise **2.31ii**, (2,3 dichlorophenyl)methanesulfonyl chloride and triethylamine were reacted with 5-amino-thiazole-4-carboxylic acid ethyl ester in 1,4-dioxane at 60 ºC for 24 hours, which afforded intermediate **2.31i** in 53% yield. **2.31i** was then hydrolysed with lithium hydroxide monohydrate in THF and methanol (1:1 v/v) at 50 ºC (18 hours) to afford **2.31ii** in 86% yield. To synthesise **2.32ii**, pyridine-3-sulfonyl chloride was reacted with 5-amino-thiazole-4-carboxylic acid ethyl ester in pyridine at 50 ºC for three hours to afford intermediate **2.32i** in 17% yield. **2.32i** was then hydrolysed, again with lithium hydroxide monohydrate in a mixture of THF and methanol (1:1 v/v) at 50 ºC (18 hours), to obtain **2.32ii** in 78% yield (Scheme 2.21).

When **2.31ii** and **2.32ii** were tested against a panel of clinically relevant MBLs (NDM-1, IMP-1, VIM-1 and VIM-2) by Dr. Gareth Langley (Schofield Group), they presented potent inhibition (Table 2.5, Figure 2.13A-D and Figure 2.14A-D)[8].



Scheme 2.21. *Synthesis of thiazole inhibitors of MBLs, 2.31ii and 2.32ii*[7]*:*

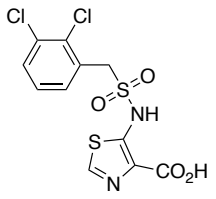
For the synthesis of 2.31ii:

a) R-SO_2Cl (1.2 equiv.), Et_3N (5 equiv.), 1,4-dioxane, 60 ºC, 24 h, 53%; b) $LiOH•H_2O$ (5 equiv.), THF/MeOH (1:1 v/v), r.t., 18 h, 86%;

For the synthesis of 2.32ii:

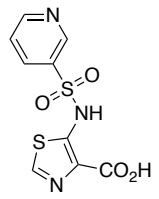
a) R-SO_2Cl (1.35 equiv.), pyridine, 50 ºC, 3 h, 17%; b) $LiOH•H_2O$ (5 equiv.), THF/MeOH (1:1 v/v), r.t., 18 h, 78%.

Table 2.5. Inhibition studies of thiazole analogues 2.31ii and 2.32ii with a panel of clinically relevant MBLs, compared against a known MBL inhibitor, L-captopril.



2.31ii

Molecular Weight: 367.22
H-bond donors: 2
H-bond acceptors: 5
CLogP: 3.047



2.32ii

Molecular Weight: 285.29
H-bond donors: 2
H-bond acceptors: 6
CLogP: 0.185

	pIC_{50}*			
Compound	NDM-1	IMP-1	VIM-1	VIM-2
2.31ii	7.5 ± 0.07	8.1 ± 0.20	7.3 ± 0.15	9.9 ± 0.03
2.32ii	6.8 ± 0.04	*3.5 ± 1.2*	5.0 ± 0.21	6.6 ± 0.03
L-Captopril**	5.0 ± 0.04	5.8 ± 0.025	5.6 ± 0.03	6.1 ± 0.02

*Inhibition studies were performed on a standard fluorogenic assay platform involving FC-5[8] and a panel of clinically relevant MBLs. Courtesy of Dr. Gareth Langley (Schofield Group).

**L-Captopril was used as a control for positive MBL inhibition.

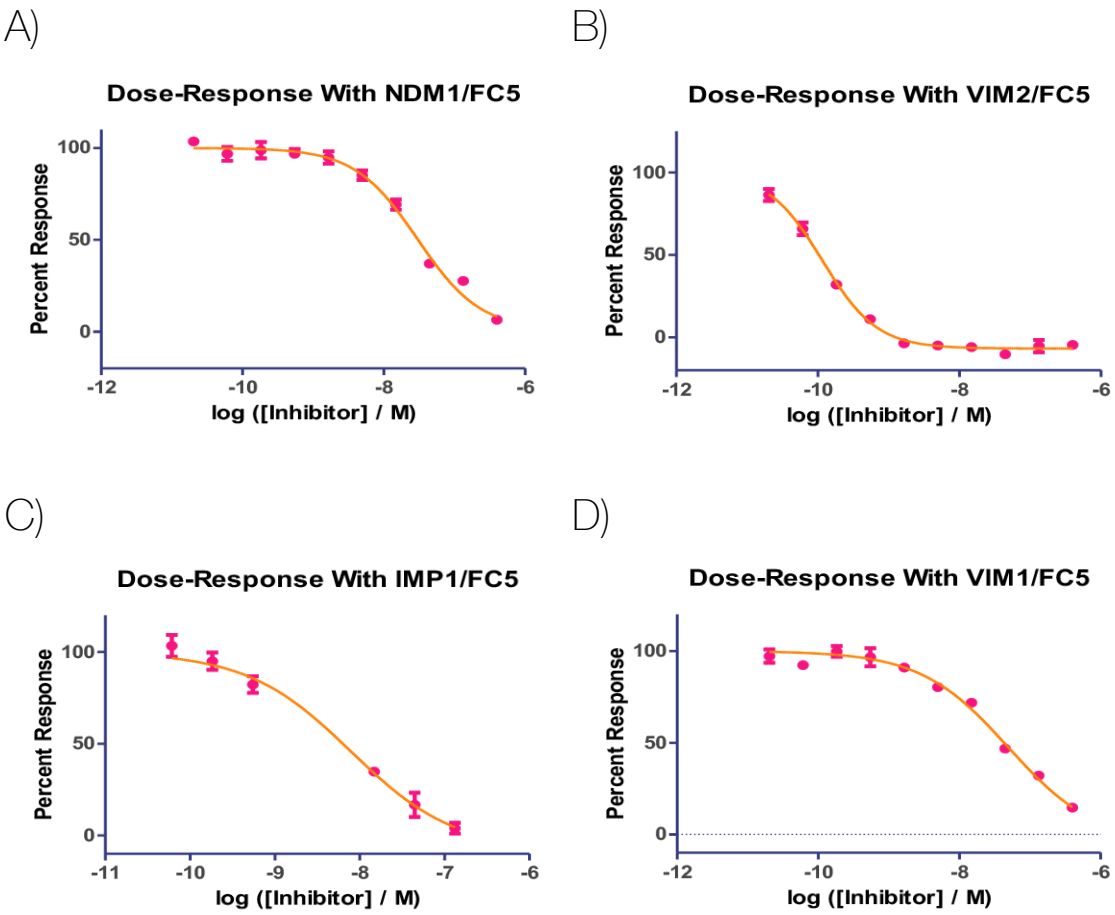


Figure 2.13. Plots showing the inhibition of various MBLs by 2.31ii, measured by the percent response illustrated by the hydrolysis of FC-5, against log (inhibitor concentration, measured in M)[8]. The MBLs tested are as follows: (A) NDM-1, (B) VIM-2, (C) IMP-1 and (D) VIM-1. Courtesy of Dr. Gareth Langley (Schofield Group).

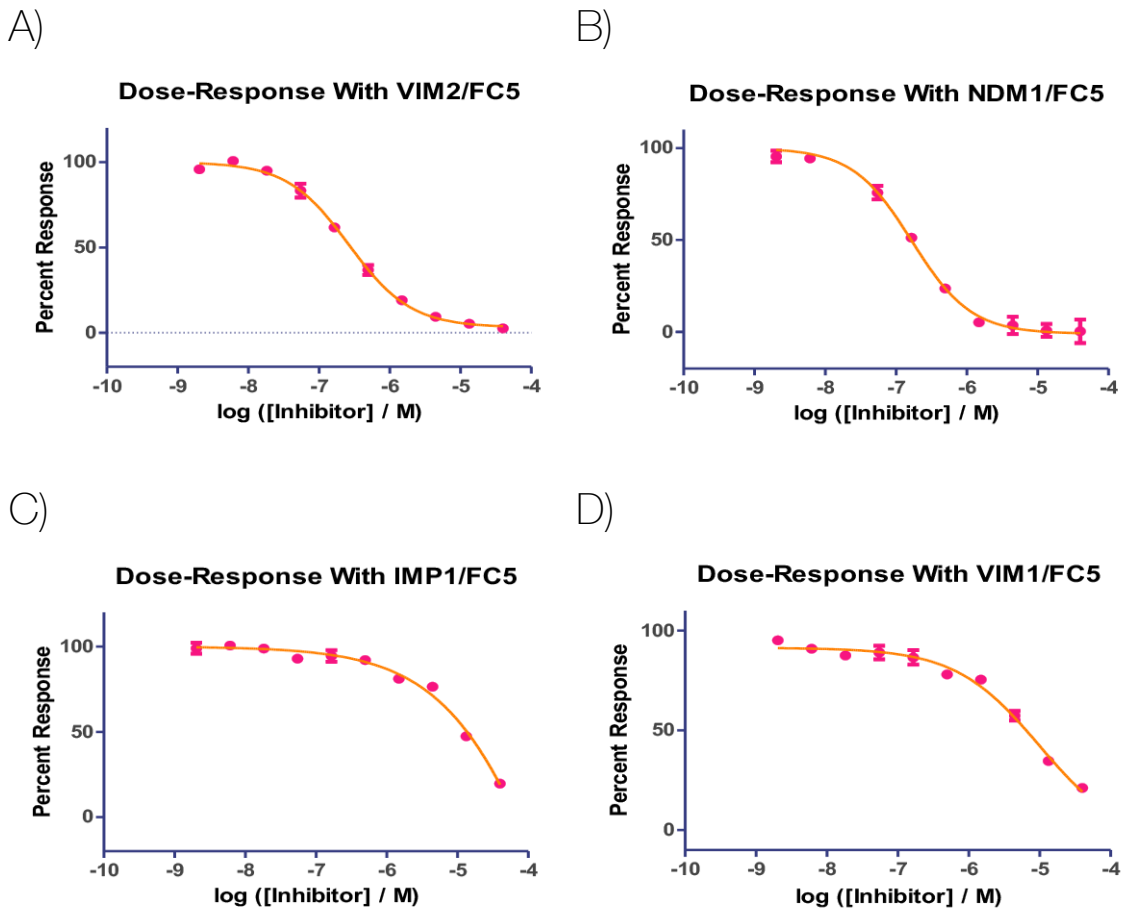


Figure 2.14. Plots showing the inhibition of various MBLs by 2.32ii, measured by the percent response illustrated by the hydrolysis of FC-5, against log (inhibitor concentration, measured in M)[8]. The MBLs tested are as follows: (A) NDM-1, (B) VIM-2, (C) IMP-1 and (D) VIM-1. Courtesy of Dr. Gareth Langley (Schofield Group).

A crystal structure of **2.31ii** bound to VIM-2 was successfully obtained by Dr. Jürgen Brem from the Schofield Group (Figure 2.15). The structure reveals a binding mode that is similar to that observed with **F32**, including chelation of Zn2 by both the nitrogen atom of the heteroaryl core as well as the 4-carboxylate group, and interactions between the C-5 sulfonamide substitution and Tyr-66 from the L3 loop. As with **F32**, there was no evidence for any direct interactions with the hydrolytic water molecule that bridges the two zinc ions (Figure 2.15).

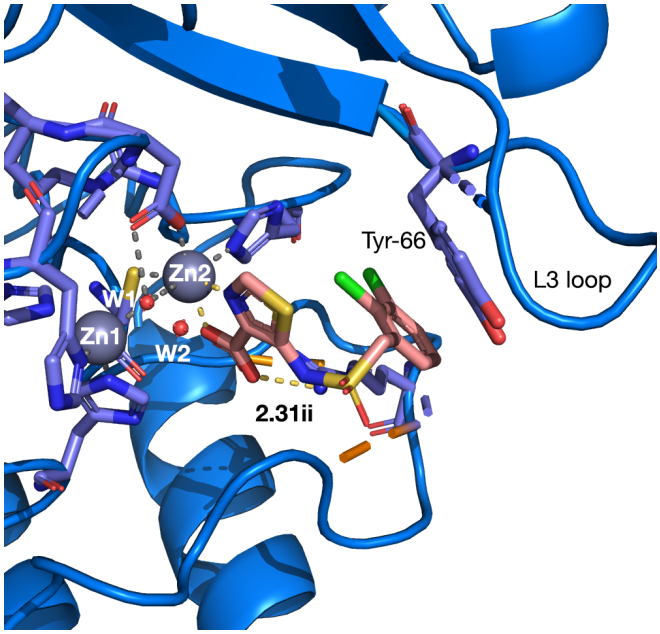


Figure 2.15. View from a crystal structure of **2.31ii** bound to VIM-2 using PyMOL. The binding mode of **2.31ii** is very similar to that of **F32**. The C-5 sulfonamide of **2.31ii** is positioned to form favourable interactions with Tyr-66 at the L3 loop. Chelation of Zn2 by both the nitrogen atom of the heteroaryl core and the 4-carboxylate group is observed. Interactions with the hydrolytic water molecule appear to be absent.

2.6. Structure-activity relationship and optimisation studies of analogues of F52

While **F32** and the related pyrrole analogues (e.g. **2.30**) may mimic the structures of five-membered hydrolysed products from *β*-lactam antibiotics featuring bicyclic 4-5 ring systems, such as penams and penems, **F52** bears resemblance to the six-membered hydrolysed products of cephems, as depicted earlier (Figure 2.4). The interactions of **F52** with the MBL active site can be further illustrated by a crystal structure of it complexed with VIM-2 (Figure 2.16). From this crystal structure, it was observed that, albeit the absence of favourable interactions with the L3 loop, interactions between F52 and both Zn2 and the bridging water molecule were evident; these involved both the pyridine nitrogen atom as well as the 2-carboxylate group. Picolinates have similar structures to **F52** and have long been known to inhibit MBLs[5]. However, the initial finding that **F35**, a benzoate, could bind to and inhibit MBL was significant, since it suggested that the presence of a heteroatom on the aromatic ring core, which was previously thought to be essential in zinc chelation, might in fact be dispensable.

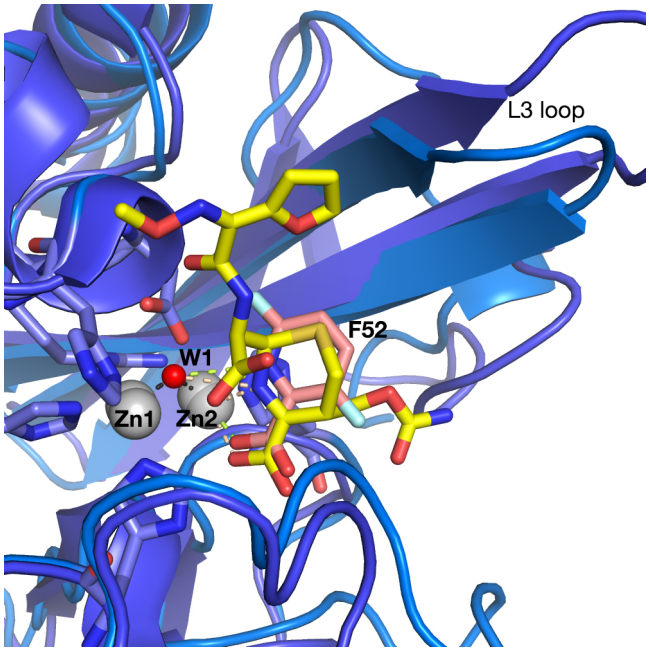
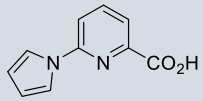
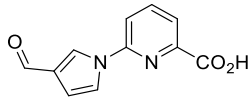
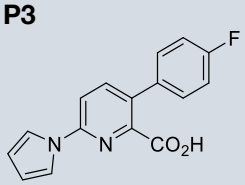


Figure 2.16. View from a crystal structure of F52 (pink) bound to VIM-2 using PyMOL. The binding mode differs from F32 in that in addition to Zn2, interactions are also observed with the bridging hydrolytic water molecule (W1), via both the pyridine nitrogen atom and the 2-carboxylate group. However, due the lack of structural complexity in this fragment, no favourable interactions are observed between F52 and the L3 loop, which suggests the possibility of optimisation via C-3 or C-4 functionalisations. This crystal structure is overlaid with the hydrolysed product of cefuroxime (yellow), a cephalosporin, which bears a six-membered ring resembling F52, while bound to NDM-1 *(RCSB PDB ID: 4RL0).*

Building the basis of this project, Dr Anna Rydzik (former Schofield Group member) had previously overlaid the structures of **F35** and **F52** with **F47**, an active site binder that did not coordinate to zincs (Figure 2.5), and subsequently synthesised pyridine-based compounds **P1**, **P2** and **P3**. Screening of these compounds[8] with a panel of clinically relevant MBLs revealed little or only weak inhibition (Table 2.6).

Table 2.6. Inhibition studies of pyridine analogues P1, P2 and P3 with a panel of clinically relevant MBLs, compared against a known inhibitor, L-captopril.

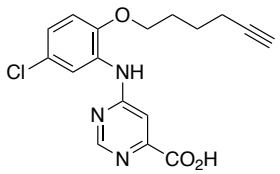
		pIC_{50}*		
Compound	NDM-1	IMP-1	VIM-1	VIM-2
P1 	< 3.0	3.1 ± 0.078	< 3.0	3.6 ± 0.18
P2 	< 3.0	< 3.0	< 3.0	2.9 ± 0.49
P3 	< 3.0	< 3.0	3.7 ± 0.03	4.3 ± 0.08
L-Captopril**	5.0 ± 0.04	5.8 ± 0.025	5.6 ± 0.03	6.1 ± 0.02

*Inhibition studies were performed on a standard fluorogenic assay platform involving FC-5[8] and a panel of clinically relevant MBLs. Courtesy of Dr. Anna Rydzik.

**L-Captopril was used as a positive inhibition control of MBLs.

A further subject of inspiration originated from a compound identified as **ELF-128**, which bears a pyrimidine 4-carboxylate core. **ELF-128** was synthesised as part of a collaboration between the Schofield Group and the European Lead Factory. **ELF-128** displayed potent inhibition against various MBLs (Table 2.7).

Table 2.7. Inhibition studies of pyrimidine analogue **ELF-128** with a panel of clinically relevant MBLs, compared against a known MBL inhibitor, L-captopril.



ELF-128
Molecular Weight: 345.78
H-bond donors: 2
H-bond acceptors: 5
CLogP: 2.488

	pIC$_{50}$*	
Compound	NDM-1	VIM-2
ELF-128	5.6**	7.3**
L-Captopril**	5.0 ± 0.04	6.1 ± 0.02

*Inhibition studies were performed on a standard fluorogenic assay platform involving FC-5[8] and a panel of clinically relevant MBLs. Courtesy of Dr. Jürgen Brem.
**Errors of pIC$_{50}$ measurements were within 10% of recorded values.
***L-Captopril was used as a positive inhibition control of MBLs.

The synthesis of analogues of either a picolinate or a pyrimidine 4-carboxylate core, with a particular focus of functionalising the C-4 and C-6 positions of the aromatic ring core respectively, was targeted (Figure 2.17). It was proposed that not only would substitution at these positions would mimic the C-6 functionalisation present in **ELF-128**, they also in part mimic the C-3 functionalisation of the pyrroles (**2.17ii** to **2.19ii**) as well as C-4 functionalisation of the thiazoles (**2.31ii** and **2.32ii**).

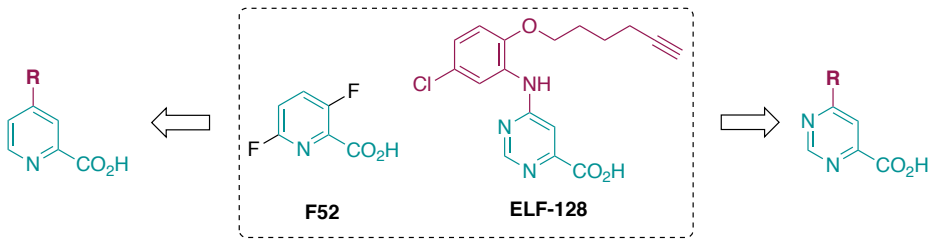


Figure 2.17. From **F52** and **ELF-128**, it was postulated that pyridine-2-carboxylates and pyrimidine-4-carboxylates, highlighted in green, offer promising leads as MBL inhibitors. In particular, functionalisation in C-4 and C-6 of the pyridine and pyrimidine ring, respectively, coloured in red, was of interest.

For the synthesis of picolinate analogues, methyl 4-bromopicolinate was identified as a possible precursor. It was envisaged that C-4 substitutions with aniline and its analogues, such as 3-chloroaniline, could be achieved via Buchwald-Hartwig cross coupling, Ullmann-type reactions or nucleophilic aromatic substitutions (Figure 2.18). However, Ullmann-type reactions were thought to be the least favourable, given that pyridines are known to chelate copper catalysts to form stable complexes. Therefore, reactions comprising Buchwald-Hartwig cross coupling and nucleophilic aromatic substitution were targeted.

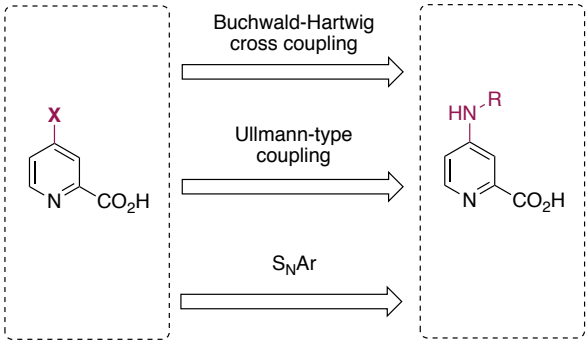


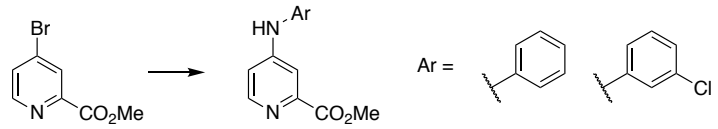
Figure 2.18. To achieve the desired C-4 substitution, it was envisioned that a Buchwald-Hartwig cross coupling, a Ullmann-type coupling or a nucleophilic aromatic substitution can be employed. As a starting point, the synthetic plan focused on amination, which resonates the structure of ELF-128.

In an attempt to carry out Buchwald-Hartwig cross coupling, methyl 4-bromopicolinate was initially reacted with aniline in a test reaction in the presence of palladium(II) acetate, 2-(dicyclohexylphosphino)3,6-dimethoxy-2',4',6'-triisopropyl-1,1'-biphenyl (BrettPhos) and potassium carbonate in *tert*-butanol at 80 °C. However, no reaction was observed despite carrying out the reaction for 48 hours.

A short study was then performed to identify the best phosphine ligand, solvent and temperature for this reaction. The conditions tested are summarised below (Table 2.8). Using LCMS to monitor the progress of reaction, it was identified that of those tested, the preferred phosphine ligand was 2-dicyclohexylphosphino-2',6'-

diisopropoxybiphenyl (RuPhos) and the best solvent was toluene at 100 ºC. Unfortunately, none of these methods yielded promising results, possibly due to the ability of picolinates to chelate the palladium catalyst.

Table 2.8. Reactions and conditions attempted achieve Buchwald-Hartwig cross coupling reactions in order to perform C-4 functionalisation of pyridines. All reactions were unsuccessful.



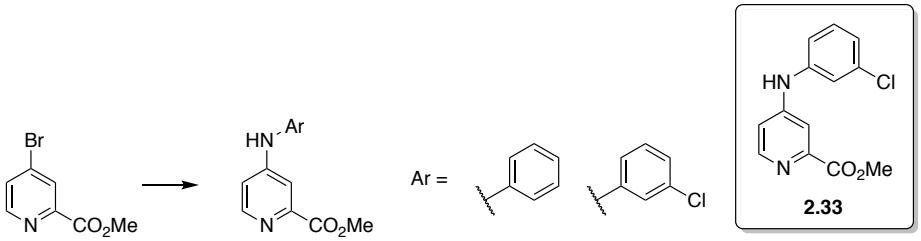
Amine	Catalyst	Phosphine ligand	Base	Solvent	Temperature
Aniline (1.5 equiv.)	$Pd(OAc)_2$ (1 mol. %)	BrettPhos (2 mol. %)	K_2CO_3 (2 equiv.)	^{t}BuOH	85 ºC
Aniline (1.5 equiv.)	$Pd(OAc)_2$ (1 mol. %)	BrettPhos (2 mol. %)	Cs_2CO_3 (2 equiv.)	^{t}BuOH	85 ºC
Aniline (1.5 equiv.)	$Pd(OAc)_2$ (1 mol. %)	XPhos (2 mol. %)	Cs_2CO_3 (2 equiv.)	^{t}BuOH	85 ºC
Aniline (1.5 equiv.)	$Pd(OAc)_2$ (1 mol. %)	RuPhos (2 mol. %)	Cs_2CO_3 (2 equiv.)	^{t}BuOH	85 ºC
Aniline (1.5 equiv.)	$Pd(OAc)_2$ (1 mol. %)	^{t}BuXPhos (2 mol. %)	Cs_2CO_3 (2 equiv.)	^{t}BuOH	85 ºC
Aniline (1.5 equiv.)	$Pd(OAc)_2$ (1 mol. %)	RuPhos (2 mol. %)	Cs_2CO_3 (2 equiv.)	Toluene	110 ºC
Aniline (1.5 equiv.)	$Pd(OAc)_2$ (1 mol. %)	RuPhos (2 mol. %)	Cs_2CO_3 (2 equiv.)	^{n}BuOH	120 ºC
Aniline (1.5 equiv.)	$Pd(OAc)_2$ (1 mol. %)	RuPhos (2 mol. %)	Cs_2CO_3 (2 equiv.)	1,4-Dioxane	100 ºC
Aniline (1.5 equiv.)	$Pd(OAc)_2$ (1 mol. %)	RuPhos (2 mol. %)	Cs_2CO_3 (2 equiv.)	THF	65 ºC
3-Chloroaniline (1.5 equiv.)	$Pd(OAc)_2$ (1 mol. %)	RuPhos (2 mol. %)	Cs_2CO_3 (2 equiv.)	Toluene	110 ºC

Reactions were carried out under inert atmospheres of nitrogen or argon and monitored for up to 48 hours.

Subsequently, nucleophilic aromatic substitution was attempted, since the C-4 position of pyridines is relatively activated towards a nucleophilic attack. It was noted that the presence of an electron-withdrawing carboxylate ester group at C-2 could possibly counteract such reaction. Thus, a base was introduced, though this could

interfere with the desired reaction, such as causing unwanted hydrolysis of the ester. Initial attempts involved using LiHMDS in THF at room temperature as well as 60 ºC; however the desired reaction was not observed. Upon further literature searches[30], LiHMDS was replaced with potassium fluoride, and the solvent swapped to either water or DMF at 100 ºC and 150 ºC respectively. From the reaction carried out in DMF at 150 ºC, a very low yield of 4% of **2.33** was obtained (Table 2.9). Hydrolysis of **2.33** to afford the final product was unsuccessful despite TLC revealing full conversion, possibly due to loss on purification due to the small scale.

Table 2.9. Reactions and conditions attempted to achieve nucleophilic aromatic substitution reactions in order to perform C-4 functionalisation of pyridines.



Amine	Base	Solvent	Temperature	Yield
Aniline (0.5 equiv.)	LiHMDS (1.5 equiv.)	THF	r.t.	-
3-Chloroaniline (0.5 equiv.)	LiHMDS (1.5 equiv.)	THF	r.t	-
Aniline (1 equiv.)	KF (2 equiv.)[30]	water	85 ºC	-
3-Chloroaniline (1 equiv.)	KF (2 equiv.)[30]	water	85 ºC	-
Aniline (1 equiv.)	KF (2 equiv.)[30]	DMF	85 ºC	-
3-Chloroaniline (1 equiv.)	KF (2 equiv.)[30]	DMF	85 ºC	4%

2.7. Structure-activity relationship studies of ELF-128

No pyrimidine analogues of **ELF-128** had been documented prior to this work. It was uncertain whether the C'-2 alkyl chain with a terminal alkyne was necessary for potent inhibition. Therefore, four pyrimidine analogues, **2.34ii** to **2.37ii**, were synthesised. These compounds were selected by breaking down the structural complexity of **ELF-128** (Figure 2.19). Using a modified literature method[31], a series of nucleophilic aromatic substitution reactions were carried out with 6-chloro-pyrimidine-4-carboxylate ethyl ester, a commercially available precursor, in the presence of corresponding aniline analogues in isopropanol. After refluxing for 24 hours, esters **2.34i** to **2.37i** were afforded. These were hydrolysed using lithium hydroxide monohydrate in THF, methanol and water (3:1:1 v/v) (50 ºC overnight) to produce **2.34ii** to **2.37ii** respectively (Scheme 2.22).

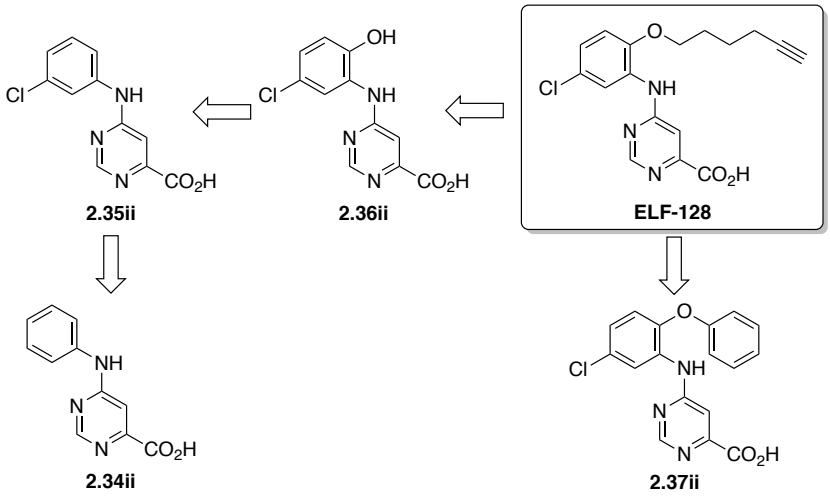
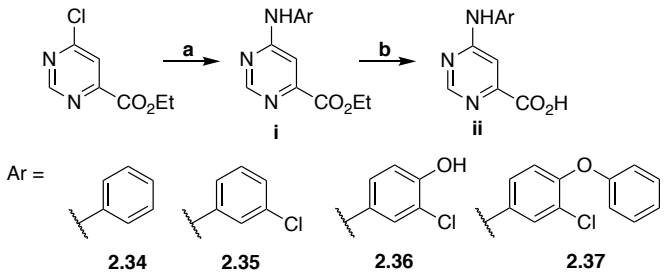
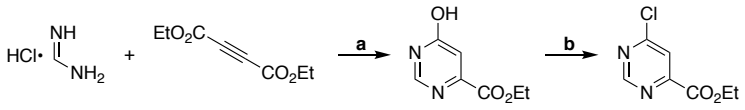


Figure 2.19. From, ELF-128, the extended alkyl chain could be removed in order to determine its impact on potency by making compound 2.36ii. Its structure could be further simplified by removing the *ortho*-hydroxyl group and *meta*-chloro group by synthesising 2.35ii and 2.34ii respectively. Further, in replacement of the extended alkyl chain, other groups such as a simple phenyl group could also be synthesised to observe its impact on potency, via the production of 2.37ii.



Scheme 2.22. *Synthesis of pyrimidine analogues[31]:*
a) Ar-NH_2 (1.2 equiv.), ^{i}PrOH, reflux, 24 h, **2.25i**: 62%, **2.26i**: 21%, **2.27i**: 21%, **2.28i**: 26%; b) LiOH•H_2O (5 equiv.), THF/MeOH/H_2O (3:1:1 v/v/v), 50 ºC, overnight, **2.25ii**: 100%, **2.26ii**: 20%, **2.27ii**: 37%, **2.28ii**: 16%.

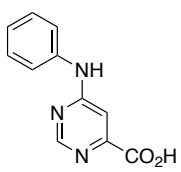
It was noted that the high cost of the starting material, 6-chloro-pyrimidine-4-carboxylate ethyl ester, could be potentially overcome by synthesis in reportedly high yield of over 80% over two steps from affordable precursors and reagents[32]. (3+3) Cycloaddition reaction between formamidine and diethyl acetylenedicarboxylate produces ethyl 6-hydroxypyrimidine-4-carboxylate[32]. Chlorination can be subsequently achieved (Scheme 2.23)[31]. However, due to time constraints, this precursor was not synthesised in-house and was commercially procured.



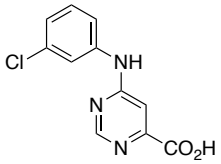
Scheme 2.23. *Example of an efficient synthetic route to access a useful precursor[32]:*
a) Et_3N (1 equiv.), MeCN, 80 ºC, 2.5 h, 86%; b) oxalyl chloride (3 equiv.), DMF (cat.), EtOAc, Ar, 75 ºC, 12 h, 100%.

Upon their successful synthesis, the four pyrimidine analogues, **2.34ii** to **2.37ii**, were tested against a panel of clinically relevant MBLs for inhibition using a platform involving FC-5 as a fluorogenic substrate[8] by Dr. Gareth Langley (Schofield Group. The results of this study are summarised in Table 2.10.

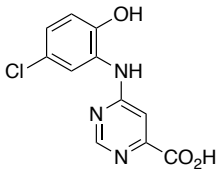
Table 2.10. Inhibition studies of various pyrimidine analogues with a panel of clinically relevant MBLs, compared against known inhibitors, L-captopril and **ELF-128**.



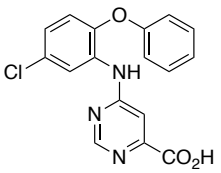
2.34ii
Molecular Weight: 215.21
H-bond donors: 2
H-bond acceptors: 4
CLogP: 0.569



2.35ii
Molecular Weight: 249.65
H-bond donors: 2
H-bond acceptors: 4
CLogP: 1.282



2.36ii
Molecular Weight: 265.65
H-bond donors: 3
H-bond acceptors: 4
CLogP: 0.615



2.37ii
Molecular Weight: 341.75
H-bond donors: 2
H-bond acceptors: 5
CLogP: 3.38

	pIC_{50}*			
Compound	NDM-1	IMP-1	VIM-1	VIM-2
2.34ii	4.5 ± 0.03	3.4 ± 0.02	4.5 ± 0.03	5.1 ± 0.02
2.35ii	3.8 ± 0.14	3.7 ± 0.05	3.7 ± 0.05	3.7 ± 0.04
2.36ii	4.7 ± 0.05	4.1 ± 0.05	6.1 ± 0.06	5.7 ± 0.04
2.37ii	5.3 ± 0.04	5.0 ± 0.03	5.3 ± 0.02	5.5 ± 0.02
ELF-128	5.6**	*N/A*	*N/A*	7.3**
L-Captopril**	5.0 ± 0.04	5.8 ± 0.025	5.6 ± 0.03	6.1 ± 0.02

*Inhibition studies were performed on a standard fluorogenic assay platform involving FC-5[8] and a panel of clinically relevant MBLs. Courtesy of Dr. Gareth Langley.

**Errors of pIC_{50} measurements were within 10% of recorded values.

***L-Captopril was used as a positive inhibition control for MBLs.

From these studies, **2.37ii** was identified as the best inhibitor compared to **2.34ii**, **2.35ii** and **2.36ii**. **2.36ii** presented relatively high selectivity for the VIM classes of MBLs, as shown by the more potent inhibition of VIM-1 and VIM-2 with **2.36ii**. However, in comparison to **ELF-128**, the potencies of all four pyrimidine analogues, **2.34ii** to **2.37ii**, were weaker. Therefore, the extended alkyl chain may contribute towards the interactions of **ELF-128** with MBLs.

From a crystal structure of **ELF-128** with VIM-2 (Figure 2.20), which was obtained by Dr. Jürgen Brem (Schofield Group), its binding mode is similar to that of **F52** with regards to the interactions with Zn2 and the bridging hydrolytic water molecule from the pyrimidine N-3 and the 4-carboxylate group. Also evident from the crystal

structure are the interactions between the C-4 functionalisation on the pyrimidine ring and the L3 loop nonpolar residues, including Phe-61 and Tyr-66. However, it was also observed that the extended alkyl chain projects away from the L3 loop of the VIM-2 MBL. Therefore, more polar substitutions may provide an opportunity to improve potency by maximising interactions with other polar residues in close proximity to the extended alkyl chain, such as Arg-206. Elongated substitutions with a terminal hydrophobic group may also enable nonpolar interactions to occur with hydrophobic residues in the regions, such as Tyr-202. Besides exploring substitutions to boost interactions in this specific active site region, substitutions on other carbon positions of the phenyl ring could be explored to facilitate interactions with other active site regions, including with the L3 loop.

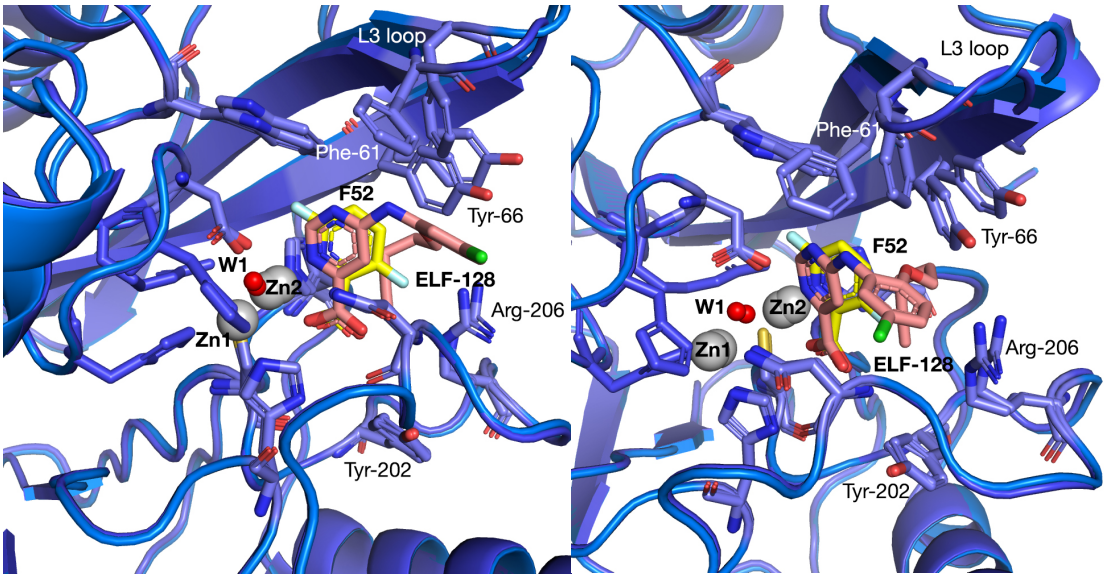


Figure 2.20. Different views from a crystal structure of **ELF-128** bound to VIM-2 using PyMOL. As seen from the overlay with **F52** against VIM-2 on the left, the binding mode is similar with regards to interactions with Zn2 and the bridging water molecule. However, the presence of additional C-4 functionalisation allows interactions with the L3 loop residues such as Phe-61 and Tyr-66, which is depicted more clearer on the right. The extended alkyl chain with a terminal alkyne could potentially be optimised to form better polar interactions with residues such as Arg-206, or nonpolar interactions with residues such as Tyr-202. Otherwise, substitutions on other carbons of that phenyl ring could be explored.

It was also noted prior to carrying out the inhibition screening assays that **2.37ii** is limited by solubility problems, as indicated by the relatively high prediction of cLogP value of 3.38 (Table 2.10). Therefore, further optimisation could also focus on reducing the lipophilicity of the compound in order to improve its aqueous solubility.

2.8. Summary of fragment optimisation work and SAR studies

In summary, through focusing particularly on derivatives of **F32**, **F52** and **ELF-128**, attempts were made to produce different series of novel MBL inhibitors, including compounds featuring the isothiazole, pyrrole and thiazole cores, which mimic five-membered hydrolysed β-lactam products such as penams and carbapenems. The synthesis of these compounds was driven by results obtained from high-throughput screening and X-ray crystallography. MBL inhibitors featuring the pyridine (e.g. **2.33**, Table 2.9) and pyrimidine cores (e.g. **2.37ii**, Scheme 2.22), which mimic six-membered hydrolysed β-lactam products such as cephems, were also synthesised. While explorations of the isothiazole and pyridine analogues were largely unsuccessful, structurally relevant compounds with MBL inhibitory properties from the pyrrole, thiazole and pyrimidine series were synthesised.

Within the pyrrole series, relatively simple pyrroles, namely **2.17ii** to **2.19ii**, did not exhibit any signs of inhibition against VIM-2, potentially due to their inability to interact favourably with the L3 loop of MBLs, illustrating the likely importance of functionalisation of their C-4 and/or C-5 position(s), i.e. functionalisation of C-3 alone is insufficient to achieve MBL inhibition. However, the nitropyrrole analogue **2.30** displayed significant inhibition against VIM-2 and could be explored in the future as a substrate to be used in chromogenic assays for MBL detection (Table 2.4).

Thiazole analogues, **2.31ii** and **2.32ii**, which were first synthesised by Antabio, were synthesised in order to characterise their inhibition profile. These inhibitors exhibited potent MBL inhibition with a panel of clinically relevant MBLs consisting of VIM-1, VIM-2, IMP-1 and NDM-1 (Table 2.5).

The inhibition by **2.31ii** was also investigated from a crystal structure obtained with VIM-2 (Figure 2.15). The structure suggests the importance of enabling interactions between the inhibitor and hydrophobic residues on the L3 loop of MBLs, such as Phe-61 and Tyr-66 in VIM-2 (Figure 2.15).

Finally, the pyrimidine analogues **2.34ii** to **2.37ii** were found to be active against a panel of clinically relevant MBLs consisting of VIM-1, VIM-2, IMP-1 and NDM-1, with **2.37ii** exhibiting the highest potency out of the four inhibitors, and **2.36ii** expressing some selectivity over the VIM class of MBLs (Table 2.10). However, their overall potencies were less than that of **ELF-128**, suggesting that the extended alkyl chain in **ELF-128** may contribute to interactions with MBLs (Table 2.10). This was supported by a crystal structure of **ELF-128** and VIM-2, suggesting that the presence of the extended alkyl chain in **ELF-128** could interact with active site residues located in the opposite direction from the L3 loop (Figure 2.20). Thus, interactions could be enhanced by the introduction of polar groups to interact with hydrophilic residues such as Arg-206, or by the introduction of nonpolar groups to interact with hydrophobic residues such as Tyr-202 (Figure 2.20). In addition, rather than focusing on the substitution on the carbon position of the phenyl ring where the existing extended alkyl chain originates from (C-6 relative to the pyrimidine core of **ELF-128**), other carbon positions of pyrimidine 4-carboxylate (e.g. C-5) could be explored to improve interactions with the L3 loop.

2.9. Experimental procedures

Reagents

Reagents were from Acros, Alfa Aesar, Enamine, Fluorochem, Key Organics, Lancaster, Sigma-Aldrich and Tokyo Chemical Industry, and used as supplied. Solvents for chemical transformation, work-up and chromatography were from Sigma-Aldrich at HPLC grade and used without further distillation. Dried solvents were obtained from Sigma-Aldrich and Alfa Aesar.

Chromatography

Silica gel 60 F 254 analytical thin layer chromatography (TLC) plates were from Merck and imaged under UV light or with appropriate staining methods. Chromatographic purification was performed using a Biotage SP1 Purification system with Biotage KP-SIL silica columns. TLC R_f values are given when column chromatography separation was performed, to the nearest 0.05 unit.

NMR spectra

^{1}H and ^{13}C NMR spectra were recorded using a Bruker AVIII 400 Nanobay machine (400 MHz). Signal positions are recorded in δ ppm using the abbreviations s, d, t, q, and m denoting singlet (s), doublet (d), triplet (t), quartet (q), and multiplet (m), respectively. For 1,2-disubstituted pyrrole compounds, the observed triplet multiplicity was reported as an apparent triplet (app. t). All NMR chemical shifts are referenced to residual solvent peaks. All coupling constants, *J*, are quoted in Hz to the nearest 0.5 Hz. Signals in both the ^{1}H and ^{13}C spectra were assigned with the aid of DEPT, COSY and HMQC.

Other characterisation

Optical rotations were recorded on a Perkin Elmer 241 or 341 polarimeter with a path length of 1 dm (using the sodium D line, 589 nm). $[\alpha]_D$ are reported in units of 10^{-1} degree (°) cm^2 g^{-1}. Concentrations are reported in g/100 mL. Temperatures are reported in degree Celsius (°C). Infrared spectra were recorded on a Bruker Tensor 27 FT-IR spectrometer. Samples were prepared as a thin film on a diamond ATR module. Absorption maxima (ν_{max}) are given in wavenumbers (cm^{-1}). Ionisation (ESI) Mass Spectrometry (MS) data (m/z) were obtained on a Fision VG Platform using a quadrupole analyser. High Resolution (HR) mass spectrometry data (m/z) data were obtained using a Bruker MicroTOF instrument with ESI source and Time of Flight (TOF) analyser. Values are reported as ratio of mass to charge in Daltons. Melting points were obtained using a Leica VMTG heated-stage microscope.

CLogP Predictions

Values of CLogP were obtained using the CLogP calculation function embedded in ChemDraw Profession 16.0.1.4(61) (PerkinElmer).

Visualisation of crystal structures

Crystal structures obtained by Dr. Jürgen Brem (Schofield Group) were visualised using PyMOL 2.0.7 (Schrödinger, Inc.).

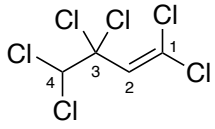
Inhibition studies on MBLs

The inhibition analysis for VIM-1, VIM-2, IMP-1 and NDM-1 conducted by colleagues from the Schofield Group using a method as previously described for MBLs[7]. Inhibition was tested by pre-incubation of the appropriate concentration of MBLs (1 nM final concentration), the inhibitor compound in an assay buffer (50 mM HEPES-NaOH buffer [pH 7.2] supplemented with 1 μg/mL BSA [to minimise enzyme

denaturation], 1 μM of $ZnSO_4$ and 0.01% Triton X-100). The concentration of FC5 employed was 5 μM for all MBLs. Nonlinear regression fitting of IC_{50} curves and reporting of pIC_{50} values (including errors) were carried out using a three-parameter dose-response curve in GraphPad Prism.

Synthesis of 2.1 (1,1,3,3,4,4-hexachlorobut-1-ene)[9]

2.1 was synthesised according to a literature procedure with minor modifications[9]. Benzoyl peroxide, BPO, (324 mg, 1.34 mmol, 1.2 mol. %) was added to 1,1,2-trichloroethylene (10 mL, 111 mmol., 1 equiv.). The reaction mixture was refluxed for 96 h, during which the mixture turned from colourless to yellow. After 96 h, the reaction mixture was cooled to r.t. Unreacted 1,1,2-trichloroethylene was removed *in vacuo*. The crude product was purified by flash column chromatography on silica (eluted with cyclohexane-ethyl acetate) give **2.1** as a yellow oil (6.49 g, 44%).



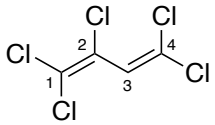
2.1

^{1}H NMR (400 MHz, DMSO-d_6) δ ppm 6.67 (s, 1H, *H4*), 5.75 (s, 1H, *H2*); **^{13}C NMR** (101 MHz, DMSO-d_6) δ ppm 128.2 (*C2*), 127.5 (*C1*), 80.3 (*C2*), 79.5 (*C4*); **IR** ν_{max} (film)/cm^{-1} 3012 (=C-H stretch), 2961 (C-H stretch), 1640 (C=C stretch), 1377 (C-H bend); **LRMS** (ESI$^+$, m/z) 260.8 [M+H]; **HRMS** (ESI$^+$) $C_4H_3Cl_6$ requires 260.8366, found [M+H] 260.8370.

Synthesis of 2.2 (1,1,2,4,4-pentachlorobuta-1,3-diene)[9]

2.1 (4.83 g, 18.4 mmol, 1 equiv.) was dissolved in methanol (14 mL). 28% Sodium methoxide-methanol solution (wt/wt; 5.3 mL, 27.5 mmol, 1.5 equiv.) was then added

dropwise. The reaction mixture was stirred at r.t. overnight, then ice-cooled. 4 M Aqueous sulfuric acid was added to neutralise the mixture. The mixture was concentrated *in vacuo* to remove volatile solvents. The resultant mixture was then dissolved in dichloromethane (25 mL), washed with water (3 x 25 mL) and brine (25 mL), dried over anhydrous magnesium sulfate and filtered. The filtrate was concentrated *in vacuo* to give **2.2** as a brown oil (2.66 g, 64%).

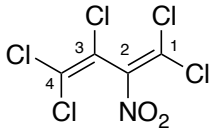


2.2

TLC 9:1 cyclohexane/ethyl acetate, R_f = 0.60; **^{1}H NMR** (400 MHz, chloroform-*d*) δ ppm 6.54 (s, 1H); **^{13}C NMR** (101 MHz, chloroform-*d*) δ ppm 129.6 (*C1*), 123.5 (*C4*), 123.2 (*C2*), 122.5 (*C3*); **IR** ν_{max} (film)/cm^{-1} 3030 (=C-H stretch), 1642 (C=C stretch), 1621 (C=C stretch); **LRMS** (ESI$^+$, m/z) 223.9 [M+H]; **HRMS** (ESI$^+$) C_4HCl_5 requires 223.8521, found [M+H] 223.8525.

Synthesis of 2.3 (1,1,2,4,4-pentachloro-3-nitrobuta-1,3-diene)[9]

2.2 (2.65 g, 11.7 mmol, 1 equiv.) was cooled in an ice bath. A mixture of concentrated sulfuric acid (0.26 mL, 4.63 mmol, 0.4 equiv.) and concentrated nitric acid (5.3 mL, 40.8 mmol, 3.5 equiv.) was added dropwise. The ice bath was removed, and the reaction mixture was warmed to r.t. and stirred for 2 days. The reaction mixture was diluted with water (25 mL) and extracted with dichloromethane (2 x 25 mL). The combined organic layers were washed with 1 M aqueous sodium hydroxide (25 mL) and brine (25 mL), dried over anhydrous magnesium sulfate, filtered and concentrated *in vacuo* to give **2.3** as a yellow oil (2.10 g, 66%).



2.3

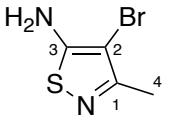
^{13}C NMR (101 MHz, DMSO-d_6) δ ppm 145.3 (*C2*), 132.7 (*C2*), 129.6 (*C1*), 126.5 (*C4*); **IR** ν_{max} (film)/cm^{-1} 3032 (=C-H stretch), 1636 (C=C stretch), 1620 (C=C stretch), 1543 (N-O stretch), 1347 (N-O stretch); **LRMS** (ESI$^+$, m/z) 269.8 [M+H]; **HRMS** (ESI$^+$) $C_4HCl_5NO_2$ requires 269.8450, found [M+H] 269.8452.

Synthesis of 2.6 (4-bromo-3-methylisothiazol-5-amine)[10]

5-Amino-3-methyl-isothiazole hydrochloride (1.00 g, 6.64 mmol, 1 equiv.) was suspended in 7 mL of water. The pH was adjusted to 10 by the addition of 1 M aqueous sodium hydroxide. After stirring at r.t. for 5 min, the mixture was extracted with Et_2O (50 mL). The organic layer was isolated and the aqueous layer was saturated with sodium chloride, which was further extracted with Et_2O (50mL). The combined ethereal extracts were washed with brine (50 mL), dried over anhydrous sodium sulfate and concentrated in vacuo to give 5-amino-3-methyl-isothiazole as a dark orange oil (0.70 g, 92%).

The crude 5-amino-3-methyl-isothiazole was dissolved in tetrachloromethane (21 mL). *N*-Bromosuccinimide, NBS, (1.09 g, 6.12 mmol, 1.3 equiv.) was added portion-wise over 10 min at r.t. The reaction mixture was stirred at 65 ºC for 2 h under nitrogen. The reaction mixture was then cooled to room temperature and diluted with Et_2O. This mixture was cooled to 5 ºC for 30 min. The precipitate formed was removed by filtration and the filtrate concentrated. The concentrated filtrate was re-dissolved in ethyl acetate (50 mL), washed with water (2 x 100 mL) and brine (100 mL), dried over

anhydrous sulfate, filtered and concentrated *in vacuo* to yield **2.6** as a dark red solid (0.86 g, 67%).

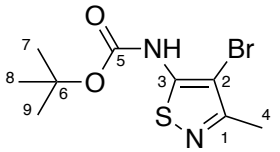


2.6

mp 98-101 °C; **TLC** 3:2 cyclohexane/ethyl acetate, R_f = 0.30; **^{1}H NMR** (400 MHz, DMSO-d_6) δ ppm 6.65 (br s, 2H, NH_2), 2.20 (s, 3H, Ar-CH_3); **^{13}C NMR** (101 MHz, DMSO-d_6) δ ppm 185.3 (*C1*), 169.0 (*C3*), 165.7 (*C2*), 16.2 (*C4*); **IR** ν_{max} (film)/cm^{-1} 3330 (N-H stretch), 3142 (N-H stretch), 1643 (aromatic C=N stretch), 1460 (aromatic C=C stretch), 1182 (aromatic C=S stretch) ; **LRMS** (ESI$^+$, m/z) 192.9 [M+H]; **HRMS** (ESI$^+$) $C_4H_6BrN_2S$ requires 192.9435, found [M+H] 192.9436.

Synthesis of 2.8 (*tert*-butyl (4-bromo-3-methylisothiazol-5-yl)carbamate)

2.6 (99 mg, 0.513 mmol, 1 equiv.) and di-*tert*-butyl decarbonate (170 mg, 0.779 mmol, 1.5 equiv.) were dissolved in dichloromethane (3 mL). Triethylamine (0.2 mL, 1.43 mmol, 3 equiv.) was added slowly. The reaction mixture was then stirred at r.t. for 4 h under nitrogen. The resultant mixture was concentrated *in vacuo* and the crude product purified by flash column chromatography on silica (eluted with pentane-ethyl acetate) to afford **2.8** as a brown solid (57 mg, 38%)



2.8

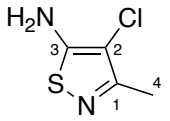
mp 95-97 °C; **TLC** 3:2 cyclohexane/ethyl acetate, R_f = 0.35; **^{1}H NMR** (400 MHz, DMSO-d_6) δ ppm 2.61 (s, 3H, Ar-CH_3), 1.52 (s, 9H, ^{t}Bu); **^{13}C NMR** (101 MHz, DMSO-

d_6) δ ppm 180.3 (*C1*), 168.2 (*C5*), 166.0 (*C3*) 163.9 (*C2*), 81.1 (*C6*), 29.7 (*C7-9*), 15.3 (*C4*); **IR** ν_{max} (film)/cm^{-1} 3350 (N-H stretch), 2976 (C-H stretch), 1645 (aromatic C=N stretch), 1423 (aromatic C=C stretch), 1163 (aromatic C=S stretch); **LRMS** (ESI^+, m/z) 293.0 [M+H]; **HRMS** (ESI^+) $C_9H_{14}BrN_2O_2S$ requires 292.9959, found [M+H] 292.9961.

Synthesis of 2.11 (4-chloro-3-methylisothiazol-5-amine)[11]

5-Amino-3-methyl-isothiazole hydrochloride (2.35 g, 15.6 mmol, 1 equiv.) was suspended in 15 mL of water. The pH was adjusted to 10 by the addition of 1 M aqueous sodium hydroxide. After stirring at r.t. for 5 min, the mixture was extracted with Et_2O (100 mL). The organic layer was isolated, and the aqueous layer was saturated with sodium chloride, which was further extracted with Et_2O (100mL). The combined ethereal extracts were washed with brine (100 mL), dried over anhydrous sodium sulfate, then concentrated *in vacuo* to afford 5-amino-3-methyl-isothiazole as a dark orange oil (1.20 g, 67%).

The crude 5-amino-3-methyl-isothiazole was dissolved in chloroform (35 mL). *N*-Chlorosuccinimide, NCS, (1.40 g, 10.5 mmol, 1 equiv.) was added portion-wise over 10 min at r.t. The reaction mixture was stirred under reflux for 4 h under nitrogen. After that, the reaction mixture was cooled to room temperature and diluted with Et_2O. This mixture was cooled to 5 ºC for 30 min. The precipitate formed was removed by filtration and the filtrate concentrated. The concentrated filtrate was re-dissolved in ethyl acetate (50 mL), washed with water (2 x 100 mL) and brine (100 mL), dried over anhydrous sulfate, filtered and concentrated *in vacuo*. The crude product was purified by flash column chromatography on silica (eluted with dichloromethane-methanol) to yield **2.11** as a red solid (1.62 g, 100%).

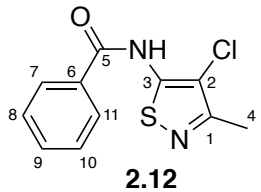


2.11

mp 72-75 °C (lit. 62-63 °C[33]); **TLC** 98:2 dichloromethane/methanol, R_f = 0.25; **^{1}H NMR** (400 MHz, DMSO-d_6) δ ppm 6.74 (br s, 2H, NH_2), 2.17 (s, 3H, Ar-CH_3); **^{13}C NMR** (101 MHz, DMSO-d_6) δ ppm 180.1 (*C1*), 166.0 (*C2*), 162.0 (*C3*), 18.4 (*C4*); **IR** ν_{max} (film)/cm^{-1} 3329 (N-H stretch), 3140 (N-H stretch), 1627 (aromatic C=N stretch), 1430 (aromatic C=C stretch), 1189 (aromatic C=S stretch); **LRMS** (ESI$^+$, m/z) 149.0 [M+H]; **HRMS** (ESI$^+$) $C_4H_6ClN_2S$ requires 148.9935, found [M+H] 148.9941.

Synthesis of 2.7 (*N*-(4-chloro-3-methylisothiazol-5-yl)benzamide)

2.6 (499 mg, 3.36 mmol, 1 equiv.) was dissolved in pyridine (2 mL). Benzoyl chloride (0.5 mL, 4.31 mmol, 1.3 equiv.) in pyridine (2 mL) was added. The resultant mixture was stirred at r.t. for 18 h. The mixture was diluted with water (100 mL) and washed with ethyl acetate (4 x 25 mL). The combined ethyl acetate layers were washed with 1M aqueous sodium hydroxide (100 mL) and 10% aqueous copper(II) sulfate solution (wt/wt; 100 mL). The organic layer was dried over magnesium sulfate, filtered and concentrated *in vacuo*, giving **2.7** as a brown solid (622 mg, 73%).



2.12

mp 83-87 °C; **TLC** 3:2 cyclohexane/ethyl acetate, R_f = 0.50; **^{1}H NMR** (400 MHz, DMSO-d_6) δ ppm 11.75 (s, 1H, NH), 7.99 (d, *J* = 7.0 Hz, 2H, *H7* and *H11*), 7.67 (t, *J* = 7.5 Hz, 1H, *H9*), 7.57 (d, *J* = 7.5 Hz, 2H, *H8* and *H10*), 2.36 (s, 3H, Ar-CH_3); **^{13}C NMR**

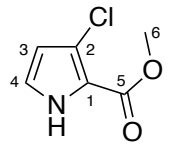
(101 MHz, DMSO-d_6) δ ppm 180.1 (*C5*), 166.4 (*C1*), 159.7 (*C3*), 153.5 (*C2*), 132.9 (*C6*), 131.4 (*C9*), 128.8 (*C8* and *C10*), 128.5 (*C7* and *C11*), 18.4 (*C4*); **IR** ν_{max} (film)/cm^{-1} 3177 (N-H stretch), 2924 (C-H stretch), 1703 (C=O stretch), 1655 (C=N stretch), 1604 (aromatic C=C stretch), 1553 (aromatic C=C stretch), 1477 (aromatic C=C stretch), 1415 (aromatic C=C stretch), 1185 (aromatic C=S stretch); **LRMS** (ESI^+, m/z) 253.0 [M+H]; **HRMS** (ESI^+) $C_{11}H_{10}ClN_2OS$ requires 253.0197, found [M+H] 253.0186.

Synthesis of 2.16 (methyl 3-chloro-1*H*-pyrrole-2-carboxylate)[18]

2.16 was synthesised according to a literature procedure[18]. 2-Methyl-1-pyrroline (2 mL, 21.1 mmol, 1 equiv.) was dissolved in THF (60 mL) and ice-cooled. NCS (22.56 g, 169 mmol, 8 equiv.) was added and the reaction mixture was stirred at 55 °C for 1 h. Upon completion, the reaction mixture was diluted with water (30 mL) and extracted with cyclohexane (4 x 30 mL). The combined organic layers were dried over anhydrous sodium sulfate, filtered and concentrated *in vacuo* to yield crude 4,4-dichloro-5-(trichloromethyl)-3,4-dihydro-2*H*-pyrrole (8.79 g, quant.) as a brown oil, which was used directly for the next step without further purification.

The crude intermediate was dissolved in methanol (25 mL) and ice-cooled. 28% Sodium methoxide-methanol (wt/wt; 38 mL) was added dropwise, and the reaction mixture was left to stir for 2 h at r.t. At the end of the reaction, the mixture was then cooled using ice, and 4 M sulfuric acid solution was added slowly to neutralise the mixture. The mixture was then concentrated under reduced pressure and the concentrated mixture was extracted with ethyl acetate (5 x 30 mL). The combined organic layers were washed with brine (50 mL), dried over anhydrous sodium sulfate, filtered and concentrated *in vacuo*. The concentrate was further purified by flash

column chromatography on silica (eluted with cyclohexane-ethyl acetate) to afford **2.16** (1.87 g, 55%) as a brown solid.



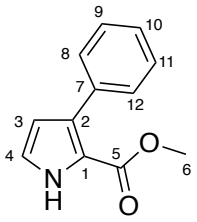
2.16

mp 86-87 °C (lit. 88.3-90.3°C[34]); **TLC** 3:2 cyclohexane/ethyl acetate, R_f = 0.50; **^{1}H NMR** (400 MHz, DMSO-d_6) δ ppm 12.11 (s, 1H, NH), 7.02 (dd, *J* = 3.5, 2.8 Hz, 1H, *H4*), 6.25 (app. t, *J* = 2.5 Hz, 1H, *H3*), 3.78 (s, 3H, OCH_3); **^{13}C NMR** (101 MHz, DMSO-d_6) δ ppm 159.6 (*C5*), 123.3 (*C1*), 117.4 (*C2*), 117.2 (*C4*), 110.9 (*C3*), 51.2 (*C6*); **IR** ν_{max} (film)/cm^{-1} 3399 (N-H stretch), 3131 (aromatic C-H stretch), 2957 (C-H stretch), 1670 (ester C=O stretch), 1439 (aromatic C=C stretch), 1398 (aromatic C=C stretch); **LRMS** (ESI$^+$, m/z) 160.0 [M+H]; **HRMS** (ESI$^-$) $C_6H_5ClNO_2$ requires 158.0014, found [M-H] 158.0008.

Synthesis of 2.17i (methyl 3-phenyl-1*H*-pyrrole-2-carboxylate)

2.16 (102 mg, 0.637 mmol, 1 equiv.) was dissolved in a mixture of 1,4-dioxane (4 mL) and water (0.8 mL) in a sealed microwave vial. With stirring, XPhos (60 mg, 0.126 mmol, 20 mol. %), palladium(II) acetate (14 mg, 0.062 mmol, 10 mol. %) and potassium carbonate (260 mg, 1.88 mmol, 3 equiv.) were added. The resultant suspension was purged with nitrogen for 5 min, then stirred at 100 ºC for 2 h. Upon cooling to ambient temperature, the reaction mixture was diluted with water (10 mL), extracted with ethyl acetate (4 x 10 mL). The combined organic fractions were washed with brine, dried over anhydrous sodium sulfate and concentrated *in vacuo*.

The crude product was purified using flash column chromatography on silica (eluting with hexane-ethyl acetate) to afford **2.17i** as a white solid (105 mg, 83%).



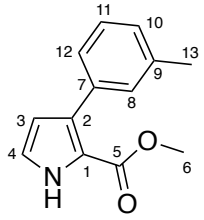
2.17i

mp 88-91 °C; **TLC** 3:2 cyclohexane/ethyl acetate, R_f = 0.35; **^{1}H NMR** (400 MHz, DMSO-d_6) δ ppm 11.85 (s, 1H, NH), 7.49 (d, *J* = 7.5 Hz, 2H, *H8* and *H12*), 7.34 (t, *J* = 7.0 Hz, 2H, *H9* and *H11*), 7.26 (t, *J* = 7.0 Hz, 1H, *H10*), 7.02 (app. t, *J* = 3.0 Hz, 1H, *H3*), 6.29 (app. t, *J* = 2.5 Hz, 1H, *H4*), 3.69 (s, 3H, OCH_3); **^{13}C NMR** (101 MHz, DMSO-d_6) δ ppm 160.8 (*C5*), 135.3 (*C7*), 131.4 (*C2*), 129.1 (*C9* and *C11*), 127.6 (*C8* and *C12*), 126.7 (*C1*), 126.5 (*C3*), 123.1 (*C10*), 111.5 (*C4*), 50.8 (*C6*); **IR** ν_{max} (film)/cm^{-1} 3400 (N-H stretch), 3030 (aromatic C-H stretch), 2957 (C-H stretch), 1670 (ester C=O stretch), 1535 (aromatic C=N stretch), 1439 (aromatic C=C stretch), 1398 (aromatic C=C stretch); **LRMS** (ESI$^+$, m/z) 202.1 [M+H]; **HRMS** (ESI$^-$) $C_{12}H_{10}NO_2$ requires 200.0717, found [M-H] 200.0720.

Synthesis of 2.18i (methyl 3-(*m*-tolyl)-1*H*-pyrrole-2-carboxylate)

2.16 (91 mg, 0.570 mmol, 1 equiv.) was dissolved in a mixture of 1,4-dioxane (4 mL) and water (0.8 mL) in a sealed microwave vial. With stirring, XPhos (61 mg, 0.128 mmol, 20 mol. %), palladium(II) acetate (15 mg, 0.067 mmol, 10 mol. %) and potassium carbonate (261 mg, 1.89 mmol, 3 equiv.) were added. The resultant suspension was purged with nitrogen for 5 min, then stirred at 100 ºC for 2 h. Upon cooling to ambient temperature, the reaction mixture was diluted with water (10 mL),

extracted with ethyl acetate (4 x 10 mL). The combined organic fractions were washed with brine, dried over anhydrous sodium sulfate and concentrated *in vacuo*. The crude product was purified using flash column chromatography on silica (eluted with hexane-ethyl acetate) to afford **2.18i** as an off-white solid (105 mg, 86%).



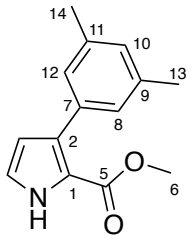
2.18i

mp 93-95 °C; **TLC** 3:2 cyclohexane/ethyl acetate, R_f = 0.40; **^{1}H NMR** (400 MHz, DMSO-d_6) δ ppm 12.11 (s, 1H, NH), 7.35-7.16 (m, 3H, *H8*, *H11* and *H12*), 7.07 (d, *J* = 7.5 Hz, 1H, *H10*), 7.01 (app. t, *J* = 3.0 Hz, 1H, *H4*), 6.26 (app. t, *J* = 2.5 Hz, 1H, *H3*), 3.68 (s, 3H, OCH_3), 2.32 (s, 3H, Ar-CH_3); **^{13}C NMR** (101 MHz, DMSO-d_6) δ ppm 160.8 (*C5*), 136.5 (*C7*), 135.3 (*C9*), 131.5 (*C2*), 129.7 (*C12*), 127.5 (*C11*), 127.1 (*C10*), 126.3 (*C8*), 123.0 (*C1*), 116.8 (*C3*), 111.5 (*C4*), 50.8 (*C6*), 21.1 (*C13*); **IR** ν_{max} (film)/cm^{-1} 3300 (N-H stretch, br), 3050 (aromatic C-H stretch), 2972 (C-H stretch), 1682 (ester C=O stretch), 1522 (aromatic C=N stretch), 1417 (aromatic C=C stretch), 1376 (aromatic C=C stretch); **LRMS** (ESI$^+$, m/z) 216.1 [M+H]; **HRMS** (ESI$^-$) $C_{13}H_{12}NO_2$ requires 214.0874, found [M-H] 214.0875.

Synthesis of 2.19i (methyl 3-(3,5-dimethylphenyl)-1*H*-pyrrole-2-carboxylate)

2.16 (104 mg, 0.652 mmol, 1 equiv.) was dissolved in a mixture of 1,4-dioxane (4 mL) and water (0.8 mL) in a sealed microwave vial. With stirring, XPhos (60 mg, 0.126 mmol, 20 mol. %), palladium(II) acetate (15 mg, 0.067 mmol, 10 mol. %) and potassium carbonate (262 mg, 1.90 mmol, 3 equiv.) were added. The resultant

suspension was purged with nitrogen for 5 min, then stirred at 100 ºC for 2 h. Upon cooling to ambient temperature, the reaction mixture was diluted with water (10 mL), extracted with ethyl acetate (4 x 10 mL). The combined organic fractions were washed with brine, dried over anhydrous sodium sulfate and concentrated in vacuo. The crude product was purified using flash column chromatography on silica (eluted with hexane-ethyl acetate) to afford **2.19i** as an off-white solid (119 mg, 81%).



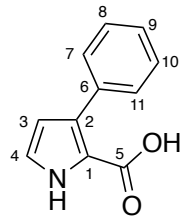
2.19i

mp 94-96 °C; **TLC** 3:2 cyclohexane/ethyl acetate, R_f = 0.45; **^{1}H NMR** (400 MHz, DMSO-d_6) δ ppm 11.79 (s, 1H, NH), 7.09 (s, 2H, *H8* and *H12*), 6.99 (app. t, *J* = 3.0 Hz, 1H, *H4*), 6.89 (s, 1H, *H10*), 6.24 (app. t, *J* = 2.5 Hz, 1H, *H3*), 3.68 (s, 3H, OCH_3), 2.27 (s, 6H, Ar-CH_3); **^{13}C NMR** (101 MHz, DMSO-d_6) δ ppm 160.8 (*C5*), 136.3 (*C9* and *C11*), 135.2 (*C7*), 131.6 (*C2*), 127.9 (*C10*), 127.0 (*C8* and *C12*), 122.9 (*C4*), 116.8 (*C1*), 111.5 (*C3*), 50.8 (*C6*), 21.0 (*C13* and *C14*); **IR** ν_{max} (film)/cm^{-1} 3350 (N-H stretch, br), 3096 (aromatic C-H stretch), 2965 (C-H stretch), 1680 (ester C=O stretch), 1532 (aromatic C=N stretch), 1421 (aromatic C=C stretch), 1380 (aromatic C=C stretch); **LRMS** (ESI$^+$, m/z) 230.1 [M+H]; **HRMS** (ESI$^-$) $C_{14}H_{16}NO_2$ requires 228.1030, found [M-H] 228.1028.

Synthesis of 2.17ii (3-phenyl-1*H*-pyrrole-2-carboxylic acid)

2.17i (100 mg, 0.497 mmol, 1 equiv.) was dissolved in a mixture of methanol (4 mL) and water (2 mL). Lithium hydroxide monohydrate (104 mg, 2.48 mmol, 5 equiv.) was added. The reaction mixture was stirred at r.t. overnight. The reaction mixture was

acidified with 1M aqueous hydrochloric acid, and the precipitate formed was filtered and dried, to give **2.17ii** as a white solid (78 mg, 84%).

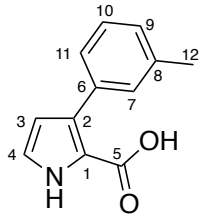


2.17ii

mp 157-159 °C; **^{1}H NMR** (400 MHz, DMSO-d_6) δ ppm 12.22 (br s, 1H, NH), 11.69 (br s, 1H, OH), 7.51 (dd, *J* = 8.5, 1.5 Hz, 2 H, *H7* and *H11*), 7.32 (dt, 7.5, 2.0 Hz, 2H, *H8* and *H10*), 7.23 (tt, *J* = 7.5, 1.5 Hz, 1H, *H9*), 6.97 (app. t, *J* = 3.0 Hz, 1H, *H4*), 6.25 (app. t, *J* = 2.5 Hz, 1H, *H3*); **^{13}C NMR** (101 MHz, DMSO-d_6) δ ppm 161.9 (*C5*), 135.7 (*C1*), 130.7 (*C2*), 129.2 (*C7* and *C11*), 127.5 (*C8* and *C10*), 126.2 (*C6*), 122.4 (*C9*), 117.8 (*C4*), 111.4 (*C3*); **IR** ν_{max} (film)/cm^{-1} 3100 (O-H stretch, br), 3050 (aromatic C-H stretch), 1712 (acid C=O stretch), 1540 (aromatic C=N stretch), 1425 (aromatic C=C stretch), 1376 (aromatic C=C stretch); **LRMS** (ESI$^-$, m/z) 186.1 [M-H]; **HRMS** (ESI$^-$) $C_{11}H_8NO_2$ requires 186.0561, found [M-H] 186.0562.

Synthesis of 2.18ii (3-(*m*-tolyl)-1*H*-pyrrole-2-carboxylic acid)

2.18i (90 mg, 0.418 mmol, 1 equiv.) was dissolved in a mixture of methanol (4 mL) and water (2 mL). Lithium hydroxide monohydrate (88 mg, 2.10 mmol, 5 equiv.) was added. The reaction mixture was stirred at r.t. overnight. The reaction mixture was acidified with 1M aqueous hydrochloric acid, and the precipitate formed was filtered and dried, to give **2.18ii** as an off-white solid (28 mg, 33%).

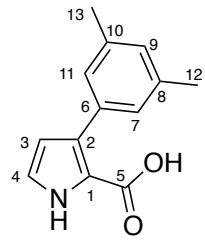


2.18ii

mp 161-162 °C;**^{1}H NMR** (400 MHz, DMSO-d_6) δ ppm 12.17 (s, 1H, NH), 11.65 (br s, 1H, OH), 7.30 (m, *H7* and *H11*), 7.20 (t, *J* = 8.0 Hz, 1H, *H10*), 7.05 (d, *J* = 7.5 Hz, 1H, *H9*), 6.95 (app. t, *J* = 3.0 Hz, 1H, *H4*), 6.23 (app. t, *J* = 2.5 Hz, 1H, *H3*), 2.31 (s, 3H, Ar-CH_3) ; **^{13}C NMR** (101 MHz, DMSO-d_6) δ ppm 161.9 (*C5*), 161.9 (*C1*), 136.3 (*C8*), 135.6 (*C6*), 129.8 (*C2*), 127.4 (*C10*), 126.9 (*C9*), 126.5 (*C7*), 122.3 (*C11*), 117.8 (*C4*), 111.4 (*C3*), 21.1 (*C12*); **IR** ν_{max} (film)/cm^{-1} 3150 (O-H stretch, br), 3050 (aromatic C-H stretch), 2960 (C-H stretch), 1708 (acid C=O stretch), 1536 (aromatic C=N stretch), 1429 (aromatic C=C stretch), 1380 (aromatic C=C stretch); **LRMS** (ESI$^-$, m/z) 200.1 [M-H]; **HRMS** (ESI$^-$) $C_{12}H_{10}NO_2$ requires 200.0717, found [M-H] 200.0716.

Synthesis of 2.19ii (3-(3,5-dimethylphenyl)-1*H*-pyrrole-2-carboxylic acid)

2.19i (108 mg, 0.471 mmol, 1 equiv.) was dissolved in a mixture of methanol (4 mL) and water (2 mL). Lithium hydroxide monohydrate (99 mg, 2.36 mmol, 5 equiv.) was added. The reaction mixture was stirred at r.t. overnight. The reaction mixture was acidified with 1 M aqueous hydrochloric acid, and the precipitate formed was filtered and dried, to give **2.19ii** as an off-white solid (62 mg, 61%).



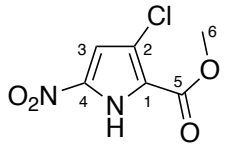
2.19ii

mp 167-169 °C;**^{1}H NMR** (400 MHz, DMSO-d_6) δ ppm 12.11 (br s, 1H, NH), 11.62 (br s, 1H, OH), 7.09 (s, *H7* and *H11*), 6.94 (app. t, *J* = 3.0 Hz, 1H, *H4*), 6.87 (s, 1H, *H9*), 6.20 (app. t, *J* = 2.5 Hz, 1H, *H3*), 2.26 (s, 6H, Ar-CH_3); **^{13}C NMR** (101 MHz, DMSO-d_6) δ ppm 161.9 (*C5*), 136.1 (*C8* and *C10*), 135.6 (*C6*), 131.0 (*C2*), 127.7 (*C9*), 127.1 (*C7* and *C11*), 122.2 (*C4*), 117.8 (*C1*), 111.4 (*C3*), 21.0 (*C12* and *C13*); **IR** ν_{max} (film)/cm^{-1} 3125 (O-H stretch, br), 3075 (aromatic C-H stretch), 2960 (C-H stretch), 1705 (acid C=O stretch), 1542 (aromatic C=N stretch), 1421 (aromatic C=C stretch), 1376 (aromatic C=C stretch); **LRMS** (ESI$^-$, m/z) 214.1 [M-H]; **HRMS** (ESI$^-$) $C_{13}H_{12}NO_2$ requires 214.0874, found [M-H] 214.0873.

Synthesis of 2.20 (methyl 3-chloro-5-nitro-1*H*-pyrrole-2-carboxylate) and 2.13 (methyl 3-chloro-4-nitro-1*H*-pyrrole-2-carboxylate)[22]

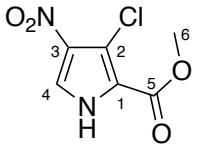
2.16 (1.87 g, 11.7 mmol, 1 equiv.) was dissolved in acetic anhydride (20 mL) and cooled to -40°C. Concentrated nitric acid (1.1 mL, 17.3 mmol, 1.5 equiv.) was added dropwise. The reaction mixture was stirred for 3 h while allowing it to slowly warm to r.t. After 3 h, the mixture was cooled to -40 °C again, poured over an ice-water mixture, and filtered to obtain the precipitate. The precipitate was washed with water, re-dissolved in ethyl acetate and concentrated *in vacuo* to give a yellow solid containing a crude mixture of **2.20** and **2.21**.

The mixture of regioisomers was separated using flash column chromatography (eluting with cyclohexane-ethyl acetate) to give **2.20** (451 mg, 24%) and **2.21** (533 mg, 29%), respectively.



2.20

mp 180-184 °C; **TLC** 4:1 cyclohexane/ethyl acetate, R_f = 0.35; **^{1}H NMR** (400 MHz, chloroform-*d*) δ ppm 10.32 (s, 1H, NH), 7.05 (s, 1H, Ar-H), 3.98 (s, 3H, OCH_3); **^{13}C NMR** (101 MHz, chloroform-*d*) δ ppm 159.3 (*C5*), 136.9 (*C4*), 121.2 (*C1*), 119.4 (*C2*), 111.1 (*C3*), 53.1 (*C6*); **IR** ν_{max} (film)/cm^{-1} 3208 (N-H stretch), 3137 (aromatic C-H stretch), 1695 (ester C=O stretch), 1517 (N-O stretch), 1467 (aromatic C=C stretch), 1413 (aromatic C=C stretch), 1370 (N-O stretch); **LRMS** (ESI$^+$, m/z) 205.1 [M+H]; **HRMS** (ESI$^-$) $C_6H_4ClN_2O_4$ requires 202.9865, found [M-H] 202.9860.

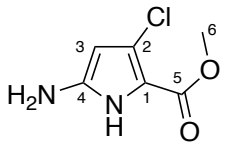


2.21

mp 231-233 °C; **TLC** 4:1 cyclohexane/ethyl acetate, R_f = 0.20; **^{1}H NMR** (400 MHz, DMSO-d_6) δ ppm 13.45 (s, 1H, NH), 8.19 (s, 1H, Ar-H), 3.85 (s, 3H, OCH_3); **^{13}C NMR** (101 MHz, chloroform-d_6) δ ppm 159.2 (*C5*), 131.8 (*C1*), 123.8 (*C2*), 119.4 (*C3*), 114.5 (*C4*), 53.0 (*C6*); **IR** ν_{max} (film)/cm^{-1} 3148 (aromatic C-H), 2875 (C-H), 1682 (ester C=O stretch), 1548 (N-O stretch), 1504 (aromatic C=C), 1442 (aromatic C=C), 1374 (N-O stretch); **LRMS** (ESI$^+$, m/z) 205.0 [M+H]; **HRMS** (ESI$^-$) $C_6H_4ClN_2O_4$ requires 202.9865, found [M-H] 202.9860.

Synthesis of 2.22 (methyl 5-amino-3-chloro)-1*H*-pyrrole-2-carboxylate)[24]

A mixture of ammonium chloride (53 mg, 0.99 mmol, 0.7 equiv.) and iron (432 mg, 7.74 mmol, 5.5 equiv.) was suspended in a mixture of ethanol and water (15 mL, v/v = 10:1), and stirred at reflux for 5 min. **2.20** (288 mg, 1.41 mmol, 1.0 equiv.) was added and the reaction mixture was allowed to stir for 1 h. The mixture was then allowed to cool to r.t. and concentrated *in vacuo*. The concentrate was re-dissolved in dichloromethane and filtered through a Celite pad with thorough washing with dichloromethane. Finally, the filtrate was concentrated under reduced pressure to give **2.22** (240 mg, 1.37 mmol, 98%) as a yellow solid, which was used for subsequent steps without further purification.



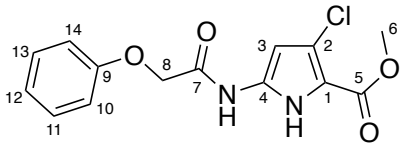
2.22

mp 190-193 °C; **TLC** 3:2 cyclohexane/ethyl acetate, R_f = 0.35; **^{1}H NMR** (400 MHz, DMSO-d_6) δ ppm 10.56 (br s, 1H, NH), 5.76 (s, 1H, Ar-H), 5.22 (s, 2H, NH_2), 3.67 (s, 3H, OCH_3); **^{13}C NMR** (101 MHz, DMSO-d_6) δ ppm 196.9 (*C5*), 181.3 (*C4*), 157.5 (*C1*), 145.0 (*C2*), 130.4 (*C3*), 88.0 (*C6*); **IR** ν_{max} (film)/cm^{-1} 3322 (N-H stretch), 3130 (N-H stretch), 3050 (aromatic C-H), 2963 (C-H), 1680 (ester C=O stretch), 1511 (aromatic C=C), 1439 (aromatic C=C); **LRMS** (ESI$^+$, m/z) 175.0 [M+H]; **HRMS** (ESI$^+$) $C_6H_8ClN_2O_2$ requires 175.0274, found [M+H] 175.0278.

Synthesis of 2.23 (methyl 5-amino-3-chloro)-1*H*-pyrrole-2-carboxylate)

2.22 (240 mg, 1.37 mmol, 1 equiv.) was dissolved in dry acetonitrile (14 mL). To this solution was added 1-hydroxybenzotriazole hydrate, or HOBt (1.05 g, 6.86 mmol, 5

equiv.), which was dissolved in dry pyridine (3.4 mL). Phenoxyacetyl chloride (0.95 mL, 6.88 mmol, 5 equiv.) was then added slowly. The resultant mixture was stirred at r.t. under nitrogen for 21 h. The mixture was then diluted with chloroform (50 mL), washed with sat. aqueous sodium bicarbonate solution (50 mL) and brine (50 mL). The organic layer was dried over anhydrous sodium sulfate, filtered and concentrated *in vacuo*. The crude product was purified by flash column chromatography on silica (eluted with cyclohexane-ethyl acetate) to obtain **2.23** as a pale-yellow solid (219 mg, 52%).

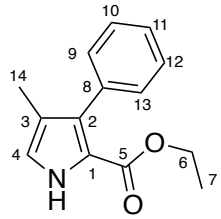


2.23

mp 156-162 °C; **TLC** 3:2 cyclohexane/ethyl acetate, R_f = 0.40; **^{1}H NMR** (400 MHz, DMSO-d_6) δ ppm 10.86 (s, 1H, C(O)NH), 8.42 (s, 1H, NH), 7.67 (d, *J* = 3.0 Hz, 1H, Ar-H), 7.06 (t, *J* = 7.5 Hz, 2H, *H12* and *H14*), 7.01 (d, *J* = 8.0 Hz, 2H, *H9* and *H11*), 6.93 (d, *J* = 8.0 Hz, 1H, *H13*), 4.65 (s, 2H, OCH_2), 3.91 (s, 3H, OCH_3); **^{13}C NMR** (101 MHz, chloroform-d_6) δ ppm 165.6 (*C7*), 160.4 (*C5*), 157.0 (*C9*), 130.1 (*C4*), 130.0 (*C11* and *C13*), 122.6 (*C1*), 121.4 (*C12*), 115.0 (*C10* and *C14*), 113.7 (*C3*), 67.4 (*C8*), 52.0 (*C6*); **IR** ν_{max} (film)/cm^{-1} 3399 (N-H stretch), 3274 (N-H stretch), 2948 (C-H stretch), 1785 (ester C=O stretch), 1685 (amide C=O stretch), 1587 (aromatic C=C stretch), 1552 (aromatic C=C stretch), 1498 (aromatic C=C stretch), 1438 (aromatic C=C stretch), 1400 (aromatic C=C stretch); **LRMS** (ESI$^+$, m/z) 331.0 [M+Na]; **HRMS** (ESI$^+$) $C_{14}H_{13}ClN_2O_4Na$ requires 331.0456, found [M+Na] 331.0456.

Synthesis of 2.25 (ethyl 4-methyl-3-phenyl-1*H*-pyrrole-2-carboxylate)[26]

2-Nitro-3-phenyl-2-propene (5.00 g, 30.6 mmol, 1 equiv.) and ethyl isocyanoacetate (3.68 mL, 33.7 mmol. 1.1 equiv.) were dissolved in a mixture of anhydrous tetrahydrofuran and anhydrous isopropanol (50 mL, 3:1 v/v). The mixture was cooled to 10°C with a cold water bath. With stirring, 1,8-diazabicyclo[5.4.0]undec-7-ene, or DBU, (9.17 mL, 61.3 mmol, 2 equiv.) was added dropwise. The reaction mixture was allowed to warm to r.t. and stirred for 4 h. Upon completion, the solvent was removed *in vacuo*. Water (30 mL) was then added to the residue and extracted with diethyl ether (3 x 50 mL). The combined organic extracts were washed with brine (2 x 30 mL) and dried over anhydrous sodium sulfate, filtered and concentrated under reduced pressure. The crude material was purified using flash column chromatography (eluted with cyclohexane-ethyl acetate) to obtain **2.25** as an off-white solid (6.50 g, 93%).



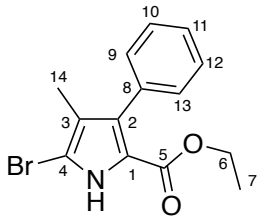
2.25

mp 63-64 ºC (lit. 63 ºC[35]); **TLC** 3:2 cyclohexane/ethyl acetate, R_f = 0.55; **^{1}H NMR** (400 MHz, chloroform-*d*) δ 8.82 (s, 1H, NH), 7.20-7.35 (m, 5H, Ph-H), 6.65 (s, 1H, *H4*), 4.13 (q, 2H, OCH_2), 1.98 (s, 3H, Ar-CH_3), 1.13 (t, -CH_3); **^{13}C NMR** (101 MHz, chloroform-*d*) δ 158.7 (*C5*), 135.4 (*C8*), 134.2 (*C2*), 127.4 (*C10*, *C12*), 126.6 (*C11*), 125.8 (*C9*, *C13*), 121.4 (*C4*), 119.1 (*C1*), 117.9 (*C3*), 58.8 (*C6*), 15.2 (*C7*), 12.6 (*C14*); **IR** ν_{max} (film)/cm^{-1} 3300 (N-H stretch), 3063 (aromatic C-H stretch), 2960 (C-H stretch), 1680 (ester C=O stretch), 1534 (aromatic C=C stretch), 1420 (aromatic C=C stretch); **LCMS** m/z

375.1 ($M+H^+$), time = 7.461 min; **HRMS** (ESI^-) $C_{14}H_{14}NO_2$ requires 228.1030, found [M-H] 228.1033.

Synthesis of 2.26 (ethyl 5-bromo-4-methyl-3-phenyl-1*H*-pyrrole-2-carboxylate)[27]

2.25 (500 mg, 2.18 mmol, 1 equiv.) was dissolved in DMF (15 mL). NBS (466 mg, 2.62 mmol, 1.2 equiv.) was added portion-wise. The reaction mixture was then stirred at r.t. for 2 h. Upon completion, the mixture was diluted with water (25 mL) and extracted with ethyl acetate (2 x 25 mL). The combined organic layer was washed with brine (25 mL), dried over anhydrous sodium sulfate, filtered and concentrated *in vacuo*. The crude product was further purified via flash column chromatography (eluted with cyclohexane-ethyl acetate) to give **2.26** as a pink solid (471 mg, 70%).

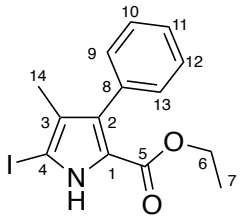


2.26

mp 92-95 °C; **TLC** 3:2 cyclohexane/ethyl acetate, R_f = 0.70; **^{1}H NMR** (400 MHz, chloroform-*d*) δ 9.40 (s, 1H, NH), 7.41-7.28 (m, 5H, Ph-H), 4.17 (q, *J* = 7.0 Hz, OCH_2), 1.93 (s, 3H, Ar-CH_3), 1.13 (t, *J* = 7.0 Hz, 3H, CH_3); **^{13}C NMR** (101 MHz, chloroform-*d*) δ 160.2 (*C5*), 134.5 (*C8*), 131.8 (*C2*), 130.1 (*C10* and *C12*), 127.9 (*C11*), 127.5 (*C9* and *C13*), 126.4 (*C3*), 123.7 (*C1*), 106.3 (*C4*), 60.8 (*C6*), 26.9 (*C7*), 14.0 (C14); **IR** ν_{max} (film)/cm^{-1} 3442 (N-H stretch), 3030 (aromatic C-H stretch), 2881 (C-H stretch), 1732 (ester C=O stretch), 1563 (aromatic C=C stretch), 1442 (aromatic C=C stretch); **LCMS** m/z 308.1 and 310.1 ($M+H^+$), time = 9.985 min. **HRMS** (ESI^+) $C_{14}H_{15}BrNO_2$ requires 308.0286, found [M+H] 308.0288.

Synthesis of 2.27 (ethyl 5-iodo-4-methyl-3-phenyl-1*H*-pyrrole-2-carboxylate)[27]

2.25 (500 mg, 2.18 mmol, 1 equiv.) was dissolved in DMF (15 mL). NIS (589 mg, 2.62 mmol, 1.2 equiv.) was added portion-wise. The reaction mixture was then stirred at r.t. for 2 h. Upon completion, the mixture was diluted with water (25 mL) and extracted with ethyl acetate (2 x 25 mL). The combined organic extracts were washed with brine (25 mL), dried over anhydrous sodium sulfate, filtered and concentrated *in vacuo*. The crude product was further purified via flash column chromatography (eluted with cyclohexane-ethyl acetate) to give **2.27** as a yellow solid (584 mg, 75%).

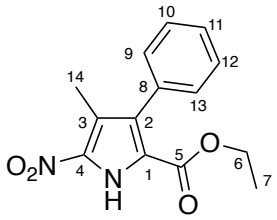


2.27

mp 101-103 °C; **TLC** 3:2 cyclohexane/ethyl acetate, R_f = 0.65; **^{1}H NMR** (400 MHz, chloroform-*d*) δ 9.68 (br s, 1H, NH), 7.41-7.27 (m, 5H, Ph-H), 4.20 (q, *J* = 7.0 Hz, 2H, OCH_2), 1.95 (s, 3H, Ar-CH_3), 1.12 (t, *J* = 7.0 Hz, 3H, CH_3); **^{13}C NMR** (101 MHz, chloroform-*d*) δ 160.4 (*C5*), 134.4 (*C8*), 131.5 (*C2*), 130.3 (*C10* and *C12*), 127.7 (*C11*), 127.2 (*C9* and *C13*), 126.3 (*C3*), 123.4 (*C1*), 74.0 (*C4*), 60.5 (*C6*), 27.1 (*C7*), 14.2 (C14); **IR** ν_{max} (film)/cm^{-1} 3440 (N-H stretch), 3032 (aromatic C-H stretch), 2896 (C-H stretch), 1738 (ester C=O stretch), 1553 (aromatic C=C stretch), 1460 (aromatic C=C stretch); **LRMS** (ESI$^+$, m/z) 356.0 [M+H]; **HRMS** (ESI$^-$) $C_{14}H_{13}INO_2$ requires 353.9996, found [M-H] 353.9994.

Synthesis of 2.28 (ethyl 4-methyl-5-nitro-3-phenyl-1*H*-pyrrole-2-carboxylate)[22]

2.28 was synthesised via nitration of **2.25** (100 mg, 0.436 mmol, 1 equiv.) using the same method that was used to synthesise **2.20** and **2.21** to give an off-white solid (39 mg, 33%).

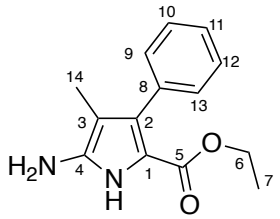


2.19

mp 183-185 °C; **TLC** 3:2 cyclohexane/ethyl acetate, R_f = 0.65; **^{1}H NMR** (400 MHz, chloroform-*d*) δ 10.32 (s, 1H, NH), 7.42-7.38 (m, 3H, *H10*, *H11* and *H12*), 7.29-7.24 (m, 2H, *H9* and *H13*), 4.23 (q, *J* = 7.0 Hz, 2H, OCH_2), 2.30 (s, 3H, Ar-CH_3), 1.13 (t, *J* = 7.0 Hz, 3H, CH_3); **^{13}C NMR** (101 MHz, chloroform-*d*) δ 167.1 (*C5*), 151.3 (*C4*), 131.1 (*C8*), 131.0 (*C2*), 130.7 (*C11*), 129.5 (*C1*), 129.3 (*C10* and *C12*), 129.0 (*C9* and *C13*), 128.3 (*C3*), 64.7 (*C6*), 27.3 (*C7*), 14.3 (*C14*); **IR** ν_{max} (film)/cm^{-1} 3442 (N-H stretch), 3030 (aromatic C-H stretch), 2873 (C-H stretch), 1740 (ester C=O stretch), 1545 (N-O stretch), 1466 (aromatic C=C stretch), 1352 (N-O stretch); **LCMS** m/z 275.1 ($M+H^+$), time = 9.961 min; **HRMS** (ESI^-) $C_{14}H_{13}N_2O_2$ requires 273.0881, found [M-H] 273.0880.

Synthesis of 2.20 (ethyl 5-amino-4-methyl-3-phenyl-1*H*-pyrrole-2-carboxylate)[24]

2.20 was synthesised via reduction of **2.19** (33 mg, 0.120 mmol, 1.0 equiv.) using the same method that was used to synthesise **2.14** to give an off-white crystal (29 mg, quant.), which was used in the subsequent step without further purification.

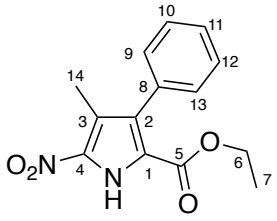


2.20

mp 203-205 °C; **TLC** 3:2 cyclohexane/ethyl acetate, R_f = 0.20; **^{1}H NMR** (400 MHz, chloroform-*d*) δ 10.54 (br s, 1H, NH), 7.44-7.39 (m, 3H, *H10*, *H11* and *H12*), 7.27-7.23 (m, 2H, *H9* and *H13*), 5.16 (s, 2H, NH_2), 4.21 (q, *J* = 7.0 Hz, 2H, OCH_2), 2.32 (s, 3H, Ar-CH_3), 1.13 (t, *J* = 7.0 Hz, 3H, CH_3); **^{13}C NMR** (101 MHz, chloroform-*d*) δ 169.2 (*C5*), 141.1 (*C4*), 132.1 (*C8*), 131.3 (*C2*), 131.0 (*C11*), 129.3 (*C1*), 129.1 (*C10* and *C12*), 128.7 (*C9* and *C13*), 128.1 (*C3*), 63.9 (*C6*), 26.8 (*C7*), 14.1 (*C14*); **IR** ν_{max} (film)/cm^{-1} 3450 (N-H stretch), 3425 (N-H stretch), 3345 (N-H stretch), 3030 (aromatic C-H stretch), 2870 (C-H stretch), 1736 (ester C=O stretch), 1521 (aromatic C=C stretch), 1487 (aromatic C=C stretch); **LRMS** (ESI$^+$, m/z) 245.1 [M+H]; **HRMS** (ESI$^+$) $C_{14}H_{17}N_2O_2$ requires 245.1290, found [M+H] 245.1292.

Synthesis of 2.30 (4-methyl-5-nitro-3-phenyl-1*H*-pyrrole-2-carboxylic acid)

2.28 (39 mg, 0.142 mmol, 1 equiv.) was dissolved in a mixture of tetrahydrofuran and methanol (3:1 v/v, 4 mL), and 1M aqueous sodium hydroxide solution (0.71 mL, 0.71 mmol, 5 equiv.) was added slowly. The reaction mixture was left to stir at r.t. for 24 h, after which it was diluted with 1 M aqueous sodium hydroxide solution (10 mL) and washed with ethyl acetate (20 mL). The aqueous layer was acidified with 2 M aqueous hydrochloric acid solution (10 mL) and extracted with ethyl acetate (20 mL). The resultant organic layer was dried over anhydrous sodium sulfate, filtered, and concentrated *in vacuo* to give **2.30** as a white solid (23 mg, 66%).



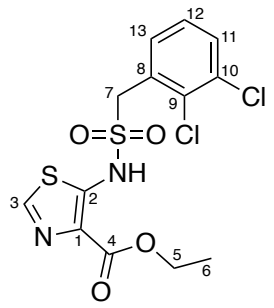
2.30

mp 203-204 °C; **TLC** 9:1 dichloromethane/methanol, R_f = 0.40; **^{1}H NMR** (400 MHz, methanol-d_4) δ 7.41-7.31 (m, 3H, *H8*, *H9* and *H10*), 7.28-7.24 (m, 2H, *H7* and *H11*), 2.22 (s, 3H, Ar-CH_3); **^{13}C NMR** (101 MHz, methanol-d_4) δ 162.6 (*C5*), 134.3 (*C4*), 132.6 (*C6*), 131.5 (*C2*), 130.7 (*C8* and *C10*), 129.4 (*C9*), 128.8 (*C1*), 128.5 (*C7* and *C11*), 123.3 (*C3*), 11.4 (*C12*); **IR** ν_{max} (film)/cm^{-1} 3300 (O-H stretch, br), 3048 (aromatic C-H stretch), 2873 (C-H stretch), 1707 (acid C=O stretch), 1532 (N-O stretch), 1512 (aromatic C=C stretch), 1461 (aromatic C=C stretch), 1356 (N-O stretch); **LRMS** (ESI$^+$, m/z) 247.1 [M+H]; **HRMS** (ESI$^-$) $C_{12}H_9N_2O_4$ requires 245.0568, found [M-H] 245.0567.

Synthesis of 2.31i (ethyl 4-(((2,3-dichlorophenyl)methyl)sulfonamido)isothiazole-3-carboxylate)[7]

2.31i was synthesised according to a modified literature procedure[7]. 5-Amino-thiazole-4-carboxylic acid ethyl ester (223 mg, 1.297 mmol, 1 equiv.) and triethylamine (0.92 mL, 6.601 mmol, 5 equiv.) were dissolved in 1,4-dioxane (6 mL). To this, (2,3 dichlorophenyl)methanesulfonyl chloride (414 mg, 1.595 mmol, 1.2 equiv.) was added at r.t. and stirred for 24 h at 60 °C. The mixture was concentrated *in vacuo* and extracted with ethyl acetate. The organic layer was washed with 1 M aqueous hydrochloric acid solution (25 mL) and water (25 mL). The organic layer was dried with anhydrous sodium sulfate, filtered and concentrated *in vacuo*. The residue was purified by column chromatography on silica (eluted with 0-50% ethyl acetate-

cyclohexane). The fractions containing the desired product were combined and the solvent removed by evaporation *in vacuo*. The solid was triturated with diethyl ether to give **2.31i** (272 mg, 53%) as an off-white solid.



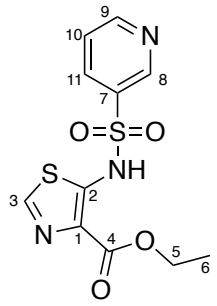
2.31i

mp 123-124 °C; **TLC** 1:1 cyclohexane/ethyl acetate, R_f = 0.80; **^{1}H NMR** (400 MHz, methanol-d_4) δ 8.33 (s, 1H, *H3*), 7.49-7.41 (m, 2H, *H11* and *H13*), 7.21 (t, *J* = 8.0 Hz, 1H, *H12*), 4.35 (q, *J* = 7.0 Hz, 2H, OCH_2), 1.34 (t, *J* = 7.0 Hz, 3H, CH_3); **^{13}C NMR** (101 MHz, methanol-d_4) δ 164.8 (*C4*), 148.4 (*C3*), 146.6 (*C8*), 134.7 (*C10*), 134.6 (*C9*), 133.0 (*C13*), 132.5 (*C2*), 130.1 (*C1*), 129.4 (*C12*), 129.0 (*C11*), 126.1 (C2), 62.7 (*C5*), 57.9 (*C7*), 14.6 (*C6*); **IR νmax** (film)/cm^{-1} 3412 (N-H stretch), 3050 (aromatic C-H stretch), 2962 (C-H stretch), 1733 (ester C=O stretch), 1621 (aromatic C=C stretch), 1554 (aromatic C=C stretch), 1363 (S=O stretch), 1123 (S=O stretch); **LCMS** m/z 395.050 ($M+H^+$) time = 7.367 min; **HRMS** (ESI^+) $C_{13}H_{12}Cl_2N_2O_2S_2$ requires 394.96883, found [M+H] 394.96876.

Synthesis of 2.32i (ethyl 4-(pyridine-3-sulfonamido)isothiazole-3-carboxylate)[7]

2.32i was synthesised according to a modified literature procedure[7]. 5-Amino-thiazole-4-carboxylic acid ethyl ester (172 mg, 1.0 mmol, 1 equiv.) was suspended in pyridine (3 mL). To this, pyridine-3-sulfonyl chloride (330 mg, 1.35 mmol, 1.35 equiv.) was added and the mixture heated at 50 °C for 3 h. The mixture was diluted with

water and extracted with ethyl acetate. The combined organic layers were dried with anhydrous sodium sulfate, filtered and concentrated *in vacuo* to dryness. The residue was purified by column chromatography on silica (eluted with 0-100% ethyl acetate-cyclohexane). The fractions containing the desired product were combined and the solvent removed by evaporation *in vacuo*. The solid was triturated with diethyl ether to give **2.32i** (52 mg, 17%) as a yellow solid.

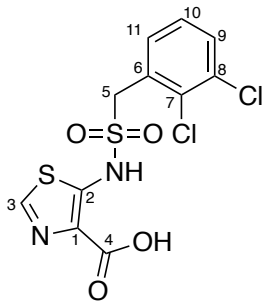


2.32i

mp 141-143 °C; **TLC** 1:1 cyclohexane/ethyl acetate, R_f = 0.15; **^{1}H NMR** (400 MHz, methanol-d_4) δ ppm 9.04 (d, *J* = 1.5 Hz, 1H, *H8*), 8.70 (dd, *J* = 5.0, 1.5 Hz, 1H, *H9*), 8.34-8.29 (m, 2H, *H3* and *H11*), 7.56 (dq, *J* = 5.0, 0.5 Hz, 1H, *H10*), 4.30 (q, *J* = 7.0 Hz, 2H, OCH_2), 1.32 (t, *J* = 7.0 Hz, 3H, CH_3); **^{13}C NMR** (151 MHz, methanol-d_4) δ 164.5 (*C4*), 153.5 (*C9*), 148.5 (*C3*), 145.1 (*C8*), 139.4 (*C7*), 137.7 (*C11*), 136.7 (*C1*), 130.2 (*C10*), 125.4 (*C2*), 62.0 (*C5*), 14.6 (C6); **IR ν_{max}** (film)/cm^{-1} 3421 (N-H stretch), 3050 (aromatic C-H stretch), 2962 (C-H stretch), 1744 (ester C=O stretch), 1607 (aromatic C=C stretch), 1531 (aromatic C=C stretch), 1370 (S=O stretch), 1156 (S=O stretch); **LCMS** m/z 314.000 ($M+H^+$) time = 5.267 min; **HRMS** (ESI^+) $C_{11}H_{11}N_3O_4S_2$ requires 314.02637, found [M+H] 314.02631.

Synthesis of 2.31ii (4-(((2,3-dichlorophenyl)methyl)sulfonamido)isothiazole-3-carboxylic acid)[7]

2.31ii was synthesised according to a modified literature procedure[7]. **2.31i** (100 mg, 0.254 mmol, 1 equiv.) was suspended in methanol (1 mL) and tetrahydrofuran (1 mL). To this, a solution of lithium hydroxide monohydrate (54 mg, 1.287 mmol, 5 equiv.) in water (2 mL) was added and the mixture heated at 50 °C for 18 hours. The mixture was cooled to r.t. and the solvents were removed *in vacuo*. The residue was diluted with water and acidified with 1 M aqueous hydrochloric acid solution. The product was collected by filtration, washed with water and dried under vacuum to give **2.31ii** (80 mg, 86%) as a pink-orange solid.

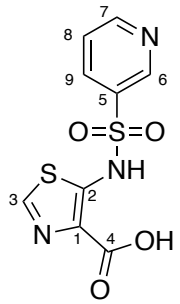


2.31ii

mp 162 °C; **^{1}H NMR** (400 MHz, DMSO-d_6) δ 8.47 (s, 1H, *H3*), 7.63 (dd, *J* = 8.0, 1.5 Hz, 1H, *H9*), 7.47 (dd, *J* = 8.0, 1.5 Hz, 1H, *H10*), 7.33 (t, *J* = 8.0 Hz, 1H, *H11*), 4.95 (s, 2H, CH_2); **^{13}C NMR** (126 MHz, DMSO-d_6) δ 164.5 (*C4*), 147.6 (*C3*), 144.7 (*C6*), 132.7 (*C8*), 132.2 (*C7*), 132.1 (*C11*), 131.0 (*C1*), 129.5 (*C10*), 128.8 (*C9*), 128.1 (*C2*), 56.2 (*C5*); **IR ν_{max}** (film)/cm^{-1} 3400 (N-H stretch), 3300 (O-H stretch, br), 3060 (aromatic C-H stretch), 2960 (C-H stretch), 1704 (acid C=O stretch), 1610 (aromatic C=C stretch), 1531 (aromatic C=C stretch), 1372 (S=O stretch), 1151 (S=O stretch); **LCMS** m/z 367.0 ($M+H^+$) time = 6.163 min; **HRMS** (ESI^+) $C_{11}H_8Cl_2N_2O_4S_2$ requires 364.92298, found [M-H] 364.92272.

Synthesis of 2.23ii (4-(pyridine-3-sulfonamido)isothiazole-3-carboxylic acid)[7]

2.32ii was synthesised according to a modified literature procedure[7]. **2.32i** (45 mg, 0.144 mmol, 1 equiv.) was suspended in methanol (1 mL) and tetrahydrofuran (1 mL). To this mixture, a solution of lithium hydroxide monohydrate (30 mg, 0.714 mmol, 5 equiv.) in water (2 mL) was added and the mixture heated at 50 °C for 18 h. The mixture was cooled to r.t. and the solvents were removed *in vacuo*. The residue was diluted with water and acidified with 1 M aqueous hydrochloric acid solution. The product was collected by filtration, washed with water and dried under vacuum to give **2.32ii** (32 mg, 78%) as a yellow solid.

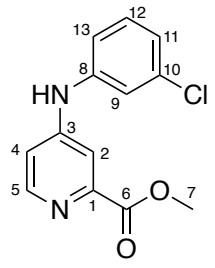


2.32ii

mp 184 °C; **^{1}H NMR** (400 MHz, DMSO-d_6) δ 8.94 (dd, *J* = 2.5, 0.5 Hz, 1H, *H6*), 8.79 (dd, *J* = 5.0, 1.5 Hz, 1H, *H7*), 8.53 (s, 1H, *H3*), 8.18 (ddd, *J* = 8.0, 2.5, 1.5 Hz, 1H, *H9*), 7.61 (ddd, *J* = 8.0, 5.0, 1.0 Hz, 1H, *H8*); **^{13}C NMR** (101 MHz, DMSO-d_6) δ 162.7 (*C4*), 153.0 (*C7*), 146.7 (*C3*), 145.2 (*C6*), 136.8 (*C5*), 135.1 (*C9*), 134.8 (*C1*), 131.1 (*C8*), 124.4 (*C2*); **IR ν_{max}** (film)/cm^{-1} 3400 (N-H stretch), 3300 (O-H stretch, br), 3080 (aromatic C-H stretch), 1703 (acid C=O stretch), 1604 (aromatic C=C stretch), 1527 (aromatic C=C stretch), 1385 (S=O stretch), 1164 (S=O stretch); **LCMS** m/z 286.100 ($M+H^+$) time = 4.157 min; **HRMS** (ESI^-) $C_9H_7N_3O_4S_2$ requires 283.98052, found [M-H] 283.98057.

Synthesis of 2.33 (methyl 4-((3-chlorophenyl)amino)picolinate)[31]

Methyl 4-bromo-pyridine-2-carboxylate (300 mg, 1.39 mmol, 1 equiv.) and potassium fluoride (161 mg, 2.77 mmol, 2 equiv.) were suspended in anhydrous DMF (1.0 mL). 3-Chloroaniline was added slowly, and the reaction was stirred at 150 °C for 48 h. The solvent was then removed under reduced pressure, and the mixture diluted with ethyl acetate (5 mL) and washed with water (5 mL). The aqueous layer was back-extracted with ethyl acetate (2 x 5 mL), and the combined organic layers were dried over anhydrous sodium sulfate, filtered and concentrated *in vacuo*. The crude product was purified by flash column chromatography on silica (eluted with cyclohexane-ethyl acetate) to afford **2.33** (16 mg, 4%).

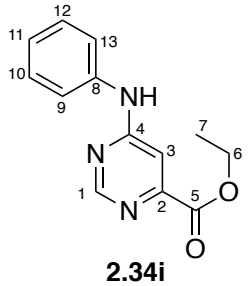


2.33

mp 102 °C; **TLC** 3:2 cyclohexane/ethyl acetate, R_f = 0.10; **^{1}H NMR** (400 MHz, chloroform-*d*) δ 8.41 (d, *J* = 5.5 Hz, 1H, *H5*), 7.67 (d, *J* = 2.0 Hz, 1H, *H2*), 7.31 (t, *J* = 8.0 Hz, 1H, *H12*), 7.21 (s, 1H, *H2*), 7.17-7.08 (m, 2H, *H11* and *H13*), 7.02 (dd, *J* = 5.5, 2.5 Hz, 1H, *H4*), 6.59 (s, 1H, *H9*), 3.98 (s, 3H, OCH_3). **^{13}C NMR** (101 MHz, chloroform-*d*) δ 184.5 (*C6*), 150.3 (*C3*), 140.3 (*C1*), 135.5 (*C8*), 130.9 (*C5*), 129.0 (*C10*), 126.8 (*C12*), 125.0 (*C11*), 122.0 (*C9*), 119.9 (*C13*), 111.9 (*C4*), 111.7 (*C2*), 53.2 (*C7*); **IR** ν_{max} (film)/cm^{-1} 3420 (N-H stretch), 3050 (aromatic C-H stretch), 2961 (C-H stretch), 1742 (ester C=O stretch), 1576 (aromatic C=C stretch), 1483 (aromatic C=C stretch); **LRMS** (ESI^+, m/z) 263.1 [M+H]; **HRMS** (ESI^+) $C_{13}H_{12}ClN_2O_2$ requires 263.0587, found [M+H] 263.0588.

Synthesis of 2.34i (ethyl 6-(phenylamino)pyrimidine-4-carboxylate)[31]

2.34i was synthesised according to a literature procedure with minor modifications[31]. Ethyl 6-bromopyrimidine-4-carboxylate (200 mg, 1.07 mmol, 1 equiv.) was dissolved in anhydrous isopropanol (10 mL). With stirring, aniline (0.10 mL, 1.10 mmol, 1.05 equiv.) was added, and the resulting solution was refluxed for 18 h. The reaction mixture was cooled to r.t. and the solvent was removed *in vacuo* to afford a yellow solid. The solid was then re-dissolved in dichloromethane (100 mL) and washed with brine (100 mL). The aqueous layer was back-extracted with dichloromethane (2 x 50 mL). The combined organic phase was dried over anhydrous sodium sulfate, filtered and evaporated to dryness. The crude product was purified by flash column chromatography on silica (eluted with cyclohexane-ethyl acetate) to afford **2.34i** as a white solid (162 mg, 62%).



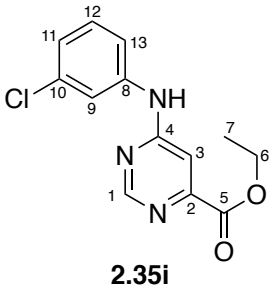
2.34i

mp 75 °C; **TLC** 3:2 cyclohexane/ethyl acetate, R_f = 0.20; **^{1}H NMR** (400 MHz, chloroform-*d*) δ 8.77 (s, 1H, H1), 7.91 (s, 1H, NH), 7.45-7.38 (m, 5H, *H3*, *H9*, *H10*, *H12* and *H13*), 7.22 (t, *J* = 8.5, 1H, *H11*), 4.42 (q, *J* = 7.0 Hz, 2H, OCH_2), 1.39 (t, *J* = 7.0 Hz, 3H, CH_3). **^{13}C NMR** (101 MHz, chloroform-*d*) δ 164.8 (*C4*), 162.3 (*C5*), 159.1 (*C2*), 154.4 (*C1*), 137.5 (*C8*), 129.8 (*C3*), 125.7 (*C10* and *C12*), 122.7 (*C9* and *C13*), 105.4 (*C11*), 62.6 (*C6*), 14.3 (*C7*); **IR** ν_{max} (film)/cm^{-1} 3422 (N-H stretch), 3050 (aromatic C-H stretch), 2950 (C-H stretch), 1741 (ester C=O stretch), 1642 (aromatic C=N stretch),

1535 (aromatic C=C stretch), 1381 (aromatic C=C stretch); **LRMS** (ESI^+, m/z) 244.1 [M+H]; **HRMS** (ESI^+) $C_{13}H_{14}ClN_3O_2$ requires 244.1086, found [M+H] 244.1088.

Synthesis of 2.35i (ethyl 6-((3-chlorophenyl)amino)pyrimidine-4-carboxylate)[31]

2.35i was synthesised using the same procedure that was used for the synthesis of **2.34i**[31], and was isolated as a white solid (40 mg, 21%).

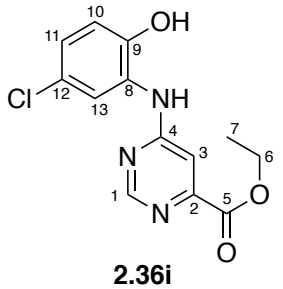


2.35i

mp 81 °C; **TLC** 1:1 pentane/ethyl acetate, R_f = 0.30; **^{1}H NMR** (400 MHz, chloroform-*d*) δ 8.86 (s, 1H, *H1*), 8.10 (s, 1H, *H9*), 7.66 (s, 1H, *H3*), 7.55 (s, 1H, NH), 7.41 (d, *J* = 7.0 Hz, 1H, *H11*), 7.32 (t, *J* = 8.0 Hz, 1H, *H12*), 7.17 (d, *J* = 7.0 Hz, 1H, *H13*), 4.44 (q, *J* = 7.0 Hz, 2H, OCH_2), 1.41 (t, *J* = 7.0 Hz, 3H, CH_3). **^{13}C NMR** (101 MHz, chloroform-*d*) δ 161.4 (*C4*), 158.0 (*C5*), 149.9 (*C2*), 142.6 (*C1*), 138.5 (*C8*), 134.9 (*C10*), 130.2 (*C3*), 125.2 (*C9*), 121.8 (*C12*), 119.8 (*C11*), 106.5 (*C13*), 62.7 (*C6*), 14.0 (*C7*); **IR** ν_{max} (film)/cm^{-1} 3420 (N-H stretch), 3050 (aromatic C-H stretch), 2950 (C-H stretch), 1735 (ester C=O stretch), 1624 (aromatic C=N stretch), 1531 (aromatic C=C stretch), 1362 (aromatic C=C stretch); **LRMS** (ESI^+, m/z) 278.1 [M+H]; **HRMS** (ESI^+) $C_{13}H_{13}ClN_3O_2$ requires 278.0696, found [M+H] 278.0694.

Synthesis of 2.36i (ethyl 6-((5-chloro-2-hydroxyphenyl)amino)pyrimidine-4-carboxylate)[31]

2.36i was synthesised using the same procedure that was used for the synthesis of **2.34i**[31], and was isolated as a yellow solid (33 mg, 21%).

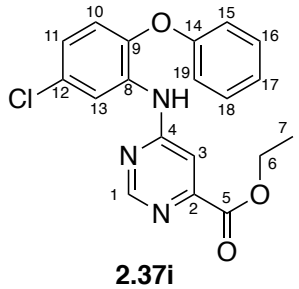


2.36i

mp 93-95 °C; **TLC** 1:1 cyclohexane/ethyl acetate, R_f = 0.30; **^{1}H NMR** (400 MHz, methanol-d_4) δ 8.67 (s, 1H, *H1*), 8.06 (s, 1H, *H13*), 7.49 (s, 1H, *H3*), 6.98 (dd, *J* = 8.5, 2.5 Hz, 1H, *H11*), 6.85 (d, *J* = 8.5 Hz, 1H, *H10*), 6.70 (d, *J* = 2.5 Hz, 1H, OH), 4.41 (q, *J* = 7.0 Hz, 2H, OCH_2), 1.40 (t, *J* = 7.0 Hz, 3H, CH_3). **^{13}C NMR** (101 MHz, methanol-d_4) δ 159.3 (*C4*), 153.9 (*C5*), 145.1 (*C2*), 142.6 (*C1*), 137.2 (*C9*), 131.4 (*C8*), 125.5 (*C12*), 125.0 (*C11*), 119.1 (*C13*), 117.3 (*C10*), 63.3 (*C6*), 14.5 (*C7*); **IR** ν_{max} (film)/cm^{-1} 3400 (N-H stretch), 3300 (O-H stretch), 3050 (aromatic C-H stretch), 2956 (C-H stretch), 1733 (ester C=O stretch), 1636 (aromatic C=N stretch), 1519 (aromatic C=C stretch), 1355 (aromatic C=C stretch); **LRMS** (ESI$^-$, m/z) 292.0 [M-H]; **HRMS** (ESI$^-$) $C_{13}H_{11}ClN_3O_3$ requires 292.0494, found [M-H] 292.0495.

Synthesis of 2.37i (ethyl 6-((5-chloro-2-phenoxyphenyl)amino)pyrimidine-4-carboxylate)[31]

2.37i was synthesised using the same procedure that was used for the synthesis of **2.34i**[31], and was isolated as a brown solid (33 mg, 21%).

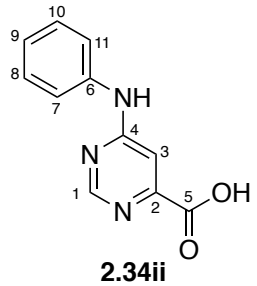


2.37i

mp 102 °C; **^{1}H NMR** (400 MHz, chloroform-*d*) δ 8.91 (d, *J* = 1.0 Hz, 1H, *H1*), 8.54 (d, *J* = 2.3 Hz, 1H, *H3*), 7.73 (s, 1H, NH), 7.42 (s, 1H, *H13*), 7.35 (t, *J* = 8.0 Hz, 2H, *H16* and *H18*), 7.15 (t, *J* = 7.5 Hz, 1H, *H17*), 7.02-6.97 (m, 3H, *H11*, *H15* and *H19*), 6.80 (d, *J* = 8.5 Hz, 1H, *H10*), 4.44 (q, *J* = 7.0 Hz, 2H, OCH_2), 1.41 (t, *J* = 7.0 Hz, 3H, CH_3). **^{13}C NMR** (101 MHz, chloroform-*d*) δ 164.2 (*C4*), 161.0 (*C5*), 158.8 (*C2*), 156.0 (*C14*), 153.8 (*C1*), 145.5 (*C9*), 130.7 (*C8*), 130.2 (*C16* and *C18*), 129.0 (*C12*), 124.5 (*C17*), 124.0 (*C10*), 121.6 (*C11*), 118.8 (*C15* and *C19*), 110.0 (*C13*), 108.2 (*C3*), 62.7 (OCH_2), 14.3 (CH_3). **IR** ν_{max} (film)/cm^{-1} 3416 (N-H stretch), 3050 (aromatic C-H stretch), 2965 (C-H stretch), 1737 (ester C=O stretch), 1640 (aromatic C=N stretch), 1521 (aromatic C=C stretch), 1372 (aromatic C=C stretch); **LRMS** (ESI^+, m/z) 370.1 [M+H]; **HRMS** (ESI^+) $C_{19}H_{17}ClN_3O_3$ requires 370.0958, found [M+H] 370.0960.

Synthesis of 2.34ii (6-(phenylamino)pyrimidine-4-carboxylic acid)

2.34i was dissolved in 2 mL of tetrahydrofuran and water (1:1 v/v). 1 M aqueous sodium hydroxide solution (0.7 mL) was added slowly and the reaction was stirred at 40 °C overnight. The reaction mixture was acidified with 2 M aqueous hydrochloric acid solution and extracted with ethyl acetate (3 x 20 mL). The combined organic layers were washed with brine and dried over anhydrous magnesium sulfate. The resultant solution was concentration *in vacuo* to yield **2.34ii** as a white solid (126 mg, 100%).

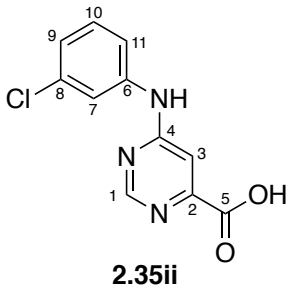


2.34ii

mp 202-203 °C; **^{1}H NMR** (400 MHz, DMSO-d_6) δ 10.17 (s, 1H, OH), 8.73 (s, 1H, *H1*), 7.70 (d, *J* = 8.0 Hz, 2H, *H7* and *H11*), 7.43-7.32 (m, 3H, *H3*, *H8* and *H10*), 7.09 (t, *J* = 7.5 Hz, 1H, *H9*). **^{13}C NMR** (101 MHz, DMSO-d_6) δ 164.92 (*C4*), 161.36 (*C5*), 157.68 (*C2*), 152.72 (*C1*), 138.95 (*C6*), 128.96 (*C8* and *C10*), 123.45 (*C7* and *C11*), 120.41 (*C9*); **IR** ν_{max} (film)/cm^{-1} 3416 (N-H stretch), 3300 (O-H stretch, br), 3050 (aromatic C-H stretch), 1708 (acid C=O stretch), 1632 (aromatic C=N stretch), 1533 (aromatic C=C stretch), 1352 (aromatic C=C stretch); **LRMS** (ESI$^-$, m/z) 214.1 [M-H]; **HRMS** (ESI$^-$) $C_{11}H_7ClN_3O_2$ requires 214.0622, found [M-H] 214.0622.

Synthesis of 2.35ii (6-((3-chlorophenyl)amino)pyrimidine-4-carboxylic acid)

2.35ii was synthesised from **2.35i** using the same procedure that was used for the synthesis of **2.34ii** and was isolated as an off-white solid (60 mg, 20%).



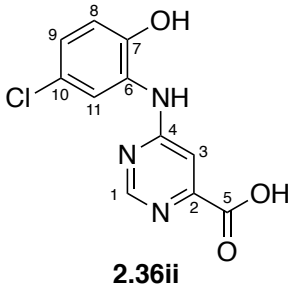
2.35ii

mp 215 °C; **^{1}H NMR** (400 MHz, DMSO-d_6) δ 10.22 (s, 1H, OH), 8.86 (s, 1H, *H1*), 7.66 (s, 1H, *H7*), 7.55 (s, 1H, *H3*), 7.41 (d, *J* = 7.0 Hz, 1H, *H9*), 7.32 (t, *J* = 8.0 Hz, 1H, *H10*), 7.17 (d, *J* = 8.0 Hz, 1H, *H11*); **^{13}C NMR** (101 MHz, DMSO-d_6) δ 163.9 (*C4*), 162.1 (*C5*),

158.9 (*C2*), 154.7 (*C1*), 147.3 (*C6*), 136.5 (*C8*), 131.8 (*C10*), 122.4 (*C9*), 116.9 (*C7*), 116.1 (*C11*), 106.2 (*C3*); **IR** ν_{max} (film)/cm^{-1} 3416 (N-H stretch), 3300 (O-H stretch, br), 3050 (aromatic C-H stretch), 1708 (acid C=O stretch), 1632 (aromatic C=N stretch), 1533 (aromatic C=C stretch), 1352 (aromatic C=C stretch); **LRMS** (ESI$^-$, m/z) 238.0 [M-H]; **HRMS** (ESI$^-$) $C_{11}H_7ClN_3O_2$ requires 248.0232, found [M-H] 248.0231.

Synthesis of 2.36ii (6-((5-chloro-2-hydroxyphenyl)amino)pyrimidine-4-carboxylic acid)

2.36i was dissolved in 1 mL of tetrahydrofuran and water (1:1 v/v). 1 M aqueous sodium hydroxide solution (0.02 mL) was added and the reaction was stirred at 40 °C overnight. The reaction mixture was acidified with 4 M hydrochloric acid solution and the resultant precipitate was filtered, washed with water and dried to give **2.36ii** as a brown solid (11 mg, 37%).



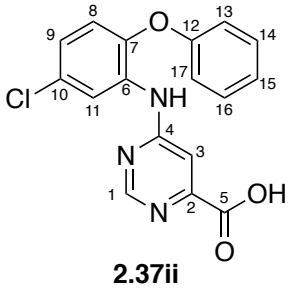
2.36ii

mp 232 °C; **^{1}H NMR** (400 MHz, DMSO-d_6) δ 10.28 (s, 1H, OH), 9.41 (s, 1H, OH), 8.70 (s, 1H, *H1*), 8.07 (s, 1H, *H3*), 7.55 (s, 1H, *H11*), 7.01 (dd, *J* = 8.5, 2.5 Hz, 1H, *H9*), 6.91 (d, *J* = 8.5 Hz, 1H, *H8*); **^{13}C NMR** (101 MHz, DMSO-d_6) δ 165.2 (*C4*), 161.6 (*C5*), 157.6 (*C2*), 153.4 (*C1*), 127.5 (*C7*), 124.0 (*C6*), 122.5 (*C10*), 122.1 (*C9*), 116.4 (*C11*), 111.4 (*C8*), 107.9 (*C3*); **IR** ν_{max} (film)/cm^{-1} 3420 (N-H stretch), 3300 (O-H stretch, br), 3050 (aromatic C-H stretch), 1706 (acid C=O stretch), 1644 (aromatic C=N stretch), 1520

(aromatic C=C stretch), 1376 (aromatic C=C stretch); **LRMS** (ESI^-, m/z) 264.0 [M-H]; **HRMS** (ESI^-) $C_{11}H_7ClN_3O_3$ requires 264.0181, found [M-H] 264.0180.

Synthesis of 2.37ii (6-((5-chloro-2-phenoxyphenyl)amino)pyrimidine-4-carboxylic acid)

2.37ii was synthesised from **2.37i** using the same procedure that was used for the synthesis of **2.34ii** and was isolated as a white solid (39 mg, 16%).



2.37ii

mp 244-245 °C; **^{1}H NMR** (400 MHz, DMSO-d_6) δ 10.42 (br s, 1H, OH), 8.89 (s, 1H, *H1*), 8.34 (s, 1H, *H3*), 7.61 (s, 1H, NH), 7.40 (s, 1H, *H11*), 7.28 (t, *J* = 8.0 Hz, 2H, *H14* and *H16*), 7.13 (t, *J* = 7.5 Hz, 1H, *H15*), 7.06-7.01 (m, 3H, *H9*, *H13* and *H17*), 6.83 (d, *J* = 8.5 Hz, 1H, *H8*); **^{13}C NMR** (101 MHz, DMSO-d_6) δ 165.3 (*C4*), 163.1 (*C5*), 159.7 (*C2*), 157.6 (*C12*), 154.9 (*C1*), 143.8 (*C7*), 130.9 (*C6*), 131.0 (*C14* and *C16*), 128.2 (*C10*), 122.4 (*C15*), 123.3 (*C8*), 121.7 (*C9*), 119.1 (*C13* and *C17*), 111.2 (*C11*), 108.5 (*C3*); **IR** ν_{max} (film)/cm^{-1} 3420 (N-H stretch), 3300 (O-H stretch, br), 3050 (aromatic C-H stretch), 1703 (acid C=O stretch), 1643 (aromatic C=N stretch), 1516 (aromatic C=C stretch), 1368 (aromatic C=C stretch); **LRMS** (ESI^-, m/z) 340.0 [M-H]; **HRMS** (ESI^-) $C_{17}H_{11}ClN_3O_3$ requires 340.0494, found [M-H] 340.0495.

2.10. References

[1] Walsh T. R.; Toleman, M. A.; Poirel, L.; Nordmann, P. *Clin. Microbiol. Rev.* **2005**, *18*, 306–325.

[2] Collins, P. M.; Ng, J. T.; Talon, R.; Nekrosiute, K.; Krojer, T.; Douangamath, A.; Brandao-Neto, J.; Wright, N.; Pearce, N. M.; Delft, F. V. *Acta Crystallogr. D Struct. Biol.* **2017**, *73*, 246–255.

[3] Krojer, T.; Talon, R.; Pearce, N.; Collins, P.; Douangamath, A.; Brandao-Neto, J.; Dias, A.; Marsden, B.; Delft, F. V. *Acta Crystallogr. D Struct. Biol.* **2017**, *73*, 267–278.

[4] Kimura, S.; Ishii, Y.; Yamaguchi, K. *Diagno. Microbiol. Infect. Dis.* **2005**, *53*, 241–244.

[5] Horsfall, L. E.; Garau, G.; Lienard, B. M. R.; Dideberg, O.; Schofield, C. J.; Frere, J. M.; Galleni, M. *Antimicrob. Agents Chemother.* **2007**, *51*, 2136–2142.

[6] Everett, M.; Sprynski, N.; Coelho, A.; Castandet, J.; Bayet, M.; Bougnon, J.; Lozano, C.; Davies, D. T.; Leiris, S.; Zalacain, M.; Morrissey, I.; Magnet, S.; Holden, K.; Warn, P.; Luca, F. D.; Docquier, J.-D.; Lemonnier, M. *Antimicrob. Agents Chemother.* **2018**, *62*, e00074-18.

[7] Antabio SAS. Antibacterial Thiazolecarboxylic Acids. International Patent WO 2014/198849 A1, Dec 18, 2014.

[8] Berkel, S. S. V.; Brem, J.; Rydzik, A. M.; Salimraj, R.; Cain, R.; Verma, A.; Owens, R. J.; Fishwick, C. W. G.; Spencer, J.; Schofield, C. J. *J. Med. Chem.* **2013**, *56*, 6945–6953.

[9] Gokmen, Z.; Deniz, N. G.; Ibis, C. *Phosphorus Sulfur Silicon Relat. Elem.* **2014**, *190*, 93–102.

[10] Schering Corporation. Methods for Inhibiting Protein Kinases. United States Patent US 2007/105864 A1, May 18, 2007.

[11] Akiba, K.; Ohkata, K.; Ohyama, Y.; Akiba, K.-Y. *Heterocycles* **1994**, *37*, 859.

[12] Pfizer Inc. Macrocyclic Derivatives for the Treatment of Proliferative Diseases. International Patent WO 2017/27310 A1, Feb 16, 2017.

[13] Teffera, Y.; Choquette, D.; Liu, J.; Colletti, A. E.; Hollis, L. S.; Lin, M.-H. J.; Zhao, Z. *Chem. Res. Toxicol.* **2010**, *23*, 1743–1752.

[14] Warner Lambert Co. Trans-6-[2-(3- or 4-carboxamido-substituted pyrrol-1-yl)alkyl]-4-hydroxypyran-2-one inhibitors of cholesterol synthesis. United States Patent US 4681893 A1, Jul 21, 1987.

[15] Cordrey, L. J. *J. Am. Geriatr. Soc.* **1976**, *24*, 440–446.

[16] Mallison, T. E. *J. Paramed. Prac.* **2017**, *9*, 522–526.

[17] Lainton, J. A.; Huffman, J. W.; Martin, B. R.; Compton, D. R. *Tetrahedron Lett.* **1995**, 36, 1401–1404.

[18] Dainippon Sumitomo Pharma Co., Ltd. Cyclic Amide Derivative. United States Patent US 2013/0217692 A1, Aug 22, 2013.

[19] Bristol-Myers Squibb Company. Pyrrolopyridazines As Potassium Channel Inhibitors. International Patent WO 2014/143607 A1, Sep, 18, 2014.

[20] Gao, M.; He, C.; Chen, H.; Bai, R.; Cheng, B.; Lei, A. *Angew. Chem. Int. Ed.* **2013**, *125*, 7096–7099.

[21] Abraham, R. J.; Bernstein, H. J. *Can. J. Chem.* **1959**, *37*, 1056–1065.

[22] Cooksey, A.; Morgan, K.; Morrey, D. *Tetrahedron* **1970**, *26*, 5101–5111.

[23] Louw, R. *Encyclopedia of reagents for organic synthesis*; J. Wiley and Sons: Chichester, 2009.

[24] Beutner, G. L.; Desai, L.; Fanfair, D.; Lobben, P.; Anderson, E.; Leung, S. W.; Eastgate, M. D. *Org. Process Res. Dev.* **2014**, *18*, 1812–1820.

[25] Ramadas, K.; Srinivasan, N. *Synth. Comm.* **1992**, *22*, 3189–3195.

[26] Chang, C. K.; Bag, N. *J. Org. Chem.* **1995**, *60*, 7030–7032.

[27] Zhou, H.; Chen, J.; Meagher, J. L.; Yang, C.-Y.; Aguilar, A.; Liu, L.; Bai, L.; Cong, X.; Cai, Q.; Fang, X.; Stuckey, J. A.; Wang, S. *J. Med. Chem.* **2012**, *55*, 4664–4682.

[28] Wolfe, J. P.; Åhman, J.; Sadighi, J. P.; Singer, R. A.; Buchwald, S. L. *Tetrahedron Lett.* **1997**, *38*, 6367–6370.

[29] Ocallaghan, C. H.; Morris, A.; Kirby, S. M.; Shingler, A. H. *Antimicrob. Agents Chemother.* **1972**, *1*, 283–288.

[30] Walsh, K.; Sneddon, H. F.; Moody, C. J. *ChemSusChem* **2013**, *6*, 1455–1460.

[31] Biomarin IGA Limited. Compounds for Treatment of Duchenne Muscular Dystrophy. International Patent WO2010/20432 A2, Feb 25, 2010.

[32] CHDI Foundation, Inc. Kynurenine-3-Monooxygenase Inhibitors, Pharmaceutical Compositions, And Methods of Use Thereof. International Patent WO2013/33085 A1, Mar 7, 2013.

[33] Ohkata, K.; Ohyama, Y.; Akiba, K. *ChemInform* **2010**, *25*.

[34] Tehrani, K. A.; Borremans, D.; Kimpe, N. D. *Tetrahedron* **1999**, *55*, 4133–4152.

[35] Boev, N. V.; Ustynyuk, Y. A. *Rus. J. Org. Chem.* **2007**, *43*, 297–304.

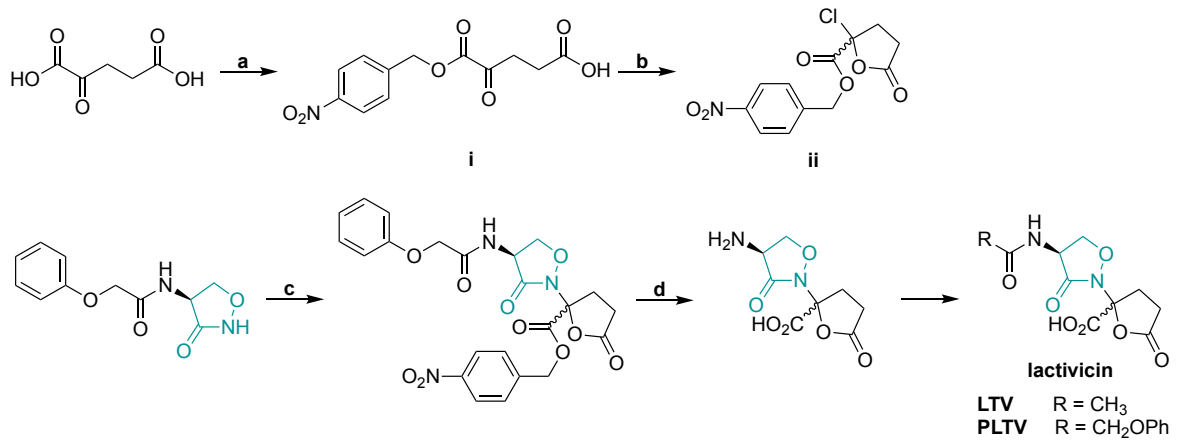
Chapter 3.
Towards Novel Lactivicin Analogues



3. Towards Novel Lactivicin Analogues

3.1. Clinical relevance of non β-lactam containing antibiotics

The success of the penicillins and subsequent generations of clinically useful *β*-lactam containing antibiotics was ultimately based on natural products. With the arguable exception of avibactam, the utilisation of modern medicinal chemistry (which encompasses high-throughput screening and structure-based design), has been unsuccessful in delivering useful scaffolds with the efficacy of *β*-lactam containing compounds for PBP and/or *β*-lactamase inhibition. The only natural product that does not contain a *β*-lactam and display PBP inhibition is lactivicin[1,2]. Compared to the *β*-lactam containing compounds, there has been few studies investigating the effects on PBPs and/or *β*-lactamases of the lactivicins.



Scheme 3.1. *A reported route to the lactivicins[1,2]:*

a) 4-nitrobenzyl bromide (1.1 equiv.), dicyclohexylamine (1 equiv.), dimethylformamide, 50-70 ºC, 15 min, 93%; **b)** sulfonyl chloride (5.5 equiv.), 1,2-dichloroethane, reflux, 10 h, 85%; **c)** method A: ii (1.3 equiv.), Et_3N (2 equiv.), CH_2Cl_2, 0 ºC to r.t., 0.5 h, or method B: i (1.3 equiv.), DCC* (1.3 equiv.), CH_2Cl_2, r.t., 14 h; **d)** H_2, Pd-C, EtOAc-pH 7.0 buffer, 0 ºC to r.t.; **e)** for **LTV**, Ac_2O (1.2 equiv.), $NaHCO_3$, THF/H_2O, 0 ºC, 28%; for **PLTV**, phenoxyacetyl chloride (1.2 equiv.), $NaHCO_3$, THF/H_2O, 0 ºC.

**N*,*N*'-Dicyclohexylcarbodiimide.

As introduced in Chapter 1, *γ*-lactams have historically evoked significant research interest, given their resemblance to *β*-lactams as well as the theoretical possibility to recyclise upon *β*-lactamase-mediated hydrolysis[3,4]. As highlighted by the recent clinical success of avibactam[5], there exists an opportunity in *γ*-lactam or *γ*-lactam-like structures to mitigate the growing threat of antimicrobial resistance. Lactivicin was the first antibacterial natural product PBP inhibitor to be isolated that contained an L-cycloserine motif which is related to a *γ*-lactam ring. D-Cycloserine, interestingly, acts independently as a therapeutic against tuberculosis, which is caused by a bacterium, *Mycobacterium tuberculosis*[6].

The original lactivicin (**LTV**), a natural product, was isolated and resynthesised by Takeda, and subsequently synthesised from derivatised L-cycloserine and activated 2-oxoglutarate (2-OG) (Scheme 3.1)[1,2]. While **LTV** and early derivatives, e.g. **PLTV**, were active against some species of both Gram-positive and Gram-negative bacteria, such as *S. aureus* and *K. pneumoniae*, their anti-PBP activities were not comparable to later generations of *β*-lactam antibiotics. Recent studies have also shown that these pioneering examples of *γ*-lactam type antibiotics are susceptible to hydrolysis, by at least some *β*-lactamases, and do not inhibit MBLs[7,8,9,9,10]. While these observations may initially suggest that lactivicins are not attractive leads to pursue, it is important to bear in mind that in comparison to newer generations of *β*-lactam antibiotics, **LTV** and **PLTV** lack in terms of the structural complexity of their side chains.

In order to boost the effectiveness of *β*-lactam antibiotics, medicinal chemists have performed extensive side chain modifications. Firstly, the C-6 (in penicillin nomenclature) amide side chain has been extensively modified, resulting in pencillins

with broader spectrum activities[10]. Side chain modifications have also been carried out on the cephalosporins and the carbapenems[11,12]. These modifications have drastically improved the activities and pharmacokinetic properties of the β-lactam antibiotics (Figure 3.1).

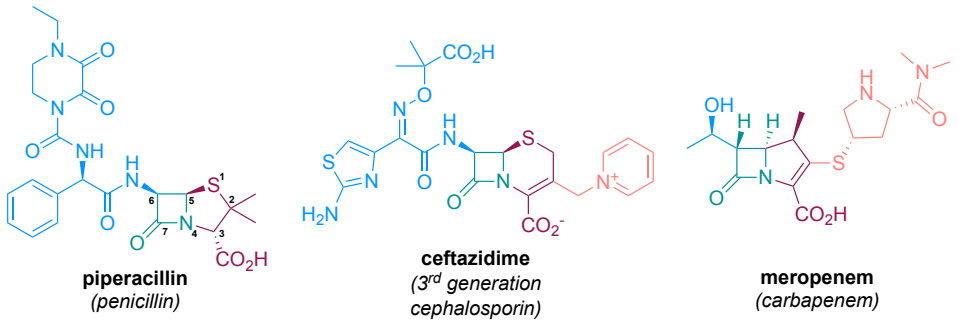


Figure 3.1. Examples of functionalisations performed on different classes of β-lactam antibiotics, i.e. the penicillins, the cephalosporins and the carbapenems, illustrated by piperacillin (with the classic penicillin numbering nomenclature), ceftazidime and meropenem, respectively. The common β-lactam rings are in green. The amide side chain (in the case of the penicillins and cephalosporins), which can be readily functionalised, and the hydroxyethyl side chain (in the case of the carbapenems), are in blue. The non β-lactam ring, coloured in red, can also be functionalised in the case of cephalosporins and carbapenems, with examples of structural features highlighted in orange.

Pfizer has demonstrated the potential of siderophore-coupled lactivicin derivatives, such as **LTV-14** and **LTV-17** (Figure 3.2)[13]. Notably, **LTV-17** has displayed interesting biological activities, with the added functionality on its lactone being a novel aspect of its structure[14]. The amide group of **LTV-17** contains a commonly used antibiotic amide side chain, i.e. the 2-amino-4-thiazolyl methoxyimino (ATMO) group. The use of this side chain has been described in numerous clinically successful β-lactam antibiotics, with aztreonam, a monobactam, being one such example[15]. The addition of a siderophore, in order to exploit the bacterial iron uptake mechanisms to boost drug intake and selectivity, and consequently, activity, was possibly in part inspired by the success of BAL30072. BAL30072 was developed by Basilea (Basel,

Switzerland) and is a siderophore-containing monobactam that showed promising *in vivo* and *in vitro* activities against multi-drug resistant Gram-negative bacteria[16].

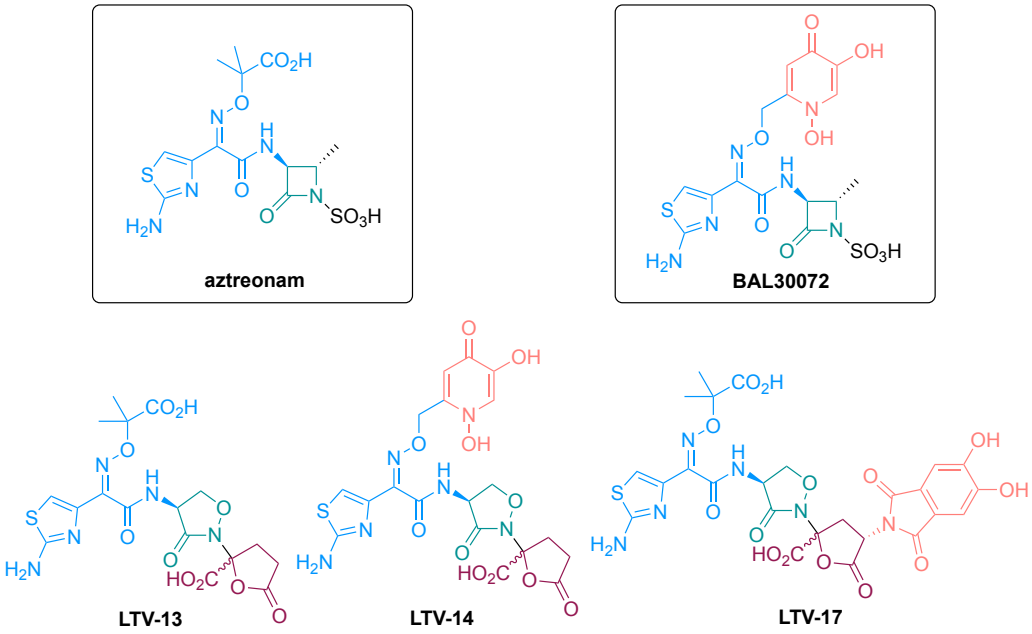
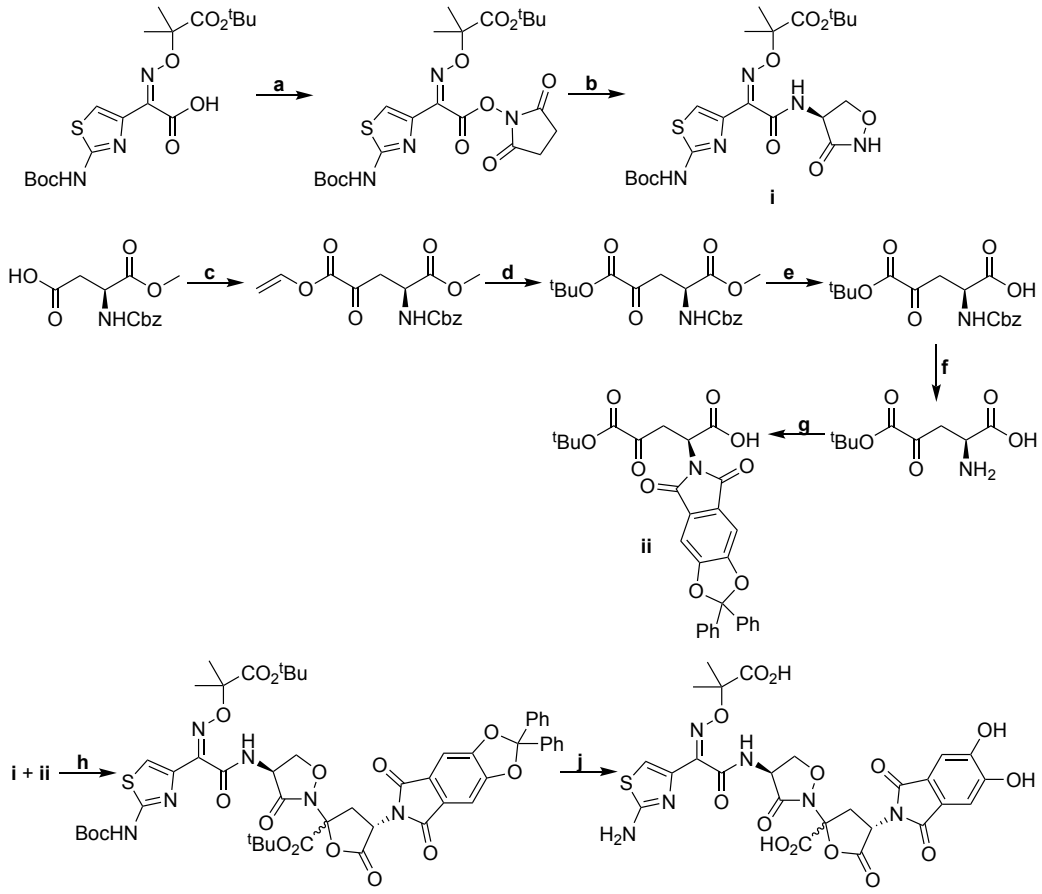


Figure 3.2. Lactivicin derivatives synthesised by Pfizer. These may have been inspired by the structure of aztreonam, a clinically important monobactam antibiotic (the common ATMO-like side chain in blue) and BAL30072, a siderophore-containing (orange) monobactam, which exploits iron uptake mechanisms to boost antibiotic intake in bacteria. The *β*-lactam ring in aztreonam and the *γ*-lactam-like ring in lactivicins are in green, while the lactivicin lactone rings are in red.

Although the synthesis of **LTV-17** was achieved via a synthetically challenging (and low yielding) reaction scheme (Scheme 3.2)[13], its promising inhibitory activities indicate that one can possibly maximise the potential of a *γ*-lactam (more accurately, a *γ*-lactam-like moiety in the case of lactivicin) by introducing more complex functionalities to the molecule, such as a siderophore group. With this goal in mind, various components were synthesised in order to enable access of new lactivicin related structures.



Scheme 3.2. *Route to the lactivicin derivative prepared by Pfizer*[13]*:*

a) *N*-hydroxysuccinimide (1.1 equiv.), DCC (1.1 equiv.), CH_2Cl_2, 23 ºC, 3.5 h; **b)** L-cycloserine hydrochloride (1.2 equiv.), $NaHCO_3$ (1.2 equiv.), EtOH, reflux, 5.5 h; **c)** (triphenylphosphoranylidene) acetonitrile (1.05 equiv.), EDCI (0.1 equiv.), anhydrous CH_2Cl_2, 23 ºC, overnight, N_2, then ozone/oxygen, vinyl alcohol, -65 ºC, 2 h, Ar; **d)** $Pd(PPh_3)_4$, morpholine (10 equiv.), anhydrous THF, r.t., 45 min, then 2-*tert*-butyl-1,3-diisopropylisourea, anhydrous THF, 23 ºC, 30 min; **e)** $LiOH•H_2O$ (1.05 equiv.), THF/H_2O, 0 to 23 ºC, 30 min; **f)** H_2, Pd-C, HCl/1,4-dioxane, THF, 23 ºC, 25 h; **g)** DMF (cat.), oxalyl chloride (1.0 equiv.), 0 ºC, 50 min, then 2,2-diphenyl-[1,3]dioxolo[4,5-*f*]isobenzofuran-5,7-dione (1.0 equiv.), pyridine, 90 ºC, 1.5 h; **h)** DCC (1.4 equiv.), 23 ºC, 16 h; **j)** BCl_3 (8 equiv.), CH_2Cl_2, -50 to -30 ºC, 2 h. Overall yield for steps **h** and **j** = 6%.

3.2. Derivatisation of *γ*-lactone for lactivicin synthesis

Previous attempts have been made to functionalise lactivicins, by Takeda[17] as well as by researchers in China[18] in the 80s and early 90s, with limited success (Figure 3.3). However, analysis of the crystal structure of lactivicins with *β*-lactamases leads to the observation of interactions, which imply scope for optimisation (Figure 3.4). The synthetic challenge posed by the lactivicins comprises two main aspects. While D-cycloserine is an affordable and commercially available material produced by *Streptomyces garyphalus*, its enantiomer, L-cycloserine, is less readily available. As described in Appendix 1, attempts were made to efficiently synthesise L-cycloserine. However, despite the exploration of various methods in literature, as well as from past preparations from the Schofield Group, an efficient and robust route was not achieved. For the purpose of uncovering new synthetic strategies for lactivicins, it was considered appropriate to experiment with the cheaper D-cycloserine in proof-of-principle work, before producing lactivicins with L-cycloserine.

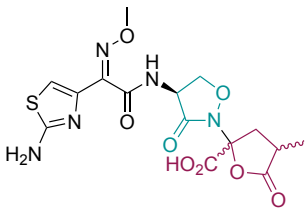


Figure 3.3. Structure of an early example of a lactivicin derivative with a methyl group added to the lactone ring, as synthesised by Takeda. This compound exhibited antibacterial properties against *S. aureus, E. coli* and *K. pneumoniae*[17].

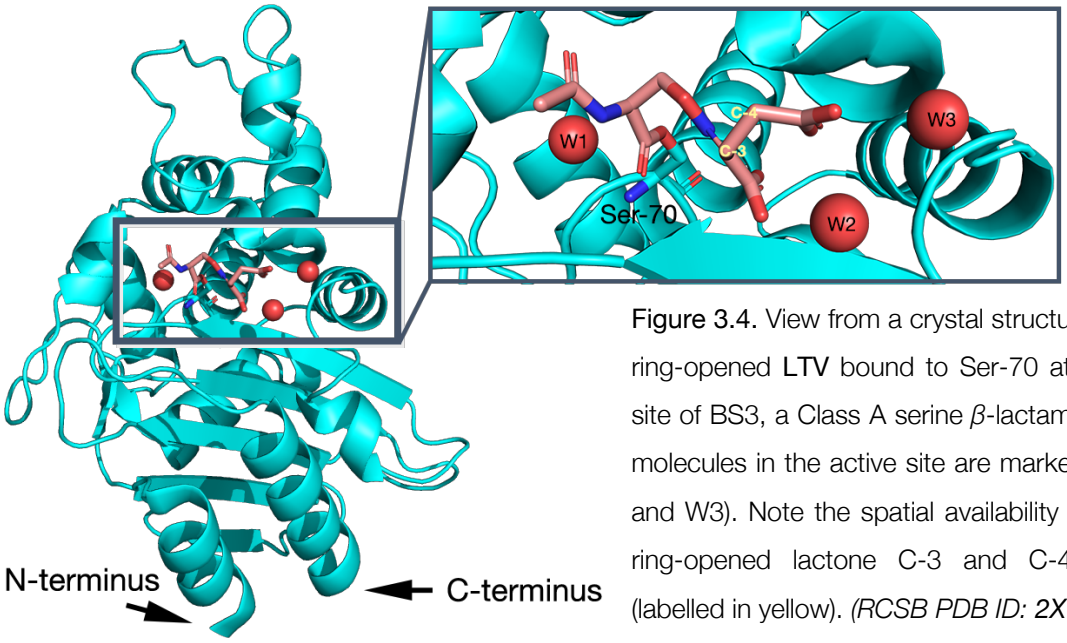


Figure 3.4. View from a crystal structure showing ring-opened LTV bound to Ser-70 at the active site of BS3, a Class A serine *β*-lactamase. Water molecules in the active site are marked (W1, W2 and W3). Note the spatial availability around the ring-opened lactone C-3 and C-4 positions (labelled in yellow). *(RCSB PDB ID: 2X71)*

Functionalising the lactone ring of the lactivicins presents challenges. Previous attempts in the Schofield Group to synthesise the more complex lactivicin derivatives using a modified version of the scheme as reported by Pfizer (Scheme 3.2)[13] had not been successful. Reported methods of lactivicin lactone functionalisation involve intermediates functionalised at the C-3 or C-4 position of 2-oxoglutarate (2-OG) esters (Figure 3.5). Therefore, new methods of obtaining functionalised lactone precursors for the synthesis of novel lactivicin derivatives were explored.

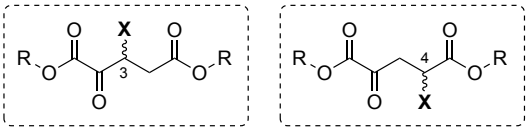
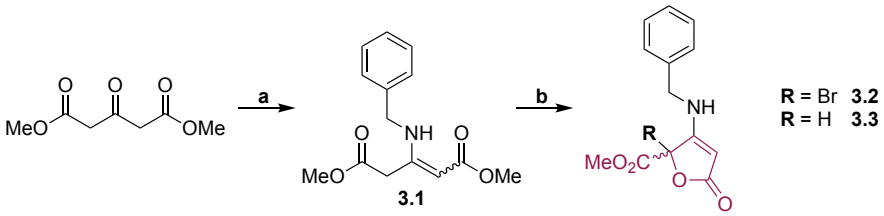


Figure 3.5. 2-OG functionalisations at either C-3 (left) or C-4 (right).

The synthesis of *α,β*-unsaturated lactones, **3.2** and **3.3**, has been reported by researchers from France[19]. The synthesis starts from an equimolar of dimethyl-1,3-acetonedicarboxylate and benzylamine in methanol, which affords **3.1** in apparent quantitative yield, followed by cyclisation using *N*-bromosuccinimide (NBS; 1.5 equiv.) in ethyl acetate at room temperature (24 hours), to produce **3.2** in a reasonable yield (Scheme 3.3)[19].



Scheme 3.3. *Synthesis of a functionalised α,β-unsaturated lactone*[19]*:*
a) benzylamine (1 equiv.), MeOH, r.t., 24 h, quantitative; **b)** NBS (1.5 equiv.), EtOAc, r.t., 24 h, **3.4**: 45%, **3.5**: 24%.

It was envisaged that **3.2** could be used to synthesise new unsaturated lactivicin derivatives with the *N*-benzyl-protected amine potentially enabling flexibility in the late-stage functionalisation of the C-3 lactone position (Figure 3.5). Potentially, this could be achieved either via deprotection of the benzyl group from the secondary amine, or by early-stage functionalisation of the amine prior to lactone formation via NBS-mediated cyclisation.

(Figure 3.5).

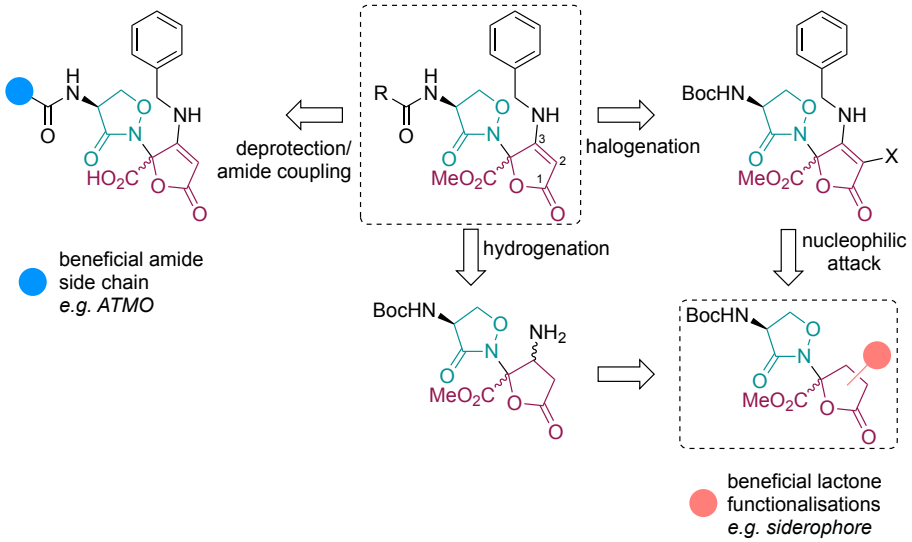
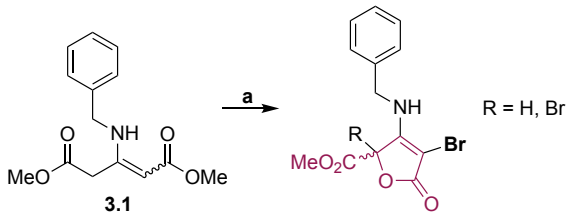


Figure 3.5. Potential routes to lactivicin analogues (centre) from *α,β*-unsaturated lactone **3.5**, as accessed from Scheme 3.3. This strategy can potentially be used to access new lactivicin species with modified amide side chains (blue), e.g. the clinically tested ATMO side chain and to enable lactone functionalisation (orange), such as by the addition of a siderophore group at C-2 or C-3 of the lactone ring.

The C-2 lactone position of the new analogue could be further brominated in the presence of excess NBS, as demonstrated by Toum et al. from **3.1** (Scheme 3.4)[19]. Furthermore, the unsaturation could potentially be removed via hydrogenation to produce a chiral centre at the C-3 lactone position, as well as an electrophilic centre at the C-2 lactone position (Figure 3.5). This would allow functionalisation to take place at a similar position as where the siderophore is attached to the lactivicin analogues synthesised by Pfizer[13].

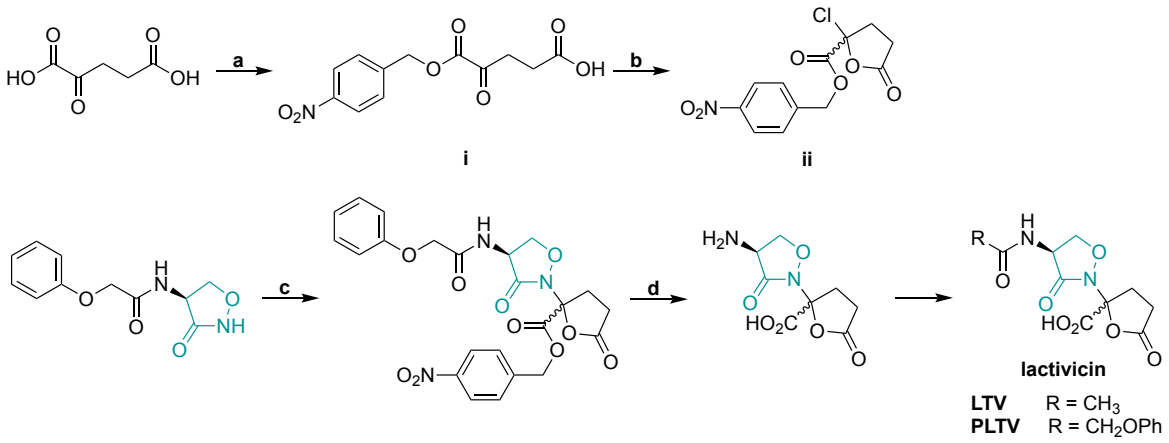


Scheme 3.4. *Example of reactions and conditions for α-bromination of a lactone from literature[19]:*
a) for R = H: NBS (3 equiv.), EtOAc, or for R = Br: NBS (2 x 1.5 equiv.), EtOAc.
In both cases, it was reported that the reactions were quenched with an aqueous solution of Na_2SO_3.

Thus, using the method of Toum et al.[19], the desired bromolactone **3.2** was synthesised from **3.1** in 45% yield (Scheme 3.3). Consistent with the observations of Toum et al.[19], a non-brominated lactone by-product, **3.3**, was also isolated, in 24% yield. The separation of **3.2** and **3.3** was successfully achieved via silica column chromatography.

3.3. Towards the synthesis of novel lactivicin analogues

Bromolactone derivative, **3.2**, is a potentially viable electrophile to obtain lactivicin derivatives from cycloserine. Although most earlier lactivicin analogue syntheses have focused mainly on *in situ* cyclisation from a reaction with 2-OG, the use of an electrophilic lactone has been explored, although manifesting lower yields (Scheme 3.5)[1,2].



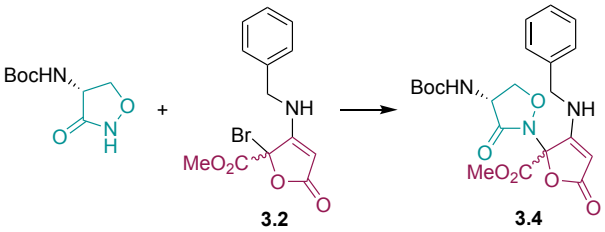
Scheme 3.5. *Literature example of **LTV** and **PLTV** synthesis as performed by Takeda[1,2]:*
a) 4-nitrobenzyl bromide (1.1 equiv.), dicyclohexylamine (1 equiv.), dimethylformamide, 50-70 ºC, 15 min, 93%; **b)** sulfonyl chloride (5.5 equiv.), 1,2-dichloroethane, reflux, 10 h, 85%; **c)** method A: ii (1.3 equiv.), Et_3N (2 equiv.), CH_2Cl_2, 0 ºC to r.t., 0.5 h, or method B: i (1.3 equiv.), DCC (1.3 equiv.), CH_2Cl_2, r.t., 14 h; **d)** H_2, Pd-C, EtOAc-pH 7.0 buffer, 0 ºC to r.t.; **e)** for **LTV**, Ac_2O (1.2 equiv.), $NaHCO_3$, THF/H_2O, 0 ºC, 28%; for **PLTV**, phenoxyacetyl chloride (1.2 equiv.), $NaHCO_3$, THF/H_2O, 0 ºC.

The scope of a nucleophilic substitution reaction that allows cycloserine to react with **3.2** to give the desired lactivicin analogue structure was thus explored. It is important to note that at this stage, the potential activities of the eventual lactivicin derivative(s) are not a major consideration, since the priority was to explore new synthetic avenues to functionalise lactivicins. With this objective in mind, a series of conditions were tested with Boc-protected D-cycloserine and **3.2**. Given the presence of a tertiary halide in **3.2**, it was considered that S_N2-type reactions might not be favoured due to

steric hindrance. Considering the fragility of the reagents as well as the desired product, a slight excess of triethylamine was initially used to facilitate the nucleophilic attack on bromolactone **3.2**. However, this condition did not produce any desired product even after 48 hours. The use of a stronger base, sodium hydride, was then attempted in tetrahydrofuran (THF). However, addition of the base at 0 °C to a solution of **3.2** (in THF) followed by an overnight reaction at room temperature did not yield any product.

The use of an excess of potassium carbonate and potassium iodide in acetonitrile was then investigated. This reaction afforded **3.4** in a satisfactory yield of 75% without optimisation (room temperature, one hour). The set of conditions tested and experimental outcomes are summarised here in Table 3.1.

Table 3.1. Reaction conditions attempted to couple Boc-cycloserine to lactone **3.2** to produce a novel lactivicin derivative, **3.4**.



Base	**3.2**	**Solvent***	**Temperature**	**Duration**	**Presence of iodide ions**	**Yield of 3.4**
Et_3N (2 equiv.)	1.3 equiv.	CH_2Cl_2*	0 °C to r.t.	48 h	-	-
NaH (2 equiv.)	2 equiv.	THF*	0 °C to r.t.	Overnight	-	-
K_2CO_3 (5 equiv.)	1.1 equiv.	MeCN	r.t.	1 h	KI (1.1 equiv.)	75%

*Anhydrous solvents were used for all reactions.

Upon arriving at the ester derivative of the novel lactivicin analogue, **3.4**, hydrolysis of the methyl ester to obtain **3.5** was desired. This was found to be challenging, likely relating to the fact that the methyl carboxylate ester is at a quaternary carbon centre bonded to two rings, resulting in steric hindrance. Various literature procedures, both chemical and enzymatical, were tested as summarised in Table 3.2.

Use of a classic hydrolysis procedure involving the addition of lithium hydroxide monohydrate (4 equiv.) in a mixture of methanol and water (2:1 v/v) at 0 °C, followed by warming to room temperature, did not give any product (after five hours). Even when the reaction duration was extended to 48 hours, no product was observed.

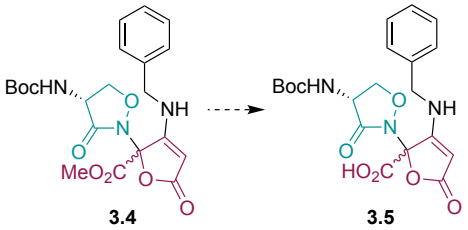
Using an acid hydrolysis, **3.4** was refluxed in concentrated hydrochloric acid, but after four hours no useful products were isolated.

Tributyltin oxide (TBTO) was attempted (2 equiv. in acetonitrile)[20] in an alternative methyl ester deprotection procedure. However, after a 24-hour reaction at room temperature, no product was observed. Similarly, the use of boron tribromide in dichloromethane (-78 °C, with warming to room temperature) was unsuccessful (no product formation was observed after an overnight reaction).

Enzymatic conditions were also attempted. Using porcine liver esterase (PLE; Sigma-Aldrich) in a mixture of 0.2 M phosphate buffer (pH 7.0) and 3.2 M ammonium sulfate buffer (20:1 v/v), a reaction was carried out at room temperature. After four days, there was no sign of any reaction. Similarly, the use of a protease from *B. lichenformis* (Type VIII, Sigma-Aldrich) in 0.3 M phosphate buffer (pH 7.5), in various solvents (acetonitrile, diethyl ether, tetrahydrofuran, methanol and chloroform) at room temperature did not yield the desired acid **3.5** (no reaction after 48 hours).

Similarly, reactions using an alcalase, Alcalase® CLEA (Sigma-Aldrich) in phosphate buffer (pH 7.5), in various solvents (acetonitrile, diethyl ether, tetrahydrofuran, methanol and chloroform) at room temperature did not manifest any reaction after 24 hours. **3.4** was also refluxed in MilliQ water for 48 hours; again no reaction was observed.

Table 3.2. Reaction conditions attempted to hydrolyse the methyl ester 3.4.

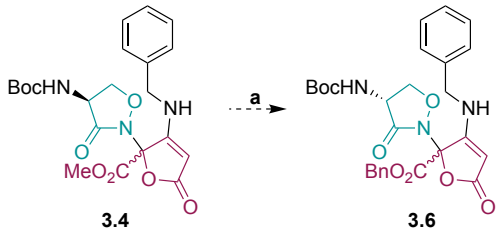


3.4 **3.5**

Mechanism	**Reagents**	**Solvent**	**Temperature**	**Duration**
Base hydrolysis	LiOH•H_2O (2 equiv.)	MeOH/H_2O	0 ºC to r.t.	5 h
Base hydrolysis	LiOH•H_2O (2 equiv.)	MeOH/H_2O	0 ºC to r.t.	48 h
Acid hydrolysis	Conc. HCl (excess)	-	Reflux	4 h
Hard nucleophilic attack	TBTO* (2 equiv.)	MeCN	R.t.	24 h
Soft nucleophilic attack	BBr_3 in CH_2Cl_2(2 equiv.)	CH_2Cl_2	-78 ºC to r.t.	Overnight
Enzymatic hydrolysis	Porcine liver esterase (PLE)	Phosphate buffer/$(NH_4)_2SO_4$ buffer (pH 7.0)	R.t.	4 days
Enzymatic hydrolysis	Protease from *B. lichenformis*, Type VIII	Phosphate buffer (pH 7.5) with: A: MeCN B: Et_2O C: THF D: MeOH E: $CHCl_3$	R.t.	48 h
Enzymatic hydrolysis	Alcalase® CLEA	Phosphate buffer (pH 7.5) with: A: MeCN B: Et_2O C: THF D: MeOH E: $CHCl_3$	R.t.	24 h
Hydrolysis	N/A	MilliQ water	Reflux	48 h

*Tributyltin oxide

As no successful result was obtained with the removal of the methyl carboxylate ester, an alternative strategy of trans-esterification was attempted to create a benzyl ester, **3.8**[21]. Using an excess of titanium(IV) isopropoxide in benzene, a large excess of benzyl alcohol was added and heated to 120 °C. Benzene and isopropyl alcohol were then distilled off until the reaction mixture reached about half its original volume. **3.4**, dissolved in benzene, was then added to the mixture and heated at 120 °C for eight hours in the presence of a Dean-Stark trap with molecular sieves (4 Å). While the desired benzyl ester was not isolated, it was observed that the Boc group did not survive this reaction (Scheme 3.6).



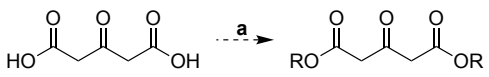
Scheme 3.6. *Reactions and conditions for trans-esterification*[21]*:*
a) $Ti(O^iPr)_4$ (5 equiv.), benzyl alcohol (25 equiv.), benzene, 120 °C, 8 h, reaction unsuccessful (Boc deprotection occurred).

Another strategy was attempted to attach a different ester group to the carboxylate, aiming to achieve a greater ease of late-stage deprotection. Conditions aimed at forming alternative esters from 1,3-acetonedicarboxylic acid were attempted (Scheme 3.7). In an attempt to obtain di-*tert*-butyl ester **3.7** from 1,3-acetonedicarboxylic acid, an excess of *N*,*N*-diisopropylethylamine (DIPEA) and *N*,*N*,*N'*,*N'*-tetramethyl-*O*-(*N*-succinimidyl)uronium tetrafluoroborate (TSTU) were added to 1,3-acetonedicarboxylic acid to activate the carboxylate groups in a mixture of *N*,*N*-dimethylformamide (DMF), 1,4-dioxane and water (2:2:1 v/v) at room temperature using a modified literature procedure[22]. A large excess of *tert*-butanol

was added after an hour, and the mixture was refluxed for 32 hours; however, no product was isolated.

In an attempt to synthesise the di-(4-nitrobenzyl) ester, **3.8**, from 1,3-acetonedicarboxylic acid, three different methods were attempted. Addition of 4-nitrobenzyl bromide and triethylamine in DMF at 0 ºC followed by an overnight reaction at room temperature afford no desired product. Addition of 4-nitrobenzyl alcohol in the presence of a catalytic amount of *p*-toluenesulfonic acid monohydrate (*p*-TsOH•H_2O) in toluene, refluxed overnight, also did not result in any product formation. Addition of 4-nitrobenzyl bromide in the presence of potassium iodide and potassium carbonate in acetonitrile followed by a 48-hour reaction at room temperature also did not to give rise to any product.

Similarly, an attempt to produce the di-benzhydryl ester, **3.9**, from 1,3-acetonedicarboxylic acid and diazodiphenylmethane failed.



R = ^{t}Bu **3.7**
R = 4-nitrobenzyl **3.8**
R = $CH(Ph)_2$ **3.9**

Scheme 3.7. *Reactions and conditions:*

3.7 (R = ^{t}Bu):

a) TSTU* (2.4 equiv.), DIPEA** (3 equiv.), ^{t}BuOH (20 equiv.), DMF/1,4-dioxane/H_2O, r.t., 1 h [22];

3.8 (R = 4-nitrobenzyl):

a) method A: 4-nitrobenzyl bromide (2.4 equiv.), Et_3N (6 equiv.), DMF, 0 ºC to r.t., overnight, or method B: 4-nitrobenzyl alcohol (6 equiv.), *p*-TsOH•H_2O*** (1 mol.%), toluene, reflux, overnight, or method C: 4-nitrobenzyl bromide (2.2 equiv.), K_2CO_3 (5 equiv.), KI (2.2 equiv.), MeCN, r.t., 48 h;

3.9 (R = $CH(Ph)_2$):

a) method A: diazodiphenylmethane (2 equiv.), THF, room temp, overnight;

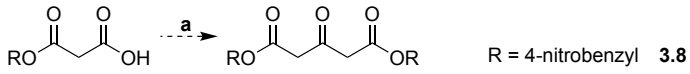
Reactions unsuccessful.

**N,N,N',N*'-Tetramethyl-*O*-(*N*-succinimidyl)uronium tetrafluoroborate.

***N,N*-Diisopropylethylamine.

*** *p*-Toluenesulfonic acid monohydrate.

In a different strategy, the use of 3-((4-nitrobenzyl)oxy)-3-oxopropanoic acid, TSTU and DIPEA (in DMF) was attempted [22], but did not give the desired product (Scheme 3.8).



Scheme 3.8. *Reactions and conditions[22]:*

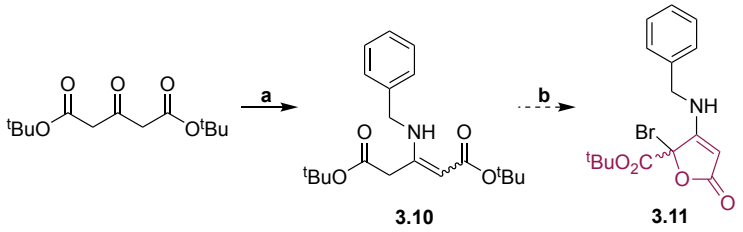
3.8 (R = 4-nitrobenzyl):

a) TSTU* (1.2 equiv.), DIPEA** (1.2 equiv.), DMF, Ar, r.t., 2 h, reaction unsuccessful.

**N,N,N',N*'-Tetramethyl-*O*-(*N*-succinimidyl)uronium tetrafluoroborate.

***N,N*-Diisopropylethylamine.

Using commercially available di-*tert*-butyl-1,3-acetonedicarboxylate, an attempt to generate the *tert*-butyl analogue of **3.2** (**3.11**) was executed using a similar method to that reported by Toum et al. (step a in Scheme 3.4)[19]. To a solution of di-*tert*-butyl-1,3-acetonedicarboxylate in methanol, benzylamine was added and stirred for 24 hours to afford the imine intermediate **3.10** in 60% crude yield. However, reacting **3.10** with NBS in ethyl acetate at room temperature for another 24 hours did not afford any lactone product (Scheme 3.9). Potentially this may be due to steric effects conferred by the *tert*-butyl group.

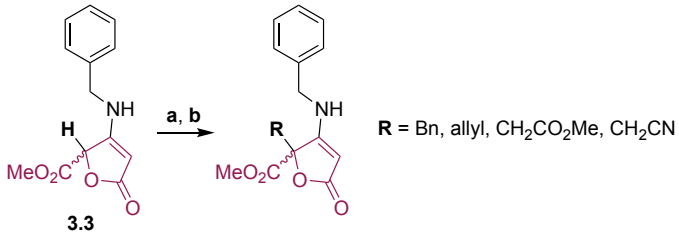


Scheme 3.9. *Reactions and conditions[19]:*

a) benzylamine (1 equiv.), MeOH, r.t., 24 h, 60%; b) NBS* (1.5 equiv.), EtOAc, r.t., 24, reaction unsuccessful.

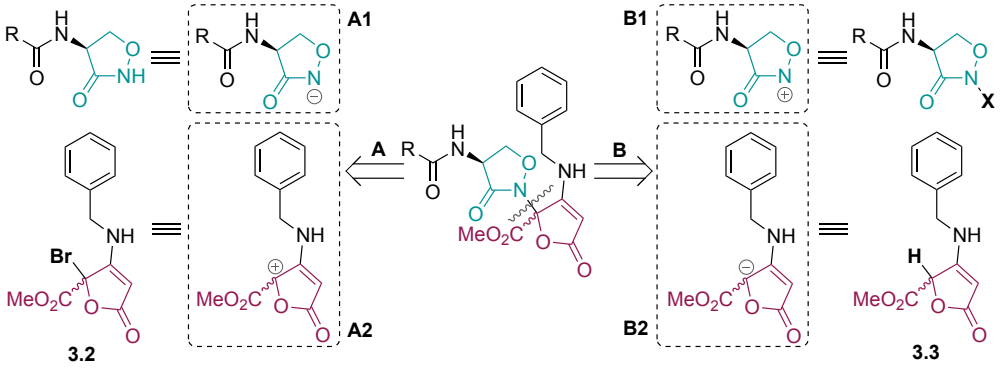
**N*-Bromosuccinimide.

In a different synthetic approach, the attention was turned to **3.3**, a by-product of the reaction highlighted in Scheme 3.4. Amongst the experiments reported by Toum et al., **3.3** was shown to undergo a Grignard reaction (Scheme 3.10)[19], thus highlighting its potential as a nucleophile, in contrast to the electrophilc bromolactone, **3.2**.



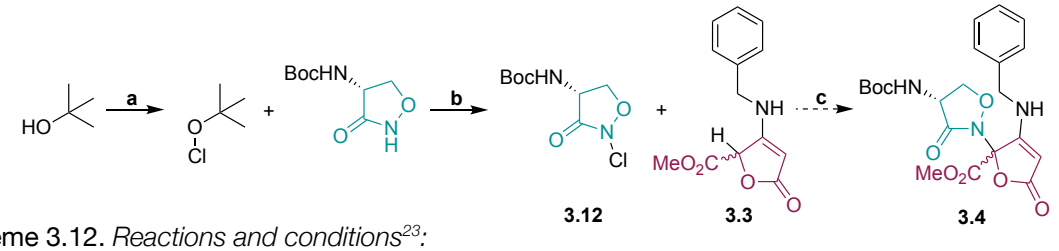
Scheme 3.10. *Examples of Grignard reaction of lactone, 3.3, as reported by Toum et al.[19]:* a) method A: K_2CO_3 (2.5 equiv.) in CH_2Cl_2, or method B: LiHMDS (1 equiv.) in THF, or method C: NaHMDS (1 equiv.) in THF, followed by *in situ* reaction with: b) RX in THF, where RX = BnBr, allyl bromide, MeI, methyl bromoacetate, or bromoacetonitrile.

As indicated in Scheme 3.10, **3.3** is relatively robust under basic conditions (e.g. K_2CO_3, LiHMDS and NaHMDS), suggesting an opportunity for hydrolysing the methyl ester in an earlier stage, and subsequently deploy other more synthetically useful carboxylate group protection strategies. It was thus proposed that the synthons in the original retrosynthetic analysis would be swapped, with the lactone as the nucleophile and the cycloserine as the electrophile (Scheme 3.11), aiming to produce the same lactivicin analogue, **3.5**.



Scheme 3.11. *Retrosynthetic analysis of a novel class of lactivicin derivatives:* Retrosynthesis via method A gives synthons A1 and A2, which corresponds to the nucleophilic substitution involving cycloserine and bromolactone **3.2**. Retrosynthesis via method B, results in a different pair of synthons: the synthetic equivalent of B1 can be a cycloserine derivative with a leaving group on the nitrogen, while the synthetic equivalent of B2 can be **3.3**, which has been reported to act as a nucleophile by Toum et al[19].

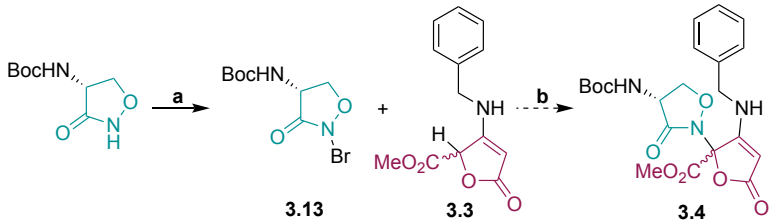
However, the question remained if a synthetic equivalent of an electrophilic cycloserine could be synthesised. Scrutiny of the literature uncovered a possibility of converting the amide hydrogen of a cycloserine to a halogen via free radical reaction. Thus, via modification of a literature method[23], *tert*-butanol was reacted with a large excess of sodium hypochlorite in acetic acid at 0 °C in the dark (ten minutes). The formation of the resultant *tert*-butyl hypochlorite intermediate was monitored by thin-layer chromatography (TLC); this intermediate was used without further purification for the attempted chlorination of Boc-protected D-cycloserine, in dichloromethane (0 °C; darkness). After 30 minutes, TLC analysis indicated that the starting material (Boc-protected D-cycloserine) was fully consumed; it was proposed that the *N*-chloro-Boc-protected D-cycloserine **3.12** had been formed. The putative **3.12** then was used without further purification in the subsequent step, where **3.3** was reacted first with LiHMDS in THF to allow deprotonation to occur, followed by the addition of **3.12** at 0 °C and an overnight reaction in darkness. Unfortunately, this reaction did not yield any of the desired lactone **3.4** (Scheme 3.12).



Scheme 3.12. *Reactions and conditions*[23]*:*

a) excess sodium hypochlorite, acetic acid, 0 °C, 10 min, dark (intermediate used without further purification); b) CH_2Cl_2, 0 °C, 30 min, dark (intermediate used without further purification); c) 3.3 (1 equiv.) LiHMDS (1.1 equiv.), THF, 0 °C to r.t., overnight, dark, reaction unsuccessful.

A further attempt was made to produce the *N*-brominated Boc-protected D-cycloserine **3.13** using bromine and a strong base. Thus, to Boc-protected D-cycloserine in THF was treated with LiHMDS, then bromine at 0 °C in the dark. Following a three-hour reaction, full consumption of the starting materials was indicated by TLC, and the putative intermediate **3.13** was used without further purification. **3.3** was then separately reacted with LiHMDS in THF to allow deprotonation, followed by the addition of **3.13** at 0 °C and an overnight reaction in darkness. However, this reaction was unsuccessful (Scheme 3.13).



Scheme 3.13. *Reactions and conditions:*

a) Bromine (1.0 equiv.), LiHMDS (1.2 equiv.), THF, 0 °C, 3 h, dark (intermediate used without further purification); b) LiHMDS (1.1 equiv.), THF, 0 °C to r.t., overnight. Reaction unsuccessful.

It was noted for the chemistry described in Scheme 3.12 and Scheme 3.13 that the formation of the *N*-chlorinated and brominated cycloserine intermediates **3.12** and **3.13**, respectively, may not have successfully taken place even though TLC has indicated the occurrence of reaction. Therefore, further spectroscopic validation of the formation of **3.12** and **3.13** is desirable.

3.4. Synthesis of aza-lactivicin derivatives via pyrazolidinones

Cycloserine is not the only γ-lactam analogue that has been previously explored by medicinal chemists as a β-lactam substitute. Another interesting type of γ-lactam analogues that has been explored are the pyrazolidinones, pioneered by Eli Lilly, which as β-lactam mimics (Figure 3.6)[24,25].

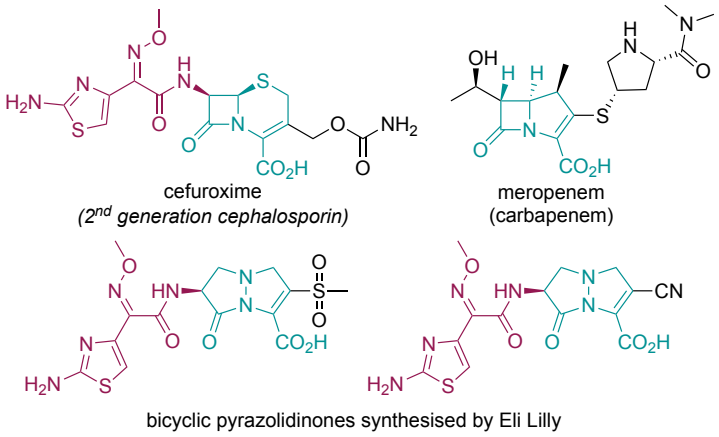
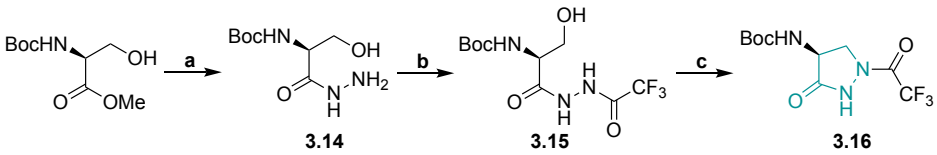


Figure 3.6. Comparison of clinically successful β-lactam containing antibiotics such as cefuroxime, a second-generation cephalosporin, and meropenem, a carbapenem, with bicyclic pyrazolidinones synthesised by Eli Lilly[24,25]. The β-lactam containing bicyclic cores as well as the analogous bicyclic pyrazolidinone containing systems are highlighted in green; the amide side chains are highlighted in red.

As in the case of the cycloserine ring in lactivicins, the presence of an electronegative (nitrogen) atom adjacent to the lactam group in the bicyclic pyrazolidinones will likely polarise the amide linkage and encourage a nucleophilic attack; it may also stabilise the acyl-enzyme complex with respect to reversible lactam formation (Figure 3.6). It was considered of interest to synthesise pyrazolidinones in order to not only access the bicyclic pyrazolidinones that have been previously synthesised, but also access the aza-analogues of lactivicins. It was considered that both could result in interesting activities with PBPs or β-lactamases.

By modifying the procedures developed at Eli Lilly[26], the trifluoroacetyl-protected pyrazolidinone, **3.16**, was successfully synthesised (Scheme 3.14). Starting from

commercially available Boc-protected L-serine methyl ester, a substitution reaction was carried out with an excess of hydrazine monohydrate in methanol under a nitrogen atmosphere (room temperature; 24 hours), providing **3.14** in apparent quantitative yield. *S*-Ethyl trifluorothioacetate was then added to **3.14** in ethanol under nitrogen, and after 70 hours (room temperature) **3.15** was generated in a crude quantitative yield. Mitsunobu cyclisation was then performed on **3.15** in the presence of triphenyl phospine and diisopropyl azodicarboxylate (DIAD) in THF under a nitrogen atmosphere. After a six-hour reaction at room temperature, **3.16** was successfully isolated in 63% yield.

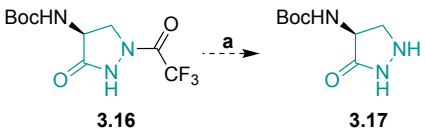


Scheme 3.14. *Synthesis of N-protected pyrazolidine-3-one*[26]*:*

a) $H_2NNH_2 \bullet H_2O$ (5 equiv.), MeOH, N_2, r.t., 24 h, quant.; b) *S*-ethyl trifluorothioacetate (1.5 equiv.), EtOH, N_2, r.t., 70 h, quant.; c) PPh_3 (1.3 equiv.), DIAD (1.3 equiv.), THF, N_2, r.t., 6 h, 63%.

*Diisopropyl azodicarboxylate.

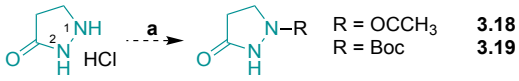
Following literature procedure[26], **3.16** was subjected to hydrolysis under basic conditions with the aim of removing the trifluoroacetate group from **3.16** to produce **3.17**, by adjusting the pH to 12 with the addition of aqueous sodium hydroxide solution and constant stirring (30 minutes). However, the product from this reaction was noted to be extremely water soluble. An attempt was made to purify the product via continuous extraction (see Experimental procedures) over 96 hours, as recommended by literature[26], but this was unsuccessful (Scheme 3.15).



Scheme 3.15. *Reactions and conditions*[26]*:*

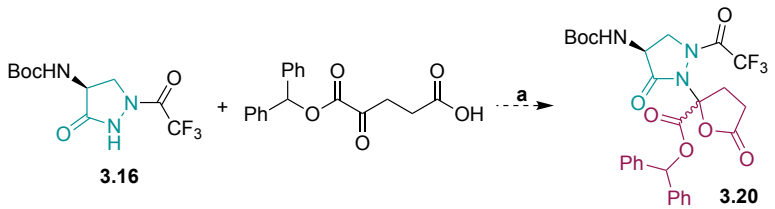
a) aqueous NaOH solution (pH 12), 30 min, then continuous extraction for 96 h, reaction unsuccessful.

A different strategy was explored to extract the polar pyrazolidinone product, by introducing a protecting group onto N1 of the pyrazolidinone core, which should alter the polarity of the compound but also can be removed via various methods. The Boc group as well as a simple acetyl group were envisioned to fulfil these criteria, and these were tested on commercially available pyrazolidin-3-one hydrochloride as a synthetic model (Scheme 3.16). No useful results were obtained from these test reactions.



Scheme 3.16. *N-protection of pyrazolidin-3-one hydrochloride:*
a) **3.16** (R = $OCCH_3$): CH_3COCl (1.1 equiv.), DIPEA* (1 equiv.), THF, r.t., 24 h. **3.17** (R = Boc): Boc anhydride (1.1 equiv.), $NaHCO_3$ (3 equiv.), THF/H_2O, 0 ºC to r.t., overnight. Reactions unsuccessful.
**N,N*-Diisopropylethylamine.

With **3.16**, an attempt was made to couple this with a 2-OG derivative via a Mitsunobu-type cyclisation to form an aza-lactivicin derivative (Scheme 3.17), in a fashion that mimics the classic synthesis of lactivicin using *N,N'*-dicyclohexylcarbodiimide (DCC) in dichloromethane (Scheme 3.1)[1,2,27]. The synthesis of this type of compounds have been previously attempted by Takeda[27]. However, the conversion was unsuccessful.



Scheme 3.17. *Reactions and conditions*[1,2,27]*:*
a) DCC* (1.6 equiv.), CH_2Cl_2, r.t., 17 h, reaction unsuccessful.
**N,N'*-Dicyclohexylcarbodiimide

3.5. Summary of synthetic strategies towards novel lactivicin derivatives

In summary, thorough re-examination and replication of previous attempts to access lactivicin derivatives revealed some weaknesses. Current methods of generating new lactivicin analogues often rely on functionalised 2-OG precursors, which are themselves challenging to synthesise. Using a recently reported *γ*-lactone in literature, **3.2**, as a precursor, a novel lactivicin analogue, **3.4**, was obtained in acceptable yield. However, the subsequent methyl ester deprotection of **3.4** to unleash the free carboxylic acid (**3.5**) was unsuccessful. Further work should aim to identify an ester deprotection strategy, as well as to repeat the work using L-cycloserine. If these aims could be achieved, the work could have potential to access a variety of new lactivicin analogues. Synthesis of the aza-lactivicin derivative (**3.20**) was also unfruitful, although these compounds may lead to new antibiotics possessing interesting activities against PBPs and *β*-lactamases.

3.6. Experimental procedures

Reagents

Reagents were from Acros, Alfa Aesar, Enamine, Fluorochem, Key Organics, Lancaster, Sigma-Aldrich and Tokyo Chemical Industry, and used as supplied. Solvents for chemical transformation, work-up and chromatography were from Sigma-Aldrich at HPLC grade and used without further distillation. Dried solvents were obtained from Sigma-Aldrich and Alfa Aesar.

Chromatography

Silica gel 60 F 254 analytical thin layer chromatography (TLC) plates were from Merck and imaged under UV light or with appropriate staining methods. Chromatographic

purification was performed using a Biotage SP1 Purification system with Biotage KP-SIL silica columns. TLC R_f values are given when column chromatography separation was performed, to the nearest 0.05 unit.

NMR spectra

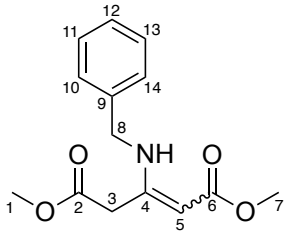
^1H and ^{13}C NMR spectra were recorded using a Bruker AVIII 400 Nanobay machine (400 MHz). Signal positions are recorded in δ ppm using the abbreviations s, d, t, q, and m denoting singlet (s), doublet (d), triplet (t), quartet (q), and multiplet (m), respectively. All NMR chemical shifts are referenced to residual solvent peaks. All coupling constants, *J*, are quoted in Hz to the nearest 0.5 Hz. Signals in both the ^1H and ^{13}C spectra were assigned with the aid of DEPT, COSY and HMQC.

Other characterisation

Optical rotations were recorded on a Perkin Elmer 241 or 341 polarimeter with a path length of 1 dm (using the sodium D line, 589 nm). $[\alpha]_D$ are reported in units of 10^{-1} degree (°) cm^2 g^{-1}. Concentrations are reported in g/100 mL. Temperatures are reported in degree Celsius (°C). Infrared spectra were recorded on a Bruker Tensor 27 FT-IR spectrometer. Samples were prepared as a thin film on a diamond ATR module. Absorption maxima (ν_{max}) are given in wavenumbers (cm^{-1}). Ionisation (ESI) Mass Spectrometry (MS) data (m/z) were obtained using a Fision VG Platform using a quadrupole analyser. High Resolution (HR) mass spectrometry data (m/z) data were obtained using a Bruker MicroTOF instrument with ESI source and Time of Flight (TOF) analyser. Values are reported as ratio of mass to charge in Daltons. Melting points were obtained using a Leica VMTG heated-stage microscope.

Synthesis of 3.1 (dimethyl 3-(benzylamino)pent-2-enedioate)[19]

1,3-Dimethyl acetonedicarboxylate (13.2 mL, 91.4 mmol, 1 equiv.) was dissolved in anhydrous methanol (80 mL). Benzylamine (10.0 mL, 91.6 mmol, 1 equiv.) was then added, and the mixture stirred at r.t. under nitrogen for 24 h. The mixture was then concentrated *in vacuo* to afford **3.1** as a crude product in the form of a yellow oil (24.68 g, quant.) as a mixture of *E* and *Z* isomers (*E*:*Z*, approximately 84:16 from ^{1}H NMR analysis).



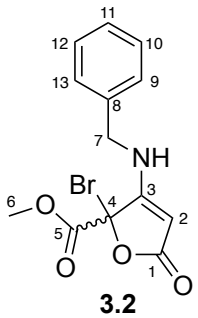
3.1

TLC 1:1 cyclohexane/ethyl acetate, R_f = 0.40; **IR** ν_{max} (film)/cm^{-1} 3320 (N-H stretch), 1742 (ester C=O stretch), 1681 (α,β-unsaturated C=O stretch); **^{1}H NMR** (400 MHz, DMSO-d_6) δ ppm 8.80 (t, *J* = 6.5 Hz, 1H, NH, *Z* isomer), 7.42 (t, *J* = 5.5 Hz, 1H, NH, *E* isomer), 7.40-7.32 (m, 5H, Ph, *E* isomer), 7.30-7.23 (m, 5H, Ph, *Z* isomer), 4.54 (s, 1H, *H5*, *Z* isomer), 4.50 (s, 1H, *H5*, *E* isomer), 4.43 (d, *J* = 6.0 Hz, 2H, CH_2Ph, *Z* isomer), 4.24 (d, *J* = 6.0 Hz, 2H, CH_2Ph, *E* isomer), 3.79 (s, 2H, CH_2C(O), *E* isomer), 3.78 (s, 2H, CH_2C(O), *Z* isomer), 3.63 (s, 3H, *C7* OCH_3, *E* isomer), 3.59 (s, 3H, *C7* OCH_3, *Z* isomer), 3.52 (s, 3H, *C1* OCH_3, *Z* isomer), 3.41 (s, 3H, *C1* OCH_3, *E* isomer); **^{13}C NMR** (101 MHz, DMSO-d_6) δ ppm 169.7 (*C6*, *Z* isomer), 169.7 (*C6*, *E* isomer), 169.0 (*C2*, *Z* isomer), 168.1 (*C2*, *E* isomer), 157.6 (*C4*, *Z* isomer), 155.7 (*C4*, *E* isomer), 138.7 (*C9*, *Z* isomer), 137.7 (*C9*, *Z* isomer), 128.6 (*C11* and *C13*, *Z* isomer), 128.4 (*C11* and *C13*, *E* isomer), 128.1 (*C12*, *Z* isomer), 127.3 (*C10* and *C14*, *Z* isomer), 127.1 (*C10* and *C14*, *E* isomer), 126.9 (*C12*, *E* isomer), 83.7 (*C5*, *Z* isomer), 82.7 (*C5*, *E* isomer), 52.0 (*C7*, *Z*

isomer), 51.5 (*C7*, *E* isomer), 49.7 (*C1*, *Z* isomer), 49.4 (*C1*, *E* isomer), 46.2 (*C8*, *Z* isomer), 46.1 (*C8*, *E* isomer), 37.8 (*C3*, *Z* isomer), 37.4 (*C3*, *E* isomer); **LRMS** (ESI^+, m/z) 264.1 [M+H]; **HRMS** (ESI^+) $C_{14}H_{18}NO_4$ requires 264.1236, found [M+H] 264.1233.

Synthesis of racemic 3.2 (methyl (±)-3-(benzylamino)-2-bromo-5-oxo-2,5-dihydrofuran-2-carboxylate) and racemic 3.3 (methyl (±)-3-(benzylamino)-5-oxo-2,5-dihydrofuran-2-carboxylate)[19]

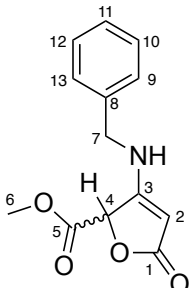
3.1 (24.68 g, 93.7 mmol, 1 equiv.) was dissolved in ethyl acetate (500 mL). *N*-Bromosuccinimide (NBS; 25.00 g, 140 mmol, 1.5 equiv.) was then added portion-wise and the mixture was stirred at r.t. for 24 h. The reaction mixture was then diluted with water (500 mL) and the organic layer was separated. The organic layer was washed with brine (500 mL), dried over anhydrous sodium sulfate and concentrated *in vacuo*. The products were separated using column chromatography on silica (eluted with pentane-diethyl ether) to afford a mixture of racemic **3.2** (13.87 g, 45%) and racemic **3.3** (5.62, 24%), in a ratio of 2.5:1, both of which were presented as yellow oils.



3.2

TLC 2:3 cyclohexane/diethyl ether, R_f = 0.30; **IR** ν_{max} (film)/cm^{-1} 3360 (N-H stretch), 1770 (ester C=O stretch), 1741 (lactone C=O stretch), 1642 (C=C stretch); **^{1}H NMR** (400 MHz, Chloroform-*d*) δ ppm 7.41-7.22 (m, 5H, PhH), 5.30 (br m, 1H, NH), 4.80 (s,

1H, *H2*), 4.32 (d, *J* = 5.0 Hz, 2H, CH_2Ph), 3.86 (s, 3H, CH_3); **^{13}C NMR** (101 MHz, Chloroform-*d*) δ ppm 171.0 (*C5*), 167.9 (*C1*), 163.9 (*C3*), 135.5 (*C8*), 128.8 (*C10* and *C12*), 128.1 (*C11*), 127.2 (*C9* and *C13*), 99.8 (*C4*), 83.8 (*C2*), 54.2 (*C6*), 49.0 (*C7*); **LRMS** (ESI^+, m/z) 326.0 [M+H]; **HRMS** (ESI^+) $C_{13}H_{13}BrNO_4$ requires 326.0028, found [M+H] 326.0033.

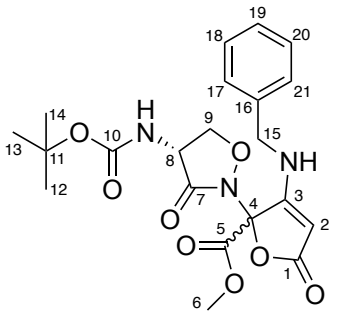


3.3

TLC 2:3 cyclohexane/diethyl ether, R_f = 0.05; **IR** ν_{max} (film)/cm^{-1} 3357 (N-H stretch), 1760 (ester C=O stretch), 1731 (lactone C=O stretch), 1628 (C=C stretch); **^{1}H NMR** (400 MHz, DMSO-d_6) δ 8.23 (t, *J* = 5.5 Hz, 1H, NH), 8.03 (t, *J* = 5.5 Hz, 1H, NH), 7.40-7.21 (m, 5H, Ph), 5.54 (s, 1H, *H4*), 4.64 (s, 1H, *H2*), 4.60 (s, 1H, *H2*), 4.33-4.25 (m, 2H, CH_2Ph), 3.76 (s, 3H, OCH_3), 3.73 (s, 3H, OCH_3); **^{13}C NMR** (101 MHz, DMSO-d_6) δ 179.4 (*C6*), 173.1 (*C6*), 171.2 (*C1*), 167.1 (*C1*), 166.8 (*C3*), 165.6 (*C3*), 137.6 (*C8*), 128.4 (*C9* and *C13*), 128.3 (*C9* and *C13*), 127.2 (*C10*, *C11* and *C12*), 127.1 (*C10*, *C11* and *C12*), 79.8 (*C4*), 79.5 (*C4*), 75.4 (*C2*), 53.0 (*C6*), 52.9 (*C6*), 47.8 (*C7*), 47.5 (*C7*); **LRMS** (ESI^-, m/z) 246.1 [M-H]; **HRMS** (ESI^-) $C_{13}H_{12}NO_4$ requires 246.0772, found [M-H] 246.0769.

Synthesis of racemic 3.4 (methyl (±)-3-(benzylamino)-2-((*R*)-4-((*tert*-butoxycarbonyl)amino)-3-oxoisoxazolidin-2-yl)-5-oxo-2,5-dihydrofuran-2-carboxylate)

Boc-D-cycloserine (5.11 g, 25.3 mmol, 1 equiv.) was dissolved in anhydrous acetonitrile (250 mL). Potassium carbonate (17.46 g, 126 mmol, 5 equiv.) and potassium iodide (4.61 g, 27.8 mmol, 1.1 equiv.) were added. The mixture was purged with nitrogen for 15 min, after which **3.2** (9.07 g, 27.8 mmol, 1.1 equiv.) dissolved in acetonitrile (250 mL), was added. The reaction was stirred at r.t under nitrogen for 1 h. The mixture was then diluted with ethyl acetate (250 mL) and washed with water (250 mL). The aqueous layer was back-extracted with ethyl acetate (100 mL). The combined organic layers were washed with water (250 mL) and brine (250 mL), dried over anhydrous sodium sulfate, filtered and concentrated *in vacuo*. The crude product was purified using flash column chromatography on silica (eluted with cyclohexane-ethyl acetate) to give **3.4** as a yellow oil (8.53 g, 75%) as a mixture of diastereomers (approx. 1:1 from ^{1}H NMR), which were not separated.



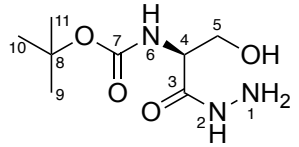
3.4

mp 121-124 °C; **TLC** 98:2 dichloromethane/methanol, R_f = 0.25; **IR** ν_{max} (film)/cm^{-1} 3421 (N-H stretch), 3398 (N-H stretch), 3032 (aromatic C-H stretch), 2988 (C-H stretch), 1720 (C=O stretch), 1677 (C=O stretch), 1641 (alkene C=C stretch), 1520 (aromatic C=C stretch); **^{1}H NMR** (400 MHz, Chloroform-*d*) δ ppm 7.38-7.20 (m, 5H,

Ph), 4.70-4.61 (m, 1H), 4.38-4.32 (m, 1H), 4.23-4.11 (m, 1H), 3.84 and 3.82 (s, 3H, OCH_3, both diastereomers), 1.42 and 1.41 (s, 9H, ^{t}Bu, both diastereomers); **^{13}C NMR** (101 MHz, Chloroform-*d*) δ ppm 172.6 and 172.3 (*C5*), 170.6 and 170.4 (*C7*), 163.5 and 163.5 (*C1*), 161.2 and 161.1 (*C3*), 155.3 and 155.2 (*C10*), 135.9 and 135.8 (*C16*), 128.8 and 128.7 (*C18* and *C20*), 127.9 and 127.8 (*C19*), 127.1 (*C17* and *C21*), 99.2 (*C4*), 89.1 and 88.6 (*C2*), 82.5 and 80.6 (*C11*), 74.3 and 71.7 (*C8*), 54.3 and 54.3 (*C9*), 53.0 and 52.6 (*C6*), 49.1 and 49.0 (*C15*), 28.1 (*C12*, *C13* and *C14*); **LRMS** (ESI^+, m/z) 448.2 [M+H]; **HRMS** (ESI^+) $C_{21}H_{26}N_3O_8$ requires 448.1720, found [M+H] 448.1723.

Synthesis of 3.14 (*N*-(*tert*-butoxycarbonyl)-(L)-serine hydrazide)[26]

N-Boc-L-serine methyl ester (5.40 g, 24.6 mmol, 1 equiv.) was dissolved in methanol (40 mL). Hydrazine monohydrate (4.0 mL, 82.5 mmol, 3.35 equiv.) was added, and the reaction mixture was stirred under nitrogen at r.t. for 24 h. The reaction mixture was then concentrated *in vacuo* (at a temperature below 30 °C) and dried under vacuum overnight to afford **3.14** as a white solid (5.39 g, 100%).



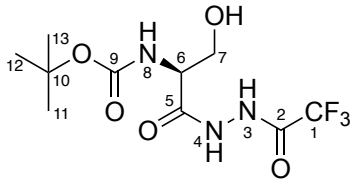
3.14

mp 118-120 °C (lit. 106-108 °C[28]); **TLC** 98:2 dichloromethane/methanol, R_f = 0.30; **$[\alpha]^{25}_D$** -4.3° (c = 0.01 g/mL, methanol) [lit. -9° (c = 0.0395 g/mL, methanol)[11]]; **IR** ν_{max} (film)/cm^{-1} 3300 (O-H stretch, br), 3280 (N-H stretch), 2982 (C-H stretch), 1703 (carbamate C=O stretch), 1667 (amide C=O stretch); **^{1}H NMR** (400 MHz, Methanol-d_4) δ ppm 4.89 (t, *J* = 5.5 Hz, *H4*), 3.70 (d, *J* = 5.5 Hz, 2H, CH_2), 1.43 (s, 9H, ^{t}Bu); **^{13}C NMR** (101 MHz, DMSO-d_6) δ ppm 171.4 (*C3*), 156.6 (*C7*), 79.5 (*C8*), 63.2 (*C5*), 56.8

(*C4*), 29.4 (*C9*, *C10* and *C11*); **LRMS** (ESI$^+$, m/z) 220.1 [M+H]; **HRMS** (ESI$^+$) $C_8H_{18}N_3O_4$ requires 220.1297, found [M+H] 220.1301.

Synthesis of 3.15 (*tert*-butyl (*S*)-(3-hydroxy-1-oxo-1-(2-(2,2,2-trifluoroacetyl)hydrazineyl)propan-2-yl)carbamate)[26]

3.14 (5.38 g, 24.5 mmol, 1 equiv.) was dissolved in ethanol (25 mL). *S*-Ethyl trifluorothioacetate (4.7 mL, 36.7 mmol, 1.5 equiv.) was added. The reaction mixture was stirred under nitrogen at r.t. for 70 h and concentrated *in vacuo* to afford crude **3.15** as a yellow oil (7.88 g, quant.), which was used in the next step without further purification.

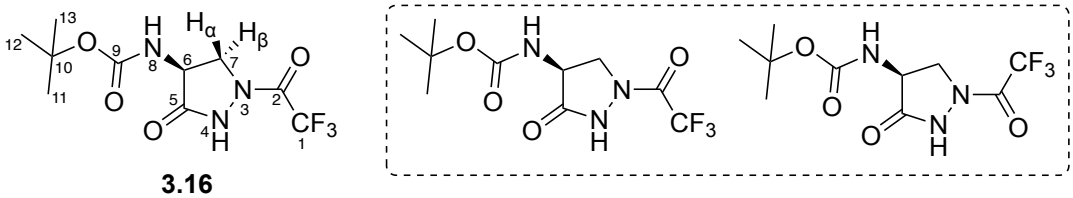


3.15

TLC 98:2 dichloromethane/methanol, R_f = 0.15; **[α]$^{25}_D$** -27.2° (c = 0.01 g/mL, methanol); **IR** ν_{max} (film)/cm^{-1} 3200 (N-H and O-H stretch), 2985 (C-H stretch), 1741 (amide C=O stretch), 1690 (carbamate C=O stretch); **^{1}H NMR** (400 MHz, DMSO-d_6) δ ppm 10.29 (br s, 1H, NH), 6.78 (d, *J* = 8.0 Hz, N*H*Boc), 6.33 (br s, 1H, NH), 4.88 (br s, 1H, OH), 4.08 (m, 1H, *H6*), 3.57 (m, 2H, CH_2), 1.37 (s, 9H, ^{t}Bu); **^{13}C NMR** (101 MHz, DMSO-d_6) δ ppm 170.3 (*C5*), 156.1 (q, *J* = 36 Hz, *C2*), 155.9 (*C9*), 116.4 (q, *J* = 289 Hz; *C1*), 78.8 (*C9*), 62.1 (*C7*), 56.1 (*C6*), 28.3 (*C11*, *C12* and *C13*); **LRMS** (ESI$^+$, m/z) 316.1 [M+H]; **HRMS** (ESI$^+$) $C_{10}H_{17}F_3N_3O_5$ requires 316.1120, found [M+H] 316.1126.

Synthesis of 3.16 (*tert*-butyl (*S*)-(3-oxo-1-(2,2,2-trifluoroacetyl)pyrazolidin-4-yl)carbamate)[26]

3.15 (411 mg, 1.30 mmol, 1 equiv.) and triphenyl phosphine (447 mg, 1.70 mmol, 1.3 equiv.) were dissolved in THF (15 mL). Diisopropyl azodicarboxylate (DIAD; 0.33 mL, 1.68 mmol, 1.3 equiv.) was added. The reaction was stirred at r.t. under nitrogen for 6 h. After that, the mixture was concentrated *in vacuo*. The residue was re-dissolved in ethyl acetate (15 mL), washed with sat. aqueous sodium bicarbonate solution (3 x 15 mL). The sodium bicarbonate washes were combined with brine (30 mL) and washed with ethyl acetate (20 mL). The aqueous portion was extracted with ethyl acetate (20 mL) and acidified with 1M aqueous hydrochloric acid solution to pH 2.5. The mixture was then further extracted with ethyl acetate (4 x 25 mL), and the final organic layer was separated, dried over anhydrous sodium sulfate, filtered and concentrated *in vacuo* to afford **3.16** as a white solid (243 mg, 63%) as a mixture of isomers (A:B = 6:5), which were not separated.



3.16

mp 160-165 °C; **TLC** 98:2 dichloromethane/methanol, R_f = 0.35; **$[\alpha]^{25}_D$** -90.1° (c = 0.01 g/mL, methanol); **IR** ν_{max} (film)/cm^{-1} 3380 (N-H stretch), 2986 (C-H stretch), 1685 (C=O stretch); **^{1}H NMR** (400 MHz, DMSO-d_6) δ ppm isomer A: 7.51 (br d, *J* = 7.2 Hz, BocNH), 4.53 (m, 1H, *H6*), 4.19 (t, 1H, *J* = 11.0 Hz, *Hα*), 3.62 (dd, 1H, *J* = 16.0, 11.0 Hz, *Hβ*), 1.33 (s, 9H, ^{t}Bu); isomer B: 7.47 (br d, *J* = 5.5 Hz, BocNH), 4.79 (m, 1H, H6), 4.53 (m, 1H, *Hα*), 3.85 (t, 1H, *J* = 8.5 Hz, *Hβ*), 1.33 (s, 9H, ^{t}Bu); **^{13}C NMR** (101 MHz, DMSO-d_6) δ ppm 168.7 and 168.2 (*C9*), 155.8 and 155.5 (*C5*), 151.7 and 148.3 (q, *J*

= 38 Hz, *C2*), 116.9 and 116.5 (q, *J* = 288 Hz and 287 Hz, *C1*), 79.3 and 79.2 (*C10*), 51.3 and 51.0 (*C6*), 50.7 and 50.1 (*C7*), 28.3 (*C11*, *C12* and *C13*); **LRMS** (ESI^-, m/z) 294.1 [M-H]; **HRMS** (ESI^-) $C_{10}H_{11}F_3N_3O_4$ requires 294.0707, found [M-H] 294.0712.

3.7. References

[1] Harada, S.; Tsubotani, S.; Hida, T.; Ono, H.; Okazaki, H. *Tetrahedron Lett.* **1986**, *27*, 6229–6232.

[2] Nozaki, Y.; Katayama, N.; Ono, H.; Tsubotani, S.; Harada, S.; Okazaki H.; Nakao, Y. *Nature* **1987**, *325*, 179–180.

[3] Wilmouth, R. C.; Westwood, N. J.; Anderson, K.; Brownlee, W.; Claridge, T. D.; Clifton, I. J.; Pritchard, G. J.; Aplin, R. T.; Schofield, C. J. *Biochemistry* **1998**, *37*, 17506–17513.

[4] Wilmouth, R. C.; Kassamally, S.; Westwood, N. J.; Sheppard, R. J.; Claridge, T. D.; Aplin, R. T.; Wright, P. A.; Pritchard, G. J.; Schofield, C. J. *Biochemistry* **1999**, *38*, 7989–7998.

[5] Wang, D. Y.; Abboud, M. I.; Markoulides, M. S.; Brem, J.; Schofield, C. J. *Future Med. Chem.* **2016**, *8*, 1063–1084.

[6] Lambert, M. P.; Neuhaus, F. C. *J. Bacteriol.* **1972**, *110*, 978-987.

[7] Nozaki, Y.; Katayama, N.; Harada, S.; Ono, H.; Okazaki, H. *J. Antibiot.* **1989**, *42*, 84–93.

[8] Macheboeuf, P.; Fisher, D.; Brown, T.; Zervosen, A.; Joris, B.; Luxen, A.; Dessen, A.; Schofield, C. J. *Nat. Chem. Biol.* **2007**, *3*, 565–569.

[9] Brown T.; Charlier, P.; Herman, R.; Schofield, C. J.; Sauvage, E. *J. Med. Chem.* **2010**, *53*, 5890–5894.

[10] White, G. W.; Malow, J. B.; Zimelis, V. M.; Pahlavanzadeh, H.; Panwalker, A. P.; Jackson, G. G. *Antimicrob. Agents Chemother.* **1979**, *15*, 540–543.

[11] Neu, H. C.; Labthavikul, P. *Antimicrob. Agents Chemother.* **1982**, *21*, 11–18.

[12] Sunagawa, M.; Matsumura, H.; Inoue, T.; Fukasawa, M.; Kato, M. *J. Antibiot.* **1990**, *43*, 519–532.

[13] Starr, J.; Brown, M. F.; Aschenbrenner, L.; Caspers, N.; Che, Y.; Gerstenberger, B. S.; Huband, M.; Knafels, J. D.; Lemmon, M. M.; Li, C.; Mccurdy, S. P.; Mcelroy, E.; Rauckhorst, M. R.; Tomaras, A. P.; Young, J. A.; Zaniewski, R. P.; Shanmugasundaram, V.; Han, S. *J. Med. Chem.* **2014**, *57*, 3845–3855.

[14] Calvopiña, K.; Umland, K.-D.; Rydzik, A. M.; Hinchliffe, P.; Brem, J.; Spencer, J.; Schofield, C. J.; Avison, M. B*. Antimicrob. Agents Chemother.* **2016**, *60*, 4170–4175.

[15] Sykes, R. B.; Bonner, D. P.; Bush, K.; Georgopapadakou, N. H. *Antimicrob. Agents Chemother.* **1982**, *21*, 85–92.

[16] Page, M. G. P.; Dantier, C.; Desarbre, E. *Antimicrob. Agents Chemother.* **2010**, *54*, 2291–2302.

[17] Takeda Pharmaceutical Co Ltd. Antibiotic 2-(3-oxo-2-isoxazolidinyl)-5-oxo-2-tetrahydrofuran-carboxylates. United States Patent US4851422A, Jul 25, 1989.

[18] Zhou, A.; Li, Z.; Li, M.; Wang, J. *Chin. J. Antibiot.* **1994**, *19*, 194–199.

[19] Toum, V.; Kadouri-Puchot, C.; Hamon, L.; Lhommet, G.; Mouriès-Mansuy, V.; Vanucci-Bacqué, C.; Dechoux, L.; *Synthesis* **2011**, *2011*, 2781–2788.

[20] Salomon, C. J.; Mata, E. G.; Mascaretti, O. A. *J. Org. Chem.* **1994**, *59*, 7259–7266.

[21] Fukuda, T.; Sugiyama, K.; Arima, S.; Harigaya, Y.; Nagamitsu, T.; Omura Satoshi. *Org. Lett.* **2008**, *10*, 4239–4242.

[22] Ryu, Y.; Scott, A. *Tetrahedron Lett.* **2003**, *44*, 7499–7502.

[23] Mintz, M. J.; Walling, C. *Org*. *Synth*. **1969**, *49*, 9.

[24] Jungheim, L. N.; Barnett, C. J.; Gray, J. E.; Horcher, L. H.; Shepherd, T. A.; Sigmund, S. K. *Tetrahedron* **1988**, *44*, 3119–3126.

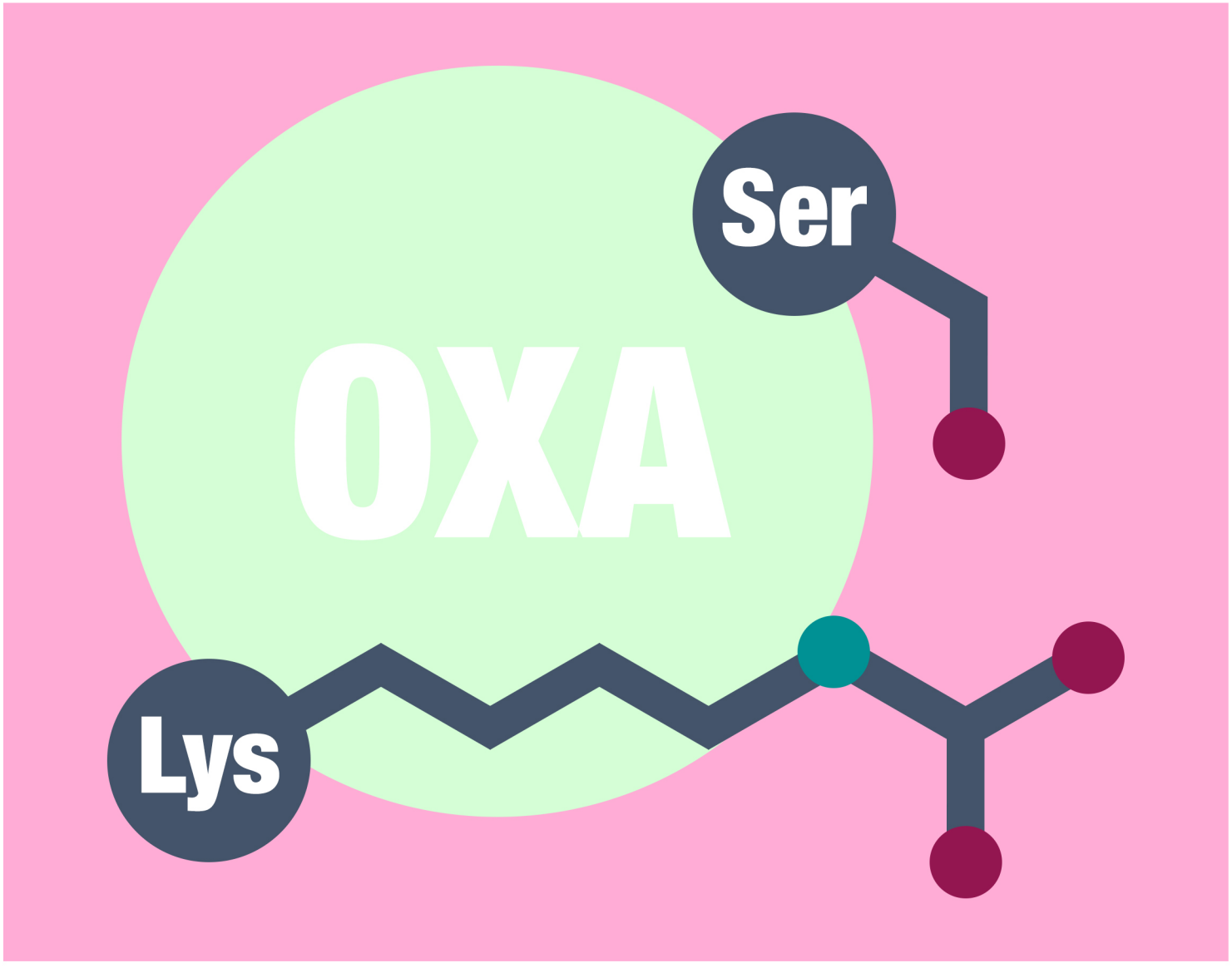
[25] Shepherd, T. A.; Jungheim, L. N. *Tetrahedron Lett.* **1988**, *29*, 5061–5064.

[26] Holmes, R. E.; Neel, D. A. *Tetrahedron Lett.* **1990**, *31*, 5567–5570.

[27] Tamura, N.; Matsushita, Y.; Yoshioka, K.; Ochiai, M. *Tetrahedron* **1988**, *44*, 3231–3240.

[28] Storey, H. T.; Beacham, J.; Cernosek, S. F.; Finn, F. M.; Yanaihara, C.; Hofmann, K. *J. Am. Chem. Soc.***1972**, *94*, 6170–6178.

Chapter 4.
Studies on OXA β-Lactamases



4. Studies on OXA β-Lactamases

4.1. Clinical relevance of OXA β-lactamases in antibiotic resistance

As introduced in Chapter 1, the rise of carbapenem-hydrolysing *β*-lactamases is a major clinical threat, particularly because carbapenems are an important last line of defence against multidrug resistant bacteria. Clinically relevant and mechanistically intriguing examples of such *β*-lactamases are the Class D *β*-lactamases, otherwise known as oxacillinases or OXA *β*-lactamases. While not all OXA *β*-lactamases have the ability to hydrolyse carbapenems at clinically relevant levels[1], some variants, notably OXA-48, exert significant pressure on healthcare systems worldwide, with outbreaks of OXA-48 identified across the entire European continent, including in the UK (Figure 1)[2].

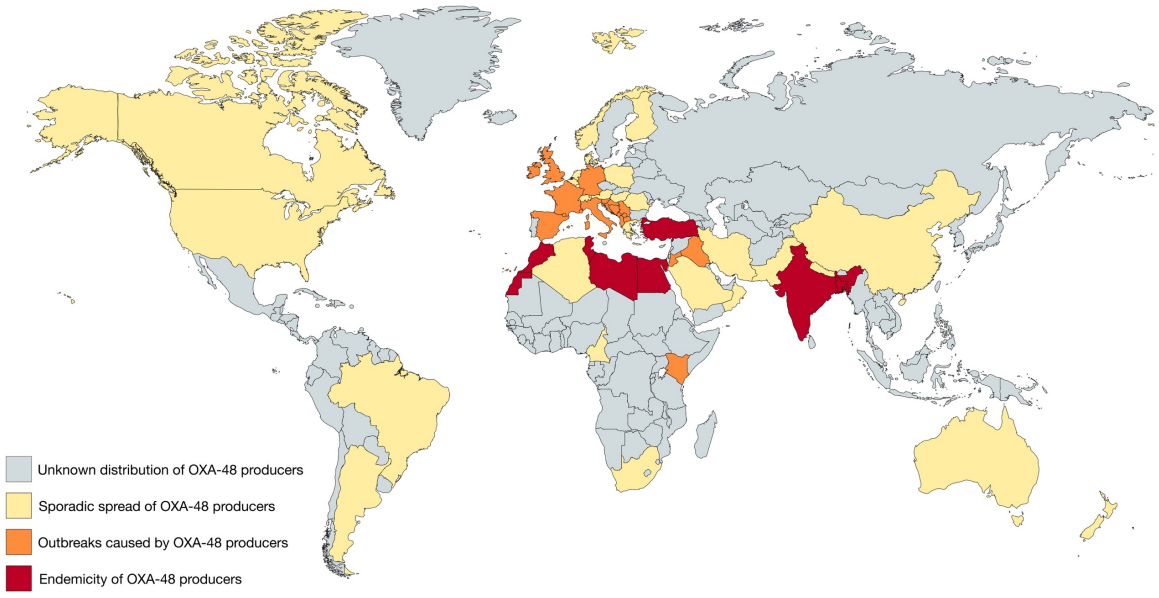


Figure 4.1. The global spread of OXA-48 producing bacterial species as of 2014, which has been observed to affect countries in every major continent. Although endemicity is currently restricted to less developed parts of the world such as South Asia and Northern Africa, outbreaks have occurred across the whole of Europe, including the UK[2].

The mechanisms of OXA *β*-lactamases differ significantly from other SBLs in that a key active site residue, Lys-70 (numbering based on OXA-10), is carbamylated[3]. This carbamylation directly affects the ability of OXA enzymes to hydrolyse *β*-lactam or *β*-lactam-like substrates (Figure 4.2)[3]. Previous studies have proposed that *β*-lactamase inhibitors that target OXA enzymes, such as avibactam, may promote decarbamylation of Lys-70[4,5]. Halide ions are also proposed to inhibit OXA enzymes through decarbamylation of Lys-70[6,7]. By exploiting this mechanistic feature of OXA enzymes, it was envisioned that further studies could enable the development of better inhibitors of the OXA *β*-lactamases.

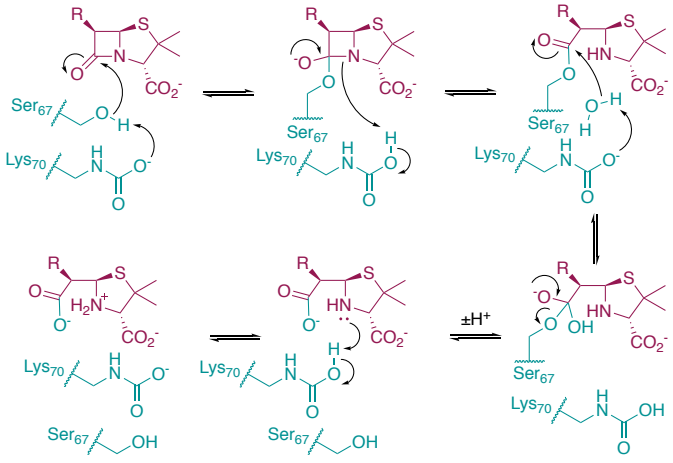


Figure 4.2. Proposed mechanistic outline of the hydrolysis of a *β*-lactam substrate, a penam, by an OXA enzyme[3]. The carbamylated Lys-70 is proposed to function as a general base in the deprotonation of Ser-63 and the active site water molecule, and as a general acid in the protonation of the nitrogen atom of the 1,3-thiazolidine ring[3]. The residue numbering is based on that for OXA-10.

Most clinically available *β*-lactamase inhibitors, including the *β*-lactams clavulanic acid, sulbactam and tazobactam, are ineffective against the OXA *β*-lactamases (Figure 4.3)[8]. The only effective OXA *β*-lactamase inhibitor that is currently employed in the clinic is the non *β*-lactam compound, avibactam[9], which has been approved by the FDA in combination with ceftazidime (Avycaz®) for the treatment of patients with hospital-acquired bacterial pneumonia and ventilator-associated bacterial pneumonia[10]. The lactivicins (discussed in Chapter 3), such as **LTV**, **PLTV** and **LTV-13** are of interest as potential (OXA) *β*-lactamase inhibitors[11]. In addition, it was envisaged that bicyclic boronates, such as **BN1** and **BN2**, which mimic the

tetrahedral intermediate in *β*-lactamase catalysed hydrolysis, might inhibit the OXA *β*-lactamases[12]. 6-Methylidene penems, such as **BLI-489**, also display inhibition of some *β*-lactamases[13,14,15]. Therefore, it was of special interest to characterise the potency of these compounds as inhibitors of the OXA *β*-lactamases (Figure 4.3). The mechanism of inhibition of OXA *β*-lactamases by halide ions was identified as a topic of potential interest.

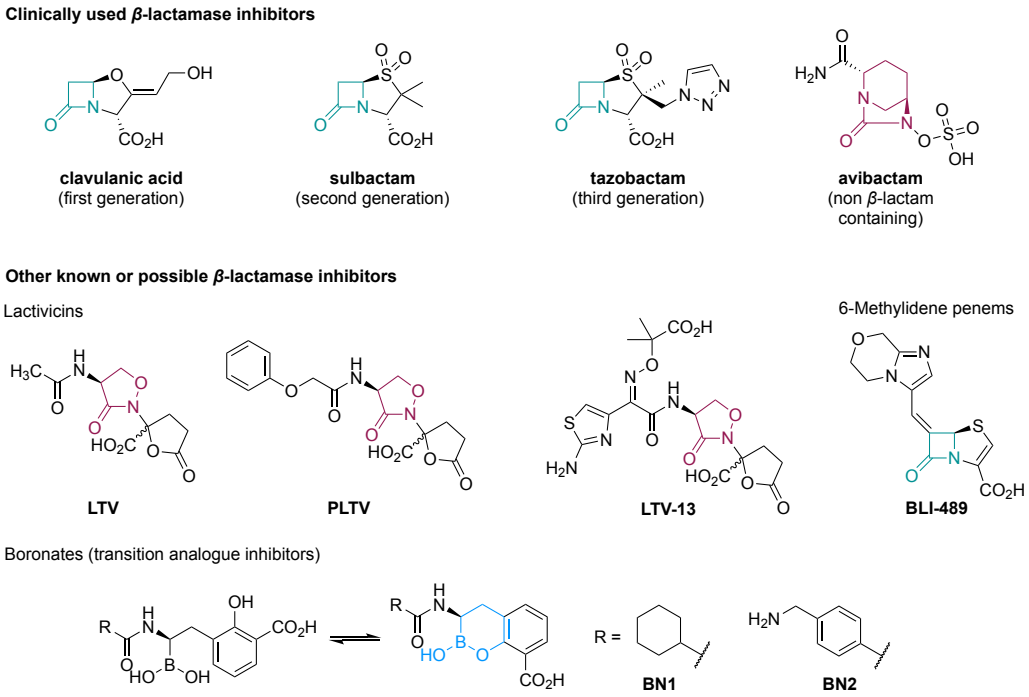


Figure 4.3. Examples of clinically used *β*-lactamase inhibitors, and other compounds in exploratory phases. *β*-Lactam containing compounds, i.e. clavulanic acid, sulbactam and tazobactam, as well as the non *β*-lactam containing inhibitor avibactam, are used in the clinic. In preclinical research, lactivicins (e.g. **LTV**, **PLTV** and **LTV-13**) inhibit *β*-lactamases and are (partially) resistant to *β*-lactamase-catalysed hydrolysis[11]. Boronates, exemplified by **BN1** and **BN2**, are tetrahedral intermediate analogue inhibitors of some *β*-lactamases[12]. 6-Methylidene penems such as **BLI-489** have been previously explored as potent *β*-lactamase inhibitors, although their activity versus the OXA *β*-lactamases had not been well studied[13,14,15]. *β*-Lactam rings are in green while other lactams are in red; the transition state mimic is in blue.

4.2. Production and purification of OXA-23 and OXA-48

In order to characterise the effects of the aforementioned compounds on OXA *β*-lactamases, OXA-23 and OXA-48 were produced and purified using an existing method[16]. The OXA *β*-lactamases were produced as N-terminal hexahistidine fusions in recombinant *Escherichia coli* BL21(DE3)[16]. The grown, induced and harvested cells were lysed by sonication, and the enzymes purified by nickel-affinity chromatography and size-exclusion chromatography[16]. The N-terminal His tag of the purified enzymes was removed using His-tagged 3C protease, which was then removed via passage through a HisTrap column. The purified enzyme fractions were identified by SDS-PAGE and concentrated by centrifugal ultrafiltration before buffer exchange and freezing[16]. The purity of both enzymes was determined by size exclusion chromatography-multi-angle laser scattering (SEC-MALS) analyses carried out by Dr. David Staunton (University of Oxford, Department of Biochemistry, Biophysics Facility).

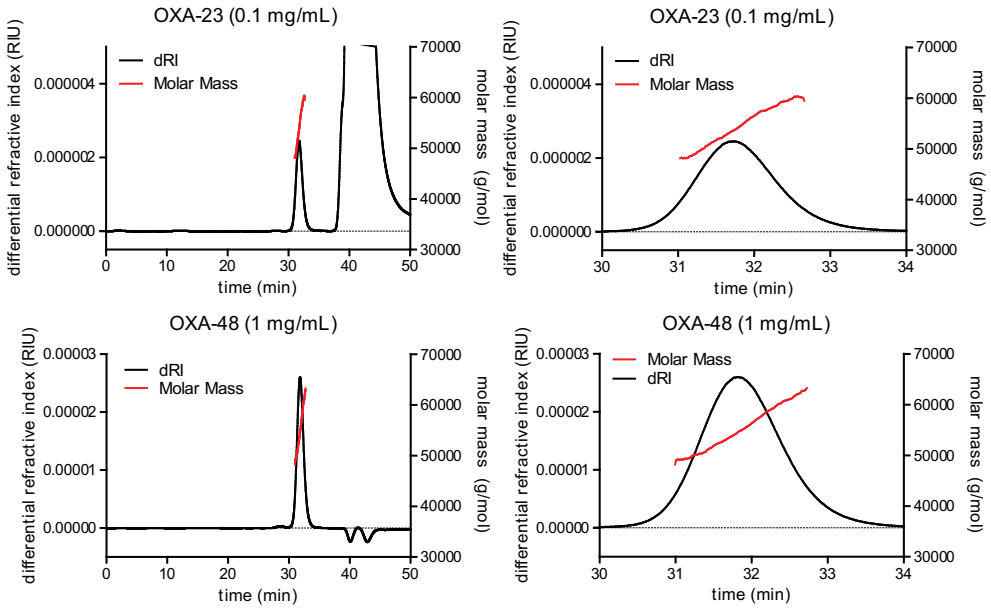


Figure 4.4. Spectra of SEC-MALS analyses showing the purity of OXA-23 and OXA-48, and evidence for the lack of aggregation. These data also suggested that both OXA-23 and OXA-48 were in a dimeric state (OXA-23: calculated 31.0 kDa, observed 54.2 kDa; OXA-48: calculated 30.4 kDa, observed 55.2 kDa).

4.3. Characterisation of kinetic parameters for OXA-23 and OXA-48

The enzymatic reaction between OXA β-lactamases and their substrates can be modelled using the Michaelis-Menten kinetics[17]. In summary, for an enzyme E, and a substrate S, it follows that:

$$E + S \underset{k_{-1}}{\overset{k_{+1}}{\rightleftharpoons}} ES \overset{k_{cat}}{\rightarrow} E + P$$

Equation 4.1

where k_{+1} denotes the forward rate constant and k_{-1} denotes the reverse rate constant for the formation of an enzyme-substrate (ES) complex; k_{cat} denotes the catalytic rate constant for the forward reaction of the ES complex to form the product. Assuming that the enzyme concentration is much less than the substrate concentration, and that the substrate is in instantaneous chemical equilibrium with the ES complex, the subsequent equation for the velocity of the reaction, which represents the rate of product formation, can be derived as follows:

$$v = \frac{d[P]}{dt} = \frac{V_{max}[S]}{K_M + [S]}$$

Equation 4.2

where V_{max} represents the maximum reaction velocity, which can also be denoted by the following:

$$V_{max} = k_{cat}[E]_0$$

Equation 4.3

where $[E]_0$ denotes the original enzyme concentration.

Based on the above-mentioned theoretical background, the kinetic parameters for OXA-23 and OXA-48 were obtained with chromogenic and fluorogenic substrates, including nitrocefin[18] and FC5[19] (Figure 4.4), both of which have been widely used in β-lactamase kinetic assays. A previously unreported substrate, FC5-Pip, which was

synthesised by Dr. Anna Rydzik (former member of the Schofield Group) and which has not been optimised for assay implementation, was also explored (Figure 4.5). It was proposed that FC5-Pip would be hydrolysed by OXA *β*-lactamases in a fashion similar to FC5, given the structural similarity[19]. For each enzyme-substrate pair, kinetic parameters including the turnover number or the catalytic rate (k_{cat}), the maximum rate (V_{max}) and the Michaelis constant (K_M) were measured, both in the presence and in the absence of sodium bicarbonate (50 mM). The data recorded were analysed using GraphPad Prism 5 (Figure 4.6) and the kinetics parameters derived accordingly (Table 4.1 [OXA-23] and Table 4.2 [OXA-48]).

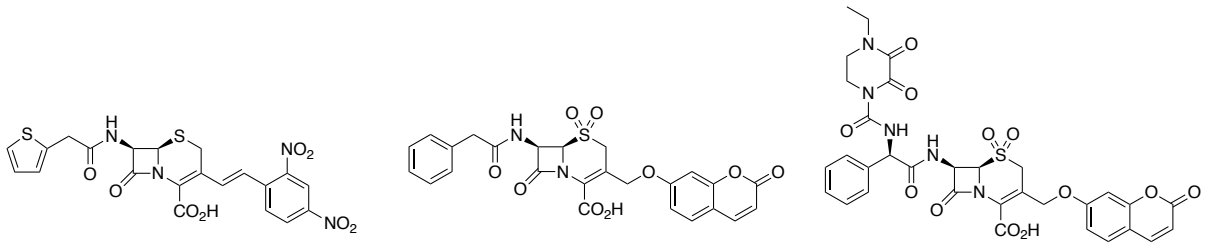


Figure 4.5. Structures of nitrocefin and FC5, which have been used in *β*-lactamase kinetic studies[18,19], and FC5-Pip, a previously uncharacterised substrate which is believed to act similarly to FC5[19].

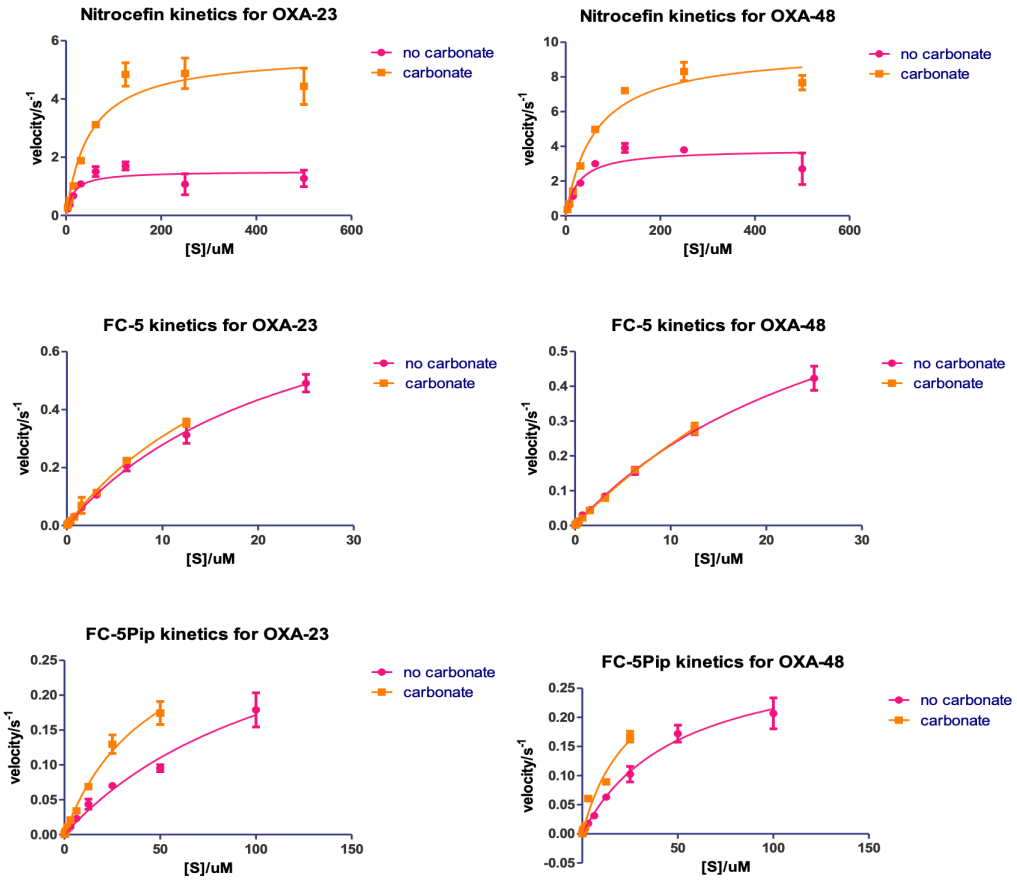


Figure 4.6. The plots of OXA-23 (left) and OXA-48 (right) kinetics data obtained for nitrocefin (top), FC-5 (middle) and FC-5 (bottom), calculated using Michaelis-Menten fitting from GraphPad Prism 5.

Table 4.1. Kinetic parameters for OXA-23 with assay substrates.

	Substrate	k_{cat} (s^{-1})*	V_{max} ($\mu M\ s^{-1}$)	K_M (μM)	k_{cat}/K_M ($s^{-1}\ \mu M^{-1}$)*
	Absence of sodium bicarbonate:				
1	Nitrocefin	759	1.518 ± 0.118	15.21 ± 4.89	49.9
2	FC5	78	0.975 ± 0.062	25.04 ± 2.63	3.12
3	FC5-Pip	31	0.389 ± 0.056	126 ± 27	0.246
	Presence of sodium bicarbonate (50 mM):				
4	Nitrocefin	2793	5.586 ± 0.318	49.99 ± 9.38	55.9
5	FC5	79	0.992 ± 0.107	22.30 ± 3.41	3.56
6	FC5-Pip	28	0.344 ± 0.028	46.65 ± 6.37	0.590

*Standard errors (n=4) were less or equal to 10% of the recorded values.

Table 4.2. Kinetic parameters for OXA-48 with assay substrates.

	Substrate	k_{cat} (s^{-1})*	V_{max} ($\mu M\ s^{-1}$)	K_M (μM)	k_{cat}/K_M ($s^{-1}\ \mu M^{-1}$)*
	Absence of sodium bicarbonate:				
1	Nitrocefin	1919	3.838 ± 0.275	27.06 ± 7.35	70.9
2	FC5	77	0.957 ± 0.067	31.50 ± 3.42	2.43
3	FC5-Pip	26	0.322 ± 0.018	50.13 ± 5.57	0.514
	Presence of sodium bicarbonate (50 mM):				
4	Nitrocefin	4806	9.612 ± 0.412	61.64 ± 8.27	78.0
5	FC5	109	1.358 ± 0.199	48.13 ± 8.52	2.26
6	FC5-Pip	26	0.326 ± 0.061	25.74 ± 8.25	1.01

*Standard errors (n=4) were less or equal to 10% of the recorded values.

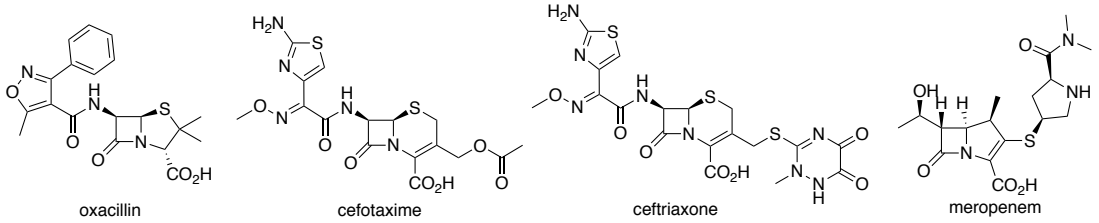
In the case of nitrocefin, the addition of sodium bicarbonate, which acts as a source of carbon dioxide, caused an approximately four-fold increase in both k_{cat} (and therefore V_{max}) and K_M in the case of OXA-23 (Table 4.1 row 1 versus row 4). In the case of OXA-48, k_{cat} and K_M increased approximately two-fold on sodium bicarbonate addition (Table 4.2 row 1 versus row 4). Consequently, the overall catalytic efficiency, which is represented by k_{cat}/K_M, displayed a slight, but appreciable, increase for both OXA-23 (Table 4.1) and OXA-48(Table 4.2), with added sodium bicarbonate. Therefore, the presence of sodium bicarbonate, which implies the presence of increased carbamylation, apparently increases the turnover while decreasing the enzyme-substrate affinity, resulting in a small increase in efficiency. The overall k_{cat}/K_M for nitrocefin was the highest for the three substrates that were tested.

For FC5, in the case of OXA-23, the presence of sodium bicarbonate did not have a significant impact on k_{cat} or K_M (Table 4.1 row 2 versus row 5). Therefore, k_{cat}/K_M was relatively unaffected. In the case of OXA-48, both k_{cat} and K_M were increased in the presence of sodium bicarbonate, by ~40% and ~55%, respectively (Table 4.2 row 2 versus row 5), which was less significant than the increases for nitrocefin (150% and 130% for k_{cat} and K_M, respectively). Consequently, k_{cat}/K_M for OXA-48 with FC-5

manifested a slight decrease of ~10% on addition of sodium bicarbonate (Table 4.2 row 2 versus row 5). Overall, however, the overall catalytic efficiencies for both OXA-23 (Table 4.1 row 2 versus row 5) and OXA-48 (Table 4.2 row 2 versus row 5) with FC5 are approximately the same with and without the addition of sodium bicarbonate. As compared to nitrocefin, the overall catalytic efficiencies for FC5 were 95% lower for OXA-23 regardless of the addition of sodium bicarbonate (Table 4.1). As for OXA-48, the overall catalytic efficiencies for FC5, when compared to nitrocefin, were >95% and 90% lower in the absence and presence of sodium bicarbonate, respectively (Table 4.2).

The suitability of FC5-Pip as a fluorogenic substrate for the OXA *β*-lactamases was next evaluated. Compared to FC5, FC5-Pip presented an approximately three-fold lower k_{cat} for OXA-23 (Table 4.1 row 5 versus row 6) and four-fold lower for OXA-48 (Table 4.2 row 5 versus row 6), i.e. FC5-Pip had the lowest turnover rates of the three substrates tested. However, like FC5, the k_{cat} for FC5-Pip was fairly consistent with and without added sodium bicarbonate (Table 4.1 and 4.2, row 3 versus row 6). By contrast with FC5, the K_M values for FC5-Pip were significantly affected by the addition of sodium bicarbonate. Thus, in the presence of sodium bicarbonate, the K_M was found to decrease by three-fold for OXA-23 (Table 4.1 row 3 versus row 6) and by two-fold for OXA-48 (Table 4.2 row 3 versus row 6). By combining the effect of sodium bicarbonate on both k_{cat} and K_M, the catalytic efficiency (k_{cat}/K_M) for FC5-Pip was found to approximately double in the presence of sodium bicarbonate for both OXA-23 (Table 4.1 row 3 versus row 6) and OXA-48 (Table 4.2 row 3 versus row 6). Nonetheless, the overall catalytic efficiency for FC5-Pip was poor when compared to nitrocefin and FC5.

Table 4.3. Kinetic parameters for OXA-23 with substrates reported in literature[7,8].



(penicillin) *(3rd generation cephalosporins)* *(carbapenem)*

Substrate	k_{cat} (s^{-1})	K_M (μM)	k_{cat}/K_M ($s^{-1}\ \mu M^{-1}$)
Oxacillin	320 ± 10	110 ± 10	3.1 ± 0.2
Cefotaxime	5.5 ± 0.1	340 ± 30	0.016 ± 0.002
Ceftriaxone	0.016 ± 0.001	3.7 ± 0.5	0.0044 ± 0.0007
Meropenem	0.068 ± 0.001	$\leq$ 2.0	$\geq$ 0.034

It is known from the literature that Class D carbapenemases, such as OXA-23 and OXA-48, cannot hydrolyse some expanded-spectrum cephalosporins[20]. The data in Table 4.3, which summarises the k_{cat} and K_M values recorded for OXA-23 with β-lactam substrates in the literature, shows that while the catalytic efficiency in the hydrolysis of extended-spectrum cephaloporins (including third-generation cephalosporins such as cefotaxime and ceftriaxone) by OXA-23 is lower in comparison to that of oxacillin and meropenem [21,22], hydrolysis of nitrocefin, FC5 and FC5-Pip display comparatively higher catalytic efficiency. Nitrocefin is structurally similar to first-generation cephalosporins which possess less complex side chains. This may explain the relatively high catalytic efficiency observed with nitrocefin for both OXA-23 and OXA-48. FC5-Pip, however, has a polar piperacillin side chain. The presence of this more complex side chain may render the compound less susceptible to hydrolysis by OXA-23 and OXA-48, consistent with the reportedly lower susceptibility of structurally complex expanded-spectrum cephalosporins towards some OXA β-lactamases[7.8].

4.4. Fluorometric kinetic assays for OXA-23 and OXA-48 with a panel of inhibitors

Following the screening of substrates for OXA-23 and OXA-48, screening of inhibitors was performed using a FC5-based fluorogenic assay[19], as adapted from a reported protocol for OXA-10[12], using 5 μM FC5 and 12.5 nM OXA-23 and OXA-48. The inhibitors studied included avibactam, sulbactam, **LTV**, **PLTV**, **LTV-13**, **BN1**, **BN2** and **BLI-489** (Figure 4.3).

The inhibitors and enzymes were pre-incubated for 0, 10, 30, 60 and 360 minutes in assay buffer with and without 50 mM sodium bicarbonate. The kinetics of inhibition were measured as IC_{50} and converted to pIC_{50}. These results are summarised in Table 4.4 (OXA-23) and Table 4.5 (OXA-48).

Table 4.4. Inhibition of OXA-23 by a panel of inhibitors.

		pIC_{50} for each incubation period				
	Inhibitor	**0 min**	**10 min**	**30 min**	**60 min**	**360 min**
	Absence of sodium bicarbonate:					
1	**Avibactam**	6.87 ± 0.05	7.87 ± 0.04	8.36 ± 0.07	8.04 ± 0.06	*N/A*
2	**Sulbactam**	<4	4.13 ± 0.12	4.76 ± 0.04	4.73 ± 0.06	5.40 ± 0.05
3	**LTV**	<4	<4	<4	<4	<4
4	**PLTV**	<4	<4	<4	<4	<4
5	**LTV-13**	<4	<4	<4	<4	<4
6	**BN1**	7.25 ± 0.02	7.41 ± 0.03	7.64 ± 0.05	7.30 ± 0.02	7.66 ± 0.11
7	**BN2**	6.22 ± 0.02	6.53 ± 0.05	6.52 ± 0.04	6.31 ± 0.03	6.32 ± 0.03
8	**BLI-489**	*ND **				
	Presence of sodium bicarbonate (50 mM):					
9	**Avibactam**	6.35 ± 0.05	6.76 ± 0.04	7.37 ± 0.04	7.66 ± 0.04	8.87 ± 0.16
10	**Sulbactam**	<4	<4	<4	<4	<4
11	**LTV**	<4	<4	<4	<4	<4
12	**PLTV**	<4	<4	<4	<4	<4
13	**LTV-13**	<4	<4	<4	<4	<4
14	**BN1**	7.60 ± 0.07	7.51 ± 0.05	7.46 ± 0.03	7.55 ± 0.05	7.47 ± 0.03
15	**BN2**	6.28 ± 0.04	6.24 ± 0.03	6.08 ± 0.03	6.18 ± 0.03	6.08 ± 0.03
16	**BLI-489****	8.25 ± 0.01	8.25 ± 0.01	8.21 ± 0.01	8.07 ± 0.01	7.74 ± 0.02

*Not determined.

**Measurements by Dr. Samuel Cahill (former Schofield Group member)[12,19].

Table 4.5. Inhibition of OXA-48 by a panel of inhibitors.

		pIC_{50} for each incubation period				
	Inhibitor	**0 min**	**10 min**	**30 min**	**60 min**	**360 min**
	Absence of sodium bicarbonate:					
1	**Avibactam**	6.39 ± 0.05	6.86 ± 0.04	7.51 ± 0.06	7.82 ± 0.07	7.07 ± 0.69
2	**Sulbactam**	<4	<4	4.28 ± 0.13	4.84 ± 0.06	5.43 ± 0.04
3	**LTV**	<4	<4	<4	<4	<4
4	**PLTV**	<4	<4	<4	<4	<4
5	**LTV-13**	<4	<4	<4	<4	<4
6	**BN1**	7.18 ± 0.03	7.25 ± 0.02	7.18 ± 0.04	7.15 ± 0.02	7.09 ± 0.02
7	**BN2**	6.29 ± 0.03	6.39 ± 0.03	6.30 ± 0.02	6.26 ± 0.03	6.27 ± 0.02
8	**BLI-489**	*ND**				
	Presence of sodium bicarbonate (50 mM):					
9	**Avibactam**	6.83 ± 0.04	6.91 ± 0.04	7.45 ± 0.05	7.85 ± 0.05	*N/A*
10	**Sulbactam**	<4	<4	<4	<4	<4
11	**LTV**	<4	<4	<4	<4	<4
12	**PLTV**	<4	<4	<4	<4	<4
13	**LTV-13**	<4	<4	<4	<4	<4
14	**BN1**	7.05 ± 0.02	7.07 ± 0.02	7.04 ± 0.03	7.00 ± 0.03	6.92 ± 0.02
15	**BN2**	6.28 ± 0.03	6.19 ± 0.04	6.07 ± 0.02	6.13 ± 0.02	6.08 ± 0.03
16	**BLI-489****	7.85 ± 0.03	7.82 ± 0.02	7.80 ± 0.02	7.66 ± 0.02	7.31 ± 0.01

*Not determined.

**Measurements by Dr. Samuel Cahill (former Schofield Group member)[12,19].

From these screens, it was established that the lactivicins, exemplified by **LTV**, **PLTV** and **LTV-13** (Figure 4.3), do not manifest any evidence of inhibition of OXA-23 and OXA-48 regardless of the incubation period; instead the lactivicins may act as substrates (Table 4.4 rows 3, 4, 5, 11, 12, 13, and Table 4.5 rows 3, 4, 5, 11, 12, 13). The inhibition of OXA-23 and OXA-48 by sulbactam was less potent as compared to the other inhibitors tested in this study (with the exception of the lactivicins). The extent of inhibition of both OXA-23 and OXA-48 by sulbactam was observed to increase with increasing incubation time, implying time dependent effects (Table 4.4 rows 2 and 10 and Table 4.5 rows 2 and 10). This may be due to the mechanism of sulbactam-mediated inhibition of *β*-lactamases. In the inhibition of the Class A *β*-

lactamases, such as TEM-1 and SHV-1, by sulbactam, crosslinking with a nucleophilic amino acid (Ser-130) may occur, which could lead to the irreversible formation of a *β*-alkoxyacrylate (Figure 4.7). The formation of the acrylate-enzyme complex is thought to increase with longer incubation[23]. The extent of inhibition for sulbactam was greater in the absence of sodium bicarbonate. In fact, inhibition was not observed for either OXA-23 or OXA-48 in the presence of sodium bicarbonate.

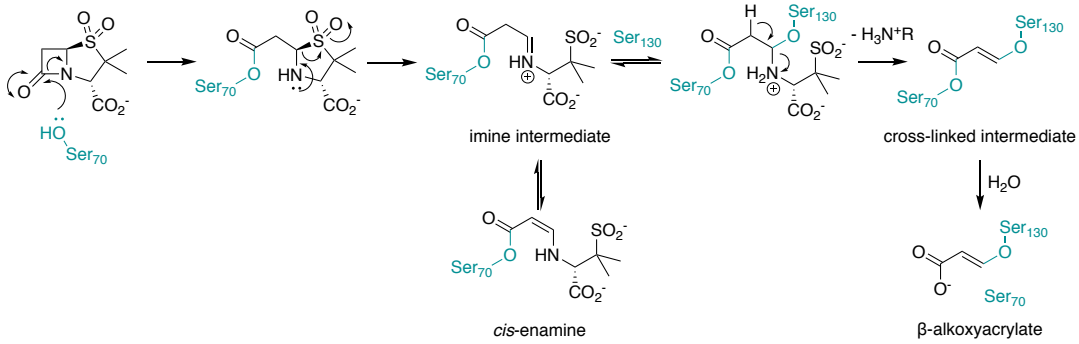


Figure 4.7. Outline of the proposed mechanism of the inhibition of a Class A *β*-lactamase (e.g. TEM-1 or SHV-1) by sulbactam, showing key intermediates and products. A pathway highlighting a second nucleophilic attack is also shown[23].

By contrast, the inhibition of OXA-23 and OXA-48 by **BLI-489** was extremely potent (Figure 4.3). In the absence of sodium bicarbonate, the extent of inhibition could not be accurately characterised in this study due to its high potency (Table 4.4 row 8 and Table 4.5 row 8). In the presence of sodium bicarbonate, **BLI-489** displayed the highest extent of inhibition for both *β*-lactamases (Table 4.4 row 16 and Table 4.5 row 16). Over longer periods of incubation, the extent of inhibition was found to decrease, which revealed time dependent effects (Figure 4.8). This observation may suggest that the acyl-enzyme complex, which contains a seven-membered 1,4-thiazepine ring and which is relatively stable (Figure 4.9)[24], may degrade over time.

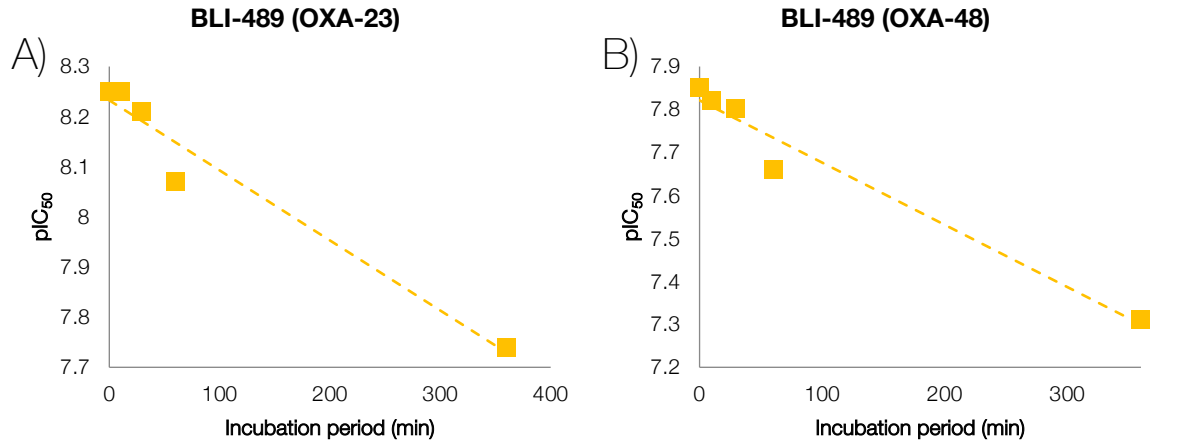


Figure 4.8. Inhibition of OXA-23 (A) and OXA-48 (B) in the presence of sodium bicarbonate (50 mM) by BLI-489. As incubation period increases, the extent of inhibition was found to decrease.

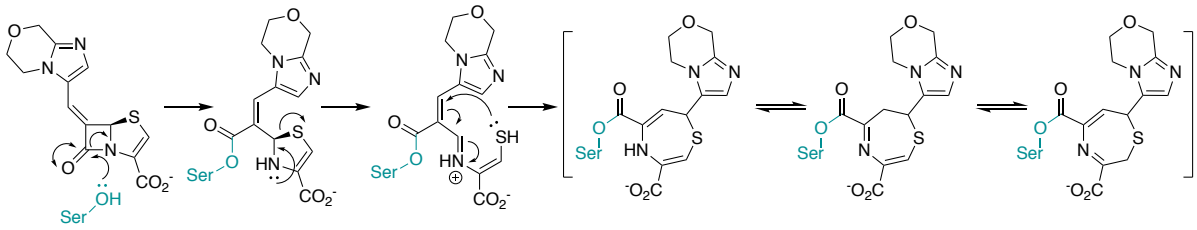


Figure 4.9. Outline of the proposed mechanism of inhibition of SBLs by BLI-489[24].

The extent of inhibition of OXA-23 and OXA-48 by bicyclic boronates **BN1** and **BN2** (Figure 4.3) was relatively stable with the different lengths of pre-incubation (Table 4.4 rows 6, 7 14, 15 and Table 4.5 rows 6, 7, 14, 15). Since the mechanism of inhibition of *β*-lactamases by bicyclic boronates has provided no evidence that it involves fragmentation (Figure 4.10), the lack of time dependency is not unexpected[25]. **BN1** exhibited a potency approximately 10-fold greater than **BN2** for both OXA-23 and OXA-48 (Figure 4.11 [OXA-23] and Figure 4.12 [OXA-48]). The extent of inhibition was higher in the absence of sodium bicarbonate as compared to that in its presence.

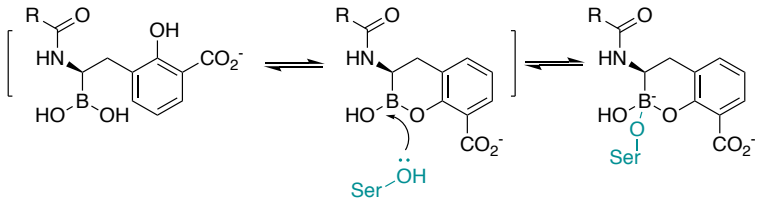


Figure 4.10. Outline of the mechanism of inhibition of an OXA β-lactamase by a bicyclic boronate[25].

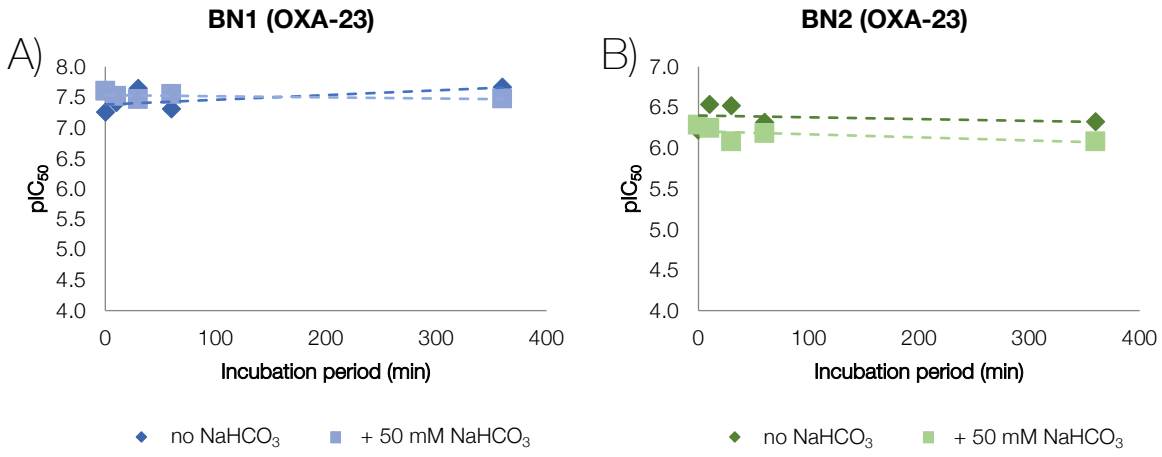


Figure 4.11. Kinetic measurements of inhibition of OXA-23 by bicyclic boronates BN1 (A) and BN2 (B). As the incubation period increases, the extent of inhibition is stable. BN1 exhibits a potency approximately 10-fold higher than BN2. Potency is also greater in the presence of sodium bicarbonate.

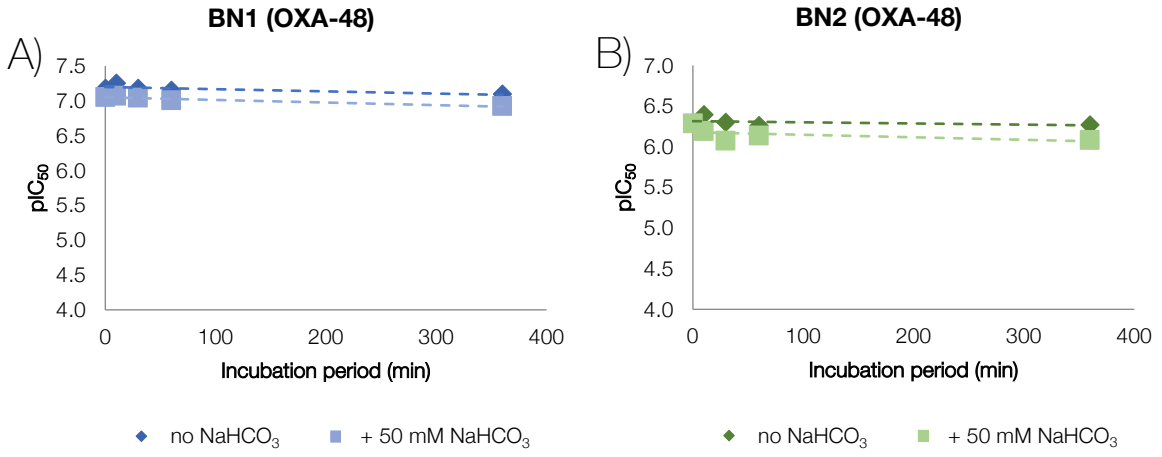


Figure 4.12. Kinetic measurements of inhibition of OXA-48 by bicyclic boronates BN1 (A) and BN2 (B). As the incubation period increases, the extent of inhibition is stable. BN1 exhibits a potency approximately 10-fold higher than BN2. Potency is also greater in the presence of sodium bicarbonate.

Avibactam displayed significantly better inhibition for both OXA-23 and OXA-48 as compared to sulbactam (Table 4.4 rows 1, 9 and Table 4.5 rows 1, 9). Similar to sulbactam, the extent of inhibition of both OXA-23 and OXA-48 by avibactam was observed to increase with increasing incubation time, again implying time dependent effects (Table 4.4 rows 1, 9 and Table 4.5 rows 1, 9). Currently there is only evidence for fragmentation of avibactam with the Class A SBL KPC-2 (Figure 4.13)[20]. Therefore, the observed time dependent effects may be caused by other factors. The high potency observed in this study agrees with previous work performed on OXA carbapenemases[9]. The impact of sodium bicarbonate on avibactam potency is less apparent. Therefore, the presence of sodium bicarbonate may not have a significant impact on lysine carbamylation and by extension, the enzymatic activity, of OXA-23 and OXA-48 in the presence of avibactam (Figure 4.14). These observations may attribute to the formation of the stable carbomyl-enzyme complex (Figure 4.13)[20].

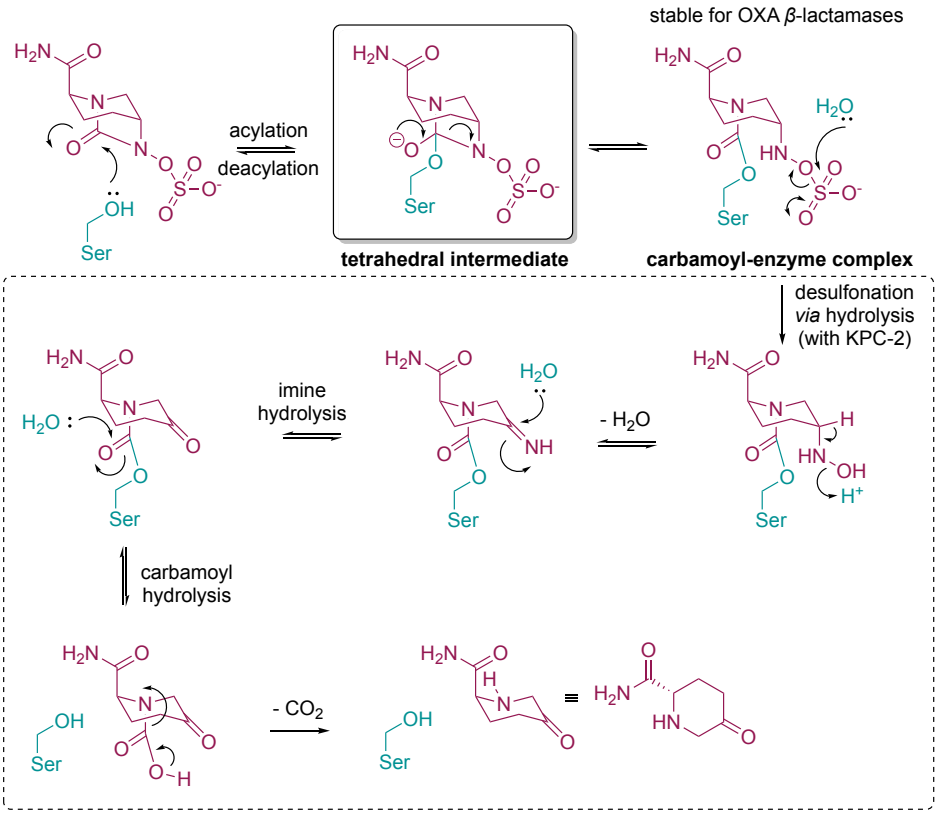


Figure 4.13. Outline of the proposed mechanism of inhibition of an OXA β-lactamase by avibactam, showing key intermediates and products[20]. Desulfonation and further fragmentation has, to date, only been observed with KPC-2, a Class A SBL[20].

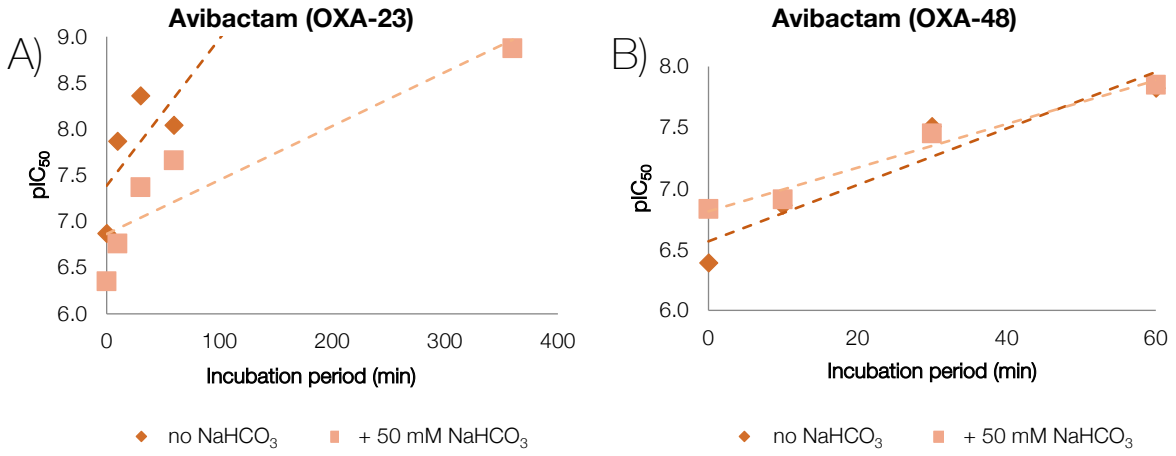


Figure 4.14. Kinetic measurements of the inhibition of OXA-23 (A) and OXA-48 (B) by avibactam. Note that as the incubation time increases, the extent of inhibition increases significantly. With the two OXA β-lactamases, the potency of inhibition by avibactam is similar. The difference in potency in the presence of sodium bicarbonate as compared to in its absence is less apparent, with only a slight difference observed with OXA-23.

4.5. Fluorometric kinetic assays for OXA-10, OXA-23 and OXA-48 with iodide

The OXA β-lactamases are inhibited by halides, although the mechanism of inhibition is yet to be fully characterised. According to classic analyses, the mode of inhibition could be competitive, uncompetitive, non-competitive or mixed[26]. To explain these different modes of inhibition, the following reaction scheme at equilibrium can be considered:

$$\begin{array}{ccccc} E & + & S & \rightleftharpoons & ES & \rightarrow & E & + & P \\ & & & & & & & & \\ +I & & & & +I & & & & \\ \downarrow\uparrow K_I & & & & \downarrow\uparrow K_I' & & & & \\ EI & & & & ESI & & & & \end{array}$$

Equation 4.4

where K_I represents the dissociation constant of the reversible combination of the inhibitor and the enzyme to form the enzyme-inhibitor (EI) complex, and K_I' represents the dissociation constant of the reversible combination of the inhibitor and the enzyme-substrate complex to form the enzyme-substrate-inhibitor (ESI) complex.[26]

In pure competitive inhibition, the inhibitor I, competes with the substrate for binding with the free enzyme only. Thus, $K_I > 0$ and $K_I' = 0$. In pure uncompetitive competition however, the inhibitor only binds to the enzyme-substrate complex. Therefore, $K_I' > 0$ and $K_I = 0$. When the inhibitor binds to both the free enzyme as well as the enzyme-substrate complex, i.e. $K_I > 0$ and $K_I' > 0$, the mode of inhibition is defined as mixed. In a special case when the inhibitor binds equally well to the free enzyme and the enzyme-substrate complex, i.e. $K_I = K_I'$, the mode of inhibition is defined as non-competitive.[26]

One way of determining the mode of halide inhibition on OXA *β*-lactamases is to apply a combination of the Dixon method[27] and the Cornish-Bowden method[28]. According to Dixon, given the following Michaelis-Menten equation for a competitive system:

$$v = \frac{V_{max}[S]}{K_M\left(1 + \frac{[I]}{K_I}\right) + [S]}$$

Equation 4.5

which can be rearranged to derive the following equation:

$$\frac{1}{v} = \frac{K_M}{V_{max}[S]} + \frac{1}{V_{max}} + \frac{K_M}{V_{max}[S]}\frac{[I]}{K_I}$$

Equation 4.6

such that a plot of the reciprocal velocity $\frac{1}{v}$ against the inhibitor concentration $[I]$ is a straight line.[27]

In the Cornish-Bowden method, taking into consideration that the inhibitor may bind to the enzyme-substrate complex, the following Michaelis-Menten equation is proposed:

$$v = \frac{V_{max}[S]}{K_M\left(1 + \frac{[I]}{K_I}\right) + [S]\left(1 + \frac{[I]}{K_I'}\right)}$$

Equation 4.7

which can be rearranged to derive the following equation:

$$\frac{[S]}{v} = \frac{K_M}{V_{max}}\left(1 + \frac{[I]}{K_I}\right) + \frac{[S]}{V_{max}}\left(1 + \frac{[I]}{K_I'}\right)$$

Equation 4.8

such that a plot of $\frac{[S]}{v}$ against $[I]$ also provides a straight line.[28]

By constructing a series of Dixon plots and Cornish-Bowden plots at different substrate concentrations and inhibitor concentrations, it is possible to compare the values of K_I and K_I' (Figure 4.15)[27,28].

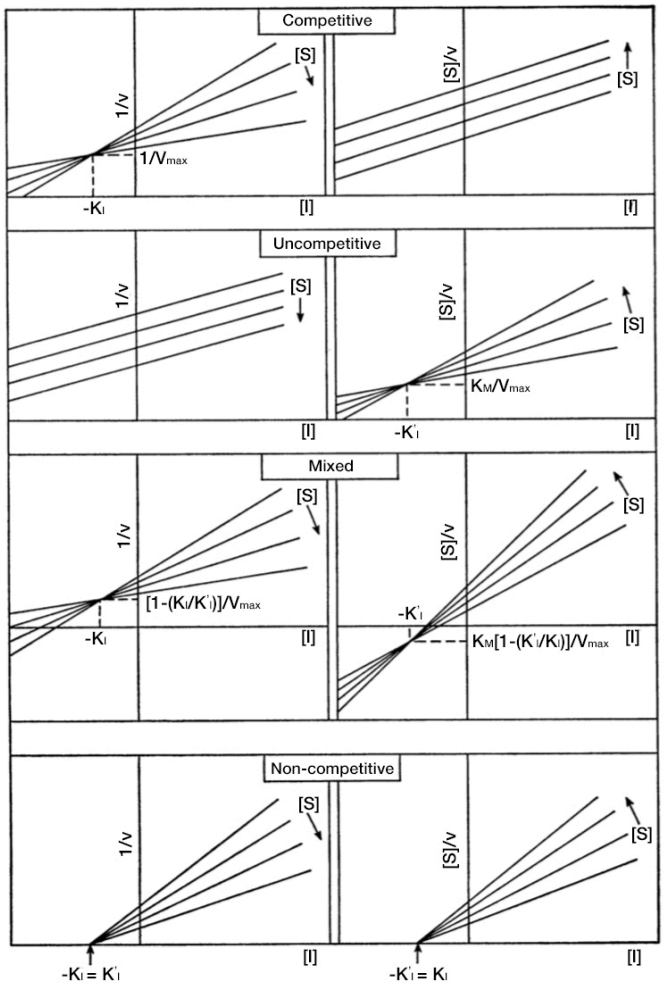


Figure 4.15. Different modes of inhibition as identified using a combination of Dixon plots (left) and Cornish-Bowden plots (right). While the Dixon method plots $\frac{1}{v}$ against $[I]$, the Cornish-Bowden method plots $\frac{[S]}{v}$ against $[I]$. The intercepts may also be used to quantitatively determine the inhibitor dissociation constants, K_I and K_I' in addition to informing on the mode of inhibition[28].

Using OXA-23 and OXA-48, as well as OXA-10 (prepared by Dr. Samuel Cahill, former member of the Schofield Group), the mode of inhibition of OXA *β*-lactamases by halides, specifically iodide, was studied using a FC5-based fluorogenic assay[12,19]. OXA-10 was used at 1 nM, OXA-23 at 10 nM and OXA-48 at 10 nM. Different substrate concentrations (100, 50, 25, 12.5, 6.25, 3.125, 1.56 and 0.781 *μ*M) and inhibitor concentrations (250, 125, 50, 10, 5, 1, 0.5 and 0 mM) were used, and the rates were determined for different substrate-inhibitor concentrations (Table 4.6 [OXA-10], Table 4.7 [OXA-23] and Table 4.8 [OXA-48]).

Table 4.6. Rate of hydrolysis of FC5 by OXA-10 with varying FC5 concentrations in the presence of different concentrations of sodium iodide (rate measured in s^{-1}).

	[NaI]/mM							
[FC5]/μM	**250**	**125**	**50**	**10**	**5**	**1**	**0.5**	**0**
100	*256.52*	*N/A*	*N/A*	*N/A*	*N/A*	*N/A*	*N/A*	*N/A*
50	*178.78*	*217.14*	*413.64*	*N/A*	*N/A*	*N/A*	*N/A*	*N/A*
25	*102.90*	*399.17*	*518.54*	*N/A*	*384.53*	*N/A*	*N/A*	*N/A*
12.5	*77.31*	*N/A*	*331.11*	*395.50*	*647.97*	*390.08*	*360.50*	*408.73*
6.25	*30.50*	*N/A*	*171.03*	*551.56*	*394.03*	*655.67*	*634.74*	*662.85*
3.13	*16.98*	*N/A*	*90.58*	*383.01*	*247.93*	*460.97*	*445.42*	*432.22*
1.56	*N/A*	*50.07*	*50.47*	*218.88*	*129.89*	*261.00*	*236.50*	*220.50*
0.781	*7.99*	*N/A*	*39.83*	*153.36*	*92.57*	*176.26*	*173.28*	*155.68*

N/A: not available.

Table 4.7. Rate of hydrolysis of FC5 by OXA-23 with varying FC5 concentrations in the presence of different concentrations of sodium iodide (rate measured in s^{-1}).

	[NaI]/mM							
[FC5]/μM	**250**	**125**	**50**	**10**	**5**	**1**	**0.5**	**0**
100	*361.23*	*380.98*	*N/A*	*N/A*	*N/A*	*N/A*	*N/A*	*N/A*
50	*183.19*	*427.96*	*723.84*	*323.97*	*264.88*	*226.99*	*371.43*	*383.49*
25	*94.64*	*212.78*	*504.18*	*784.81*	*818.99*	*869.93*	*702.01*	*778.88*
12.5	*49.77*	*N/A*	*255.14*	*424.50*	*458.29*	*485.85*	*366.05*	*398.54*
6.25	*24.38*	*N/A*	*73.88*	*200.51*	*254.89*	*220.14*	*167.36*	*200.55*
3.13	*13.10*	*29.03*	*N/A*	*101.73*	*121.51*	*113.04*	*86.18*	*107.42*
1.56	*7.81*	*16.25*	*31.44*	*94.38*	*49.84*	*52.08*	*N/A*	*55.68*
0.781	*3.15*	*7.83*	*17.28*	*24.48*	*24.17*	*28.93*	*21.62*	*29.53*

N/A: not available.

Table 4.8. Rate of hydrolysis of FC5 by OXA-48 with varying FC5 concentrations in the presence of different concentrations of sodium iodide (rate measured in s^{-1}).

	[NaI]/mM							
[FC5]/μM	**250**	**125**	**50**	**10**	**5**	**1**	**0.5**	**0**
100	*264.99*	*N/A*	*N/A*	*N/A*	*N/A*	*N/A*	*N/A*	*N/A*
50	*275.18*	*292.67*	*708.64*	*N/A*	*N/A*	*N/A*	*N/A*	*N/A*
25	*126.42*	*471.18*	*442.88*	*43.52*	*807.13*	*N/A*	*N/A*	*N/A*
12.5	*71.35*	*248.21*	*238.11*	*820.93*	*657.88*	*899.86*	*898.43*	*568.32*
6.25	*21.63*	*115.88*	*81.02*	*502.00*	*340.18*	*575.89*	*590.33*	*783.44*
3.13	*17.37*	*69.48*	*N/A*	*279.80*	*169.34*	*289.25*	*420.49*	*372.45*
1.56	*8.10*	*31.84*	*30.89*	*160.24*	*97.18*	*155.82*	*158.53*	*185.58*
0.781	*2.92*	*10.21*	*16.73*	*77.05*	*46.03*	*75.41*	*83.09*	*102.20*

N/A: not available.

From the rates of hydrolysis at varying substrate-inhibitor concentrations, the inverse of the velocity parameter, $\frac{1}{v}$ (reciprocal velocity), was obtained for the three OXA β-lactamases (Table 4.9 [OXA-10], Table 4.10 [OXA-23] and Table 4.11 [OXA-48]).

Table 4.9. Reciprocal velocity ($\frac{1}{v}$) of OXA-10 with varying FC5 concentrations in the presence of different concentrations of sodium iodide (reciprocal velocity measured in s).

	[NaI]/mM							
[FC5]/μM	**250**	**125**	**50**	**10**	**5**	**1**	**0.5**	**0**
100	*0.00390*	*N/A*	*N/A*	*N/A*	*N/A*	*N/A*	*N/A*	*N/A*
50	*0.00559*	*0.00461*	*0.00242*	*N/A*	*N/A*	*N/A*	*N/A*	*N/A*
25	*0.00972*	*0.00251*	*0.00193*	*N/A*	*0.00260*	*N/A*	*N/A*	*N/A*
12.5	*0.01293*	*N/A*	*0.00302*	*0.00253*	*0.00154*	*0.00256*	*0.00277*	*0.00245*
6.25	*0.03279*	*N/A*	*0.00585*	*0.00181*	*0.00254*	*0.00153*	*0.00158*	*0.00151*
3.13	*0.05888*	*N/A*	*0.01104*	*0.00261*	*0.00403*	*0.00217*	*0.00225*	*0.00231*
1.56	*N/A*	*0.01997*	*0.01982*	*0.00457*	*0.00770*	*0.00383*	*0.00423*	*0.00454*
0.781	*0.12520*	*N/A*	*0.02511*	*0.00652*	*0.01080*	*0.00567*	*0.00577*	*0.00642*

N/A: not available.

Table 4.10. Reciprocal velocity ($\frac{1}{v}$) of OXA-23 with varying FC5 concentrations in the presence of different concentrations of sodium iodide (reciprocal velocity measured in s).

	[NaI]/mM							
[FC5]/μM	**250**	**125**	**50**	**10**	**5**	**1**	**0.5**	**0**
100	*0.00262*	*N/A*	*N/A*	*N/A*	*N/A*	*N/A*	*N/A*	*0.00262*
50	*0.00234*	*0.00138*	*0.00309*	*0.00378*	*0.00441*	*0.00269*	*0.00261*	*0.00234*
25	*0.00470*	*0.00198*	*0.00127*	*0.00122*	*0.00115*	*0.00142*	*0.00128*	*0.00470*
12.5	*N/A*	*0.00392*	*0.00236*	*0.00218*	*0.00206*	*0.00273*	*0.00251*	*N/A*
6.25	*N/A*	*0.01354*	*0.00499*	*0.00392*	*0.00454*	*0.00598*	*0.00499*	*N/A*
3.13	*0.03445*	*N/A*	*0.00983*	*0.00823*	*0.00885*	*0.01160*	*0.00931*	*0.03445*
1.56	*0.06154*	*0.03180*	*0.01060*	*0.02006*	*0.01920*	*N/A*	*0.01796*	*0.06154*
0.781	*0.12766*	*0.05789*	*0.04084*	*0.04138*	*0.03457*	*0.04626*	*0.03386*	*0.12766*

N/A: not available.

Table 4.11. Reciprocal velocity ($\frac{1}{v}$) of OXA-48 with varying substrate concentrations in the presence of different concentrations of sodium iodide (reciprocal velocity measured in s).

	[NaI]/mM							
[FC5]/μM	**250**	**125**	**50**	**10**	**5**	**1**	**0.5**	**0**
100	*0.00377*	*N/A*	*N/A*	*N/A*	*N/A*	*N/A*	*N/A*	*N/A*
50	*0.00363*	*0.00342*	*0.00141*	*N/A*	*N/A*	*N/A*	*N/A*	*N/A*
25	*0.00791*	*0.00212*	*0.00226*	*0.02298*	*0.00124*	*N/A*	*N/A*	*N/A*
12.5	*0.01402*	*0.00403*	*0.00420*	*0.00122*	*0.00152*	*0.00111*	*0.00111*	*0.00176*
6.25	*0.04624*	*0.00863*	*0.01234*	*0.00199*	*0.00294*	*0.00174*	*0.00169*	*0.00128*
3.13	*0.05758*	*0.01439*	*N/A*	*0.00357*	*0.00591*	*0.00346*	*0.00238*	*0.00268*
1.56	*0.12346*	*0.03141*	*0.03237*	*0.00624*	*0.01029*	*0.00642*	*0.00631*	*0.00539*
0.781	*0.34286*	*0.09796*	*0.05976*	*0.01298*	*0.02172*	*0.01326*	*0.01203*	*0.00978*

N/A: not available.

In order to determine the inhibition mode, Dixon plots for the inhibition of each OXA β-lactamase by sodium iodide were obtained by plotting $\frac{1}{v}$ against inhibitor concentration, $[I]$ (Figure 4.16 [OXA-10], Figure 4.17 [OXA-23] and Figure 4.18 [OXA-48])[27].

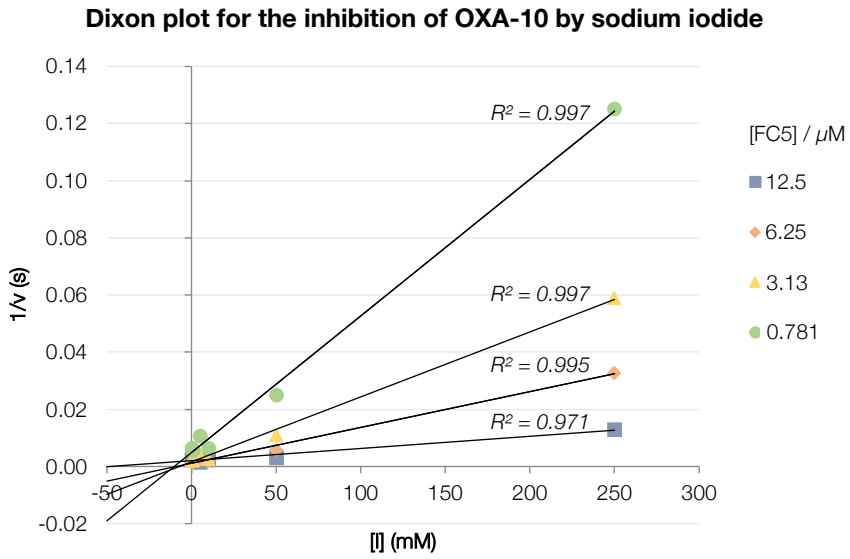


Figure 4.16. Dixon plot of $\frac{1}{v}$ (s) against $[I]$ (mM), where $\frac{1}{v}$ represents the inverse of the rate of hydrolysis of FC5 by OXA-10, and $[I]$ represents the concentration of sodium iodide.[27]

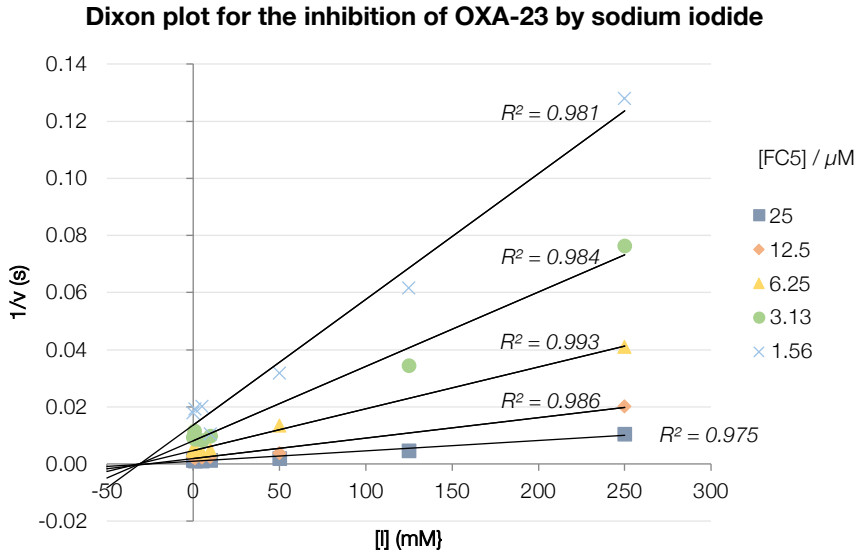


Figure 4.17. Dixon plot of $\frac{1}{v}$ (s) against $[I]$ (mM), where $\frac{1}{v}$ represents the inverse of the rate of hydrolysis of FC5 by OXA-23, and $[I]$ represents the concentration of sodium iodide.[27]

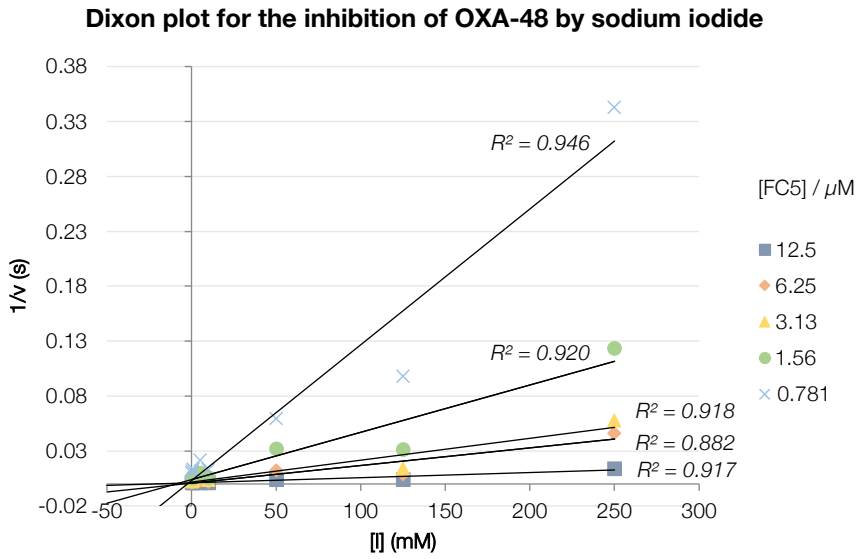


Figure 4.18. Dixon plot of $\frac{1}{v}$ (s) against $[I]$ (mM), where $\frac{1}{v}$ represents the inverse of the rate of hydrolysis of FC5 by OXA-48, and $[I]$ represents the concentration of sodium iodide. [27]

The Dixon method alone, however, is insufficient to distinguish between competitive and mixed inhibition[27]. Therefore, from the values used to generate the Dixon plots, $\frac{[S]}{v}$ values were obtained by multiplying the reciprocal velocity values, $\frac{1}{v}$, with the FC5 substrate concentration, $[S]$ (Table 4.12 [OXA-10], Table 4.13 [OXA-23] and Table 4.14 [OXA-48]), in order to apply the Cornish-Bowden method of identifying the mode of inhibition[28].

Table 4.12. Substrate concentration over the rate of FC5 hydrolysis ($\frac{[S]}{v}$) for OXA-10 with varying FC5 concentrations in the presence of different concentrations of sodium iodide ($\frac{[S]}{v}$ measured in μM s).

	[NaI]/mM							
[FC5]/μM	**250**	**125**	**50**	**10**	**5**	**1**	**0.5**	**0**
100	*0.38983*	*N/A*	*N/A*	*N/A*	*N/A*	*N/A*	*N/A*	*N/A*
50	*0.27967*	*0.23027*	*0.12088*	*N/A*	*N/A*	*N/A*	*N/A*	*N/A*
25	*0.24294*	*0.06263*	*0.04821*	*N/A*	*0.06501*	*N/A*	*N/A*	*N/A*
12.5	*0.16168*	*N/A*	*0.03775*	*0.03161*	*0.01929*	*0.03204*	*0.03467*	*0.03058*
6.25	*0.20495*	*N/A*	*0.03654*	*0.01133*	*0.01586*	*0.00953*	*0.00985*	*0.00943*
3.13	*0.18400*	*N/A*	*0.03450*	*0.00816*	*0.01260*	*0.00678*	*0.00702*	*0.00723*
1.56	*N/A*	*0.03121*	*0.03096*	*0.00714*	*0.01203*	*0.00599*	*0.00661*	*0.00709*
0.781	*0.09781*	*N/A*	*0.01962*	*0.00509*	*0.00844*	*0.00443*	*0.00451*	*0.00502*

N/A: not available.

Table 4.13. Substrate concentration over the rate of FC5 hydrolysis ($\frac{[S]}{v}$) for OXA-23 with varying FC5 concentrations in the presence of different concentrations of sodium iodide ($\frac{[S]}{v}$ measured in μM s).

	[NaI]/mM							
[FC5]/μM	**250**	**125**	**50**	**10**	**5**	**1**	**0.5**	**0**
100	*0.27684*	*0.26248*	*N/A*	*N/A*	*N/A*	*N/A*	*N/A*	*N/A*
50	*0.27294*	*0.11683*	*0.06908*	*0.15434*	*0.18877*	*0.22027*	*0.13462*	*0.13038*
25	*0.26415*	*0.11750*	*0.04959*	*0.03185*	*0.03053*	*0.02874*	*0.03561*	*0.03210*
12.5	*0.25117*	*N/A*	*0.04899*	*0.02945*	*0.02728*	*0.02573*	*0.03415*	*0.03136*
6.25	*0.25632*	*N/A*	*0.08460*	*0.03117*	*0.02452*	*0.02839*	*0.03735*	*0.03116*
3.13	*0.23855*	*0.10767*	*N/A*	*0.03072*	*0.02572*	*0.02764*	*0.03626*	*0.02909*
1.56	*0.20011*	*0.09615*	*0.04970*	*0.01656*	*0.03135*	*0.03000*	*N/A*	*0.02806*
0.781	*0.24802*	*0.09973*	*0.04522*	*0.03191*	*0.03233*	*0.02701*	*0.03614*	*0.02645*

N/A: not available.

Table 4.14. Substrate concentration over the rate of FC5 hydrolysis ($\frac{[S]}{v}$) for OXA-48 with varying FC5 concentrations in the presence of different concentrations of sodium iodide ($\frac{[S]}{v}$ measured in μM s).

	[NaI]/mM							
[FC5]/μM	**250**	**125**	**50**	**10**	**5**	**1**	**0.5**	**0**
100	*0.37737*	*N/A*	*N/A*	*N/A*	*N/A*	*N/A*	*N/A*	*N/A*
50	*0.18170*	*0.17084*	*0.07056*	*N/A*	*N/A*	*N/A*	*N/A*	*N/A*
25	*0.19776*	*0.05306*	*0.05645*	*0.57449*	*0.03097*	*0.00000*	*N/A*	*N/A*
12.5	*0.17519*	*N/A*	*0.05250*	*0.01523*	*0.01900*	*0.01389*	*0.01391*	*0.02199*
6.25	*0.28902*	*N/A*	*0.07714*	*0.01245*	*0.01837*	*0.01085*	*0.01059*	*0.00798*
3.13	*0.17994*	*0.04498*	*N/A*	*0.01117*	*0.01845*	*0.01080*	*0.00743*	*0.00839*
1.56	*0.19290*	*N/A*	*0.05058*	*0.00975*	*0.01608*	*0.01003*	*0.00986*	*0.00842*
0.781	*0.26786*	*0.07653*	*0.04669*	*0.01014*	*0.01697*	*0.01036*	*0.00940*	*0.00764*

N/A: not available.

Using these values, three Cornish-Bowden plots were generated by plotting $\frac{[S]}{v}$ against $[I]$ (Figure 4.19 [OXA-10], Figure 4.20 [OXA-23] and Figure 4.21 [OXA-48])[28].



Figure 4.19. Cornish-Bowden plot of $\frac{[S]}{v}$ (μM s) against $[I]$ (mM), where $\frac{[S]}{v}$ represents the concentration of substrate, i.e. FC5, over the rate of FC5 hydrolysis by OXA-10, and $[I]$ represents the concentration of sodium iodide.[28]

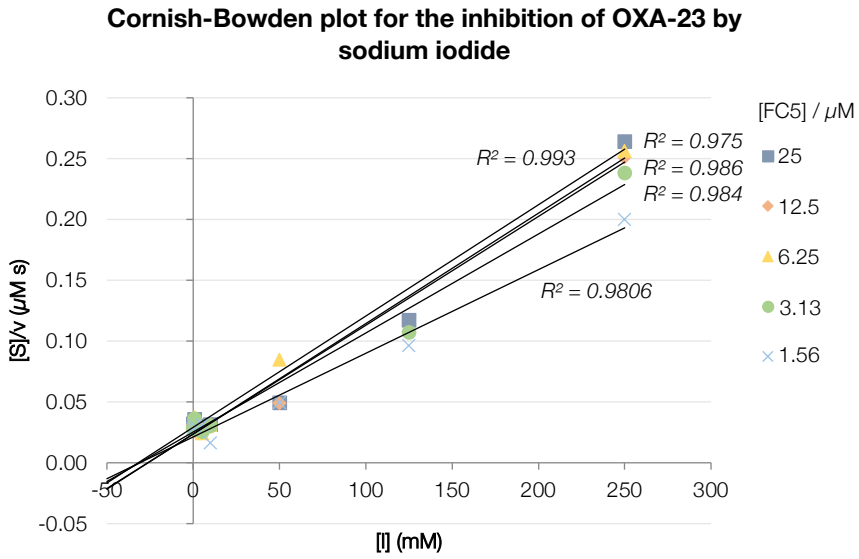


Figure 4.20. Cornish-Bowden plot of $\frac{[S]}{v}$ (μM s) against $[I]$ (mM), where $\frac{[S]}{v}$ represents the concentration of substrate, i.e. FC5, over the rate of FC5 hydrolysis by OXA-23, and $[I]$ represents the concentration of sodium iodide.[28]

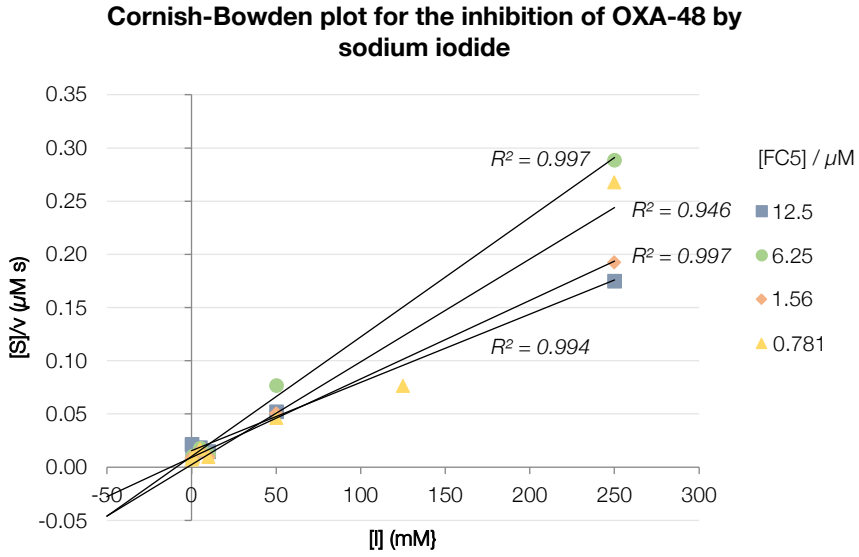


Figure 4.21. Cornish-Bowden plot of $\frac{[S]}{v}$ (μM s) against $[I]$ (mM), where $\frac{[S]}{v}$ represents the concentration of substrate, i.e. FC5, over the rate of FC5 hydrolysis by OXA-48, and $[I]$ represents the concentration of sodium iodide.[28]

From the Dixon plots for the three OXA *β*-lactamases, it was observed that the lines appear to converge slightly above the X-axis, albeit very closely to the abscissa. Due to the fact that the lines were not parallel in these plots, the mode of inhibition is unlikely to be, or at least not exclusively, uncompetitive[27]. From the Cornish-Bowden plots for all three OXA *β*-lactamases, it is apparent that the lines do not converge on the abscissa. Since the lines in the Cornish-Bowden plots were not parallel, the type of inhibition is unlikely to be, or at least not exclusively, competitive[28]. Therefore, based on these plots, a mixed mode of inhibition of OXA *β*-lactamases by sodium iodide is proposed[27,28].

The probable mixed mode inhibition of OXA *β*-lactamases by sodium iodide is consistent with the dual effects observed for halides, in studies conducted by Dr. Christopher Lohans in the Schofield Group[29]. When ^{13}C-labelled OXA-23 was treated with sodium iodide at 0, 50 and 500 mM, no decarbamylation was observed by NMR spectroscopy[29]. However, in the presence of avibactam (15 mM), it was found that increasing sodium iodide concentrations led to a greater extent of decarbamylation (Figure 4.22A)[29]. This indicates that halides may enhance carbamylation if the active site nucleophilic serine is not acylated or modified, but may diminish carbamylation when the serine residue undergoes modification, such as when it is carbamoylated (or acylated) by an inhibitor such as avibactam (or a substrate). The impact of serine modification on lysine carbamylation may be attributed to the loss of the serine as a hydrogen bond donor, which may be caused by either steric hindrance or increasing the pK_a of the lysine side chain as a result of dipolar interactions with avibactam[4,21]. The rate of ampicillin hydrolysis by OXA-10 was also found to decrease with increasing concentrations of sodium iodide (Figure 4.22B). Crystallographic evidence

suggests that in the OXA-10 : avibactam complex, iodide ions may be bound to two different positions in the active site: between Lys-70 and Trp-154, or in the position of the proposed hydrolytic water molecule (Figure 4.22C). Thus, it may be possible that iodide inhibits OXA *β*-lactamases by promoting decarbamylation of Lys-70, as well as (or instead) by blocking productive approach of the hydrolytic water molecule to the acyl-enzyme complex.

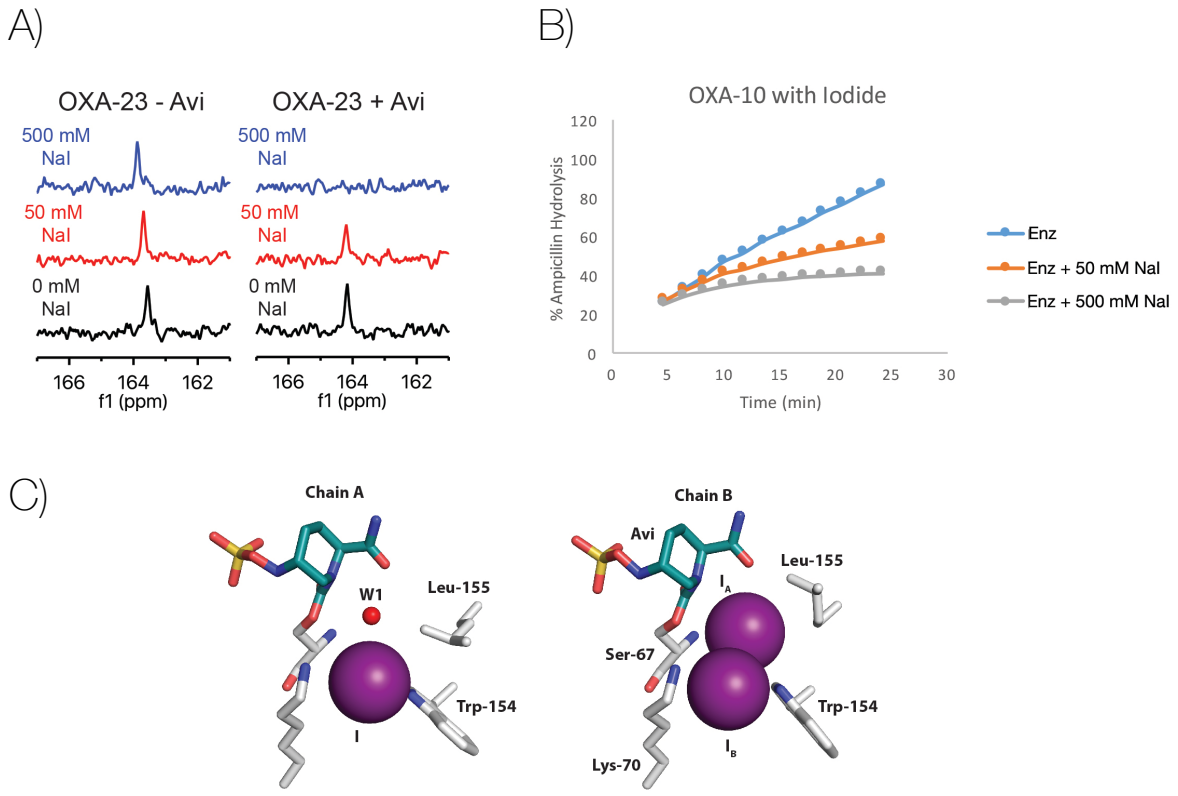


Figure 4.22. Lysine carbamylation in OXA-23 as monitored by ^{13}C NMR spectroscopy (employing $NaH^{13}CO_2$) in the indicated levels of sodium iodide and avibactam (15 mM when present) **(A)**; extent of hydrolysis of ampicillin by OXA-10 in different sodium iodide concentrations **(B)**; view from a crystal structure of the OXA-10 : avibactam complex bound to iodide, showing two binding sites **(C)** (*RCSB PDB ID: 5MOZ*)[29].

4.6. Summary of studies on OXA enzymes

In summary, procedures for the production and purification of recombinant forms of OXA-23 and OXA-48 were achieved, with kinetic parameters of these enzymes being defined using nitrocefin, FC5 and FC5-Pip as substrates for inhibition assays. It was found that for OXA-23 and OXA-48, the overall catalytic efficiency was the highest for nitrocefin and the lowest for FC5-Pip. The latter observation supported the initial hypothesis that the presence of the polar piperacillin side chain may hinder catalysis by *β*-lactamases (including OXA enzymes), which is consistent with the lower catalytic efficiency of OXA carbapenemases (which includes OXA-23 and OXA-48) observed with some extended-spectrum cephalosporins that possess more complex side chains[7,8].

The impact of the status of Lys-70 carbamylation (as determined by addition of sodium bicarbonate) on the kinetic parameters, i.e. the turnover number (k_{cat}), the enzyme-substrate affinity (K_M) and, by extension, the catalytic efficiency (k_{cat} / K_M) are rather profound. For nitrocefin, the presence of sodium bicarbonate increased the k_{cat} while decreasing the K_M, resulting in a small increase in the overall k_{cat} / K_M.

For FC5 in the presence of sodium bicarbonate, with OXA-23, the k_{cat} and the K_M values, and thus the overall k_{cat} / K_M values, were unchanged; with OXA-48 the k_{cat} and the K_M values were raised with a negligible change to the overall k_{cat} / K_M.

For FC5-Pip, with the addition of sodium bicarbonate, the k_{cat} remained unchanged but the K_M was halved, which resulted in the doubling of the overall k_{cat} / K_M for both OXA-23 and OXA-48. These observations suggest that different substrates are affected differently by the carbamylation status of Lys-70. The addition of sodium

bicarbonate resulted in either an increase in catalytic efficiency or a lack of noticeable change in catalytic efficiency.

From further kinetic assays, it was found that avibactam, the bicyclic boronates (**BN1** and **BN2**) and the 6-methylidene penem **BLI-489** were inhibitors of OXA-23 and OXA-48 (Figure 4.14, 4.11, 4.12 and 4.8). Sulbactam, in the absence of sodium bicarbonate, displayed signs of inhibition, though the extent of inhibition was relatively low as compared to other inhibitors. **BLI-489** was observed to be the most potent inhibitor in the presence of sodium bicarbonate, although its pIC_{50} values in the absence of sodium bicarbonate could not be accurately captured due to its high potency. Interestingly, the bicyclic boronate inhibitors **BN1** and **BN2** were apparently insensitive to the presence of sodium bicarbonate, while the inhibitory activities of avibactam were much more significantly affected, showing a decrease in potency with OXA-23 and an increase in potency with OXA-48 upon the addition of sodium bicarbonate. The tested lactivicins (**LTV**, **PLTV**, **LTV-13**) did not manifest any detectable inhibition of OXA-23 and OXA-48.

The presence of time dependent effects may be related to the mechanism of inhibition exhibited by different inhibitors. For example, time dependent effects were observed in this study for sulbactam, avibactam and **BLI-489**. For sulbactam, this may be due to crosslinking and fragmentation[14]; for avibactam however, the reason remains unclear and factors other than fragmentation may be involved. **BLI-489**, on the other hand, is known to cyclise to form an acyl-enzyme complex containing a 1,4-thiazepine ring[15]. There is a lack of time dependency with both bicyclic boronate inhibitors **BN1** and **BN2**, and mechanistically there is no evidence that they undergo crosslinking and/or fragmentation.

Finally, the effect of iodide ions on OXA-10, OXA-23 and OXA-48 was studied using the FC5 assay platform[12,19]. By deriving Dixon plots[27] and Cornish-Bowden plots[28] for the iodide inhibition of each OXA *β*-lactamase, it was concluded that a mixed inhibition mode is likely, which is consistent with the dual effects of halide observed with OXA *β*-lactamases from other studies[29]. This mixed inhibition mode presented by iodide may be attributed to (at least) two factors. Firstly, modification of the nucleophilic serine may render it easier to effect decarbamylation of the key lysine (Lys-70), while carbamylation may be changed in the absence of serine modification. This may be due to the loss of a hydrogen bond donor upon carbamoylation of serine (Ser-67) by avibactam, which may be due to either steric hindrance or pK_a effects from lysine-avibactam interactions[3,29]. Secondly, iodide may bind to two different sites in the active sites of OXA *β*-lactamases, i.e. between Lys-70 and Trp-154, or in the proposed site occupied by the hydrolytic water molecule. Therefore, inhibition of OXA *β*-lactamases by iodide may be a result of both lysine decarbamylation and displacement of the hydrolytic water[29].

4.7. Experimental procedures

Production and purification of OXA-23 and OXA-48[12]

In order to characterise the effects of *β*-lactamases inhibitors on OXA *β*-lactamases, OXA-23 and OXA-48 *β*-lactamases were expressed as N-terminal hexahistidine fusions in *E. coli* BL21(DE3) transformed with pOPINF-OXA-23 and pOPINF-OXA-48 respectively. The cells were grown using an autoinduction medium supplemented with 50 *μ*g/mL of ampicillin. After the cells were grown for four hours at 37 ºC, they were cooled to 18 ºC, and their growth continued overnight with shaking. The cells

were then harvested by centrifugation (10 minutes, 10,000 x *g*), resuspended in 50 mL lysis buffer (50 mM HEPES, pH 7.5, 500 mM NaCl, 5 mM imidazole) supplemented with DNase I, and lysed by sonication. The supernatant was loaded onto a 5 mL HisTrap HP column, washed with 50 mM HEPES, pH 7.5, 500 mM NaCl and 5 mM imidazole, and eluted with an imidazole gradient from 20 to 500 mM. Fractions containing the purified enzymes were concentrated by centrifugal ultrafiltration (Amicon Ultra [Millipore]; 15 mL, 10 kDa molecular weight cutoff). The resultant solution was injected onto Superdex S200 column (300 mL) and eluted with 50 mM HEPES, pH 7.5 and 200 mM NaCl. Fractions containing pure His-tagged enzymes were incubated overnight at 4 °C with His-tagged 3C protease (1:100, wt/wt) to remove the N-terminal His tag. The 3C protease, together with any uncleaved protein in the digestion mixture, was removed by passage through a second HisTrap HP column, preequilibrated with 50 mM HEPES at pH 7.5, 500 mM NaCl and 20 mM imidazole, and eluted with an imidazole gradient from 20 to 500 mM. The purified enzyme fractions were analysed by SDS-PAGE, pooled and concentrated by centrifugal ultrafiltration before buffer exchange into 25 mM HEPES, pH 7.5 and 100 mM NaCl. The concentrations of the purified proteins were determined using a NanoDrop ND-1000 spectrophotometer (Thermo Scientific; ε = 43430 and 63930 M^{-1} cm^{-1} for OXA-23 and OXA-48 respectively), aliquoted and frozen in liquid nitrogen. The purity of both *β*-lactamases was determined via size exclusion chromatography-multi-angle laser scattering (SEC-MALS) analyses carried out by Dr. David Staunton (University of Oxford, Department of Biochemistry, Biophysics Facility). Chromatography was performed using a Superdex 75 HR10/30 column on a Shimadzu HPLC system, with a mobile phase of 50 mM sodium phosphate, pH 7.5.

Detection was achieved using a Wyatt Dawn HELEOS-II 8-angle light scattering detector, a Wyatt Optilab rEX refractive index monitor, and an SPD20A UV/Vis detector (Figure 4.4).

Steady-state kinetic studies[12,19]

Steady-state kinetics studies used a PHERAstar FS microplate reader (BMG LABTECH, Germany) with UV-STAR® 96-well, half area, μclear® plates (Greiner Bio-One) for nitrocefin experiments and 384-well, half area, black, μclear® plates (Greiner Bio-One) for FC5 and FC5-Pip[12]. Buffers employed were 100 mM sodium phosphate, pH 7.5, 50 mM sodium bicarbonate, 0.01% Triton X-100 for OXA-23 and OXA-48. Reaction progress was monitored at 298 K by following changes in absorbance at 485 nm for nitrocefin, and changes in fluorescence intensity (λ_{ex} = 380 nm, λ_{em} = 480 nm) for FC5 and FC5-Pip. Suitable enzyme concentrations for kinetic analysis were determined by monitoring changes in absorbance/fluorescence for enzyme concentrations between 20 nM and 20 pM as summarised in Table 4.15. For FC5 and FC-5Pip, an umbelliferone absorbance calibration curve was also obtained (Figure 4.23).

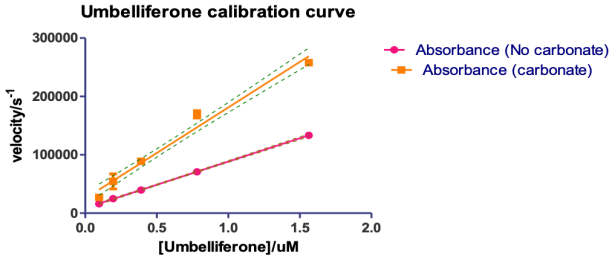


Figure 4.23. Linear regression fitting of umbelliferone absorbance at different concentrations, which is used in the kinetics analyses of FC-5 and FC-5Pip with OXA-23 and OXA-48.

Kinetic constants were determined using the initial rates of hydrolysis, with the reaction initiated through the addition of enzyme to a pre-prepared substrate mixture. Substrate concentrations ranged between 400 μM and 0.4 μM. The Michaelis-Menten equation was fitted to data by non-linear regression using GraphPad Prism software to calculate kinetic values.

Table 4.15. Suitable enzyme concentrations for kinetic analysis for different substrates.

	[E] (nM)		
Enzyme	**Nitrocefin**	**FC5**	**FC5-Pip**
OXA-23	2	12.5	12.5
OXA-48	2	12.5	12.5

Inhibition assays[12,19]

Inhibition assays were carried out using FC5 as a fluorogenic reporter substrate[19]. The enzyme concentrations used were the same as those employed in steady-state kinetic studies (Table 4.15). Different buffer solutions were used to test the impact of carbamylation: (A) 100 mM sodium phosphate, pH 7.4, 0.01% Triton X-100 and (B) 100 mM sodium phosphate, pH 7.4, 50 mM sodium bicarbonate, 0.01% Triton X-100. The concentration of FC5 employed was 5 μM for both OXA-23 and OXA-48. IC_{50} values were determined by preincubating the enzyme with the inhibitor in the assay buffer at room temperature for 10, 30, 60, or 360 minutes prior to the addition of substrate. Data with 0 min pre-incubation were obtained by addition of enzyme to a premixed solution of inhibitor and substrate. Residual enzyme activity was determined for a range of inhibitor concentrations. Nonlinear regression fitting of IC_{50} curves and reporting of pIC_{50} values (including errors) were carried out using a three-parameter dose-response curve in GraphPad Prism.

For studies of iodide inhibition of OXA *β*-lactamases, OXA-10 was used at 1 nM, OXA-23 at 10 nM and OXA-48 at 10 nM. Different substrate concentrations (100, 50, 25, 12.5, 6.25, 3.125, 1.56 and 0.781 *μ*M) and inhibitor concentrations (250, 125, 50, 10, 5, 1, 0.5 and 0 mM) were used, and the rates were determined for different substrate-inhibitor concentrations. Calculations and subsequent Dixon/Cornish-Bowden plots were performed using MS Excel.

4.8. References

[1] Antunes, N. T.; Lamoureaux, T. L.; Toth, M.; Stewart, N. K.; Frase, H.; Vakulenko, S. B. *Antimicrob. Agents Chemother.* **2014**, *58*, 2119–2125.

[2] Nordmann, P.; Poirel, L. *Clin. Microb. Infect.* **2014**, *20*, 821–830.

[3] Evans, B. A.; Amyes, S. G. B. *Clin. Microbiol. Rev.* **2014**, *27*, 241–263.

[4] King, D. T.; King, A. M.; Lal, S. M.; Wright, G. D.; Strynadka, N. C. J. *ACS Infect. Dis.* **2015**, *1*, 175–184.

[5] Lahiri, S. D.; Mangani, S.; Jahić, H.; Benvenuti, M.; Durand-Reville, T. F.; Luca, F. D.; Ehmann, D. E.; Rossolini, G. M.; Alm, R. A.; Docquier, J.-D. *ACS Chem. Bio.* **2014**, *10*, 591–600.

[6] Vercheval, L.; Bauvois, C.; Di Paolo, A.; Borel, F.; Ferrer, J.-L.; Sauvage, E.; Matagne, A.; Frère, J.-M.; Charlier, P.; Galleni, M.; Kerff, F. *Biochem. J.* **2010**, *432*, 495–506.

[7] Stojanoski, V.; Chow, D.-C.; Fryszczyn, B.; Hu, L.; Nordmann, P.; Poirel, L.; Sankaran, B.; Prasad, B. V. V.; Palzkill, T. *Biochemistry* **2015**, *54*, 3370–3380.

[8] Totir, M. A.; Cha, J.; Ishiwata, A.; Wang, B.; Sheri, A.; Anderson, V. E.; Buynak, J.; Mobashery, S.; Carey, P. R. *Biochemistry* **2008**, *47*, 4094–4101.

[9] Ehmann, D. E.; Jahić, H.; Ross, P. L.; Gu, R.-F.; Hu, J.; Durand-Réville, T. F.; Lahiri, S.; Thresher, J.; Livchak, S.; Gao, N.; Palmer, T.; Walkup, G. K.; Fisher, S. L. *J. Biol. Chem.* **2013**, *288*, 27960–27971.

[10] *States News Service*. February 25, 2015.

[11] Brown, T.; Charlier, P.; Herman, R.; Schofield, C. J.; Sauvage, E. *J. Med. Chem.* **2010**, *53*, 5890–5894.

[12] Brem, J.; Cain, R.; Cahill, S.; Mcdonough, M. A.; Clifton, I. J.; Jiménez-Castellanos, J.-C.; Avison, M. B.; Spencer, J.; Fishwick, C. W. G.; Schofield, C. J. *Nat. Comm.* **2016**, *7*, 12406.

[13] Venkatesan, A. M.; Agarwal, A.; Abe, T.; Ushirogochi, H.; Yamamura, I.; Kumagai, T.; Petersen, P. J.; Weiss, W. J.; Lenoy, E.; Yang, Y.; Shlaes, D. M.; Ryan, J. L.; Mansour, T. S. *Bioorg. Med. Chem.* **2004**, *12*, 5807–5817.

[14] Venkatesan, A. M.; Gu, Y.; Santos, O. D.; Abe, T.; Agarwal, A.; Yang, Y.; Petersen, P. J.; Weiss, W. J.; Mansour, T. S.; Nukaga, M.; Hujer, A. M.; Bonomo, R. A.; Knox, J. R. *J. Med. Chem.* **2004**, *47*, 6556–6568.

[15] Weiss, W. J.; Petersen, P. J.; Murphy, T. M.; Tardio, L.; Yang, Y.; Bradford, P. A.; Venkatesan, A. M.; Abe, T.; Isoda, T.; Mihira, A.; Ushirogochi, H.; Takasake, T.; Projan, S.; Oconnell, J.; Mansour, T. S. *Antimicrob. Agents Chemother.* **2004**, *48*, 4589–4596.

[16] Baurin, S.; Vercheval, L.; Bouillenne, F.; Falzone, C.; Brans, A.; Jacquamet, L.; Ferrer, J.-L.; Sauvage, E.; Dehareng, D.; Frère, J.-M.; Charlier, P.; Galleni, M.; Kerff, F. *Biochemistry* **2009**, *48*, 11252–11263.

[17] Michaelis, L.; Menten, M. L. *Biochem Z*. **1913**, *49*, 333–369.

[18] Ocallaghan, C. H.; Morris, A.; Kirby, S. M.; Shingler, A. H. *Antimicrob. Agents Chemother.* **1972**, *1*, 283–288.

[19] Berkel, S. S. V.; Brem, J.; Rydzik, A. M.; Salimraj, R.; Cain, R.; Verma, A.; Owens, R. J.; Fishwick, C. W. G.; Spencer, J.; Schofield, C. J. *J. Med. Chem.* **2013**, *56*, 6945–6953.

[20] Poirel, L.; Naas, T.; Nordmann, P. *Antimicrob. Agents Chemother.* **2009**, *54*, 24–38.

[21] Kaitany, K.-C. J.; Klinger, N. V.; June, C. M.; Ramey, M. E.; Bonomo, R. A.; Powers, R. A.; Leonard, D. A. *Antimicrob. Agents Chemother.* **2013**, *57*, 4848–4855.

[22] Antunes, N. T.; Lamoureaux, T. L.; Toth, M.; Stewart, N. K.; Frase, H.; Vakulenko, S. B. *Antimicrob. Agents Chemother.* **2014**, *58*, 2119–2125.

[23] Totir, M. A.; Helfand, M. S.; Carey, M. P.; Sheri, A.; Buynak, J. D.; Bonomo, R. A.; Carey, P. R. *Biochemistry* **2007**, *46*, 8980–8987.

[24] Bethel, C. R.; Distler, A. M.; Ruszczycky, M. W.; Carey, M. P.; Carey, P. R.; Hujer, A. M.; Taracila, M.; Helfand, M. S.; Thomson, J. M.; Kalp, M.; Anderson, V. E.; Leonard, D. A.; Hujer, K. M.; Abe, T.; Venkatesan, A. M.; Mansour, T. S.; Bonomo, R. A. *Antimicrob. Agents Chemother.* **2008**, *52*, 3135–3143.

[25] Cahill, S. T.; Cain, R.; Wang, D. Y.; Lohans, C. T.; Wareham, D. W.; Oswin, H. P.; Mohammed, J.; Spencer, J.; Fishwick, C. W. G.; Mcdonough, M. A.; Schofield, C. J.; Brem, J. *Antimicrob. Agents Chemother.* **2017**, *61*.

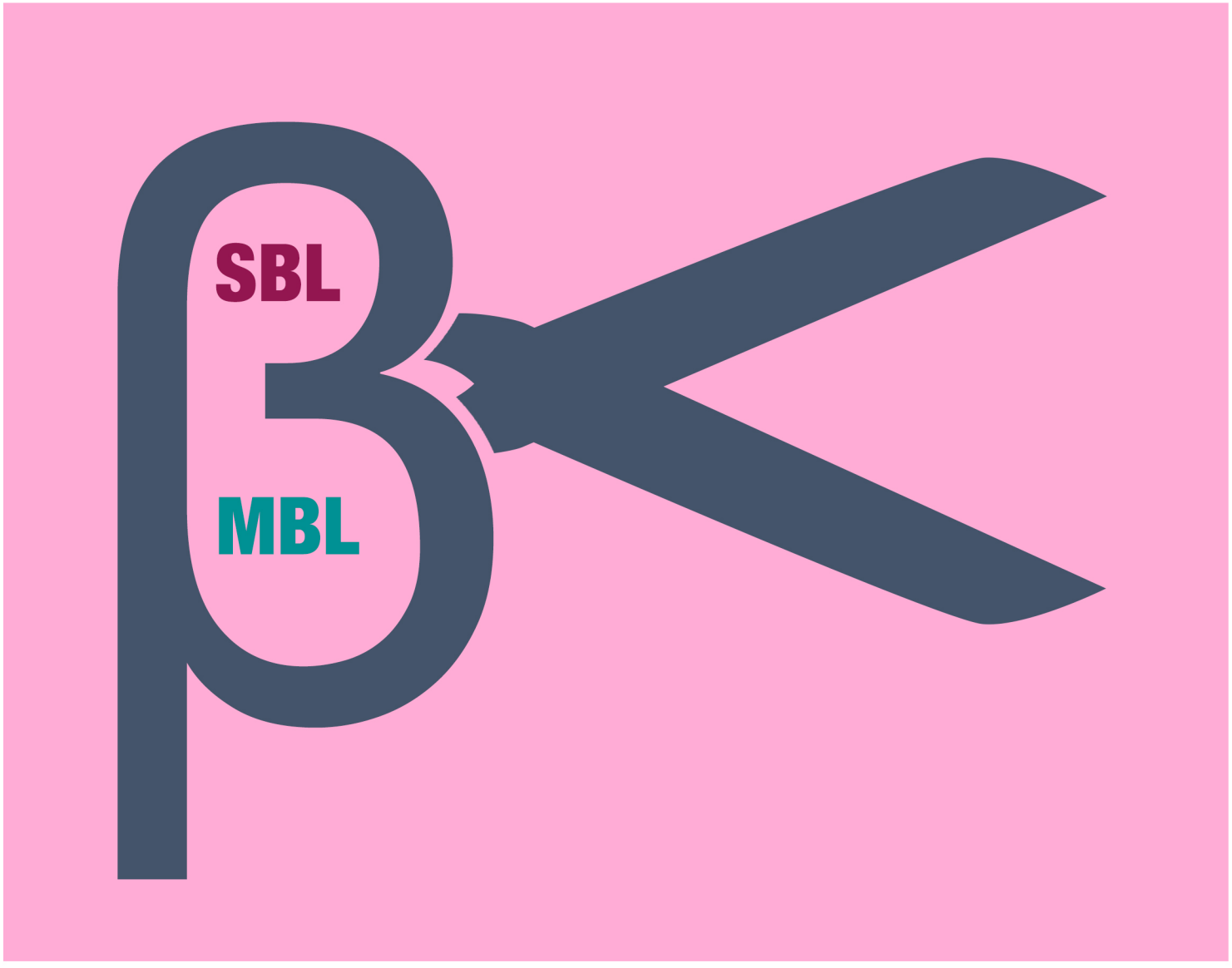
[26] Cleland W. W. *Biochim. Biophys. Acta* **1963**, *67*, 173–187.

[27] Dixon, M. *Biochem. J.* **1953**, *55*, 170–171.

[28] Cornish-Bowden, A. *Biochem. J.* **1974**, *137*, 143–144.

[29] Lohans, C. T.; Wang, D. Y.; Jorgensen, C.; Cahill, S. T.; Clifton, I. J.; Mcdonough, M. A.; Oswin, H. P.; Spencer, J.; Domene, C.; Claridge, T. D. W.; Brem, J.; Schofield, C. J. *Org. Biomol. Chem.* **2017**, *15*, 6024–6032.

Chapter 5. Conclusions and Future Work



5. Conclusions and Future Work

5.1. Conclusions and Future Work

From the work described in Chapter 2 of this thesis, it has been demonstrated that compounds containing certain heteroaryl carboxylate cores, such as 2-pyrrole carboxylates, 4-thiazole carboxylates and 4-pyrimidine carboxylates, have the potential to, at the very least, inhibit a panel of clinically relevant B1 MBLs consisting of NDM-1, IMP-1, VIM-1 and VIM-2. The structures of compounds which demonstrated potent inhibition are shown in Figure 5.1.

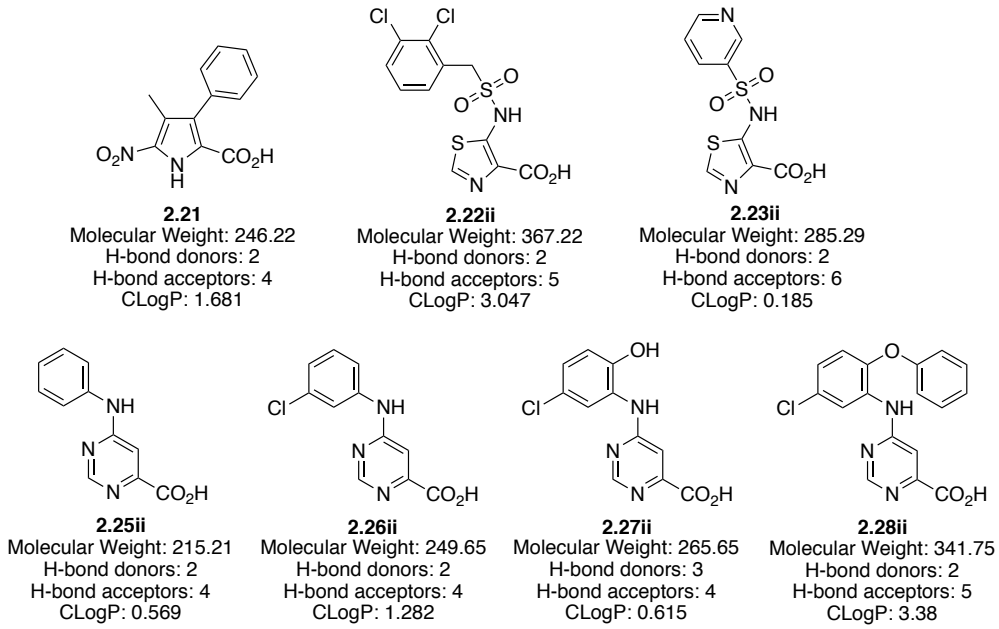
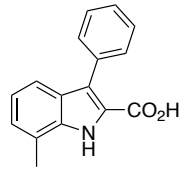


Figure 5.1. Structures of potent inhibitors of MBLs identified in this work. **2.21** contains a 2-pyrrole carboxylate core; **2.22ii** and **2.23ii** contain a 4-thiazole carboxylate core; **2.25ii**, **2.26ii**, **2.27ii** and **2.28ii** contain a 4-pyrimidine carboxylate core.

Parallel studies conducted by other members of the Schofield Group have also identified 2-indole carboxylates as potent broad-spectrum inhibitors of MBLs (Table 5.1); these compounds have been optimised and are presently undergoing *in vivo* studies. Future research could focus on the synthesis of potential MBL inhibitors that are indole, thiazole or pyrimidine-based. It is notable that it should be possible to

prepare such compounds efficiently on a large scale; this is important because 'cost of goods' is an issue in antibiotic development, especially because MBL-mediated resistance is presently most important in the developing world.

Table 5.1. Example of a 2-indole carboxylate inhibitor of MBLs.



Molecular Weight: 251.29
H-bond donors: 2
H-bond acceptors: 2
CLogP: 3.462

	pIC_{50}*	
NDM-1	IMP-1	VIM-2
7.5	5.0	6,4

*Inhibition studies were performed on a standard fluorogenic assay platform involving FC-5 and a panel of clinically relevant MBLs. Errors of pIC_{50} measurements were within 10% of recorded values. Courtesy of Dr. Madeleine Kavanaugh (former Schofield Group member).

In addition, compounds bearing a pyridine 2-carboxylate core with substitution in the 3-position as well as pyrimidine 4-carboxylate with substitution in the 5-position are of interest (Figure 5.2). One problem that was encountered with the pyrimidine series was lipophilicity. Thus, future work could also focus on synthesising compounds with polar functional groups, such as sulfonamide derivatives, as present in **2.22ii** and **2.23ii**.

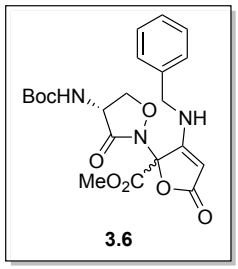


Figure 5.2. Examples of (potential) MBL inhibitors which contain a pyridine 2-carboxylate core with substitution in the 3-position (left), or a pyrimidine 4-carboxylate core with substitution in the 5-position (right).

Given the ability of heteroaryl carboxylate compounds to function as metal chelators, the inhibition of other metalloenzymes by such compounds, as well as toxicology studies, should be investigated, should any of these compounds be identified as promising leads for clinical evaluation. In line of selectivity screens, human MBLs are of potential interest, since many of these enzymes play crucial roles, e.g. in DNA damage repair and detoxification[1].

The nitropyrrole **2.21** has potential for use in mechanistical imaging studies of MBLs. The fluorescence activity of **2.21** could be further evaluated, both in its free state as well as when it is bound to various MBLs, in order to inform on its suitability as a probe in fluorescence detection assays for MBL studies.

As highlighted in Chapter 3, the lactivicins have clinical potential, as the only naturally occurring non β-lactams acting similarly to β-lactams. The successful synthesis of a novel unsaturated and densely functionalised lactivicin analogue, **3.6** was described using D-cycloserine as a precursor due to its low cost. It was envisaged that a structurally similar precursor that contains an L-cycloserine core could be synthesised in the same fashion (Figure 5.3).



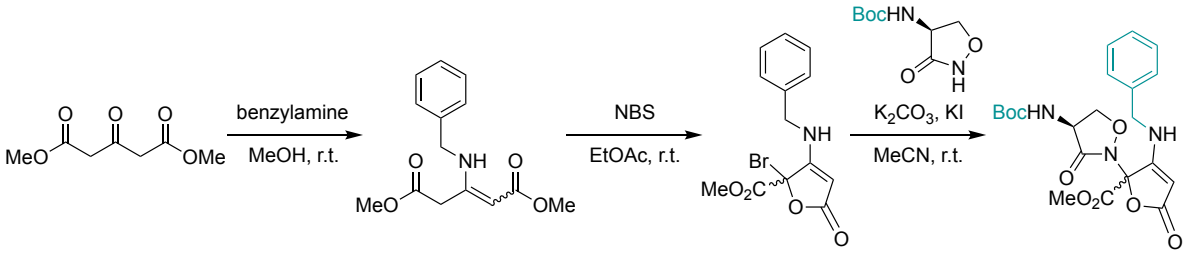


Figure 5.3. A possible synthetic route to access a stereoisomer of **3.6** from L-cycloserine, using a methodology described in Chapter 3.

The hydrolysis of the methyl ester needs to be more thoroughly investigated, with the potential option of synthesising precursors with other more readily deprotected esters, in order to ultimately afford the carboxylic acid, which is likely essential for PBP (or *β*-lactamase) inhibition activity (Figure 5.4).

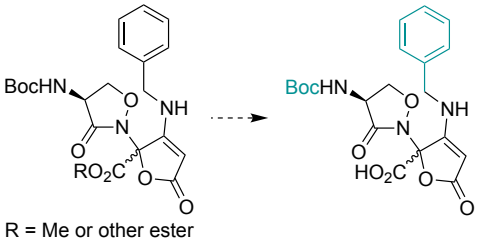


Figure 5.4. Lactivicin ester precursors featuring an L-cycloserine core could be hydrolysed to produce the free acid, which is likely essential for *β*-lactamase inhibition.

Upon accessing the free carboxylic acid from successful ester removal, it is of interest to selectively remove both the Boc group and the benzyl group, to enable functionalisation of the two amino groups – one on the cycloserine (*γ*-lactam like) core and another on the *γ*-lactone core. Examples of functionalisations that could be useful include coupling the new lactivicin core to a siderophore, which could potentially improve both bacterial uptake and selectivity, as reported for LTV-17[2,3] (Figure 5.5).

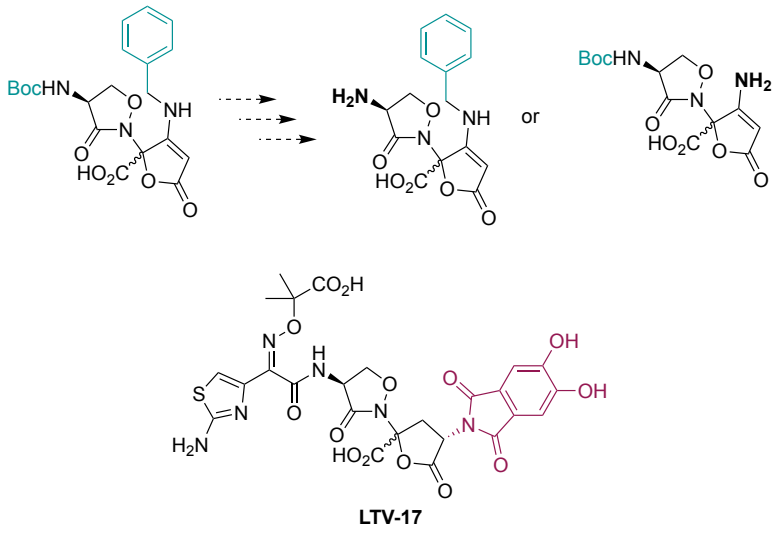


Figure 5.5. Removal of either the Boc and/or benzyl groups would reveal amino groups (top) for further functionalisation, such as attaching a siderophore, as in the suitable LTV-17 (bottom; siderophore coloured in red).

It could also be possible to attempt halogenation at the *α*-position of the *α*,*β*-unsaturated lactone, in order to enable further functionalisation at the lactone *α*-position (Figure 5.6).

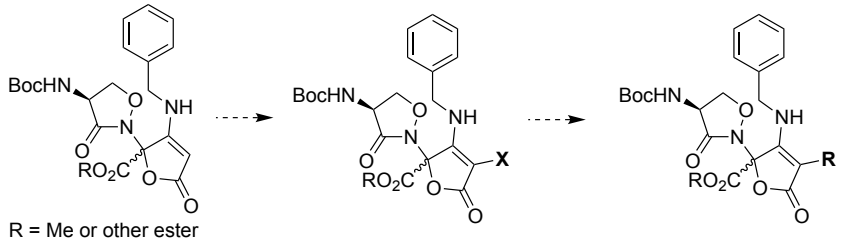


Figure 5.6. Halogenation of a lactivicin ester precursor could be achieved to enable further functionalisation at the lactone *α*-position.

It is also envisaged that via hydrogenation of the *α*,*β*-unsaturated lactone could be achieved, giving rise to a new chiral centre (Figure 5.7).

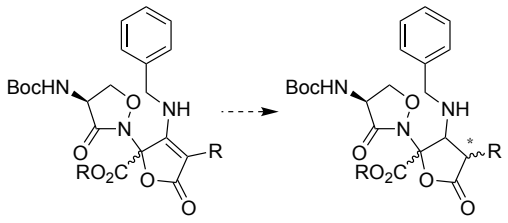


Figure 5.7. Saturation of the *α*,*β*-unsaturated lactone could lead to the formation of a new chiral centre, which may inspire the synthesis of new lactivicin derivatives.

In Chapter 4, through various fluorometric kinetic assays, it was demonstrated that iodide ions may exhibit a mixed mode of inhibition on OXA *β*-lactamases (Figure 4.14 to 4.18). The mechanism(s) of inhibition are presently unknown, but may involve protein modification, lysine decarbamylation and/or hydrolytic water displacement. The results of testing the OXA *β*-lactamases with a range of potential inhibitors including lactivicins, bicyclic boronates, BLI-489, sulbactam and avibactam, revealed very different extents of inhibition. The level of inhibition of OXA *β*-lactamases by certain some inhibitors is substantially affected by the presence of bicarbonate ions. Time dependent effects were observed with some inhibitors, e.g. avibactam, likely verifying a mechanism including protein modification (e.g. decarbamylation). The use of biological methods, such as NMR and X-ray crystallography, may inform on the mechanisms of inhibition by OXA *β*-lactamases.

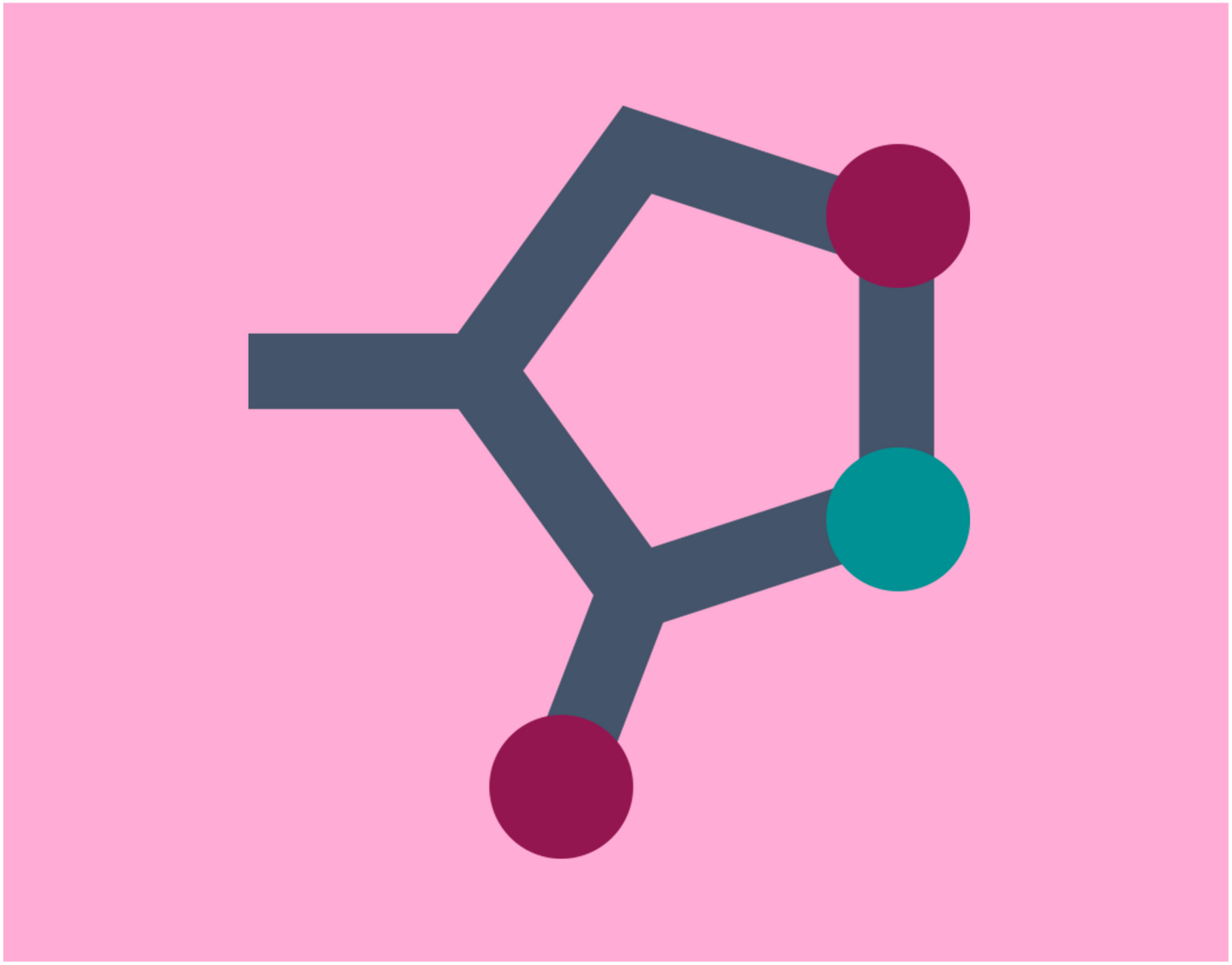
5.2. Reference

[1] Pettinati, I.; Brem, J.; Lee, S. Y.; Mchugh, P. J.; Schofield, C. J. *Trends Biochem. Sci.* **2016**, *41*, 338–355.

[2] Starr, J.; Brown, M. F.; Aschenbrenner, L.; Caspers, N.; Che, Y.; Gerstenberger, B. S.; Huband, M.; Knafels, J. D.; Lemmon, M. M.; Li, C.; Mccurdy, S. P.; Mcelroy, E.; Rauckhorst, M. R.; Tomaras, A. P.; Young, J. A.; Zaniewski, R. P.; Shanmugasundaram, V.; Han, S. *J. Med. Chem.* **2014**, *57*, 3845–3855.

[3] Calvopiña, K.; Umland, K.-D.; Rydzik, A. M.; Hinchliffe, P.; Brem, J.; Spencer, J.; Schofield, C. J.; Avison, M. B. *Antimicrob. Agents Chemother.* **2016**, *60*, 4170–4175.

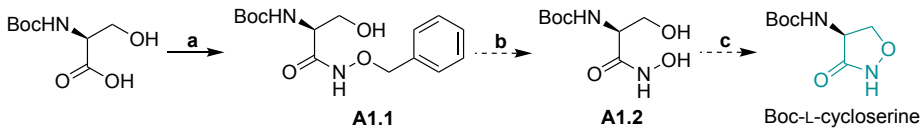
Appendix



Appendix

A1.1. Towards the efficient synthesis of cycloserine

An integral structural component of the lactivicins is their cycloserine core. Cycloserine was first isolated from two species Streptomyces as a natural product, separately by Merck and Eli Lilly[1]. Subsequently, cycloserine was first synthesised in racemic form at Merck[2,3]. In addition to the use of cycloserine as an antibiotic against *Mycobacterium tuberculosis*, which causes tuberculosis (via the use of the D-enantiomer, which acts as a cyclic analogue of D-alanine)[4], the other notable relevance of cycloserine to medicinal chemistry pertains to the presence of L-cycloserine in the lactivicins[5,6].



Scheme A1.1. *Reactions and conditions for cycloserine synthesis previously used in the Schofield Group[7]:*

a) *O*-benzyl-hydroxylamine (1 equiv.), EDCI•HCl* (0.8 equiv.), *N*-methylmorpholine (1.4 equiv.), CH_2Cl_2, -15 °C to r.t., 2 h, 63%; b) method A[7]: Pd-C 10% (1 equiv.), H_2, MeOH, r.t. or method B: Pd-C 10% (0.25 equiv.), ammonium formate (5.5 equiv.), MeOH, reflux, 1 h; c) DIAD** (1.5 equiv.), PPh_3 (1.5 equiv.), THF, 0 °C to r.t. Reactions unsuccessful.

*1-Ethyl-3-(3-dimethylaminopropyl)carbodiimide hydrochloride.

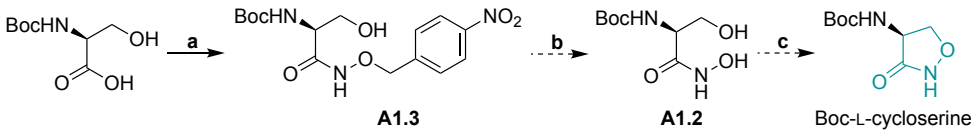
** Diisopropyl azodicarboxylate.

A synthetic strategy to access cycloserine has been previously developed by the Schofield Group[7]. This strategy was first replicated, where initially, Boc-protected L-serine was added to *O*-benzyl-hydroxylamine dichloromenthane, in the presence of 1-ethyl-3-(3-dimethylaminopropyl)carbodiimide hydrochloride (EDCI•HCl) and *N*-methylmorpholine as a base, at -15 °C, before to room temperature, which gave **A1.1** in 63% yield after a two-hour reaction (Scheme A1.1).

To afford **A1.2** from **A1.1**, hydrogenation was first carried out with 10% palladium on carbon (Pd-C) in methanol, under a hydrogen atmosphere at room temperature (Scheme A1.1). However, this procedure was unsuccessful. It was proposed that the extent of hydrogenation of **A1.1** may be inadequate due to low hydrogen gas pressure. Therefore, methods of generating hydrogen *in situ* were examined. One method using a catalytic amount of 10% Pd-C and an excess of ammonium formate in methanol was attempted on **A1.1**[8]. However, after refluxing the reaction mixture for an hour, significant over-reduction was observed, as indicated by the formation of a primary amide (Scheme A1.1).

Attempts were also made to substitute the benzyl group with a 4-nitrobenzyl group (**A1.3**) to achieve better results with hydrogenation. From Boc-protected L-serine, *O*-(4-nitrobenzyl)-hydroxylamine, EDCI•HCl and *N*-methylmorpholine were dissolved in dichloromethane at -20 °C, then warmed to room temperature and stir for 22 hours, to give **A1.3** in apparent quantitative yield.

Subsequent hydrogenation of **A1.3** was attempted via both methods attempted on **A1.1**, i.e. with Pd-C/H_2 and Pd-C/ammonium formate. In addition, an indium-catalysed reduction was performed[9], using a large excess of indium powder in a mixture of methanol and saturated ammonium chloride solution under reflux (24 hours). Unfortunately, none of these methods were successful. It was proposed that hydrogenation with Pd-C/ammonium formate would remain a viable option, but different reaction duration and temperature should be studied to identify a useful working condition.



Scheme 3.4. *Reactions and conditions:*

a) *O*-(4-nitrobenzyl)-hydroxylamine (1.3 equiv.), EDCI•HCl* (1.3 equiv.), *N*-methylmorpholine (1.3 equiv.), CH_2Cl_2, -20 °C to r.t., 22 h, quant.; b) method A: Pd-C 10% (1 equiv.), H_2, MeOH, r.t. or method B: Pd-C 10% (0.25 equiv.), ammonium formate (5.5 equiv.), MeOH, reflux, 1 h, or method C: indium (9 equiv.), MeOH, sat. NH_4Cl solution, reflux, 24 h; c) Mitsunobu cyclisation. Reactions unsuccessful.

*1-Ethyl-3-(3-dimethylaminopropyl)carbodiimide hydrochloride.

In addition to problems with hydrogenation, disadvantage of this method lies in the fact that the final compound can be contaminated with triphenylphosphine oxide, the by-product of a Mitsunobu reaction, which is difficult to eliminate. This was observed when the reaction was performed with ordinary triphenylphosphine, which made purification impossible. However, this can be potentially be resolved by the usage of polymer-bound triphenylphosphine[7], although this method is expensive, given that the price of the polymer-bound triphenylphosphine exceeds the price of commercially available L-cycloserine.

In the interest of time, resources and meeting the project outcome of synthesising new lactivicin derivatives, it became more viable to utilise the commercially available and comparatively more affordable D-cycloserine to establish the underlying synthetic methodologies of accessing new lactivicin analogues, as described in Chapter 3.

A1.2. Experimental procedures

Reagents

Reagents were from Acros, Alfa Aesar, Enamine, Fluorochem, Key Organics, Lancaster, Sigma-Aldrich and Tokyo Chemical Industry, and used as supplied. Solvents for chemical transformation, work-up and chromatography were from Sigma-Aldrich at HPLC grade and used without further distillation. Dried solvents were obtained from Sigma-Aldrich and Alfa Aesar.

Chromatography

Silica gel 60 F 254 analytical thin layer chromatography (TLC) plates were from Merck and imaged under UV light or with appropriate staining methods. Chromatographic purifications were performed using a Biotage SP1 Purification system with Biotage KP-SIL silica columns. TLC R_f values are given when column chromatography separation was performed, to the nearest 0.05 unit.

NMR spectra

^{1}H and ^{13}C NMR spectra were recorded using a Bruker AVIII 400 nanobay (400 MHz). Signal positions were recorded in δ ppm with the abbreviations s, d, t, q, and m denoting singlet (s), doublet (d), triplet (t), quartet (q) and multiplet (m), respectively. All NMR chemical shifts were referenced to residual solvent peaks. All coupling constants, *J*, are quoted in Hz to the nearest 0.5 Hz. Signals in both the ^{1}H and ^{13}C spectra were assigned with the aid of DEPT, COSY and HMQC.

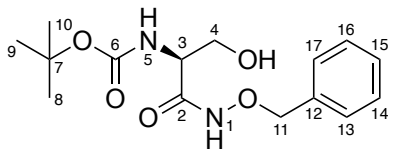
Other characterisation

Optical rotations were recorded on a Perkin Elmer 241 or 341 polarimeter with a path length of 1 dm (using the sodium D line, 589 nm). $[\alpha]_D$ are reported in units of 10^{-1} degree (^{o}) cm^2 g^{-1}. Concentrations are reported in g/100 mL. Temperatures are

reported in degree Celsius (°C). Infrared spectra were recorded on a Bruker Tensor 27 FT-IR spectrometer. Samples were prepared as a thin film on a diamond ATR module. Absorption maxima (ν_{max}) are given in wavenumbers (cm^{-1}). Ionisation (ESI) Mass Spectrometry (MS) data (m/z) were obtained on a Fision VG Platform using a quadrupole analyser. High Resolution (HR) mass spectrometry data (m/z) data were obtained from a Bruker MicroTOF instrument using ESI source and Time of Flight (TOF) analyser. Values are reported as ratio of mass to charge in Daltons. Melting points were obtained using a Leica VMTG heated-stage microscope.

Synthesis of A1.1 (*tert*-butyl (*S*)-(1-((benzyloxy)amino)-3-hydroxy-1-oxopropan-2-yl)carbamate)[7]

N-Boc-L-serine (4.00 g, 19.5 mmol, 1 equiv.) was dissolved in dichloromethane (80 mL) and cooled to -20 °C in an ice/salt bath. *O*-Benzylhydroxylamine (2.48 g, 20.1 mmol, 1.03 equiv.) and *N*-methylmorpholine (2.2 mL, 20.0 mmol, 1.03 equiv.) were added. After stirring for 5 min, EDAC•HCl (3.85 g, 20.1 mmol, 1.03 equiv.) was added. The mixture was allowed to warm to r.t. and stirred for 2 h. After quenching with 1M aqueous hydrochloric acid solution, the organic layer was separated, washed with sat. sodium bicarbonate solution (2 x 60 mL) and dried with anhydrous sodium sulfate. The solvent was removed *in vacuo*. The crude product was purified by flash column chromatography on silica (eluted with dichloromethane-methanol), to yield **A1.1** (3.42 g, 57%).

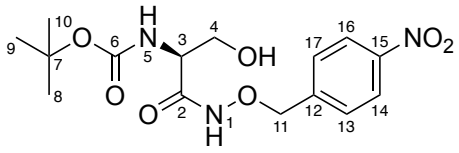


A1.1

mp 128-130 °C (lit. 130-131 °C[10]); **TLC** 95:5 dichloromethane/methanol, R_f = 0.40; **[α]$^{25}_D$** -47.0° (c = 0.01 g/mL, chloroform) [lit. -37.7° (c = 0.02 g/mL, methanol)[10]]; **IR** ν_{max} (film)/cm^{-1} 3360 (N-H stretch), 3300 (O-H stretch, br), 3190 (N-H stretch), 2995 (C-H stretch), 1715 (carbamate C=O stretch), 1670 (amide C=O stretch), 1520 (aromatic C=C stretch); **^{1}H NMR** (400 MHz, DMSO-d_6) δ ppm 7.31-7.47 (m, 5H, Ph), 6.89 (d, *J* = 8.0 Hz, 1H, C(O)NH), 4.85-4.91 (m, 1H, OH), 4.78 (s, 2H, OCH_2Ph), 3.80-3.89 (m, 1H, *H3*), 3.46-3.55 (m, 2H, CH_2OH), 1.39 (s, 9H, ^{t}Bu); **^{13}C NMR** (101 MHz, DMSO-d_6) δ ppm 167.5 (*C2*), 155.2 (*C6*), 135.9 (*C12*), 128.9 (*C14* and *C16*), 128.3 (*C13*, *C15* and *C17*), 78.2 (*C7*), 76.8 (*C11*), 61.3 (*C4*), 54.7 (*C3*), 28.2 (*C8*, *C9* and *C10*); **LRMS** (ESI$^-$, m/z) 309.3 [M-H]; **HRMS** (ESI$^-$) $C_{15}H_{22}N_2O_5$ requires 309.1456, found [M-H] 309.1445.

Synthesis of A1.2 (*tert*-butyl (*S*)-(3-hydroxy-1-(((4-nitrobenzyl)oxy)amino)-1-oxopropan-2-yl)carbamate)[7]

N-Boc-L-Serine (490 mg, 2.39 mmol, 1 equiv.) was dissolved in dichloromethane (10 mL) and cooled to -20 °C in an ice/salt bath. *O*-(4-Nitrobenzyl)hydroxylamine hydrochloride (636 mg, 3.11 mmol, 1.3 equiv.) and *N*-methylmorpholine (0.35 mL, 3.18 mmol, 1.3 equiv.) were added. After stirring for 5 min, EDAC•HCl (598 mg, 3.11 mmol, 1.3 eq.) was added. The mixture was allowed to warm to r.t. and stirred under nitrogen for 22 h. After quenching with 1M aqueous hydrochloric acid solution, the organic layer was separated, washed with sat. aqueous sodium bicarbonate solution (2 x 60 mL) and dried with anhydrous sodium sulfate. The solvent was removed *in vacuo*. The crude product was purified by flash column chromatography on silica (eluted with dichloromethane-methanol), to yield **A1.2** (849 mg, 100%).



A1.2

mp 171-172 °C; **TLC** 9:1 dichloromethane/methanol, R_f = 0.45; **[α]$^{25}_D$** -33.2° (c = 0.01 g/mL, chloroform); **IR** ν_{max} (film)/cm^{-1} 3350 (N-H stretch), 3300 (O-H stretch, br), 3190 (N-H stretch), 2986 (C-H stretch), 1713 (carbamate C=O stretch), 1668 (amide C=O stretch), 1572 (N-O stretch), 1531 (aromatic C=C stretch), 1363 (N-O stretch); **^{1}H NMR** (400 MHz, DMSO-d_6) δ ppm 11.32 (s, 1H, amide NH), 8.23 (d, *J* = 8.5 Hz, 2H, *H14* and *H16*), 7.69 (d, *J* = 8.5 Hz, 2H, *H13* and *H17*), 6.73 (d, *J* = 8.0 Hz, carbamate NH), 4.90 (s, 2H, CH_2Ar), 3.86-3.76 (m, 1H, *H3*), 3.53-3.42 (m, 2H, CH_2OH), 1.37 (9H, s, ^{t}Bu); **^{13}C NMR** (101 MHz, DMSO-d_6) δ ppm 167.2 (*C2*), 154.9 (*C6*), 147.1 (*C15*), 142.2 (*C12*), 127.8 (*C13* and *C17*), 124.2 (*C14* and *C16*), 78.3 (*C7*), 77.3 (*C11*), 61.6 (*C4*), 54.4 (*C3*), 28.1 (*C8*, *C9* and *C10*); **LRMS** (ESI$^-$, m/z) 354.1 [M-H]; **HRMS** (ESI$^-$) $C_{15}H_{20}N_3O_7$ requires 354.1307, found [M-H] 354.1301.

A1.3. References

[1] Kuehl, F. A.; Wolf, F. J.; Trenner, N. R.; Peck, R. L.; Buhs, R. P.; Howe, E.; Putter, I.; Hunnewell, B. D.; Ormond, R.; Downing, G.; Lyons, J. E.; Newstead, E.; Chaiet, L.; Folkers, K. *J. Am. Chem. Soc.* **1955**, *77*, 2344–2345.

[2] Stammer, C. H.; Wilson, A. N.; Holly, F. W.; Folkers, K. *J. Am. Chem. Soc.* **1955**, *77*, 2346–2347.

[3] Hidy, P. H.; Hodge, E. B.; Young, V. V.; Harned, R. L.; Brewer, G. A.; Phillips, W. F.; Runge, W. F.; Stavely, H. E.; Pohland, A.; Boaz, H.; Sullivan, H. R. *J. Am. Chem. Soc.* **1955**, *77*, 2345–2346.

[4] Epstein, I. G.; Nair, K.; Boyd, L. J. *Dis. Chest* **1956**, *29*, 241–257.

[5] Harada, S.; Tsubotani, S.; Hida, T.; Ono, H.; Okazaki, H. *Tetrahedron Lett.* **1986**, *27*, 6229–6232.

[6] Nozaki, Y.; Katayama, N.; Ono, H.; Tsubotani, S.; Harada, S.; Okazaki H.; Nakao, Y. *Nature* **1987**, *325*, 179–180.

[7] Hopkins, R. The development of synthetic strategies towards analogues of the natural product lactivicin. Part II thesis, 2007.

[8] Ram, S.; Spicer, L. D. *Synth. Comm.* **1987**, *17*, 415–418.

[9] Pitts, M. R.; Harrison, J. R.; Moody, C. J. *J. Chem. Soc., Perkin Trans. 1* **2001**, *9*, 955–977.

[10] Gissot, A.; Volonterio, A.; Zanda, M. *J. Org. Chem.* **2005**, *70*, 6925–6928.